Regulation of UsnRNP biogenesis

Inaugural-Dissertation

zur Erlangung des Doktorgrades
der Mathematisch-Naturwissenschaftlichen Fakultät
der Heinrich-Heine-Universität Düsseldorf

vorgelegt von

Lea Marie Esser

aus Grevenbroich

Düsseldorf, Januar 2024

aus dem Institut für Molekulare Medizin I

der Heinrich-Heine-Universität Düsseldorf

Gedruckt mit der Genehmigung der
Mathematisch-Naturwissenschaftlichen Fakultät
der Heinrich-Heine-Universität Düsseldorf

Berichterstatter:
1. Univ.-Prof. Dr. Sebastian Wesselborg
2. Univ.-Prof. Dr. Henrike Heise

Tag der mündlichen Prüfung: 29.08.2024

Table of Contents

1 Abstract

The spliceosome regulates mRNA maturation via the exclusion of non-coding sequences in the pre-mRNA and consists of uridine-rich small nuclear ribonucleoproteins (UsnRNPs). The focus of this thesis is to analyze the regulation of the two key protein complexes acting in the assembly of UsnRNPs *in vivo*: the protein arginine methyltransferase 5 (PRMT5) and the survival motor neuron (SMN) complex.

A new substrate of the PRMT5 methyltransferase, the RNA binding protein nuclear factor 90 (NF90), was characterized as a project of this thesis (Chapter 7.1). It was demonstrated that NF90 is fully methylated *in vivo*, recruited by the adapter protein RIO Kinase 1 (RioK1), the antagonist of the adapter protein chloride conductance regulatory protein (pICln), (Chapter 7.1).

Former studies revealed that the pICln protein builds a stable, hexameric, RNA-free intermediate with the Sm proteins SmD1, D2, E, F, and G, which is termed the 6S complex. Within the 6S complex, the Sm proteins are kinetically trapped. The cell needs to overcome this structure so that the five Sm proteins, together with the two missing Sm proteins SmB and D3, can assemble onto the specific uridine-rich snRNA (UsnRNA) with the help of the SMN complex. We were able to show that the Ser/Thr kinase Unc-51-like kinase 1 (ULK1) solves this key regulatory step in UsnRNP biogenesis in a role independent from autophagy, via the phosphorylation of pICln in the C-terminus (Chapter 7.2, 7.3). The ULK1-dependent phosphorylation of pICln enforces an open ring structure of the 6S complex by lowering the binding affinity at the pICln-SmG contact side, allowing the binding of the missing Sm proteins B and D3 (Chapter 7.2). Consequently, this increases the transfer efficiency of Sm proteins onto the SMN complex and finally the splicing activity (Chapter 7.3), and thus the UsnRNP biogenesis in the further course of the signaling pathway (Chapter 7.2, Chapter 7.3).

Gemin2 is the acceptor of Sm proteins within the SMN complex. We identified a novel interaction of Gemin2 with the ribosomal protein S6 kinase beta-1 (p70S6K) and a subsequent p70S6K-dependent phosphorylation (Chapter 7.4). In contrast to previous research, which only predicts a putative role of phosphorylation in UsnRNP biogenesis, this work identified defined molecular targets and their respective kinase-substrate interactions, thereby demonstrating the dependency of UsnRNP biogenesis on post-translational modifications (PTMs) *in vivo* and their dependency on cellular energy levels.

2 Zusammenfassung

Das Spleißosom reguliert die mRNA-Reifung durch den Ausschluss von nicht-kodierenden Sequenzen in der prä-mRNA und besteht aus *uridine-rich small nuclear ribonucleoproteins* (UsnRNPs). Der Schwerpunkt dieser Arbeit liegt in der Analyse der Regulierung der beiden Schlüsselproteinkomplexe, die beim Zusammenbau von UsnRNPs *in vivo* eine Rolle spielen: der Protein-Arginin-Methyltransferase 5 (PRMT5) Komplex und der *survival motor neuron* (SMN) Komplex.

Ein neues Substrat der PRMT5-Methyltransferase, das RNA-bindende Protein *nuclear factor 90* (NF90), wurde im Rahmen dieser Arbeit charakterisiert (Kapitel 7.1). Es konnte gezeigt werden, dass NF90 *in vivo* vollständig methyliert wird, rekrutiert durch das Adapterprotein *RIO Kinase 1* (RioK1), dem Antagonisten zum Adapterprotein *chloride conductance regulatory protein* (pICln), (Kapitel 7.1).

Frühere Untersuchungen ergaben, dass das pICln-Protein ein stabiles, hexameres, RNA-freies Zwischenprodukt mit den Sm-Proteinen SmD1, D2, E, F, und G bildet, das als 6S-Komplex bezeichnet wird. Innerhalb des 6S-Komplexes bilden die Sm-Proteine eine energetisch stabile Zwischenform. Die Zelle muss diese Struktur überwinden, damit sich die fünf Sm-Proteine, zusammen mit den beiden fehlenden Sm-Proteinen SmB und D3, durch Hilfe des SMN-Komplexes an die spezifische uridin-reiche snRNA (UsnRNA) anlagern können. Wir konnten zeigen, dass die Ser/Thr-Kinase *Unc-51-like kinase 1* (ULK1) diesen wichtigen regulatorischen Schritt in der UsnRNP-Biogenese in einer von der Autophagie unabhängigen Rolle über die Phosphorylierung von pICln im C-Terminus löst (Kapitel 7.2, 7.3). Die ULK1-abhängige Phosphorylierung von pICln führt zu einer Öffnung der Ringstruktur des 6S-Komplexes, indem es die Bindungsaffinität an der pICln-SmG-Kontaktstelle senkt was als Konsequenz die Bindung der fehlenden Sm-Proteine B und D3 ermöglicht (Kapitel 7.2). Dies erhöht folglich die Transfereffizienz der Sm-Proteine auf den SMN-Komplex und in letzter Konsequenz die Spleißaktivität (Kapitel 7.3), und damit die UsnRNP-Biogenese im weiteren Verlauf des Signalweges (Kapitel 7.2, Kapitel 7.3).

Gemin2 fungiert als Akzeptor von Sm-Proteinen innerhalb des SMN-Komplexes. Wir identifizierten eine neue Interaktion von Gemin2 mit der *ribosomal protein S6 kinase beta-1* (p70S6K) und eine anschließende p70S6K-abhängige Phosphorylierung (Kapitel 7.4). Im Gegensatz zu früheren Forschungsarbeiten, die nur eine vermeintliche Rolle der Phosphorylierung bei der UsnRNP-Biogenese vorhersagen, wurden in dieser Arbeit

definierte molekulare Ziele und ihre jeweiligen Kinase-Substrat-Interaktionen identifiziert, wodurch die Abhängigkeit der UsnRNP-Biogenese von posttranslationalen Modifikationen (PTMs) *in vivo* und ihre Abhängigkeit vom zellulären Energieniveau aufgezeigt wird.

3 List of figures

All figures were created with *BioRender.com*

4 Abbreviations

(v/v)	volume per volume
(w/v)	weight per volume
[32P]-ATP	32-P (phosphate) adenosine triphosphate, radioactive
[32P]-UTP	32-P (phosphate) uridine triphosphate, radioactive
[35S]-methionine	35-S (sulfur) methionine, radioactive
[3-H]-SAM	3-H (tritium) S-Adenosyl methionine, radioactive
µg	microgram
µl	microliter
µM	micromolar
AA	amino acid
AB	amido black
ADMA	Asymmetric dimethylarginine
Adox	Adenosine dialdehyde
ALS	amyotrophic lateral sclerosis
AR	autoradiography
ASO	antisence oligonucleotide
ATG	Autophagy-related
ATP	Adenosine triphosphate
AUC	analytical ultracentrifugation
bp	base pair
BSA	Bovine serum albumin
CBs	cajal bodies
CS	coomassie blue staining
CTD	C-terminal domain
DKO	double knockout
DMEM	Dulbecco’s modified Eagle’s medium
DMSO	Dimethyl sulfoxide
DNA	deoxyribonucleic acid

DPBS	Dulbecco´s phosphate-buffered saline
DRBM	double-stranded RNA-binding motif
dsRNA	double-stranded RNA
DTT	Dithiothreitol
DZF	domain associated with zinc fingers
E. coli	*Escherichia coli*
e.g.	for example
EBSS	Earle's Balanced Salt Solution
EDTA	Ethylenediaminetetraacetic acid
EGTA	ethylene glycol-bis(β-aminoethyl ether)-tetraacetic acid
FCS	Fetal calve serum
Fig.	figure
FIP200	focal adhesion kinase-interacting protein of 200 kDa
g	gram
Gemin	Gem nuclear organelle associated protein
GFP	Green fluorescent protein
GSH	Glutathione
GST	Glutathione S-transferase
h	hour
HEK293	Human embryonic kidney 293 cells
HPLC	High-performance liquid chromatography
ILF3	Interleukin enhancer-binding factor 3
IP	Immunoprecipitation
IPTG	Isopropyl β-D-1-thiogalactopyranoside
k. dom.	kinase domain
KD	dissociation constant
kDa	kilo dalton
LB	lysogeny broth
LC-MS	Liquid chromatography–mass spectrometry

MBP	myelin basic protein
mCi	microcurie
MDa	mega dalton
MEF	Mouse embryonic fibroblast
MEP50	methylosome protein 50
Mg	milligram
min	minutes
ml	milliliter
mM	millimolar
MMA	Monomethylarginine
MMTS	Methylmethanethiosulfonate
mRNA	messenger RNA
ms	millisecond
mTOR	mechanistic target of rapamycin
mTORC1	mTOR complex 1
NF90	Nuclear factor 90
Ni-NTA	Nickel nitrilotriacetic acid
nl	nanoliter
NLS	nuclear localization signal
nM	nanomolar
nm	nanometer
NMR	Nuclear magnetic resonance
p70S6K	ribosomal protein S6 kinase beta-1
pICln	Chloride conductance regulatory protein
PRMT	Protein arginine N-methyltransferase
PRMT5	Protein arginine methyltransferase 5
PTM	Post-translational modification
RG-rich	Arginine-Glycine-rich
RioK1	right open reading frame Kinase 1

RNA	ribonucleic acid
rpm	revolutions per minute
RT	room temperature
S100	cytoplasm extract
SAH	S-adenosyl-L-homocysteine
SAM	S-adenosyl methionine
SB	super broth
SDMA	Symmetric dimethylarginine
SDS	Sodium dodecyl sulfate
SDS-PAGE	sodium dodecyl sulphate–polyacrylamide gel electrophoresis
SIP1	SMN interacting protein 1
siRNA	small interfering RNA
SMA	spinal muscular atrophy
SMN	Survival of motor neuron
SNAPc	snRNA-activating protein complex
snRNA	small nuclear RNA
SPR	surface plasmon resonance
starv.	starvation
SV	Sedimentation velocity
U	enzyme unit
U1 snRNP	U1 small nuclear ribonucleoprotein
UsnRNPs	uridine-rich small nuclear ribonucleoproteins
ULK1	Uncoordinated [unc-51]-like kinase 1
Unrip	UNR-interacting protein
WB	western blot
WD45	WD Repeat Domain 45 protein
wt	wild type

Amino Acid	One letter code	Three letter code
Alanine	A	Ala
Cysteine	C	Cys
Aspartic acid	D	Asp
Glutamic acid	E	Glu
Phenylalanine	F	Phe
Glycine	G	Gly
Histidine	H	His
Isoleucine	I	Ile
Lysine	K	Lys
Leucine	L	Leu
Methionine	M	Met
Asparagine	N	Asn
Proline	P	Pro
Glutamine	Q	Gln
Arginine	R	Arg
Serine	S	Ser
Threonine	T	Thr
Valine	V	Val
Tryptophan	W	Trp
Tyrosine	Y	Tyr

5 Introduction

The main feature of the human genome is its diversity, which is maintained by mechanisms like alternative splicing, transcription initiation, and alternative polyadenylation (de Klerk et al., 2015, Bludau et al., 2020). Around 86% of the human genes are spliced, showing the important contribution of this process to the diversity of the human transcriptome (Nilsen et al., 2010, Bludau et al., 2020). The proper maturation of mRNAs during splicing is important for the subsequent protein synthesis (Nilsen et al., 2010). Since proteins play an important role in cellular signaling pathways and functions, and therefore dysfunctional proteins can cause diseases, they developed into a key feature for drug targeting to date (Araujo et al., 2007, Perrett, 2007, Yildirim et al., 2007). Furthermore, PTMs increase the diversity at the proteome level (Bludau et al., 2020), through the regulation of the protein activity. Therefore, both, the genome stability maintained through splicing, as well as the proteome level of a signaling pathway are interesting research targets for the curing of a disease.

5.1 The process of mRNA maturation - Splicing

Splicing is the cellular process in eukaryotes that processes the pre-mRNA transcript into the mature mRNA, which occurs after the transcription within the nucleus (Matera et al., 2014). The main task of the splicing is to remove the intervening sequences (introns) from the pre-mRNA, therefore the expressed sequences (exons) join together to the mature mRNA (Berget et al., 1977, Chow et al., 1977). Splicing is catalyzed by a protein-RNA complex (Lerner et al., 1980), termed the spliceosome, that requires a lot of energy throughout the splicing process (Will et al., 2011).

5.1.1 The spliceosome and its unique regulatory unit - The UsnRNP

There are two forms of the spliceosome within a cell (Patel et al., 2003). The main spliceosome catalyzes over 99% of the splice reactions within eukaryotes, which is known as canonical splicing (Burset et al., 2000), whereas the site spliceosome is only responsible for 0,5% of all splicing processes (Turunen et al., 2013). The main spliceosome is composed of five UsnRNPs, which are termed after their unique snRNA they are composed of, the U1, U2, U4/6, and U5 (Will et al., 2011). The site spliceosome, however, has four different forms of snRNPs, U11, U12, U4atac, and U6atac, whereas the U5 snRNP is shared by the site and main spliceosome (Will et al., 2011).

The snRNPs joining the canonical splicing pathway are further associated with a common set of proteins, the Sm proteins B/B′, D1, D2, D3, E, F, and G, joining together to form the mature snRNP (Will et al., 2011). Except for the U6 UsnRNA, all others share a characteristic structure (Branlant et al., 1982, Mattaj, 1986): The 5′-term trimethylguanosin (m ^{2,2,7}G) structure which is termed the m G-Cap, and a single-stranded sequence, flanked by hairpin structures known as the Sm protein binding site (Figure 1).

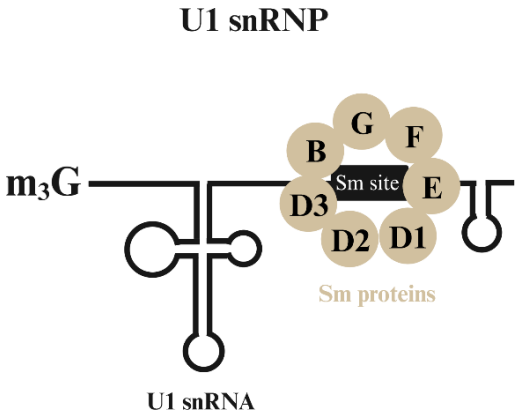

Figure 1: Schematic representation of the composition of a U1 snRNP. Shown is the human U1 snRNA with the 5′ m_3G cap and the Sm binding site. The Sm proteins bind in a ring-shaped manner onto the Sm site. *Created with BioRender.com*

5.2 The biogenesis of UsnRNPs

The biogenesis of UsnRNPs is a highly regulated, stepwise organized cellular process, which has a distinct cellular compartmentation (Figure 2), (Matera et al., 2014). At first, the transcription of the Sm-class snRNA (U1, U2, U4, U4atac, U5, U11, and U12), is catalyzed by the RNA polymerase II in the nucleus, which is initiated by the binding of the snRNA-activating protein complex (SNAPc) (Henry et al., 1998, Hung et al., 2011). After the capping of the 5′ end of the snRNA with an m^{7}G cap, and the cleavage and maturation of the 3′ end (Hernandez et al., 1986, Baillat et al., 2005), the newly synthesized snRNA is exported to the cytoplasm (Figure 2), (Ohno et al., 2002, Cullen, 2003).

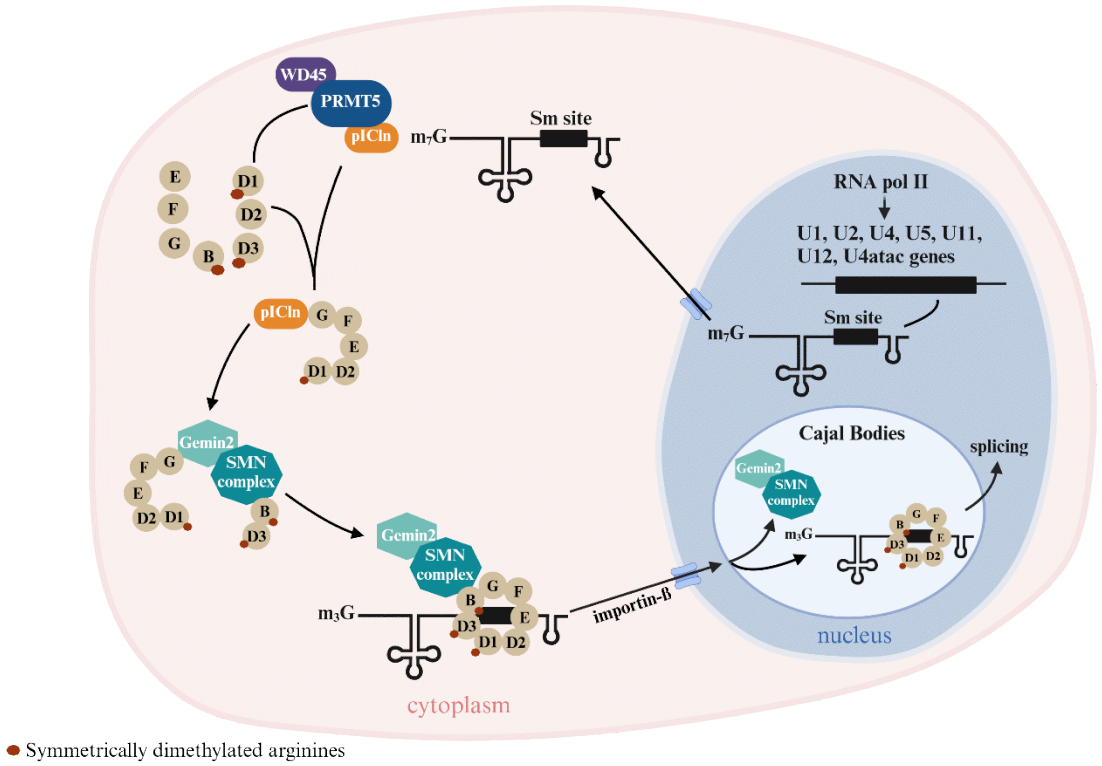

Figure 2: Schematic overview of the biogenesis of UsnRNPs. The cycle of UsnRNPs starts with the transcription of UsnRNAs within the nucleus. After their export to the cytoplasm, the assembly of the so-called Sm core is regulated by the cooperation of the PRMT5 and the SMN complex. The heptameric ring of the seven Sm proteins B, D3, D1, D2, E, F, and G is therefore bound to the Sm site of the snRNA. After the modification of the m_7G cap of the RNA to an m_3G cap the whole complex consisting of the UsnRNP and SMN complex is reimported into the nucleus via importin-ß, thereby the SMN complex probably dissociates from the UsnRNP. As a last step, the UsnRNPs mature in circular structures within the nucleus, the Cajal bodies, before contributing their role in mRNA splicing. *Created with BioRender.com*

Within the cytoplasm, a stable but inactive form, a pre-snRNP is generated. This mechanism allows proper quality control, to ensure that only assembled snRNPs come in contact with their substrates (Matera et al., 2014). *In vitro* studies on Sm core assembly revealed a hierarchical pathway, showing the Sm proteins to form three RNA-free hetero-oligomers (Raker et al., 1996): D3/B, D1/D2, and E/F/G. In an additional step, a Sm subcore intermediate consisting of D1/D2 and E/F/G binds to the UsnRNA. To finally mature to the Sm core, the Sm proteins D3/B must join (Raker et al., 1996, Will et al., 2001). To fulfill this task *in vivo*, the activity of the protein arginine methyltransferase 5 (PRMT5) complex is crucial, as it regulates the methylation of Sm proteins (Friesen et al., 2001b, Meister et al., 2001b), and the chaperone delivery of the Sm proteins (Figure 2), (Chari et al., 2008). In addition, the SMN complex, with the survival motor neuron (SMN) protein as the name-giving central core, and its associated proteins are involved in the regulation of the cytoplasmic phase of this snRNP cycle *in vivo* (Meister et al., 2001a, Massenet et al., 2002).

The SMN complex is responsible for the recruitment of nuclear-exported snRNAs and their assembly with the seven Sm proteins, which bind to the RNA binding site of the snRNA in a ring-shaped manner (Figure 2), (Meister et al., 2001a, Meister et al., 2002a, Pellizzoni et al., 2002b). The assembly of the Sm core is on the one hand stabilizing the snRNA, and on the other hand, required for the downstream RNA processing in the end culminating in the nuclear import that is catalyzed by the import receptor importin-beta (Matera et al., 2014). Within the nucleus, UsnRNPs mature in so-called Cajal bodies (CBs), before they fulfill their role in mRNA splicing (Figure 2), (Liu et al., 1996, Mao et al., 2011).

5.2.1 Role of PRMT5 complex and the methylosome subunit pICln in UsnRNP biogenesis

The PRMT5 complex, consisting of PRMT5, the WD repeat domain 45 protein (WD45), and pICln, is one out of two major protein complexes regulating the UsnRNP biogenesis (Friesen et al., 2001b, Meister et al., 2001b, Friesen et al., 2002, Meister et al., 2002b). While searching for the function of pICln, the PRMT5 protein was originally identified as a pICln interacting protein (Krapivinsky et al. 1998). Within UsnRNP biogenesis, PRMT5 has a unique regulatory role via the symmetrical dimethylation of the Sm proteins B, D1, and D3, which influences the transfer of Sm proteins onto the SMN complex in the ongoing pathway (Figure 2), (Brahms et al., 2001, Friesen et al., 2001b, Meister et al., 2002b). It is interesting to note, that the modification to symmetrical dimethylarginines (sDMAs) is especially introduced into the RG-rich tails of the Sm proteins (Meister et al., 2001b). PRMT5, in its role as a methyltransferase, thus influences the selectivity and promotes a stepwise organization of the assembly of UsnRNPs, as it is known that the SMN protein only binds symmetrical dimethylated Sm proteins (Friesen et al., 2001a). The WD45 protein, also termed methylosome protein 50 (MEP50), directly binds to PRMT5 and is required for methylosome activity by increasing the substrate affinity of PRMT5 (Meister et al., 2001b, Antonysamy et al., 2012). However, PRMT5 is extending its core complex, consisting of PRMT5 and WD45, by different adapter proteins known as pICln, RioK1, and COPR5 (Krapivinsky et al. 1998; Lacroix et al. 2008; Guderian et al. 2011). PRMT5 builds two subcomplexes *in vivo* (PRMT5-WD45-RioK1 and PRMT5-WD45-pICln), both with a composition of a 1:1:1 stoichiometry, able to recruit complex-specific substrates (Guderian et al. 2011). The methylosome subunit pICln, on the one hand, recruits the Sm proteins for

methylation (Friesen et al., 2001b, Meister et al., 2001b), and on the other hand pICln was shown to build a stable, RNA-free, ring-shaped 6S structure with the Sm proteins D1, D2, E, F, and G (Figure 2), (Chari et al. 2008). Thereby, pICln functions as an assembly chaperone by inhibiting premature or unspecific interactions and thus promotes the assembly of macromolecular complexes (Chari et al. 2008). In the ongoing pathway, the Sm proteins need to be transferred from the PRMT5 onto the SMN complex, this occurs with the help of pICln (Meister et al., 2002b, Chari et al., 2008).

5.2.2 Role of SMN complex and the core subunit Gemin2 in UsnRNP biogenesis

The overall function of the SMN complex within the UsnRNP biogenesis is receiving the Sm proteins from the PRMT5 complex and transferring them onto the snRNA to maintain proper Sm core assembly and maturation (Matera et al., 2014). To maintain this regulatory aspect, every protein within the complex has a unique function (Fischer et al., 1997, Friesen et al., 2001a, Meister et al., 2002b, Zhang et al., 2011). Although the assembly of the Sm core occurs spontaneously *in vitro* (Raker et al. 1999), the formation of Sm core assembly *in vivo* is dependent on the SMN complex, since the complex ensures Sm core assembly only on snRNAs (Fischer et al., 1997, Liu et al., 1997, Meister et al., 2001a, Pellizzoni et al., 2002b). Initial studies on the SMN-SIP1 complex (Gemin2=Gem Nuclear Organelle Associated Protein 2 was initially termed SIP1=SMN interacting protein 1) in *Xenopus* oocytes have already revealed a crucial function of the complex within the UsnRNP biogenesis. After the injection of antibodies against Gemin2 into the oocyte, the Sm core assembly of spliceosomal snRNPs was strongly inhibited, especially since their transport from the cytoplasm to the nucleus was blocked (Fischer et al., 1997). In contrast, the anti-SMN antibodies stimulated the formation of the Sm core domain. This experiment provides clear evidence that both, the SMN protein as well as Gemin2, are directly involved in the biogenesis of snRNPs through different, but related functions (Fischer et al., 1997). Nowadays, this hypothesis could be verified, by identifying the SMN-Gemin2 complex as the functional core of the SMN complex, involved in the transfer of Sm proteins onto the Sm site of the UsnRNA (Figure 2), (Pellizzoni et al., 2002b, Kroiss et al., 2008, Zhang et al., 2011). The SMN protein builds a platform for the other complex members to bind (Kroiss et al., 2008). It can interact simultaneously with the Sm proteins and Gemin2, via two different domains (Liu et al., 1997), and occupies a space for the Sm proteins B and D3 during the pentamer transfer from the PRMT5 to the SMN complex (Grimm et al., 2013). Gemin2 has

a crucial role within this process, via the binding of the Sm proteins SmD1, D2, E, F, and G thereby preventing unspecific interactions with the UsnRNA (Zhang et al., 2011). In addition to the functional core of the SMN complex, it consists of the Gemins2-8, and the UNR interacting protein (Unrip), whereas Gemin3 is an RNA-helicase and Gemin5 is responsible for the recruitment of the snRNA (Liu et al., 1997, Charroux et al., 1999, Charroux et al., 2000, Baccon et al., 2002, Gubitz et al., 2002, Pellizzoni et al., 2002a, Grimmler et al., 2005b, Carissimi et al., 2006). An interaction map of the SMN complex revealed that SMN, together with Gemin7 and Gemin8, serves as the backbone of the complex (Otter et al., 2007). SMN binds directly to Gemin2 (Liu et al. 1997), Gemin3 (Charroux et al. 1999), and Gemin8 (Carissimi et al., 2006). Gemin8 itself also interacts with Gemin4 and Gemin7 and Unrip and Gemin6 joins to complex via binding to Gemin7 (Baccon et al., 2002, Carissimia, 2005, Grimmler et al., 2005b). Further studies revealed a tight association between Gemins3 and 4 (Charroux et al., 2000). Within this complex, all interactions are stable, except for Gemin5, which is associated with the complex via a weak interaction with Gemin2 (Otter et al. 2007). Although these findings revealed mechanistic insights of the Sm core assembly, the regulation of the SMN complex activity within UsnRNP biogenesis remains unclear.

5.3 The disease spinal muscular atrophy

Spinal muscular atrophy (SMA) is a neuromuscular disease resulting in the degeneration of α-motor neurons in the spinal cord, therefore leading to progressive muscle weakness (Lefebvre et al., 1995, Crawford et al., 1996). Moreover, patients with SMA are limited in movement, muscle tone, and muscle-related functions such as breathing (Pearn, 1980). SMA is the leading cause of infant death, one of every 6000 to 10000 newborns is affected by this disease (Lunn et al., 2008, Tisdale et al., 2015). SMA can be classified into the following different types, dependent on the age of onset and the varying degrees of symptoms (Eggert et al., 2006, Zhou et al., 2012, Tisdale et al., 2015): Type 0 SMA is an embryonal lethal form of the disease. The type I form of SMA is the most common one, with an age of onset <6 months, and patients never gaining the ability to sit and usually dying within two years after birth. Patients with type II SMA show the first symptoms around two years after birth and can sit but never stand or walk alone, they die until the 20th year of life. Type III SMA develops after the second year of birth. Patients are able to sit and stand alone, and they can gain the ability to walk with restrictions. SMA type IV is the mildest course of the disease

with patients developing the symptoms around the middle of their 30th year of life. This form is rare and has no influence on the life span of the patients.

5.3.1 The genetic background of SMA

SMA is the most common autosomal recessive genetic disorder next to cystic fibrosis (Lunn et al., 2008). Although the different types of SMA are quite heterogeneous, the genetic cause for all types of the disease could be mapped to one single gene locus, the q13 within chromosome 5 (Brzustowicz et al., 1990, Melki et al., 1990). The disease-causing gene for SMA was identified in 1995 and termed the *survival motor neuron* (*SMN*) gene (Lefebvre et al., 1995). There are two inverted copies of this gene, with a consensus of around 99% within this gene section, which were later termed *SMN1* and *SMN2* (Lefebvre et al., 1995, Lefebvre et al., 1998). The sequence of the *SMN1* and *SMN2* genes just differs by only 5 nucleotides, causing a shortened transcript processed from the *SMN2* mRNA that misses the exon 7, and therefore leads to an SMN protein that is unstable and mostly dysfunctional (Lorson et al., 1999, Monani et al., 1999, Lorson et al., 2000). In a healthy person, this is compensated by the expression of the *SMN1* gene, and in the case of SMA, mutations or deletions of the *SMN1* gene lead to an inactive form (Eggert et al., 2006). In summary, the dysfunction in *SMN2* transcribed SMN, in addition to the deficiency in active SMN protein caused by the change in the *SMN1* gene, leads to a low level of functional SMN within the cell, which causes SMA (Figure 3), (Lefebvre et al., 1997, Monani et al., 1999).

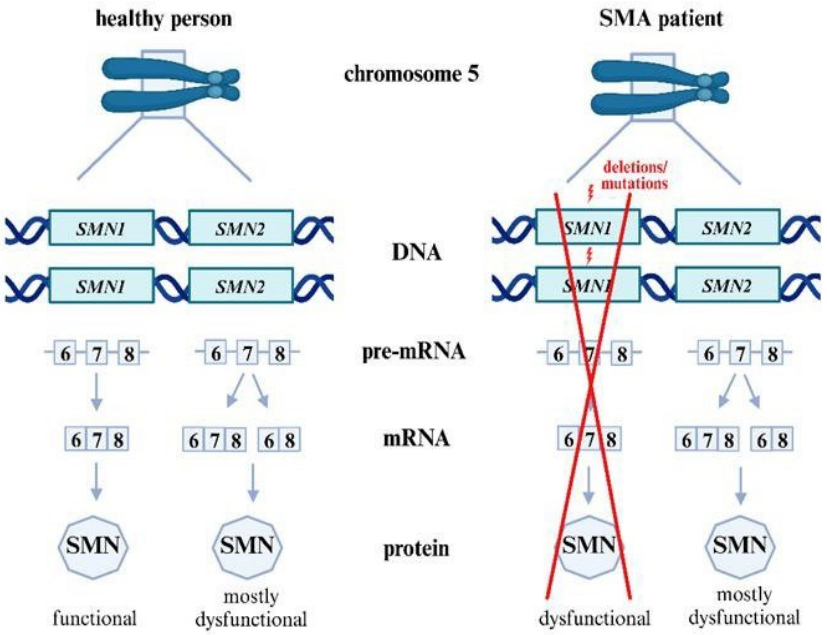

Figure 3: Schematic overview of the genetic background of spinal muscular atrophy (SMA). Within the human genome, there are two copies of the *SMN* gene called *SMN1* and *SMN2*, which are located within chromosome 5. In a healthy person, the *SMN1* gene produces the major amount of the functional SMN protein, as the *SMN2* mRNA mostly lacks the exon 7, thus resulting in a dysfunctional SMN protein. Within SMA patients, the *SMN1* gene is mutated or deleted, therefore causing the SMA phenotype. *Inspired by (Eggert et al., 2006); Created with BioRender.com*

Interestingly, the amount of *SMN2* gene copies is directly related to the severity of the disease, the more *SMN2* gene copies, the less pronounced the disease (Harada et al., 2002, Tisdale et al., 2015). Within the cell, the main role of the SMN protein is the regulation of the assembly of snRNPs, therefore a mutant of the SMN protein, lacking the first 27 amino acids, has a negative effect on UsnRNP biogenesis and pre-mRNA splicing (Pellizzoni et al., 1998). Furthermore, reduced activity of the biogenesis of snRNPs in the spinal cord of SMA mice was shown, thus linking the disease to the biogenesis pathway (Gabanella et al., 2007). In addition, a link between the late phase of SMA and a defect in splicing was verified (Bäumer et al., 2009).

5.3.2 Therapy approaches for the treatment against SMA

So far, therapy approaches mainly target the synthesis of factors that influence SMN expression. One approach focuses on the insertion of exon 7 into the *SMN2* mRNA and another one on the exogenous expression of the SMN protein. Nowadays, a treatment with so-called antisense oligonucleotides (ASOs) is the most promising potential therapy approach for SMA (Hua et al., 2010, Porensky et al., 2012). ASOs make use of the fact that

a series of splice enhancers and silencers regulate the incorporation of exon 7 in *SMN2*, an ASO can block this to alter *SMN2* transcript splicing, thereby promoting the formation of an *SMN1* identical protein (Hua et al., 2010, Porensky et al., 2012). By using a mice model of type III SMA (Hsieh-Li et al., 2000), an ASO rescuing the SMA phenotype by a single embryonic or neonatal intracerebroventricular (ICV) injection could be verified (Hua et al., 2010). The ASO rescued the SMN amount at the mRNA and protein levels in the spinal cord of motor neurons (Hua et al., 2010). Based on this research (Hua et al., 2010, Porensky et al., 2012), the approved ASO drug nusinersen against SMA came on the market (Finkel et al., 2016). The drug is injected into the central nerve system (CNS), regulating alternative splicing of *SMN2* pre-mRNA, where it blocks a splice modulator and therefore increases the amount of active SMN protein (Finkel et al., 2016). Another therapy approach is the gene therapy of SMA, which directly targets the dysfunctional *SMN1* gene. Therefore, an Adeno-Associated Viral serotype 9 (AAV9) vector was developed, carrying an intact copy of wild-type SMN, this drug was called Zolgensma (Schorling et al., 2020). Whereas nusinersen must be applied long-term at defined time intervals, the drug Zolgensma only requires a one-time intravenous injection (Prior et al., 1993). This blocks the progression of the disease but does not cure SMA.

6 Aims

This thesis aimed to analyze the regulation of UsnRNP biogenesis on the level of the PRMT5 and the SMN complex. Therefore, the pICln protein was further characterized concerning its role as a kinetic trap for the Sm proteins D1, D2, E, F, and G, the so-called 6S complex (Chari et al., 2008), during the UsnRNP biogenesis. To analyze this survey, it was essential to answer the question of how this kinetic trap is solved *in vivo.* As it is known that the assembly of Sm cores is ATP-dependent (Meister et al., 2001a), the role of PTMs was explored to adress this question. Within the first part of the thesis, pICln could be identified as a specific interaction partner and phosphorylation substrate of the ULK1 kinase. Furthermore, the role of this ULK1-dependent activity regulation of the pICln protein in the view of the UsnRNP biogenesis, which consequently solves the kinetic trap to ensure Sm core assembly, was investigated *in vitro* as well as *in vivo*, via the generation of a phospho-specific pICln antibody.

In the ongoing UsnRNP biogenesis pathway, the pentamer of Sm proteins needs to be transferred from the PRMT5 to the SMN complex, therefore the SMN-Gemin2 subcomplex builds the core unit through Sm protein binding and the transfer of Sm proteins onto the snRNA (Pellizzoni et al., 2002b, Kroiss et al., 2008, Zhang et al., 2011). In this scenario, Gemin2 has a crucial role. Like the pICln protein, Gemin2 was identified to bind the Sm proteins D1, D2, E, F, and G in an RNA-free intermediate structure (Zhang et al., 2011). As Gemin2 was hypothesized to be a potential phosphorylation target (Husedzinovic et al., 2014), another aim of this thesis was to identify the specific kinase regulating Gemin2 activity *in vivo* and to answer the question how this influences the UsnRNP biogenesis pathway.

7 Publications

Chapter 7.1

NF90/NFAR (nuclear factors associated with dsRNA) – a new methylation substrate of the PRMT5-WD45-RioK1 complex

Jan Cox, **Lea Marie Esser**, Maximilian Jüdt, Katharina Schmitz, Kaja Reiffert, Matthias Grimmler, Björn Stork, Sebastian Wesselborg and Christoph Peter

Biological Chemistry (IF:3.7), ***August 2022****. 403: 907-15.*

DOI: 10.1515/hsz-2022-0136

Chapter 7.2

An essential role of the autophagy activating kinase ULK1 in snRNP biogenesis

Katharina Schmitz*, Jan Cox*, **Lea Marie Esser***, Martin Voss, Katja Sander, Antje Löffler, Frank Hillebrand, Steffen Erkelenz, Heiner Schaal, Thilo Kähne, Stefan Klinker, Tao Zhang, Luitgard Nagel-Steger, Dieter Willbold, Sabine Seggewiß, David Schlütermann, Björn Stork, Matthias Grimmler, Sebastian Wesselborg and Christoph Peter

*These authors contributed equally to the work

Nucleic Acids Research (IF:19.16), ***June 2021****. 49: 6437-55.*

DOI: 10.1093/nar/gkab452

Chapter 7.3

Phosphorylation of pICln by the autophagy activating kinase ULK1 regulates snRNP biogenesis and splice activity of the cell

Lea Marie Esser, Katharina Schmitz, Frank Hillebrand, Steffen Erkelenz, Heiner Schaal, Björn Stork, Matthias Grimmler, Sebastian Wesselborg and Christoph Peter

Computational and Structural Biotechnology Journal (IF:6.0), ***March 2023****. 21: 2100-09.*

DOI: 10.1016/j.csbj.2023.03.015

Chapter 7.4

The Impact of p70S6 Kinase-Dependent Phosphorylation of Gemin2 in UsnRNP Biogenesis

Lea Marie Esser, Qiaoping Li, Maximilian Jüdt, Thilo Kähne, Björn Stork, Matthias Grimmler, SebastianWesselborg and Christoph Peter

International Journal of Molecular Sciences (IF: 5.6), **October 2023**. 24.

DOI: 10.3390/ijms242115552

The author contributed to other publications outside the focus of this dissertation:

Development of Macrocyclic PRMT5-Adaptor Protein Interaction Inhibitors

Adrian Krzyzanowski, **Lea Marie Esser**, Anthony Willaume, Renaud Prudent, Christoph Peter, Peter ‘t Hart and Herbert Waldmann

Journal of Medicinal Chemistry (IF: 7.3), **November 2022**. 65: 15300-11.

DOI: 10.1021/acs.jmedchem.2c01273

Comprehensive Comparison of the Capacity of Functionalized Sepharose, Magnetic Core, and Polystyrene Nanoparticles to Immuno-Precipitate Procalcitonin from Human Material for the Subsequent Quantification by LC-MS/MS

Thomas Masetto, Kai Matzenbach, Thomas Reuschel, Sebastian-Alexander Tölke, Klaus Schneider, **Lea Marie Esser**, Marco Reinhart, Laura Bindila, Christoph Peter and Matthias Grimmler

International Journal of Molecular Sciences (IF: 5.6), **June 2023**. 24.

DOI: 10.3390/ijms241310963

7.1 Chapter 1 - NF90/NFAR (nuclear factors associated with dsRNA) – a new methylation substrate of the PRMT5-WD45-RioK1 complex

Title:	**NF90/NFAR (nuclear factors associated with dsRNA) – a new methylation substrate of the PRMT5-WD45-RioK1 complex**
Authors:	Jan Cox, Lea Marie Esser, Maximilian Jüdt, Katharina Schmitz, Kaja Reiffert, Matthias Grimmler, Björn Stork, Sebastian Wesselborg and Christoph Peter
Published in:	*Biological Chemistry* Volume 31, Issue 10, 21 **August 2022**, Pages 907-915 DOI: 10.1515/hsz-2022-0136
Impact factor:	3.7
Proportional work on this manuscript:	10% Immunopurification studies Preparation of figure Contributing in writing the manuscript

NF90/NFAR (nuclear factors associated with dsRNA) – a new methylation substrate of the PRMT5-WD45-RioK1 complex

Jan Cox[1], Lea Marie Esser[1], Maximilian Jüdt[1], Katharina Schmitz[1], Kaja Reiffert[1], Matthias Grimmler[2,3], Björn Stork[1], Sebastian Wesselborg[1], Christoph Peter[1*]

[1]Institute of Molecular Medicine I, Medical Faculty and University Hospital Düsseldorf, Heinrich Heine University Düsseldorf, Düsseldorf, Germany; [2]Hochschule Fresenius gGmbH, University of Applied Sciences, Limburger Straße 2, 65510 Idstein, Germany; [3]DiaSys Diagnostic Systems GmbH, Alte Strasse 9, 65558 Holzheim, Germany

* To whom correspondence should be addressed. Tel: +49 (0) 211 81-12196; Email: christoph.peter@uni-duesseldorf.de

ABSTRACT

Protein-arginine methylation is a common posttranslational modification, crucial to various cellular processes, such as protein-protein interactions or binding to nucleic acids. The central enzyme of symmetric protein arginine methylation in mammals is the protein arginine methyltransferase 5 (PRMT5). While the methylation reaction itself is well understood, recruitment and differentiation among substrates remain less clear. One mechanism to regulate the diversity of PRMT5 substrate recognition is the mutual binding to the adaptor proteins pICln or RioK1.

Here, we describe the specific interaction of Nuclear Factor 90 (NF90) with the PRMT5-WD45-RioK1 complex. We show for the first time that NF90 is symmetrically dimethylated by PRMT5 within the RG-rich region in its C-terminus. Since upregulation of PRMT5 is a hallmark of many cancer cells, the characterization of its dimethylation and modulation by specific commercial inhibitors *in vivo* presented here may contribute to a better understanding of PRMT5 function and its role in cancer.

Keywords: NF90; PRMT5; protein-arginine methylation; RioK1

INTRODUCTION

Posttranslational modifications are an important mechanism to regulate the functions of cellular proteins. The methylation of nitrogen in the side chain of arginine is one of the most common modifications and plays an important role in a variety of cellular processes such as histone methylation, RNA splicing, transcription and translation regulation, nuclear export of proteins, and protein-protein interactions (Blanc et al., 2017, Murn et al., 2017). To date, more than 5,500 human proteins have been detected to be methylated, highlighting the central function of this modification (Murn et al., 2017). Three arginine methylation patterns are differentiated (Blanc et al., 2017). Methylation of one nitrogen leads to an N^G-monomethyl arginine (MMA). If both nitrogen atoms are methylated, symmetrical dimethylation (SDMA) and asymmetrical dimethylation (ADMA) are differentiated. In SDMA, both nitrogen atoms are individually methylated, resulting in an N^G, N'^G-dimethylarginine. In ADMA, one of the two nitrogen atoms is double methylated, resulting in an N^G, N^G-dimethylarginine. Responsible for this kind of dual modification is the family of protein arginine methyltransferases (PRMTs), which transfer the methyl group of S-adenosylmethionine (SAM) onto the guanidine group in the side chain of arginine (Bedford et al., 2009). The methyltransferase PRMT5 is the only methyltransferase that catalyzes symmetric dimethylation of arginines *in vivo*. Consequently, the loss of PRMT5 leads to a nearly complete loss of SDMA (Hadjikyriacou et al., 2015). PRMT5 together with the WD repeat-containing protein 45 (WD45) forms a hetero-octameric complex of ~450 kDa (Antonysamy et al., 2012). This structure represents the basic core complex and can be extended by the adapter proteins pICln or RioK1, which regulate the substrate specificity of PRMT5 (Guderian et al., 2011, Krzyzanowski et al., 2021, Mulvaney et al., 2021).

Here, we identified the nucleic acid-binding protein NF90 as a novel substrate of the PRMT5/WD45/RioK1 complex. Strikingly, NF90 has RG-rich sequences in the C-terminus, representing potential PRMT5-dependent methylation sites, but no methylation has yet been shown. In this work, we demonstrate that NF90 is recruited exclusively via the adapter protein RioK1 to the PRMT5-WD45 complex, where it is rapidly methylated in its C-terminal region at the RG-boxes. In immunopurification studies, we further show that both endogenous NF90 and overexpressed NF90 are fully methylated in cells.

RESULTS

NF90 interacts with the PRMT5/WD45/RioK1 complex

In previous work, NF90 was identified as a new potential interaction partner of the PRMT5/WD45/RioK1 complex by mass spectrometry (Guderian et al., 2011). In this follow-up study, we show that NF90 is indeed a binding partner and a new substrate of PRMT5 *in vitro* and *in vivo*. To investigate the complex composition and the recruitment of NF90, we generated cell lines, stably overexpressing PRMT5, WD45, pICln, and RioK1 as GFP fusion proteins. By immunoprecipitation studies, we observed co-immunoprecipitation of NF90 with GFP-PRMT5, GFP-WD45, and GFP-RioK1, whereas we could not precipitate NF90 with GFP-pICln (Fig. 1A). Data by Guderian et al showed, that the substrate specificity and recruitment of new substrates of PRMT5 are controlled by its adaptor proteins RioK1 or pICln (Guderian et al., 2011). NF90, predominantly purified by GFP-RioK1 but not by pICln, supports this model of regulating the mutual substrate specificity of PRMT5. Further pulldown experiments, utilizing heterologous expressed GST fusion proteins from *E. coli*, confirmed these results: endogenous NF90 from HEK293 lysates bound to GST-RioK1 and GST-PRMT5 but not to GST-pICln (Fig. 1B).

Figure 1

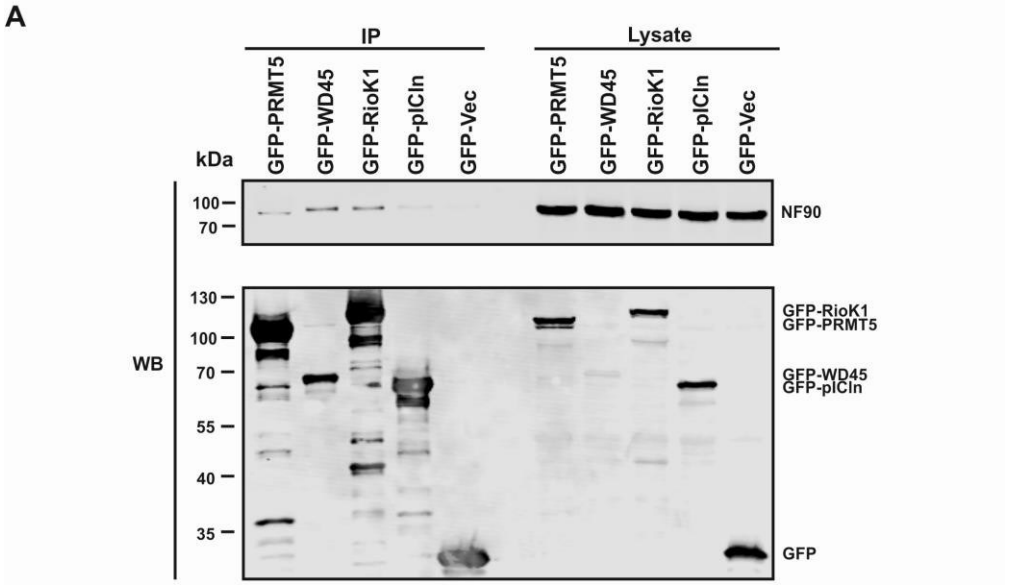

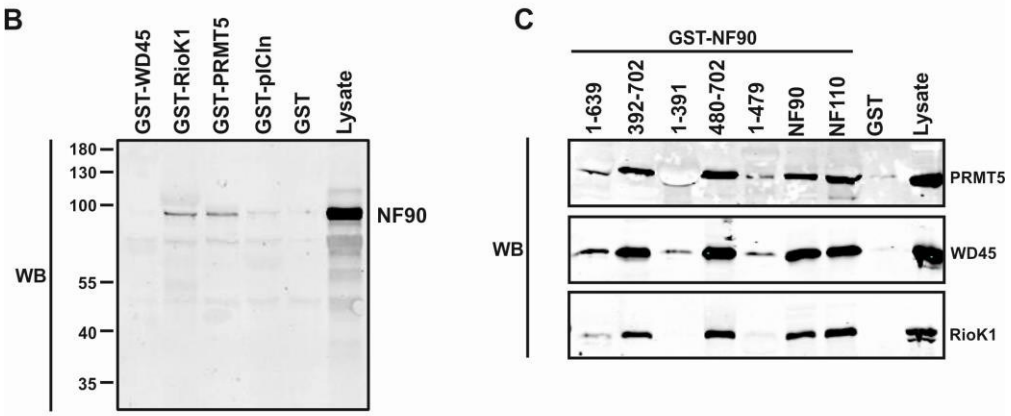

D

Dissociation constant (K_D)	RioK1	WD45	NF90	NF90+WD45	NF90+WD45+RioK1
GST-PRMT5	100 nM ±29 nM	622 nM ±251 nM	57 nM ±18 nM	68 nM ±22 nM	84 nM ±25 nM

Figure 1: NF90 interacts with the PRMT5/WD45/RioK1 complex. (A) Immunoprecipitation from GFP-PRMT5, -WD45, -Riok1, -pICln, and GFP overexpressing cells. Protein expression was induced with 0.1 µg/ml doxycycline for 24 h and as input 25 µg of total protein was loaded. After cell lysis, GFP-IP was performed and analyzed by Tris/Glycine-SDS-PAGE and western blotting, using antibodies against GFP and NF90. NF90 was co-immunoprecipitated with GFP-PRMT5, GFP-WD45 and GFP-RioK1. **(B)** Pulldown assays with recombinant GST-PRMT5, -WD45, -pICln, -RioK1, and GST purified from *E. coli* were executed in HEK293 lysate overnight at 4 °C. Co-precipitation of NF90 was analyzed using NF90 antibody and was detectable for GST-RioK1 and GST-PRMT5. **(C)** Pulldown assay as described above with different truncated forms of GST-NF90 purified from *E. coli*. Detection of co-precipitated proteins was performed with RioK1, WD45, and PRMT5 antibodies. Only the C-terminus of NF90 interacts with RioK1, WD45, and PRMT5. **(D)** Interaction studies using microscale thermophoresis measurements (MST). GST-PRMT5 was labeled with AlexaFluor488 fluorescent dye and measured against the interaction partners RioK1, WD45, and NF90. GST-PRMT5 showed a high affinity to its substrate NF90 with 57 nM. WB: western blotting.

Interaction with the PRMT5/WD45/RioK1 complex occurs via the C-terminus of NF90

NF90 is a multi-domain protein consisting of two double-stranded RNA-binding motifs (DRBM), a domain associated with zinc fingers (DZF), a bipartite nuclear localization signal (NLS), and an RG-motif (see also Figure 2 C). Due to the multi-domain structure of NF90, we generated truncated forms of NF90 (Fig. 2C) to characterize the interaction of NF90 with the proteins of the PRMT5/WD45/RioK1 complex in more detail (Fig. 1C). To this end truncations of NF90 were generated by dividing the two DRBMs (NF90 aa1-479 and NF90 aa480-702) and also dividing between the DZF domain and both DRBMs (NF90 aa1-391 and NF90 aa392-702) (Fig. 2C). Another truncated form represents NF90 without the RG-motif in the C-terminal region (NF90 aa1-639) (Fig. 2C). Interaction studies based on these forms of NF90 revealed an interaction of the PRMT5/WD45/RioK1 complex with the C-terminal region of NF90 spanning from amino acid 392 to 702 (Fig. 1C). Interestingly, the truncated form aa1-639, which represents almost the entire protein except for the RG-motif, showed only weak interaction. This indicates that the interaction predominantly occurs in the RG-rich region at the C-terminus of NF90 (Fig. 1C and Fig. 2C). To determine the affinities among the components of the PRMT5 complex and with the substrate protein NF90, microscale thermophoresis experiments were performed. For this purpose, GST-PRMT5 was labeled with Alexa flour 488 fluorescent dye and first measured against the known interaction partners of the complex, RioK1 and WD45. PRMT5 showed a strong affinity for RioK1 with a K_D of 100 nM and still a strong attachment to WD45 with a K_D of 622 nM (Fig. 1D, SD Fig. 1). In contrast, the affinity of the substrate protein NF90 towards the methyltransferase PRMT5 was determined with a high affinity of 57 nM (Fig. 1D, SD Fig. 1). Only marginal changes of affinity could be observed if WD45 was added or WD45 and RioK1 in combination. The data so far lead to the assumption that NF90 is a strong binding partner of PRMT5 *in vitro* and that substrate binding directly occurs to PRMT5 by the RG-rich stretch of NF90.

NF90 is a new substrate of PRMT5

Based on this strong *in vitro* interaction, we performed radioactive *in vitro* methylation assays with recombinant NF90 and active PRMT5 to test whether NF90 is methylated by PRMT5. Indeed, the radioactive methyl group from [3H]-SAM was transferred to GST-NF90 (Fig. 2A). Treatment with the PRMT5-specific inhibitor EPZ015666 did not result in

radioactive incorporation (Chan-Penebre et al., 2015). Both experiments prove that NF90 is symmetrically methylated by PRMT5 *in vitro* (Fig. 2A).

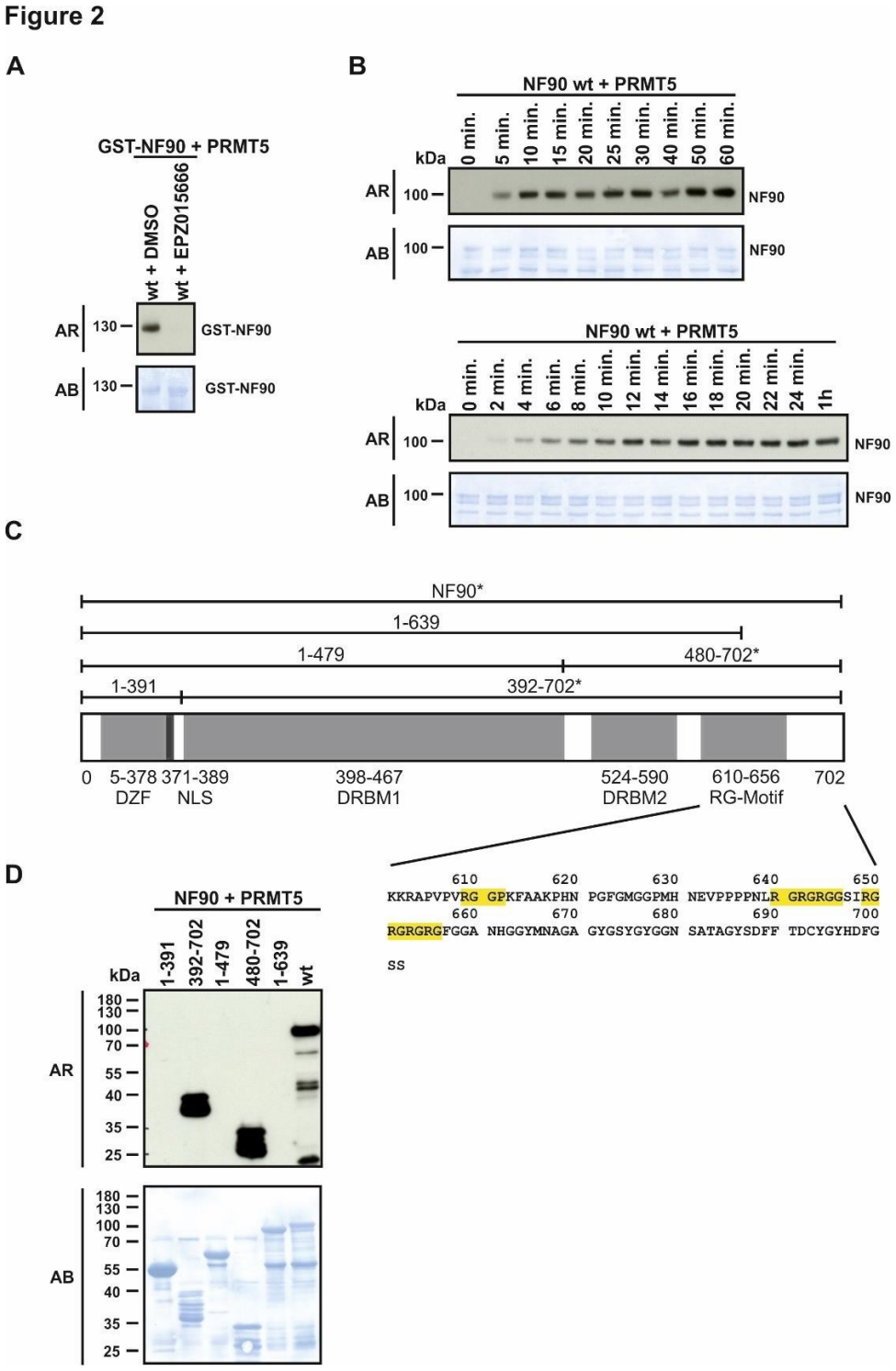

Figure 2: The C-terminus of NF90 is methylated by PRMT5. (A) Radioactive *in vitro* methylation assay using GST-NF90 purified from *E. coli* and 200 ng recombinant PRMT5 and 1 µCi [3-H]-SAM was performed with and without 1 mM PRMT5 inhibitor EPZ015666. Samples were separated by Tris/Glycine-SDS-PAGE and radioactive incorporation was analyzed by western blotting and autoradiography. The addition of 1 mM PRMT5 inhibitor EPZ015666 inhibits the methylation of NF90 by PRMT5. **(B)** Investigation of the time-

dependent methylation of NF90. 880 ng NF90 purified from *E. coli* without GST-tag was incubated with 200 ng recombinant PRMT5 and 1 µCi [3-H]-SAM. The reaction was terminated by addition of SDS sample buffer and the samples were analyzed as described in (A). **(C)** Schematic overview of the domains and truncated forms of NF90 used in this work. The asterisks indicate methylatable forms and the distinctive RG- boxes have been highlighted in yellow. **(D)** Methylation assay of truncated NF90 forms purified from *E. coli* as described in (A). NF90 is methylated in the C-terminus between amino acids 640 and 702 by PRMT5. AR: autoradiography, AB: amido black staining.

To assess the kinetics of NF90 methylation, we performed a titration of the methylation reaction. As evident in Fig. 2B, a saturation of NF90 methylation did occur already within 10 minutes. To gain a more detailed view on the methylation dynamics of NF90, 2 min steps, up to 24 minutes were performed. Again, no increase in methylation could be observed after 12 min (Fig. 2B). The NF90 protein contains several putative methylation sites (arginine-glycine-repeats, RG-Box) in the C-terminus between the amino acids 609 to 656. To further determine the location of the methylation sites within the NF90 protein we analyzed truncated forms (Fig. 2D) by methylation assays. We identified eight arginine residues as potential targets in this region (Fig. 2C, highlighted in yellow), in particular, we observed methylation of the C-terminal forms NF90 aa392-702 and NF90 aa480-702 and the wild-type NF90 protein (Fig. 2D). In contrast, no methylation was observed for the N-terminal forms NF90 aa1-391, NF90 aa1-479, and NF90-aa1-639 (Fig. 2D). These results clearly show methylation of NF90 by PRMT5 exclusively is located within the C-terminal RG-rich sequence ranging from amino acid 640 to 702.

NF90 is methylated *in vivo* by PRMT5 in an RG-rich region in the C-terminus

Based on these data, we focused on the RG-motif in the C-terminal region of NF90 in more detail. This RG-rich region contains seven glycine-arginine residues that potentially may serve as methylatable residues to PRMT5 (Fig. 2C). All arginines in the RG-rich region of NF90 at positions 640, 642, 644, 649, 651, 653, and 655 were exchanged to the structurally similar but non-methylatable lysines. The obtained methylation deficient mutant (NF90-7x R-to-K) and the NF90 wildtype protein were expressed in *E. coli* and the purified recombinant proteins were subsequently analyzed by methylation assays (Fig. 3A). In contrast to wild-type NF90, no methylation could be detected in the methylation-deficient mutant, indicating that the methylation sites are located in the region of amino acids 640 to 655 in the C-terminus of NF90.

Figure 3

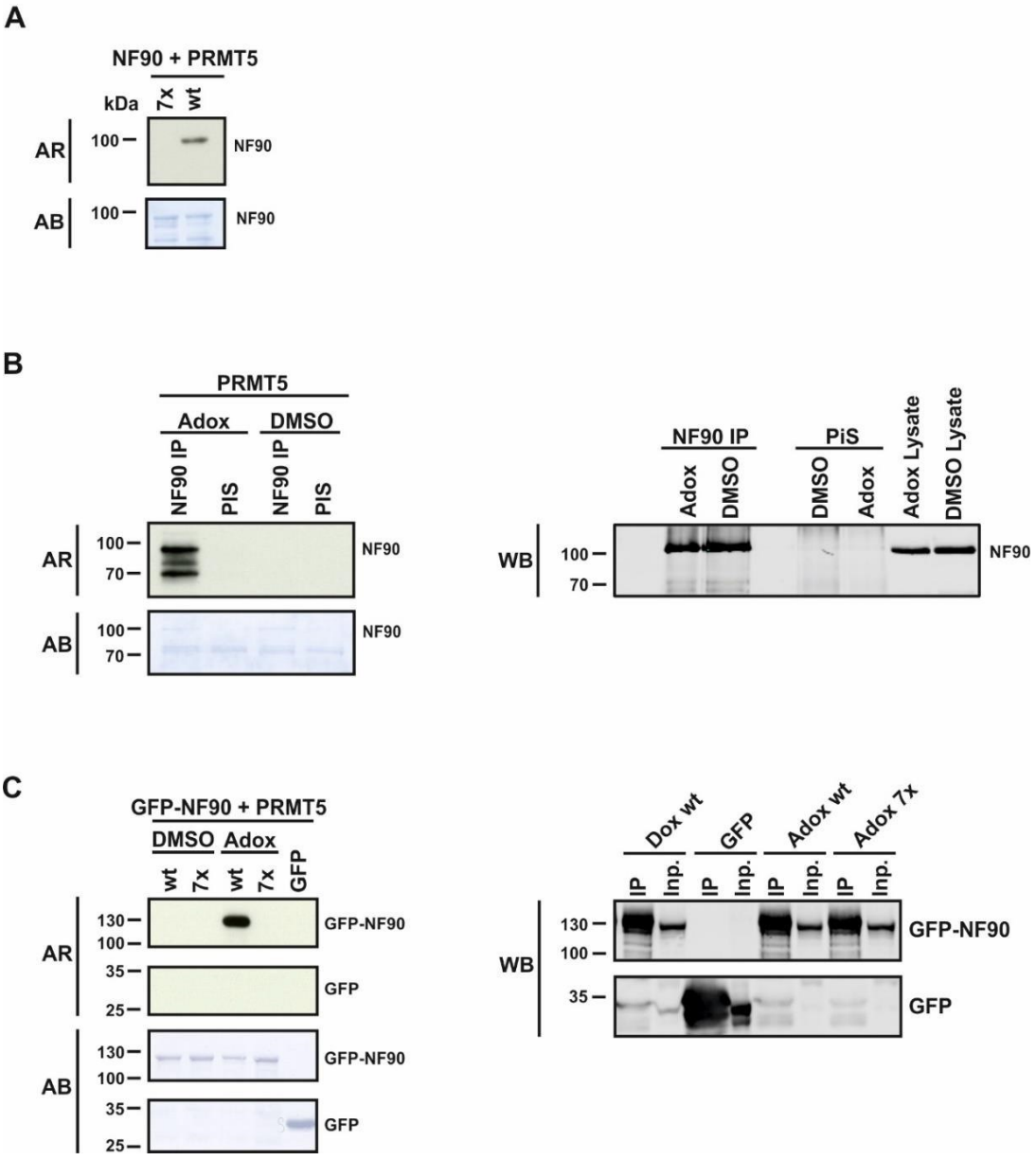

Figure 3: NF90 arginine mutants and *in vivo* inhibitor studies. (A) Recombinant NF90 wt, and NF90 7x from *E. coli* was incubated with 200 ng recombinant PRMT5 and 1 µCi [3-H]-SAM. Samples were separated by Tris/Glycine-SDS-PAGE and radioactive incorporation was analyzed by western blotting and autoradiography. In the NF90 7x mutant, all seven potential arginine methylation sites are mutated to lysines (see Fig. 2C). PRMT5 was not able to methylate the sevenfold arginine to lysine mutant. **(B)** HEK293 cells were treated with 20 µM of the S-adenosylmethionine-dependent methyltransferase inhibitor adenosine dialdehyde (Adox). 500 µg lysate with 1 µg NF90 antibody or as control Preimmunserum (PIS) and Protein G Sepharose was incubated for 1.5 h and immunopurified NF90 was subjected to a methylation assay as described in (A). Only NF90 from Adox-treated cells could be methylated *in vitro*. **(C)** Flp-In T-REx 293 cells stably expressing GFP-NF90 wt and GFP-NF90 7x were stimulated with 0.1 µg/ml doxycycline for 24 h and treated with Adox as described in (B). After GFP-IP, a methylation assay was performed. No methylation of purified GFP-NF90 occurred in control cells (DMSO), whereas NF90 immunopurified from cells treated with Adox could be methylated *in vitro*. The sevenfold lysine mutant GFP-NF90 7x showed no methylation in all conditions. AR: autoradiography, AB: amido black staining, WB: western blotting.

Next, we investigated the intracellular methylation status of endogenous NF90 from HEK cells. For this purpose, we immunoprecipitated endogenous NF90 from HEK cells and used it as a substrate for an *in vitro* methylation assay. However, endogenous NF90 showed no incorporation of radioactive ^{3}H (Fig. 3B), leading to the assumption, that NF90 is already completely methylated *in vivo*. To substantiate this hypothesis, HEK293 cells were treated with 20 µM adenosine dialdehyde (Adox) to disable endogenous methylation, before the respective cell extract was subjected to immunoprecipitation of NF90. Adox is a well-known broad inhibitor of methyltransferases (Chen et al., 2004). In consequence, newly synthesized proteins remain hypomethylated upon Adox treatment (Chen et al., 2004) and therefore are receptive for *in vitro* methylation if purified from the respective extracts. By using immunoprecipitated endogenous NF90 with and without treatment by Adox, we clearly could show methylation by Adox treated NF90, but not by DMSO/control-treated NF90 upon incubation with recombinant PRMT5 (Fig. 3B). To this point, treatment of HEK293 cells with Adox does not alter NF90 cellular expression nor efficiency of immunoprecipitation (Fig. 3B) but does alter endogenous methylation status of NF90. Upon the observed rate of methylation of Adox pretreated NF90 substrate protein, endogenous NF90 probably is fully methylated in the cell under normal conditions. To prove this finding, we repeated the experiments with HEK293 Flp-In T-REx cell lines inducibly overexpressing NF90 wildtype as a GFP-fusion protein (GFP-NF90 wt) or the methylation-deficient GFP-NF90 7x mutant (Fig. 3C). First, the intracellular protein methylation was blocked by Adox treatment, and subsequently, NF90 protein expression was induced. GFP-immunoprecipitations allowed for exclusive precipitation and measurement of newly synthesized NF90, excluding endogenous, untagged NF90. Again, no methylation of purified GFP-NF90 occurred in control cells (DMSO), whereas NF90 from Adox treated cells could be methylated *in vitro* (Fig. 3C). Taken together, these experiments indicate that endogenous as well as overexpressed NF90 are completely methylated in the normal cellular setting.

DISCUSSION

Although the RG-motif of NF90 has been postulated as a potential methylation site by PRMT5 (Richard et al., 2005), no methylation has yet been detected. In this work, we

describe for the first time NF90 as a new interaction partner of the PRMT5/WD45/RioK1 complex and as a new symmetrically methylated substrate of the methyltransferase PRMT5.

Due to the ability of RioK1 to bind numerous proteins containing RG-motifs, it increases the substrate diversity of PRMT5 and recruits new substrates to the methyltransferase (Guderian et al., 2011). Here, we observed NF90 co-immunoprecipitation within the PRMT5/RioK1 complex but not with pICln (Fig. 1A, Fig. 1B). These data confirm that NF90 recruitment occurs only via the RioK1-containing complex and not via pICln. For this, NF90 is a novel interaction partner of the PRMT5/WD45/RioK1 complex. Moreover, the C- terminal region of NF90 (aa 640 - 702) was identified as the interaction surface with this complex (Fig. 1C). The determined dissociation constant (K_D) of 100 ± 29 nM within the protein complex for RioK1 and PRMT5 (Fig. 1D) matches to 34 nM, reported in previous studies (Krzyzanowski et al., 2021). A dissociation constant of 57 ± 18 nM was observed for PRMT5 and NF90, indicating a high affinity of PRMT5 for NF90. The addition of RioK1 did not significantly alter the dissociation constants, nor did it affect NF90 methylation, as recombinant NF90 is methylated just as rapidly in the presence or absence of RioK1 under *in vitro* conditions (Fig. 2B and Supplemental Data Figure 2A). Also, *in vitro* methylation experiments with the SmB protein show that under these conditions methylation can occur independently of pICln (Supplemental Data Figure 2B). This is in line with the results of previous studies, which described a direct enzyme-substrate interaction for PRMT5 to its substrates histones H2A, H3, and the myelin basic protein (Pollack et al., 1999, Pal et al., 2004).

However, for recruiting NF90 to the PRMT5 complex in the cell, the adapter protein RioK1 may play an essential role like pICln for the Sm proteins. The specific role of PRMT5 adapter proteins (e.g. pICln and RioK1) to regulate substrate specificity of methyltransferases is a very important and exciting question. Recent approaches to answer this question aim to develop novel inhibitors for the adapter proteins and thus identify adapter protein-dependent as well as independent substrates and thus also control the activity of PRMT5 concerning targeted substrates (Krzyzanowski et al., 2021, McKinney et al., 2021, Mulvaney et al., 2021). As both proteins, NF90 and PRMT5, attribute a crucial function in ribosome biosynthesis a cooperative function of both proteins at the ribosome is conceivable (Widmann et al., 2012, Wandrey et al., 2015). To gain complete functionality in ribosome biosynthesis NF90 may require full methylation. To this end, RioK1 may recruit PRMT5 towards the ribosome for this purpose. RioK1 in this scenario attributes a comparable role

as pICln does in recruiting Sm proteins during snRNP biogenesis (Chari et al., 2008, Schmitz et al., 2021).

Investigation of the protein sequence of NF90 showed that there is a glycine-arginine-rich (GAR) motif in the C-terminal region. GAR motifs are described as a consensus sequence of protein methylation (Lapeyre et al., 1986) and GR repeats that have glycine at position -1 are predominantly methylated by PRMT5 (Musiani et al., 2019). In the C-terminal region of NF90, the sequence "R^{640}GRGRGGSIRGRGRGRGF^{657}" contains a triple RG repetition followed by a quadruple RG repetition sequence, flanked by glycines (Fig. 2C).

So far, the methylation status of NF90 *in vivo* was unclear. We observed that immunoprecipitated NF90 could not be methylated in an *in vitro* methylation assay by recombinant PRMT5 (Fig. 3B). As evident by Adox treatment (Fig. 3B), endogenous NF90 is predominantly present as a hypermethylated protein since subsequent efficient methylation of immunoprecipitated NF90 by PRMT5 was possible. The treatment of cells by Adox results in a loss of methyl groups in newly formed proteins and free methylation sites, capably to be methylated in a subsequent *in vitro* methylation assay of respective precipitated substrate proteins. Also beforehand *in vitro* investigations based on the NF90 7x mutant (Fig. 3A; C) confirmed the exclusive methylation of the seven arginine residues in the C-terminus of NF90 *in vivo* hence by Adox treatment, no methylation of this mutant could be observed. This observation also clearly excludes other PRMT5-specific arginine methylation sites of NF90, for example at positions 90, 247, 537, or 609. Strikingly, even when strongly overexpressed in HEK293 cells, GFP-NF90 wt is completely methylated (Fig. 3C). This finding as well as rapid methylation of NF90 (Fig. 2B) implies the stringency of the cell's methylation system and supports a general necessity for complete methylation of NF90 *in vivo* (Fig. 3C). In this work, we prove that NF90 is fully methylated in the cell under normal conditions and does not harbor any free methyl acceptor sites. These results are well supported by earlier work, which also described almost complete methylation of proteins, such as heterogeneous nuclear ribonucleoprotein U (hnRNP U) (Herrmann et al., 2004), nucleolin, or fibrillarin (Lischwe et al., 1982, Lischwe et al., 1985).

Currently, it is assumed that symmetric methylation of NF90 is irreversible and persists throughout the lifetime of the protein. Little is known about demethylases but the Jumonji domain-containing 6 protein (JMJD6) was described as arginine demethylase (Chang et al., 2007). However, the results could not be reproduced in other studies (Webby et al., 2009, Han et al., 2012) whereas arginine demethylation activity was observed in recent studies

(Liu et al., 2013, Poulard et al., 2014, Tsai et al., 2017). Therefore, arginine demethylation by JMJD6 remains highly controversial (Bottger et al., 2015). This raises the question of the biological function of irreversible methylation of NF90. Since many proteins have more than one methylation site but demethylation reactions have rarely been observed and are critically viewed, a regulatory function through turnover as in phosphorylation is unlikely (Simms et al., 1987, Herrmann et al., 2004). However, the production of SAM certainly consumes ATP and the cell does not make this effort unnecessarily in NF90.

It will be interesting in further studies to investigate the impact of the methylation of NF90 discovered here in this work in terms of functionality, as NF90 is a protein involved in a variety of signaling cascades.

MATERIAL AND METHODS

Cloning and Plasmids

NF90 (CCDS12247.1) cDNA was generated from HEK293 cells with cDNA Transcription Kit (4368814, Applied Biosystems) and cloned into pGEX-6P-1 (28954648, Cytiva) and pcDNA5-FRT-TO (V601020, Invitrogen) using Gibson assembly (NEB, E2621S) or restriction enzyme cloning. Phusion Polymerase (M0530, NEB) and the following primers (Sigma-Aldrich) were used:

pGEX-6P-1-NF90 wt, 5’-GTGAATTCATGCGTCCAATGCGAATT-3’
and 5’-GTGCGGCCGCCTAGGAAGACCCAAAATCATGAT-3’;
pGEX-6P-1-NF90AA1-639,
5’-CACAAGAGGAGCTGGAGGCAGTCCAGAACATGGTG-3’
and 5’- TCCAGCTCCTCTTGTGTTGGATAAACGGAAGAATG-3’
and 5’-AACCTTTAGGCGGCCGCATCGTGACTGACTG-3’
and 5’-CGGCCGCCTAAAGGTTGGGGGGTGGGGGCAC-3’;
pGEX-6P-1-NF90 AA1-479, 5’-GTGAATTCATGCGTCCAATGCGAATT-3’
and 5’-GTGCGGCCGCCCCCTTGCTCGAGTCC-3’;
pGEX-6P-1-NF90 AA480-702, 5’-GTGAATTCGAGGACTCGGCTGAGGAG-3’
and 5’-GTGCGGCCGCCTAGGAAGACCCAAAATCATGAT-3’;
pGEX-6P-1-NF90 AA1-391, 5’-GTGAATTCATGCGTCCAATGCGAATT-3’
and 5’-GTGCGGCCGCCTACTGAATCTTCTTCTTCTTTTTGCTG-3’;
pGEX-6P-1-NF90 AA392-702, 5’-GTGAATTCAAGAAAGAGGAGAAGGCAGAG-3’

and 5’-GTGCGGCCGCCTAGGAAGACCCAAAATCATGAT-3’;
pGEX-6P-1-NF90 AA609 R->K, 5’-AGCCCCAGTACCCGTCAAAGGGGGACC-3’
and 5’-GGTCCCCCTTTGACGGGTACTGGGGCT-3’;
pGEX-6P-1-NF90 7x AA640, 642, 644, 649, 651, 653, 655 R->K (GeneArt Gene Synthesis, Invitrogen);
pGEX-6P-1-NF90 AA640 R->K,
5’-CCCCAACCTTAAAGGGCGGGGAAGAGGCGGGAG-3’
and 5’-CCCCGCCCTTTAAGGTTGGGGGGTGGGGGCAC-3’;
pGEX-6P-1-NF90 AA642 R->K,
5’-TCGAGGGAAGGGAAGAGGCGGGAGCATCCGGGGAC-3’
and 5’-CCGCCTCTTCCCTTCCCTCGAAGGTTGGGGGGTGG-3’;
pGEX-6P-1-NF90 AA644 R->K,
5’-TCGAGGGCGGGGAAAAGGCGGGAGCATCCGGGGAC-3’
and 5’-CCGCCTTTTCCCCGCCCTCGAAGGTTGGGGGGTG-3’;
pGEX-6P-1-NF90 AA649 R->K,
5’-AGGCGGGAGCATCAAGGGACGAGGGCGCGGGCGAG-3’
and 5’-CGTCCCTTGATGCTCCCGCCTCTTCCCCGCCCTC-3’;
pGEX-6P-1-NF90 AA651 R->K,
5’-ATCCGGGGAAAAGGGCGCGGGCGAGGATTTGG-3’
and 5’-CCCGCGCCCTTTTCCCCGGATGCTCCCGCCTC-3’;
pGEX-6P-1-NF90 AA653 R->K,
5’-ACGAGGGAAGGGGCGAGGATTTGGTGGCGCCAAC-3’
and 5’-AATCCTCGCCCCTTCCCTCGTCCCCGGATGCTCC-3’;
pGEX-6P-1-NF90 AA655 R->K,
5’-GGGCGCGGGAAAGGATTTGGTGGCGCCAACCATGG-3’
and 5’-ACCAAATCCTTTCCCGCGCCCTCGTCCCCGGATG-3’.

Plasmids:

pcDNA5-FRT-TO-NF90 wt, pcDNA5-FRT-TO-NF90 AA640, 642, 644, 649, 651, 653, 655 R->K (7x), 5’-ATGCGTCCAATGCGAATTTTTGTGAATGATGAC-3’
and 5’-TCGCATTGGACGCATGGATCCGAGCTCGGTACCAAGC-3’
and 5’-TTTGGGTCTTCCTAGGCGGCCGCTCGAGTCTAGAGG-3’
and 5’-CTAGGAAGACCCAAAATCATGATAGCCGTAG-3’;

pcDNA5-FRT-TO-eGFP-NF90 wt and pcDNA5-FRT-TO-eGFP-NF90 AA640, 642, 644, 649, 651, 653, 655 R->K (7x),
5'-ATCCATGCGTCCAATGCGAATTTTTGTGAATGATGAC-3'
and 5'-CATTGGACGCATGGATCCGAGTCCGGACTTGTACAG-3'
and 5'-TTTGGGTCTTCCTAGGCGGCCGCTCGAGTCTAGAGG-3'
and 5'-CTAGGAAGACCCAAAATCATGATAGCCGTAG-3';
pcDNA5-FRT-TO-eGFP-PRMT5, 5'-GGATCCATGGCGGCGATGGCGGT-3'
and 5'-GCGGCCGCCTAGAGGCCAATGGTATAT-3';
pcDNA5-FRT-TO-eGFP-RioK1, 5'-GGATCCATGGACTACCGGCGGCTTC-3'
and 5'-GCGGCCGCCTATTTGCCTTTTTTCGTCT-3';
pcDNA5-FRT-TO-eGFP-pICln, 5'-GGATCCATGAGCTTCCTCAAAAGTTTCCC-3'
and 5'-GTCTCGAGTCAGTGATCAACATCTGCATCC-3';
pcDNA5-FRT-TO-eGFP-WD45, 5'-GGATCCATGCGGAAGGAAACCCCAC-3'
and 5'-GCGGCCGCCTACTCAGTAACACTTGCAGGTCC-3'.
Generation of pGEX-6P-1-PRMT5, pGEX-6P-1-WD45, pGEX-6P-1-RioK1 (Guderian et al., 2011), and pGEX-6P-1-pICln (Schmitz et al., 2021), and pcDNA5-FRT-TO-eGFP (Loffler et al., 2011) plasmids have been described previously.

Protein expression and purification

E. coli BL21 was transformed and grown overnight at 37 °C on selection plates (100 µg/mL ampicillin). 150 ml LB medium was inoculated and grown overnight at 37 °C. 1 L SB media (35 g/L Tryptone, 20 g/L Yeast extract, 5 g/L NaCl) culture was grown to an OD_{600} of 0.8. Protein expression was induced with 1 mM IPTG at 18 °C overnight. The bacteria were lysed in 300 mM NaCl, 50 mM Tris pH 7.5, 5 mM EDTA, 5 mM EGTA, 0.01% (v/v) Igepal, protease inhibitors (cOmplete Protease Inhibitor, 4693132001, Roche) and 50 mg/ml lysozyme. After sonication, lysates were centrifuged for 30 min at 10,000 g, incubated for 1.5 h at 4 °C with Glutathione-Sepharose 4B (Cytiva, 17075601), and washed three times with lysis buffer. The GST-tag was cleaved with PreScission Protease (Cytiva, 27084301) overnight at 4 °C.

The active PRMT5/WD45 complex was purchased from Active Motif (31521). GFP-tagged proteins were expressed in HEK293 cells and purified by GFP-Trap Agarose (gta-20, Chromotek).

Antibodies

Primary antibodies: α-NF90 (A303-651A, Bethyl), α-PRMT5 (2252, CST), α-WD45 (2823, CST), α-RioK1 (NBP1-30103, Novus Biologicals), α-pICln (sc-393525, Santa Cruz), α-GFP (3H9, Chromotek). Secondary antibodies using LI-COR Odyssey Imaging System: IRDye 680LT goat α-rabbit, IRDye 680LT goat α-mouse, IRDye 800CW donkey α-rabbit, IRDye 800CW donkey α-mouse, IRDye 800CW goat α-rat (LI-COR Biosciences).

Cell culture and cell lines

HEK293 cells were cultured in high glucose DMEM (41965039, Gibco) with 10% (v/v) tetracycline-free FCS (10270106, Gibco) and 100 units/mL of Penicillin and 100 µg/mL Streptomycin (15140122, Gibco) in a 5% CO_2 atmosphere at 37 °C. Cells were washed with PBS (14190169, Gibco) and treated with Trypsin-EDTA (25300054, Gibco).

Inducible Flp-In T-REx 293 cell lines (R78007, Invitrogen), stably expressing NF90 wt, NF90 7x, GFP-NF90 wt, GFP-NF90 7x, GFP-PRMT5, GFP-WD45, GFP-pICln, and GFP-RioK1 were generated by co-transfecting 4.5 µg pOG44 and 0.5 µg pcDNA5 plasmids with FuGENE HD (E2311, Promega). Cells were selected with 200 µg/ml Hygromycin B Gold (ant-hg-1, Invivogen) and 5 µg/ml Blasticidin (ant-bl-05, Invivogen) for three weeks. GFP-pICln cells were generated as described in (Schmitz et al., 2021). Protein expression was induced with 0.1 µg/ml Doxycycline and cells were harvested after 24 h. For methylation inhibition 20 µM of the S-adenosylhomocysteine hydrolase inhibitor Adenosine Dialdehyde (Adox) (Cay15644, Cayman Chemical) was used.

Immunoprecipitation and immunoblotting

Cell lysates were generated using lysis buffer with 50 mM Tris pH 7.5, 150 mM NaCl, 1 mM EDTA, 1 mM EGTA, 1% Triton X-100 and 1x Protease inhibitor (P2714, Sigma-Aldrich). Protein concentration was measured by Bradford assay (5000006, Bio-Rad). 500 µg cell lysate was used for immunoprecipitation together with 1 µg of antibodies and Protein G Sepharose (17061801, Cytiva) at 4 °C for 1.5 h with rotation. As input 25 µg of total protein was loaded. GFP-tagged proteins were purified by GFP-Trap Agarose (gta-20, Chromotek) at 4 °C for 1.5 h with rotation. Samples were washed three times with washing buffer (lysis buffer without Triton X-100 and protease inhibitors) and eluted in sample buffer (375 mM

Tris pH 7.5, 25.8% (w/v) Glycerol, 12.3% (w/v) SDS, 0.06% (w/v) Bromophenol blue, 6% (v/v) β-Mercaptoethanol, pH 6.8). Subsequently, samples were separated by Tris/Glycine-SDS-PAGE and transferred to a PVDF membrane (Immobilon-FL, Merck Millipore). The immunoblot detection was carried out using the indicated primary and fluorescent-labeled secondary antibodies and the LI-COR Odyssey Imaging System.

In vitro methylation

Target proteins were incubated with 150 ng of Flag-PRMT5/WD45 from Sf9 cells (Active Motif, 31521) and 1 µCi Adenosyl-L-Methionine, S-[methyl-3H] (Hartmann-Analytic, ART0288) in 50 mM Tris pH 7.5, 1 mM EGTA and 1 mM EDTA for 1.5 h at 37 °C. The reaction was stopped by adding sample buffer. Samples were separated by Tris/Glycine-SDS-PAGE and, after blotting and amido black staining (40% Methanol (v/v), 10% Acetic acid (v/v), 0.1% Amido black 10B (w/v)), analyzed by autoradiography with Amersham Hyperfilm MP (28906844, Cytiva) and BioMax TranScreen LE (1622034, Carestream).

Microscale thermophoresis

A Monolith NT 115 (NanoTemper Technologies) was used for microscale thermophoresis binding studies. Purified recombinant proteins GST-PRMT5, RioK1 or NF90 were labeled with AlexaFluor488-NHS (A20000, Invitrogen) in 50 mM HEPES, 300 mM NaCl, pH 7.5. 50 nM of labeled proteins and 4-14 µM of unlabeled proteins were used for interaction studies and measured as triplicates with 50% MST power and 50% LED power in premium or hydrophobic capillaries.

ACKNOWLEDGEMENTS

We also thank our colleagues David Schlütermann, Niklas Berleth, and Fabian Stuhldreier for their comments on the manuscript. This work was supported by grants from Deutsche Forschungsgemeinschaft [RTG 2158 (to B.S. and S.W.), RTG 2578 (to B.S. and S.W.), and STO 864/4-3, STO 864/5-1, STO 864/6-1 (to B.S.)] and the Düsseldorf School of Oncology (funded by the Comprehensive Cancer Center Düsseldorf/Deutsche Krebshilfe and the Medical Faculty of the Heinrich Heine University Düsseldorf; to B.S. and S.W.).

REFERENCES

Antonysamy, S., Z. Bonday, R. M. Campbell, B. Doyle, Z. Druzina, T. Gheyi, B. Han, L. N. Jungheim, Y. Qian, C. Rauch, M. Russell, J. M. Sauder, S. R. Wasserman, K. Weichert, F. S. Willard, A. Zhang, and S. Emtage. 2012. '*Crystal structure of the human PRMT5:MEP50 complex*', ***Proc Natl Acad Sci U S A***, 109: 17960-5.

Bedford, M. T., and S. G. Clarke. 2009. '*Protein arginine methylation in mammals: who, what, and why*', ***Mol Cell***, 33: 1-13.

Blanc, R. S., and S. Richard. 2017. '*Arginine Methylation: The Coming of Age*', ***Mol Cell***, 65: 8-24.

Bottger, A., M. S. Islam, R. Chowdhury, C. J. Schofield, and A. Wolf. 2015. '*The oxygenase Jmjd6--a case study in conflicting assignments*', ***Biochem J***, 468: 191-202.

Chan-Penebre, E., K. G. Kuplast, C. R. Majer, P. A. Boriack-Sjodin, T. J. Wigle, L. D. Johnston, N. Rioux, M. J. Munchhof, L. Jin, S. L. Jacques, K. A. West, T. Lingaraj, K. Stickland, S. A. Ribich, A. Raimondi, M. P. Scott, N. J. Waters, R. M. Pollock, J. J. Smith, O. Barbash, M. Pappalardi, T. F. Ho, K. Nurse, K. P. Oza, K. T. Gallagher, R. Kruger, M. P. Moyer, R. A. Copeland, R. Chesworth, and K. W. Duncan. 2015. '*A selective inhibitor of PRMT5 with in vivo and in vitro potency in MCL models*', ***Nat Chem Biol***, 11: 432-7.

Chang, B., Y. Chen, Y. Zhao, and R. K. Bruick. 2007. '*JMJD6 is a histone arginine demethylase*', ***Science***, 318: 444-7.

Chari, A., M. M. Golas, M. Klingenhäger, N. Neuenkirchen, B. Sander, C. Englbrecht, A. Sickmann, H. Stark, and U. Fischer. 2008. '*An assembly chaperone collaborates with the SMN complex to generate spliceosomal SnRNPs*', ***Cell***, 135: 497-509.

Chen, D. H., K. T. Wu, C. J. Hung, M. Hsieh, and C. Li. 2004. '*Effects of adenosine dialdehyde treatment on in vitro and in vivo stable protein methylation in HeLa cells*', ***J Biochem***, 136: 371-6.

Guderian, G., C. Peter, J. Wiesner, A. Sickmann, K. Schulze-Osthoff, U. Fischer, and M. Grimmler. 2011. '*RioK1, a new interactor of protein arginine methyltransferase 5 (PRMT5), competes with pICln for binding and modulates PRMT5 complex composition and substrate specificity*', ***J Biol Chem***, 286: 1976-86.

Hadjikyriacou, A., Y. Yang, A. Espejo, M. T. Bedford, and S. G. Clarke. 2015. '*Unique Features of Human Protein Arginine Methyltransferase 9 (PRMT9) and Its Substrate RNA Splicing Factor SF3B2*', ***J Biol Chem***, 290: 16723-43.

Han, G., J. Li, Y. Wang, X. Li, H. Mao, Y. Liu, and C. D. Chen. 2012. '*The hydroxylation activity of Jmjd6 is required for its homo-oligomerization*', ***J Cell Biochem***, 113: 1663-70.

Herrmann, F., M. Bossert, A. Schwander, E. Akgün, and F. O. Fackelmayer. 2004. '*Arginine methylation of scaffold attachment factor A by heterogeneous nuclear ribonucleoprotein particle-associated PRMT1*', ***J Biol Chem***, 279: 48774-9.

Krzyzanowski, A., R. Gasper, H. Adihou, P. t Hart, and H. Waldmann. 2021. '*Biochemical Investigation of the Interaction of pICln, RioK1 and COPR5 with the PRMT5-MEP50 Complex*', ***Chembiochem***.

Lapeyre, B., F. Amalric, S. H. Ghaffari, S. V. Rao, T. S. Dumbar, and M. O. Olson. 1986. '*Protein and cDNA sequence of a glycine-rich, dimethylarginine-containing region*

located near the carboxyl-terminal end of nucleolin (C23 and 100 kDa)', ***J Biol Chem***, 261: 9167-73.

Lischwe, M. A., R. L. Ochs, R. Reddy, R. G. Cook, L. C. Yeoman, E. M. Tan, M. Reichlin, and H. Busch. 1985. '*Purification and partial characterization of a nucleolar scleroderma antigen (Mr = 34,000; pI, 8.5) rich in NG,NG-dimethylarginine*', ***J Biol Chem***, 260: 14304-10.

Lischwe, M. A., K. D. Roberts, L. C. Yeoman, and H. Busch. 1982. '*Nucleolar specific acidic phosphoprotein C23 is highly methylated*', ***J Biol Chem***, 257: 14600-2.

Liu, W., Q. Ma, K. Wong, W. Li, K. Ohgi, J. Zhang, A. Aggarwal, and M. G. Rosenfeld. 2013. '*Brd4 and JMJD6-associated anti-pause enhancers in regulation of transcriptional pause release*', ***Cell***, 155: 1581-95.

McKinney, D. C., B. J. McMillan, M. J. Ranaghan, J. A. Moroco, M. Brousseau, Z. Mullin-Bernstein, M. O'Keefe, P. McCarren, M. F. Mesleh, K. M. Mulvaney, F. Robinson, R. Singh, B. Bajrami, F. F. Wagner, R. Hilgraf, M. J. Drysdale, A. J. Campbell, A. Skepner, D. E. Timm, D. Porter, V. K. Kaushik, W. R. Sellers, and A. Ianari. 2021. '*Discovery of a First-in-Class Inhibitor of the PRMT5-Substrate Adaptor Interaction*', ***J Med Chem***, 64: 11148-68.

Mulvaney, K. M., C. Blomquist, N. Acharya, R. Li, M. J. Ranaghan, M. O'Keefe, D. J. Rodriguez, M. J. Young, D. Kesar, D. Pal, M. Stokes, A. J. Nelson, S. S. Jain, A. Yang, Z. Mullin-Bernstein, J. Columbus, F. K. Bozal, A. Skepner, D. Raymond, S. LaRussa, D. C. McKinney, Y. Freyzon, Y. Baidi, D. Porter, A. J. Aguirre, A. Ianari, B. McMillan, and W. R. Sellers. 2021. '*Molecular basis for substrate recruitment to the PRMT5 methylosome*', ***Mol Cell***, 81: 3481-95 e7.

Murn, J., and Y. Shi. 2017. '*The winding path of protein methylation research: milestones and new frontiers*', ***Nat Rev Mol Cell Biol***, 18: 517-27.

Musiani, D., J. Bok, E. Massignani, L. Wu, T. Tabaglio, M. R. Ippolito, A. Cuomo, U. Ozbek, H. Zorgati, U. Ghoshdastider, R. C. Robinson, E. Guccione, and T. Bonaldi. 2019. '*Proteomics profiling of arginine methylation defines PRMT5 substrate specificity*', ***Sci Signal***, 12.

Pal, S., S. N. Vishwanath, H. Erdjument-Bromage, P. Tempst, and S. Sif. 2004. '*Human SWI/SNF-associated PRMT5 methylates histone H3 arginine 8 and negatively regulates expression of ST7 and NM23 tumor suppressor genes*', ***Mol Cell Biol***, 24: 9630-45.

Pollack, B. P., S. V. Kotenko, W. He, L. S. Izotova, B. L. Barnoski, and S. Pestka. 1999. '*The human homologue of the yeast proteins Skb1 and Hsl7p interacts with Jak kinases and contains protein methyltransferase activity*', ***J Biol Chem***, 274: 31531-42.

Poulard, C., J. Rambaud, N. Hussein, L. Corbo, and M. Le Romancer. 2014. '*JMJD6 regulates ERalpha methylation on arginine*', ***PLoS One***, 9: e87982.

Richard, S., M. Morel, and P. Cleroux. 2005. '*Arginine methylation regulates IL-2 gene expression: a role for protein arginine methyltransferase 5 (PRMT5)*', ***Biochem J***, 388: 379-86.

Schmitz, K., J. Cox, L. M. Esser, M. Voss, K. Sander, A. Loffler, F. Hillebrand, S. Erkelenz, H. Schaal, T. Kahne, S. Klinker, T. Zhang, L. Nagel-Steger, D. Willbold, S. Seggewiss, D. Schlutermann, B. Stork, M. Grimmler, S. Wesselborg, and C. Peter. 2021. '*An essential role of the autophagy activating kinase ULK1 in snRNP biogenesis*', ***Nucleic Acids Res***.

Simms, S. A., A. M. Stock, and J. B. Stock. 1987. '*Purification and characterization of the*

S-adenosylmethionine:glutamyl methyltransferase that modifies membrane chemoreceptor proteins in bacteria', ***J Biol Chem***, 262: 8537-43.

Tsai, W. C., L. C. Reineke, A. Jain, S. Y. Jung, and R. E. Lloyd. 2017. '*Histone arginine demethylase JMJD6 is linked to stress granule assembly through demethylation of the stress granule-nucleating protein G3BP1*', ***J Biol Chem***, 292: 18886-96.

Wandrey, Franziska, Christian Montellese, Krisztian Koos, Lukas Badertscher, Lukas Bammert, Atlanta G. Cook, Ivo Zemp, Peter Horvath, and Ulrike Kutay. 2015. '*The NF45/NF90 Heterodimer Contributes to the Biogenesis of 60S Ribosomal Subunits and Influences Nucleolar Morphology*', ***Molecular and Cellular Biology***, 35: 3491-503.

Webby, C. J., A. Wolf, N. Gromak, M. Dreger, H. Kramer, B. Kessler, M. L. Nielsen, C. Schmitz, D. S. Butler, J. R. Yates, 3rd, C. M. Delahunty, P. Hahn, A. Lengeling, M. Mann, N. J. Proudfoot, C. J. Schofield, and A. Bottger. 2009. '*Jmjd6 catalyses lysyl-hydroxylation of U2AF65, a protein associated with RNA splicing*', ***Science***, 325: 90-3.

Widmann, B., F. Wandrey, L. Badertscher, E. Wyler, J. Pfannstiel, I. Zemp, and U. Kutay. 2012. '*The kinase activity of human Rio1 is required for final steps of cytoplasmic maturation of 40S subunits*', ***Mol Biol Cell***, 23: 22-35.

Supplementary Data 1

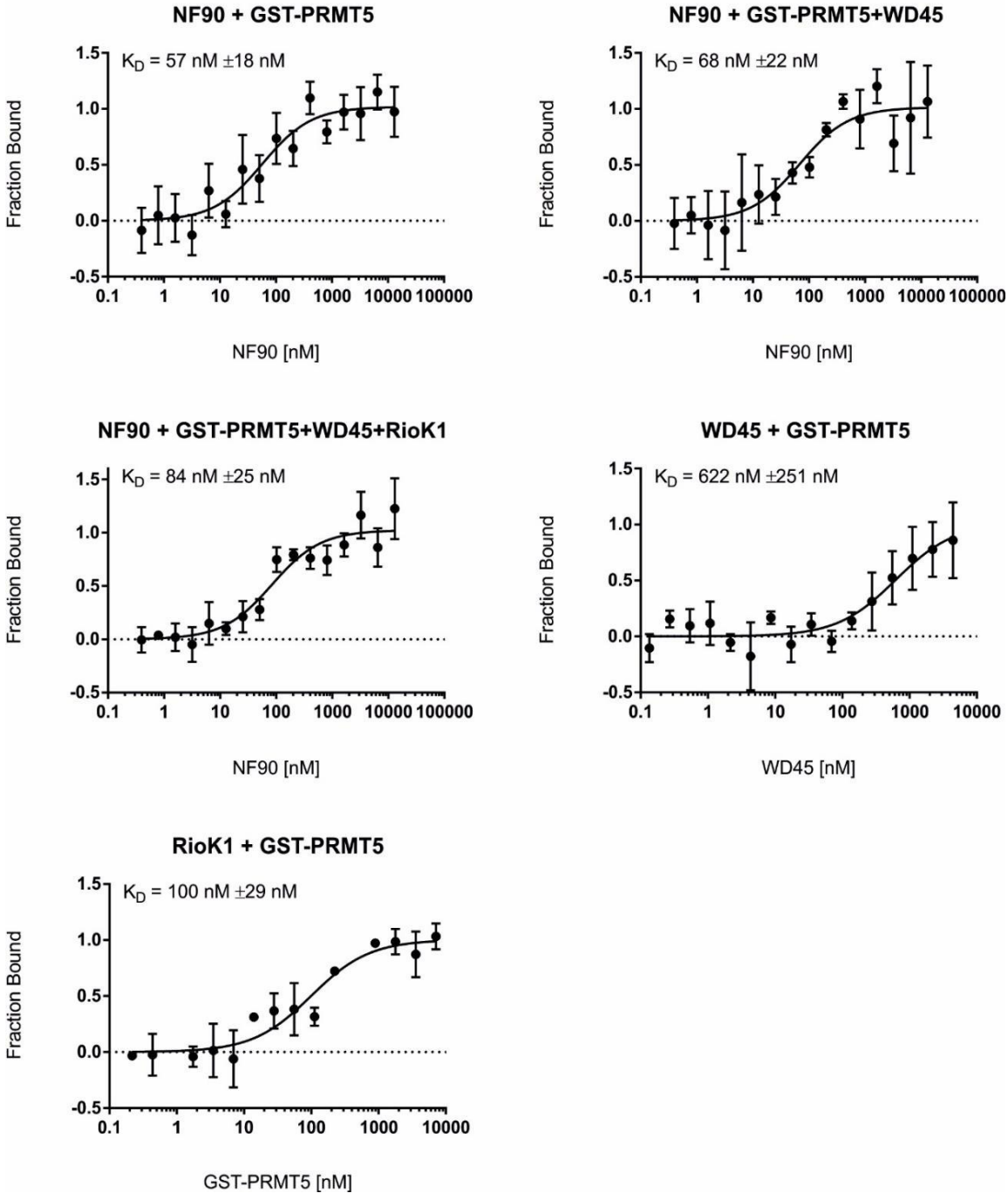

Supplementary Data Figure 1
Quantitative binding studies of NF90, PRMT5, WD45, and RioK1 by microscale thermophoresis (related to Figure 1D). Purified recombinant proteins GST-PRMT5, NF90 or RioK1 were labeled with AlexaFluor488-NHS (A20000, Invitrogen) in 50 mM HEPES, 300 mM NaCl, pH 7.5. 50 nM of labeled proteins and 4-14 µM of unlabeled proteins were used for interaction studies. All measurements were run in triplicates. Data acquisition was performed on a Nanotemper Monolith NT.115. Curve fitting was done using GraphPad Prism version 7.

Supplementary Data 2

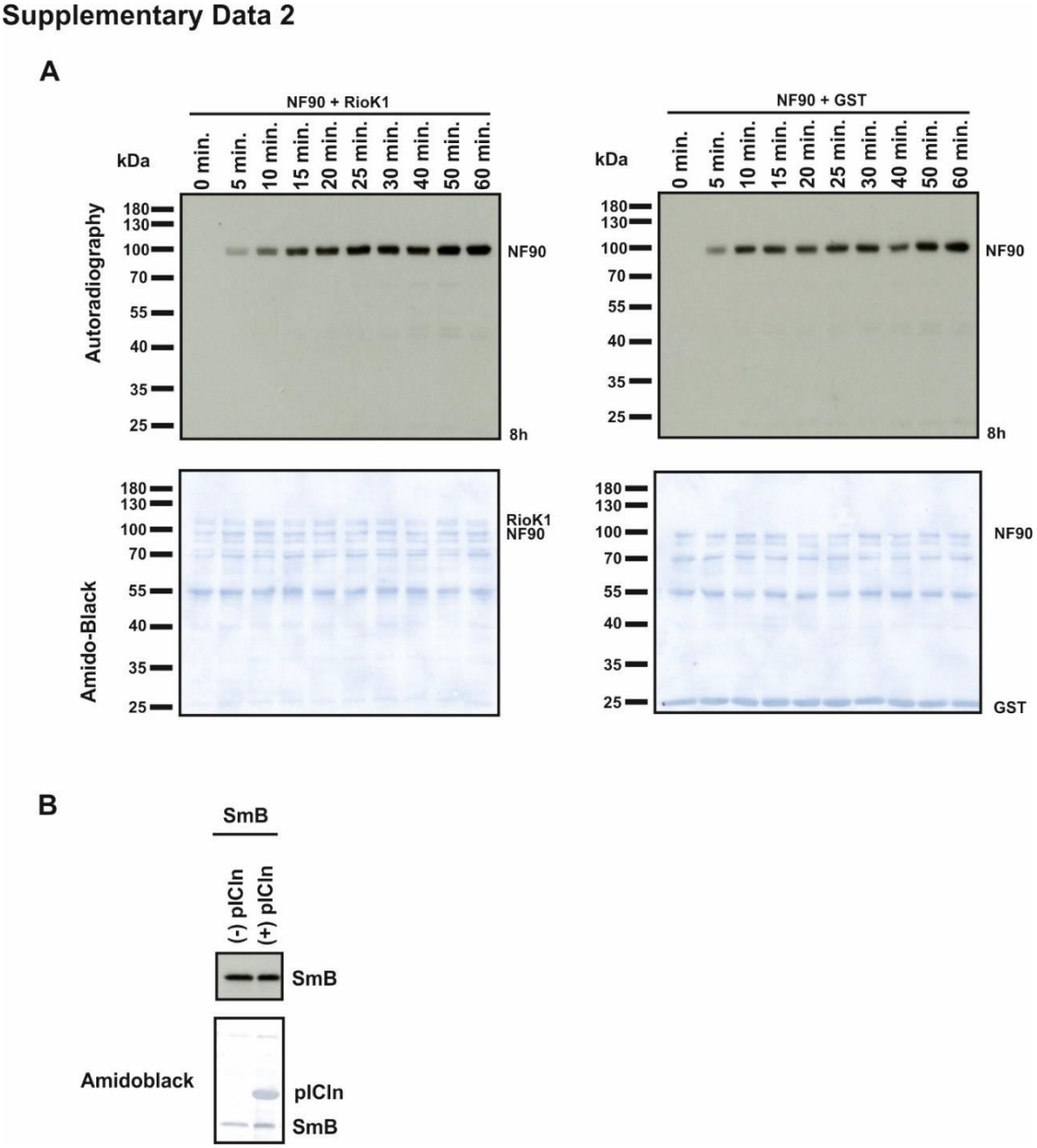

Supplementary Data Figure 2:
(A) Investigation of the influence of RioK1 on the methylation of NF90. 880 ng NF90 purified from *E. coli* without GST-tag was incubated with 200 ng recombinant PRMT5 and 1 µCi [3-H]-SAM after preincubation for 1 h with 1,5 µg recombinant RioK1 or GST protein. The reaction was terminated by addition of SDS sample buffer and the samples were analyzed as described in Figure 2.
(B) Investigation of the influence of pICln on the methylation of SmB. 500 ng SmB purified from *E. coli* without GST-tag was incubated with 200 ng recombinant PRMT5 and 1 µCi [3-H]-SAM after preincubation for 1 h with or without 1 µg recombinant pICln protein. The reaction was terminated by addition of SDS sample buffer and the samples were analyzed as described in Figure 2.

7.2 Chapter 2 - An essential role of the autophagy activating kinase ULK1 in snRNP biogenesis

Title:	**An essential role of the autophagy activating kinase ULK1 in snRNP biogenesis**
Authors:	Katharina Schmitz*, Jan Cox*, Lea Marie Esser*, Martin Voss, Katja Sander, Antje Löffler, Frank Hillebrand, Steffen Erkelenz, Heiner Schaal, Thilo Kähne, Stefan Klinker, Tao Zhang, Luitgard Nagel-Steger, Dieter Willbold, Sabine Seggewiß, David Schlütermann, Björn Stork, Matthias Grimmler, Sebastian Wesselborg and Christoph Peter *These authors contributed equally to the work
Published in:	*Nucleic Acids Research* Volume 49, Issue 11, **June 2021**, Pages 6437–6455 DOI: 10.1093/nar/gkab452
Impact factor:	19,16
Proportional work on this manuscript:	20% Protein purifications *In vitro* kinase assays Size exclusion experiments Immunopurification experiments Immunofluorescence analysis and quantification *In vitro* assembly assays Preparation of figures Contributing in writing the manuscript

An Essential Role of the autophagy activating kinase ULK1 in snRNP Biogenesis

Katharina Schmitz[1,9], Jan Cox[1,9], Lea Marie Esser[1,9], Martin Voss[1,2], Katja Sander[1], Antje Löffler[1], Frank Hillebrand[3], Steffen Erkelenz[3,4], Heiner Schaal[3], Thilo Kähne[5], Stefan Klinker[6], Tao Zhang[6,7], Luitgard Nagel-Steger[6,7], Dieter Willbold[6,7], Sabine Seggewiß[1], David Schlütermann[1], Björn Stork[1], Matthias Grimmler[8], Sebastian Wesselborg[1], Christoph Peter[1*]

1Institute of Molecular Medicine I, Medical Faculty, Heinrich Heine University Düsseldorf, Düsseldorf, Germany, 2Institute of Biochemistry, University of Cologne, Cologne, Germany, 3Institute of Virology, University Hospital Düsseldorf, Düsseldorf, Germany, 4Institute for Genetics and Cologne Excellence Cluster on Cellular Stress Responses in Aging-Associated Diseases (CECAD), University of Cologne, Cologne, Germany, 5Institute of Experimental Internal Medicine, Otto von Guericke University, Magdeburg, Germany, 6Institut für Physikalische Biologie, Heinrich-Heine-Universität Düsseldorf, Germany, 7Institute of Complex Systems: Structural Biochemistry (ICS-6), Forschungszentrum Jülich, Jülich, Germany, 8Hochschule Fresenius, Idstein, Germany

***** To whom correspondence should be addressed. Tel: **+49 (0) 211 81-11591**; Email: **christoph.peter@uni-duesseldorf.de**

[9] The authors wish it to be known that, in their opinion, the first three authors should be regarded as joint First Authors

ABSTRACT

The biogenesis of small uridine-rich nuclear ribonucleoproteins (UsnRNPs) depends on methylation of Sm proteins catalyzed by the methylosome and the subsequent action of the SMN complex, which assembles the heptameric Sm protein ring onto small nuclear RNAs (snRNAs). In this sophisticated process, the methylosome subunit pICln (chloride conductance regulatory protein) is attributed to an exceptional key position as an "assembly chaperone" by building up a stable precursor Sm protein ring structure. Here, we show that – apart from its autophagic role – the Ser/Thr kinase ULK1 functions as a novel key regulator in UsnRNP biogenesis by phosphorylation of the C-terminus of pICln. As a consequence, phosphorylated pICln is no longer capable to hold up the precursor Sm ring structure. Consequently, inhibition of ULK1 results in a reduction of efficient UsnRNP core assembly. Thus ULK1, depending on its complex formation, exerts different functions in autophagy or snRNP biosynthesis.

INTRODUCTION

Splicing of mRNA precursors is essential for the maintenance and function of the cellular proteome. This ubiquitous process is mediated by RNA-protein complexes termed spliceosomal U-rich small nuclear ribonucleoprotein particles (UsnRNP), which are composed of one specific small nuclear RNA (snRNA) and a heptameric ring of the seven common (Sm) proteins B, D1, D2, D3, E, F and G (Kambach et al., 1999, Newman et al., 2010, Matera et al., 2014). The assembly of the UsnRNPs is a sophisticated and stepwise process regulated by the protein arginine methyltransferase 5 (PRMT5), also known as methylosome, and the survival motor neuron (SMN) complex (Fischer et al., 1997, Liu et al., 1997, Friesen et al., 2001b, Meister et al., 2001a, Meister et al., 2001b, Friesen et al., 2002, Meister et al., 2002b, Zhang et al., 2011).

In this segmented process, the methylosome subunit pICln is attributed an exceptional key position as an "assembly chaperone" (Chari et al., 2008, Chari et al., 2010, Matera et al., 2014). During this assembly reaction pICln functions as a kinetic trap by building up a stable heterohexameric precursor ring structure together with the Sm proteins D1, D2, E, F and G (Chari et al., 2008). For the consecutive assembly reaction of the UsnRNP core, it is essential that catalytic snRNA is transferred onto this ring structure by the help of the SMN complex. In vitro as well as by in vivo experimental systems / cellular extracts the completion of

UsnRNP assembly strongly depends on metabolic energy by ATP hydrolysis (Meister et al., 2001a, Pellizzoni et al., 2002b). However, the involved regulating elements and the detailed structural and molecular mechanism of ATP dependent UsnRNP core assembly have remained elusive to date.

Here, we identify the autophagy activating Ser/Thr Unc-51-like kinase (ULK1) as a novel key regulator in this process. We demonstrate that pICln is a specific new substrate of ULK1 and that the newly identified phosphorylation sites in the C-terminus of pICln are responsible for breaking up the Sm ring structure at the newly identified SmG-pICln contact surface. We demonstrate that phosphorylation of pICln by ULK1 is an essential regulatory step to promote efficient biogenesis of the UsnRNP. Thus, we show that ULK1 comprises a crucial key function in two distinct cellular processes: autophagy as well as UsnRNP biogenesis, a process which is known to be highly dependent on protein methylation and phosphorylation events (Meister et al., 2001b, Grimmler et al., 2005a, Husedzinovic et al., 2014).

MATERIAL AND METHODS

Antibodies

The following primary antibodies were used for immunoblotting and immunofluorescence: α-FIP200 (A301-574A, Bethyl), α-ULK1 (8054; CST), α-ATG13 (M183-3, MBL; SAB4200100, Sigma-Aldrich), α-ATG101 (SAB4200175, Sigma-Aldrich), α-PRMT5 (2252, CST), α-WD45 (2823, CST), α-GFP (3H9, Chromotek), α-SmB (S0698, Sigma-Aldrich), α-SmD1 (ab79977, Abcam), α-SmD2 (SAB2102257, Sigma-Aldrich), α-SmE (NBP2-43792, Novus), α-SmF (SAB2102258, Sigma-Aldrich), α-SmG (HPA064152, Sigma-Aldrich), α-SMN (clone 2B1, 05-1532, Merck Millipore), α-Gemin 2 (clone 2E17, MA1-5777, Invitrogen), α-SNRPB (Y12, MA5-13449, Invitrogen) and α-Coilin (PA5-29531, Invitrogen). Antibody recognizing pICln has been described previously (Guderian et al., 2011). The detection of proteins was carried out with the following fluorescent secondary antibodies: IRDye 680LT goat α-rabbit, IRDye 680LT goat α-mouse, IRDye 800CW donkey α-rabbit, IRDye 800CW donkey α-mouse, IRDye 800CW goat anti-rat. For the detection of proteins in vivo via IF the following secondary antibodies were used: Alexa Fluor 568 donkey anti-mouse (A10037, Invitrogen) and Alexa Fluor 647 donkey anti-rabbit (A31573, Invitrogen).

Plasmids and proteins

For in vitro assays and pulldown experiments plasmids encoding full-length cDNAs of pICln (X91788.1), SmB (X17567.1), SmD3 (U15009.1), and SmG (X85373.1) were cloned from HEK293T, HeLa or Jurkat cDNA (High Capacity cDNA Reverse Transcription Kit, Applied Biosystems) into pET-28a (69864-3, EMD Biosciences) or pGEX-6P-1 (27-4597-01, Amersham) with the following primers: pICln, 5'-GGATCCATGAGCTTCCTCAAAAGTTTCCC-3' and 5'-GTCTCGAGTCAGTGATCAACATCTGCATCC-3'; SmB, 5'-ATGAATTCATGACGGTGGGCAAGAGC-3' and 5'ATGCGGCCGCTCAAAGAAGGCCTCGCATC-3'; SmD3, 5'ATGAATTCATGTCTATTGGTGTGCCG-3' and 5'-ATCTCGAGTTATCTTCGCTTTTGAAAGATG-3'; SmG, 5'-ATGGAATTCATGAGCAAAGCTCACCCT-3' and 5'ATGCTCGAGTTATCGTTCCAAGGCTT-3'. For cloning the pICln phosphorylation mutants the Pfu DNA Polymerase (Promega) and the following primers were used: S193, 195, 197A, 5'-GATTAGAAGGAATGCTTGCTCAGGCTGTGGCCAGCCAGTATAATATG-3' and 5'-CATATTATACTGGCTGGCCACAGCCTGAGCAAGCATTCCTTCTAATC-3'; S193, 195, 197D, 5'-GATTAGAAGGAATGCTTGATCAGGATGTGGACAGCCAGTATAATATG-3' and 5'-CATATTATACTGGCTGTCCACATCCTGATCAAGCATTCCTTCTAATC-3'.

Generation of pGEX6P-1-PRMT5; -WD45 (Guderian et al., 2011); -SmD1; pET28a-SmD1 (Grimmler et al., 2005b); pcDNA-FRT-TO-GFP; -GFP-ULK1; -GFP-ULK1kd; -GFP-ULK1/ΔCTD (Löffler et al., 2011) and pMSCVbsd/GFP-ULK1 plasmids have been described previously (Hieke et al., 2015). pET100/D-TOPO-SmE; -SmF; -SmD2 and pcDNA5-FRT-TO-GFP-ULK1 C-terminal domain (AA828-1050) and ULK1-GABARAP domain (AA287-416) were synthesized by GeneArt (Thermo Fisher Scientific).

For interaction studies, pMSCVbsd/GFP and pMSCVbsd/GFP-ULK1 kinase domain plasmids were generated by using pMSCVbsd/GFP-ULK1 and the following primers: 5'-CATGGACGAGCTGTACAAGTGAGGACTCGGATCCCTGGAG-3' (GFP) and 5'-GTTTTTTCATCACCCTTTCTAACTCGATGCCAGCCCC-3' (ULK1 kinase domain).

For purification GST-tagged Proteins and Pulldown Assays with those Glutathione Sepharose 4B from GE Healthcare was used. For HIS-tagged Proteins HisPur™ Ni-NTA Resin from Thermo Fischer was used. For Pulldown Assays recombinant Proteins were incubated 1,5 h at 4°C then sepharose was added and after another hour of incubation analysis of the proteins per SDS-PAGE and western blotting with specific antibodies occurred.

Recombinant active ULK1, ULK2, and PRMT5 were purchased from Sigma-Aldrich (SRP5096, SRP5097, SRP0145). ULK1/2 inhibitor MRT67307 was obtained through the MRC PPU Reagents and Services facility (MRC PPU, College of Life Sciences, University of Dundee, Scotland, mrcppureagents.dundee.ac.uk).

Cell lines and cell culture

Generation of inducible Flp-In T-REx 293 cells system expressing GFP, GFP-ULK1, GFP-ULK1kd, GFP-ULK1/ΔCTD, and GFP-pICln was carried out according to the manufacturer's instructions (Invitrogen, Thermo Fisher Scientific) and has been described previously (Löffler et al., 2011). For induction of GFP, GFP-ULK1, GFP-ULK1kd, and GFP-ULK1/ΔCTD expression, Flp-In T-REx 293 cell lines were stimulated with 0.1 µg/ml Doxycycline (Clontech) for 18 h. For starvation treatment, cells were incubated in Earle's Balanced Salt Solution (EBSS; Gibco, Thermo Fisher Scientific) for 1 h. For ULK1 knockdown HEK293T cells were transfected using DharmaFECT1 (GE Dharmacon) with 50 nM ULK1 siRNA (L-005049-00-0010, SMARTpool, ON-TARGETplus, GE Dharmacon) for 48 h.

For interaction studies, HEK293T were transiently transfected with pcDNA5-FRT-TO-GFP-ULK1 GABARAP domain and -ULK1 C-terminal domain constructs using Lipofectamine 3000 (Invitrogen, L3000-015). The cells were harvested 24 h after transfection. Additionally, HEK293T cells stably expressing the GFP-ULK1 kinase domain and GFP were generated. Therefore Plat-E cells were used as packaging cell line and transfected with the retroviral pMSCVbsd expression vectors using FuGENE6 (Promega, E2692). HEK293T cells were incubated with the retroviral supernatant containing 3 mg/ml Polybrene (Sigma-Aldrich, H9268-106) and selected with Blasticidin.

All cell lines were cultured in DMEM (4.5 g/l D-glucose; Gibco, Thermo Fisher Scientific) supplemented with 10% (v/v) FCS (Biochrom, Merck), 100 U/ml Penicillin and 100 µg/ml

Streptomycin (Gibco, Thermo Fisher Scientific) in a 5% CO2 humidified atmosphere at 37°C.

Protein expression and purification

Proteins were overexpressed in BL21 competent E. coli for 4h at RT after induction with 1 mM IPTG. Cells were lysed in 300 mM NaCl, 50 mM Tris/HCl pH 7.5, 5 mM EDTA, 5 mM EGTA, 0.01% (v/v) Igepal, protease inhibitors (cOmplete, EDTA-free protease inhibitor cocktail tablets, Roche), 50 mg/ml Lysozyme (Serva) and by sonication. After centrifugation at 10,000 g for 30 min. the lysate was incubated with glutathione sepharose 4B (GE Healthcare) for 1.5 h at 4 °C and subsequently washed 3 times with lysis buffer.

Immunoblotting and immunopurification

Protein amounts of cleared S100 cytoplasm extract were determined by the Bradford method. Samples were separated by Tris/Tricine or Tris/Glycine SDS gel electrophoresis (Laemmli, 1970) and transferred to PVDF membranes (Immobilon-FL, Merck Millipore). The immunoblot analysis was performed using the indicated antibodies and signals were detected with an Odyssey LI-COR Imaging System. For GFP immunopurification S100 extracts were incubated with GFP-Trap_A beads (ChromoTek) at 4 °C for at least 1.5 h with rotation. Purified proteins were washed 3 times with washing buffer (lysis buffer without Triton X-100 and protease inhibitors), eluted in sample buffer [375mM Tris pH 7.5; 25.8% (w/v) glycerol; 12.3% (w/v) SDS; 0.06% (w/v) Bromophenol blue; 6% (v/v) β-mercaptoethanol; pH 6.8] and analyzed by immunoblotting.

Immunofluorescence microscopy

HEK293T and Flp-In T-REx 293 cells were seeded on coverslips in DMEM high glucose media (4,5g/L D-glucose) with 10% (v/v) FCS (Biochrom, Merck), 100 U/ml Penicillin and 100 µg/ml Streptomycin (Gibco, Thermo Fisher Scientific) one day before staining. On the next day after washing the cells once with Dulbecco´s phosphate-buffered saline (DPBS), fixing was performed with 4% paraformaldehyde for 10 minutes. Cells were permeabilized with 0,2% Triton X-100/PBS for 10 minutes and blocked with 5% BSA for 30 minutes. Proteins were detected with anti-SMN clone 2B1 (1:1000) and anti-Coilin antibody

(1:1000), incubation time 2 hours. As a secondary antibody, Alexa Fluor 568 (1:200; shown in green) and Alexa Fluor 647 (1:200; shown in red) were used. Analysis of the staining was performed with the ZEISS Apotome.2 and a 40x oil immersion objective.

Cytoplasm extraction (S100) and size exclusion chromatography

HEK293T cells were incubated with Roeder A buffer (Dignam et al., 1983) in an appropriate amount for 10 min at room temperature, dounced 10 times, and adjusted to 150 mM NaCl. After centrifugation at 17,000 g for 30 min the supernatants (S100 extracts) were filtrated with Millex-HA, 0,45 µm filter unit (Merck Millipore) and applied to a Superdex 200 HiLoad 16/600 or Superdex 200 increase 10/300 GL column (GE Healthcare). 2 ml respectively 0.5 ml fractions were collected in running buffer (150 mM NaCl, 50 mM Tris/HCl pH 7.5) and analyzed by immunoblotting. The columns were calibrated with thyroglobulin (669 kDa), ferritin (440 kDa), catalase (232 kDa), aldolase (158 kDa), albumin (67 kDa), ovalbumin (43 kDa), and RNase (14 kDa) (GE Healthcare).

***In vitro* phosphorylation**

GST-PRMT5, -WD45, and -pICln was purified from E. coli, GFP-ULK1, and GFP-ULK1kd from Flp-In T-REx 293 cells. GST-ULK1 (1-649) and GST-ULK2 (1-631) were used from Sigma-Aldrich. Recombinant active GST-ULK1/2 or purified GFP-ULK1 and GST substrate in appropriate amounts were incubated in 2 µM ATP, 10 µCi [32P]-ATP (Hartmann Analytic), 2.5 mM Tris/HCl pH 7.5, 5 µM EGTA, 50 µM DTT and 3.75 mM Mg(CH3COO)2 for 45 min at 30 °C. Gel filtration fractions were incubated 1:1 with kinase buffer (50 mM NaCl, 25 mM Tris/HCl pH 7.5, 10 mM MgCl2, 2 mM CaCl2), GST-pICln and 10 µCi [32P]-ATP for 45 min at 30 °C and washed 3 times with kinase washing buffer (300 mM NaCl, 50 mM Tris/HCl pH 7.5, 5 mM EGTA, 5 mM EDTA, 0.01% (v/v) Igepal). The reaction was terminated by adding sample buffer, samples were subjected to SDS-PAGE, and after coomassie or silver staining autoradiography was performed.

***In vitro* translation and interaction assay**

[35S] methionine-labeled (Hartmann Analytic) proteins were made using the TNT Quick Coupled Transcription/Translation System (Promega). For binding assay in vitro translated

proteins were incubated with GST fusion proteins bounded on glutathione sepharose 4B (GE Healthcare) in interaction buffer (300 mM NaCl, 50 mM Tris/HCl pH 7.5, 1 mM EGTA, 1 mM EDTA, 1 mM DTT and 0.01% (v/v) Igepal) for 1.5 h at 4 °C under rotation. After washing 2 times with interaction buffer bounded proteins were eluted by adding sample buffer, separated by SDS-PAGE, and analyzed by coomassie staining and autoradiography.

In vitro methylation

GST-SmD1 was purified from E. coli, GFP-ULK1 from Flp-In T-REx 293 cells. Active Flag-PRMT5/His-WD45 and an appropriate amount of GST-SmD1 or GFP-ULK1 were incubated in 1 µCi Adenosyl-L-Methionine, S-[methyl-3H] (Perkin Elmer), 50 mM Tris/HCl pH 7.5, 1 mM EGTA and 1 mM EDTA for 1 h at 37 °C. The reaction was terminated by adding sample buffer, samples were subjected to SDS-PAGE, and after coomassie staining autoradiography was performed.

In vitro transcription and assembly of UsnRNPs

The U1 snRNA was in vitro transcribed and labeled with 10 µCi [32P]-UTP (Hartmann Analytic). For the analysis of the UsnRNP assembly in vitro, a GFP-pICln immunoprecipitation was performed with 1 mg cytoplasmic extract (S100). The efficiency of the UsnRNP biogenesis of this immunoprecipitation was analyzed by adding U1 snRNA to the immunoprecipitation in the presence/absence of ATP and active ULK1 kinase. The reactions were incubated at 35 °C for 45 min with 800 counts [32P]-UTP labeled, U1 snRNA, 2 µg t-RNA, 5 mM ATP, and 1 µl RNAsin in a final volume of 20 µl PBS. The assembly reactions were analyzed by a native RNA gel electrophoresis.

Analysis of ULK1 mediated pICln phosphorylation by LC-MS/MS

Samples were separated by SDS-PAGE after in vitro kinase assay. Gel areas containing GST-pICln were excised and subjected to in-gel digestion in an adapted manner according (Shevchenko et al., 1996). NanoLC-MS/MS analysis was performed on a hybrid dual-pressure linear ion trap/orbitrap mass spectrometer (LTQ Orbitrap Velos Pro, Thermo Fisher Scientific) equipped with a U3000 nano-flow HPLC (Thermo Fisher Scientific) as described (Niewalda et al., 2015). The procedure in brief: Samples were separated on a 75 µm I.D., 25

cm PepMap C18-column (Dionex Thermo Fisher Scientific) applying a gradient from 2% (v/v) ACN to 35% (v/v) ACN in 0.1% (v/v) formic acid over 95 min at 300 nl/min. The LTQ Orbitrap Velos Pro MS used exclusively CID-fragmentation with wideband activation (pseudo-MS3 for neutral losses of phosphate residues) when acquiring MS/MS spectra. The spectra acquisition consisted of an orbitrap full MS scan (FTMS; resolution 60,000; m/z range 400-2000) followed by up to 15 LTQ MS/MS experiments (Linear Trap; minimum signal threshold: 500; wideband isolation; dynamic exclusion time setting: 30 s; singly-charged ions were excluded from selection, normalized collision energy: 35%; activation time: 10 ms). Raw data processing, protein identification, and phosphopeptide assignment of the high-resolution orbitrap data were performed by PEAKS Studio 7.0 (Bioinformatics Solutions Inc.). The false discovery rate (FDR) was set to < 1%. Phosphorylation sites were accepted as confident for P< 0.005 (modified t-test, included in PEAKS Studio 7.0) and PhosphoRS score> 90 (Taus et al., 2011).

Analysis of pICln complex formation by quantitative LC-MS/MS

5 µg of GST-pICln wt and mutants have been incubated with 1 mg HEK293T S100 extract overnight at 4 °C. After the addition of 30 µl glutathione sepharose 4B (GE Healthcare) and further incubation at 4 C for 4 h purified proteins were washed 3 times with washing buffer (see above) and 3 times with PBS. Then GST-pICln bound to GSH-beads were subjected to "on beads digestion" as described earlier (Dubiel et al., 2017). The procedure in brief: GST-pICln bound to beads were resuspended in 50 mM ammonium bicarbonate. Cysteines were reduced by adding 2 mM dithiothreitol (DTT) for 30 min at room temperature and subsequently β-methylthiolated by addition of 10 mM methylmethanethiosulfonate (MMTS). Digestion was performed by the addition of 0.5 µg trypsin (Promega) and incubation overnight at 37 °C. Peptides were extracted by pooling the primary supernatant and the supernatant of a subsequent washing step using 0.1% (v/v) trifluoroacetic acid (TFA). Peptides were purified with reversed-phase C18 ZipTip nano-columns (EMD Millipore), eluted with 0.1% (v/v) TFA/70% (v/v) ACN, and dried. Protein identification was performed by high-resolution mass spectrometry on a hybrid dual-pressure linear ion trap/orbitrap mass spectrometer as described above. Relative protein quantification was achieved using Skyline analysis platform (MacLean et al., 2010) for MS-peak integration on extracted ion chromatograms of the following selected peptides: sp|P54105|ICLN_HUMAN: K.GLGTGTLYIAESR.L [30, 42],

K.FEEESKEPVADEEEEDSDDDVEPITEFR.F [85, 112], R.LEGMLSQSVSSQYNMAGVR.T [187, 205]; sp|P62308|RUXG_HUMAN: R.GNSIIMLEALER.V [63, 74], R.GNSIIMLEALER.V [63, 74]; sp|P62306|RUXF_HUMAN: R.CNNVLYIR.G [65, 72], sp|P62304|RUXE_HUMAN: K.VMVQPINLIFR.Y [12, 22], K.GDNITLLQSVSN.- [80, 91]; sp|P62314|SMD1_HUMAN: K.LSHETVTIELK.N [9, 19], K.NREPVQLETLSIR.G [48, 60], R.YFILPDSLPLDTLLVDVEPK.V [66, 85]; sp|P62316|SMD2_HUMAN: K.NNTQVLINCR.N [37, 46], R.GDSVIVVLR.N [102, 110]; sp|P62318|SMD3_HUMAN: R.VAQLEQVYIR.G [54, 63], R.FLILPDMLK.N [69, 77]; sp|P14678|RSMB_HUMAN: R.VLGLVLLR.G [65, 72], R.GENLVSMTVEGPPPK.D [73, 87]. pICln peptides have been used for internal normalization.

Surface Plasmon Resonance

The affinity dissociation constants (Kd) of pICln wt and pICln aspartate mutant for SmG were determined by surface plasmon resonance (SPR) using a T200 device (Biacore, GE Healthcare). The immobilization of the ligand was performed under mild acidic condition by dissolving the respective protein stock solution (50 mM Hepes, 150 mM NaCl, 1 mM EDTA, pH 7.0) in 10 mM sodium acetate buffer pH 5.0 and injection onto the N-hydroxysuccinimide (NHS) 1-ethyl-3-(3 dimethylaminopropyl)carbodiimide (EDC) activated series S CM5 sensor chip (Biacore, GE Healthcare) surface. By sequential injection of several µl of ligand solvent, the target immobilization level of 400 RU for the 51 kDa ligand GST-pICln was reached. The remaining activated surface of the ligand flow cell, as well as the activated reference flow cell, was blocked by the injection of 1 M ethanolamine pH 8.5 for 7 min. Affinity measurements were performed in running buffer (300 mM NaCl, 50 mM Tris/HCl pH 7.5, 1 mM EDTA and 1 mM EGTA). The analytes were stored in purification buffer and freshly dissolved in sample buffer (300 mM NaCl, 50mM Tris/HCl pH7.5, 1 mM EDTA, 1 mM EGTA, 1 mg/ml BSA, 1 mM DTT and 0.01% (v/v) Igepal) before analysis. During measurement analyte samples were sealed against evaporation and stored at 10°C until injection. For affinity determination of the analytes, multi-cycle kinetic experiments were applied at 20 °C and 10 µl min−1 flow rate. In between each cycle, a regeneration command (200 s injection of 10 mM glycine pH 10 at 30 µl min-1, followed by a stabilization period of 500 s with running buffer) was executed if dissociation phase time was not sufficient to dissociate the formed complex of ligand and analyte. Association

and dissociation phase of 100 s and 600 s for GST-pICln – SmG analysis was chosen. As a quality control for the activity of used analyte batch, wild type, and respective mutants were run sequentially on the same sensor chip. The reference flow cell and buffer cycles were used for double referencing of the sensorgrams. For evaluation, the sensorgrams were fitted applying the steady-state fit model of the Biacore T200 Evaluation Software 2.0 (GE Healthcare) and the offset was constantly set to zero.

Sedimentation velocity analysis

Sedimentation velocity analytical ultracentrifugation (SV-AUC) was carried out using a ProteomLab XL-A ultracentrifuge (Beckman Coulter, Brea, CA, USA) equipped with a fluorescence detection system (Aviv Biomedical inc., Lakewood, NJ, USA). Samples were filled into 3-mm double-sector titanium cells (Nanolytics, Potsdam, Germany) with a volume of 100 µl, respectively. Quartz windows were used for all cell assemblies. Radial fluorescence scans were collected continuously at 40,000 rpm using a 488 nm laser for excitation and 520 nm cut-off emission filter using a constant photomultiplier voltage. A radial resolution of 20 µm was used for data acquisition. The gains for all samples were adjusted for optimum signal-to-noise ratios. All samples were thermally equilibrated to 20 °C for about 1.5 hours before starting the measurement. The experiments were performed at 40,000 rpm (equivalent to 129,024$\times g$) at 20 °C for 5 h. All SV data was then analyzed with continuous distribution c(s) Lamm equation model with maximum entropy regularization, which is implemented in the software package SEDFIT (version 15.01b, http://www.analyticalultracentrifugation.com/) (Schuck, Schuck, 2000). The fitting parameters, including the partial specific volumes ($\bar{\nu}$), buffer density (ρ), and viscosity (η), were calculated based on the protein sequences and buffer composition, respectively, by applying SEDNTERP (version 20130813 BETA, http://bitcwiki.sr.unh.edu/index.php/Main_Page). The size distributions as well as the sedimentation profiles were presented by GUSSI (version 1.2.1) (Brautigam, 2015). The final sedimentation coefficients were normalized to the s-values at 20 °C in pure water solvent (s20, w).

RESULTS

ULK1 is a new interaction partner of the PRMT5 complex

To identify new interaction partners of ULK1 we established an inducible expression system of GFP-ULK1 in Flp-In T-REx 293 cells. Utilizing this system, we identified and characterized new substrates of ULK1 by subsequent co-immunopurification and mass spectrometry like the AMP-activated protein kinase (α, β, and γ AMPK) (Löffler et al., 2011). This survey also revealed a putative association of ULK1 with the Protein arginine N-methyltransferase 5 (PRMT5) as well as its binding partners the methylosome protein 50 (MEP50/WD45) and the chloride conductance regulatory protein (pICln).

To validate our mass spectrometry results we performed immunoblot analysis from Flp-In T-REx 293 cells expressing inducible GFP-ULK1 or a GFP control. Only immunopurification of GFP-ULK1 but not GFP alone revealed an interaction with PRMT5, WD45, and pICln (Fig. 1A). Furthermore, the interaction of the methylosome with ULK1 seems to be independent of autophagy induction since PRMT5 and its binding partners were co-immunopurified to the same extent upon incubation with starvation medium for induction of autophagy (Fig. 1A, SD Fig. 1A).

Figure 1

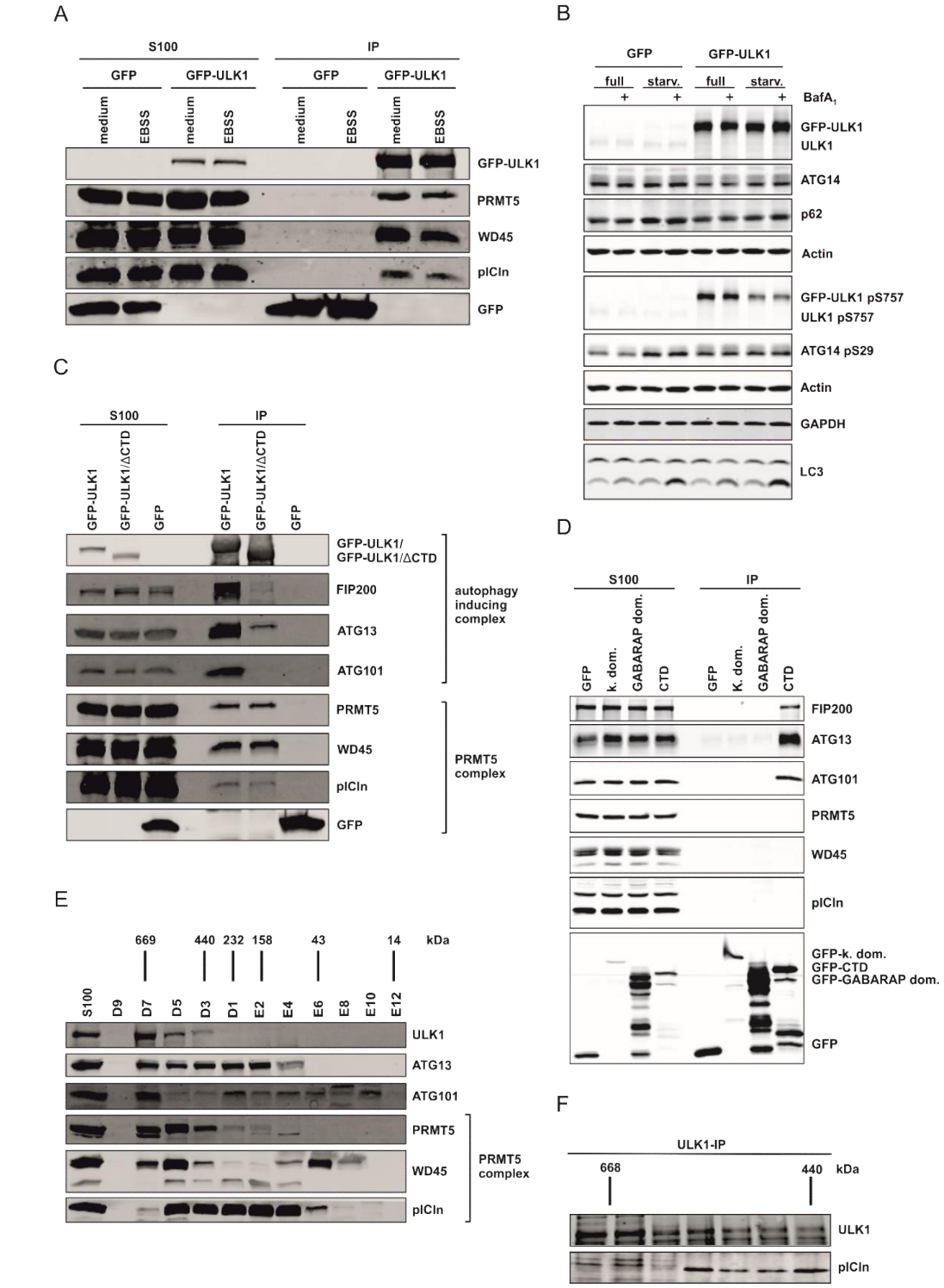

Figure 1. ULK1 interacts directly with the PRMT5 complex independent of its role in autophagy. (A) Flp-In T-REx 293-GFP-ULK1 and Flp-In T-REx 293-GFP cells were stimulated with 0.1 µg/ml doxycycline for 18 h, followed by 1 h of starvation treatment with EBSS. After cytoplasm extraction (S100) GFP-IP was performed and analyzed by Tris/Glycine-SDS-PAGE and western blotting using antibodies against GFP, PRMT5, WD45, and pICln. (B) Flp-In T-REx 293-GFP-ULK1 and Flp-In T-REx 293-GFP cells were stimulated with 0.1 µg/ml doxycycline for 18 h, followed by treatment with full or starvation medium (EBSS) in absence or presence of bafilomycin A1 (BafA1; 10 nM) for 1 h. Afterwards, cells were harvested, lysed and cleared cellular lysates were subjected to Tris/Glycine-SDS-PAGE and immunoblotting for GFP, ULK1 pS757, ATG14, ATG14 pS29, p62, LC3, GAPDH, and Actin. (C) Flp-In T-REx 293-GFP-ULK1, -GFP-ULK1/ΔCTD and -GFP cells were stimulated with 0.1 µg/ml doxycycline for 18 h. After cytoplasm extraction

(S100) GFP-IP was performed and analyzed by Tris/Glycine-SDS-PAGE and western blotting using antibodies against FIP200, GFP, PRMT5, ATG13, WD45, pICln, and ATG101. (D) HEK293T cells were stably transfected with pMSCVbsd-GFP-ULK1 kinase domain (k. dom.) and pMSCVbsd-GFP constructs. Additionally, HEK293T cells were transient transfected with pcDNA5-FRT-TO-GFP-ULK1 GABARAP domain (GABARAP dom.) and -ULK1 C-terminal domain (CTD) constructs. After cytoplasm extraction (S100) GFP-IP was performed and analyzed by Tris/Glycine-SDS-PAGE and western blotting using antibodies against GFP, FIP200, ATG13, ATG101, PRMT5, WD45 and pICln. (E) S100 extract was generated of HEK293T cells and applied to a Superdex 200 increase column. Fractions were analyzed by Tris/Glycine-SDS-PAGE and immunoblotting using antibodies against ULK1, ATG13, ATG101, PRMT5, WD45, and pICln. (F) S100 extract of HEK293T cells was applied to a Superdex 200 increase column and afterward, endogenous immunoprecipitation with antibody against ULK1 was performed. Immunoprecipitation was analyzed by Tris/Glycine-SDS-PAGE using antibodies against ULK1 and pICln.

During autophagy, ULK1 is associated with ATG13, ATG101, and RB1CC1/FIP200 in a high molecular weight complex of 2 MDa (Hosokawa et al., 2009). The formation of this autophagy inducing complex requires the C-terminal domain (CTD) of ULK1 (Chan et al., 2009). When we used Flp-In T-REx 293 cells inducibly expressing a mutant lacking the CTD of ULK1 (GFP-ULK1/ΔCTD) we still can co-immunopurify comparable amounts of PRMT5, WD45, and pICln (Fig. 1B). In contrast ATG13, ATG101 and FIP200 could only be co-immunopurified with full-length ULK1 (Fig. 1B) or with the C-terminal domain of ULK1 (SD Fig. 1B). Thus, the interaction of ULK1 with the methylosome is independent of the C-terminal domain of ULK1 and additionally independent of its kinase and GABARAP domain (SD Fig. 1B). This intriguing observation suggests that apart from its central role in autophagy, ULK1 may also play a crucial part in UsnRNP biogenesis and activity.

In addition to the established and well-characterized autophagy-inducing complex with a size of >2000 kDa (Hosokawa et al., 2009), overexpressed ULK1 can be detected in a smaller population in a CTD-independent manner with a molecular mass of 400 to 500 kDa (Chan et al., 2009). Since the PRMT5 complex also has a molecular size of 400 to 600 kDa (Friesen et al., 2001b, Friesen et al., 2002), we used Superdex 200 increase column size exclusion chromatography to analyze the co-migration of ULK1 with the PRMT5 complex. Consistent with the results from Chan and coworkers (Chan et al., 2009) we detected endogenous ULK1 from HEK293T cells in a size range of 400 to 600 kDa (Fig. 1C). We could identify the co-migration of ULK1 with the endogenous PRMT5 complex in these fractions (Fig. 1C).

These results posed the question if ULK1 is a new substrate of the methylosome. Subsequent radioactive *in vitro* methylation assays with active PRMT5 could not provide evidence for this, whereas the Sm protein D1, a known substrate of PRMT5 (Friesen et al., 2001b), was efficiently methylated (Fig. 1D).

The methylosome subunit pICln is a new substrate of the autophagy initiating kinase ULK1

Recent studies have shown that besides methylation UsnRNP biogenesis crucially depends on ATP levels (Meister et al., 2001a, Pellizzoni et al., 2002b, Grimmler et al., 2005a, Husedzinovic et al., 2014). Moreover, the PRMT5 complex subunit pICln is highly phosphorylated *in vitro* and *in vivo* (Sanchez-Olea et al., 1998, Grimmler et al., 2005a).

To test if the methylosome is a substrate of ULK1, we performed *in vitro* kinase assays using recombinant purified GST fusion proteins of PRMT5, WD45, and pICln as substrates and active GST-ULK1 purified from Sf9 insect cells. Surprisingly, among all used substrates only pICln showed strong ^{32}P incorporation upon incubation with active GST-ULK1 (Fig. 2A), indicating that pICln represents a new substrate of ULK1. To prove if the observed phosphorylation of pICln is ULK1 specific, we conducted the kinase assay with a kinase-dead mutant of ULK1 (GFP-ULK1kd) (Fig. 2B) (Löffler et al., 2011). Consistent with the previous results, only immunopurified active GFP-ULK1 was able to phosphorylate pICln. In contrast, pICln incubated with the kinase-dead mutant GFP-ULK1kd did not exhibit ^{32}P incorporation at all (Fig. 2B).

Figure 2

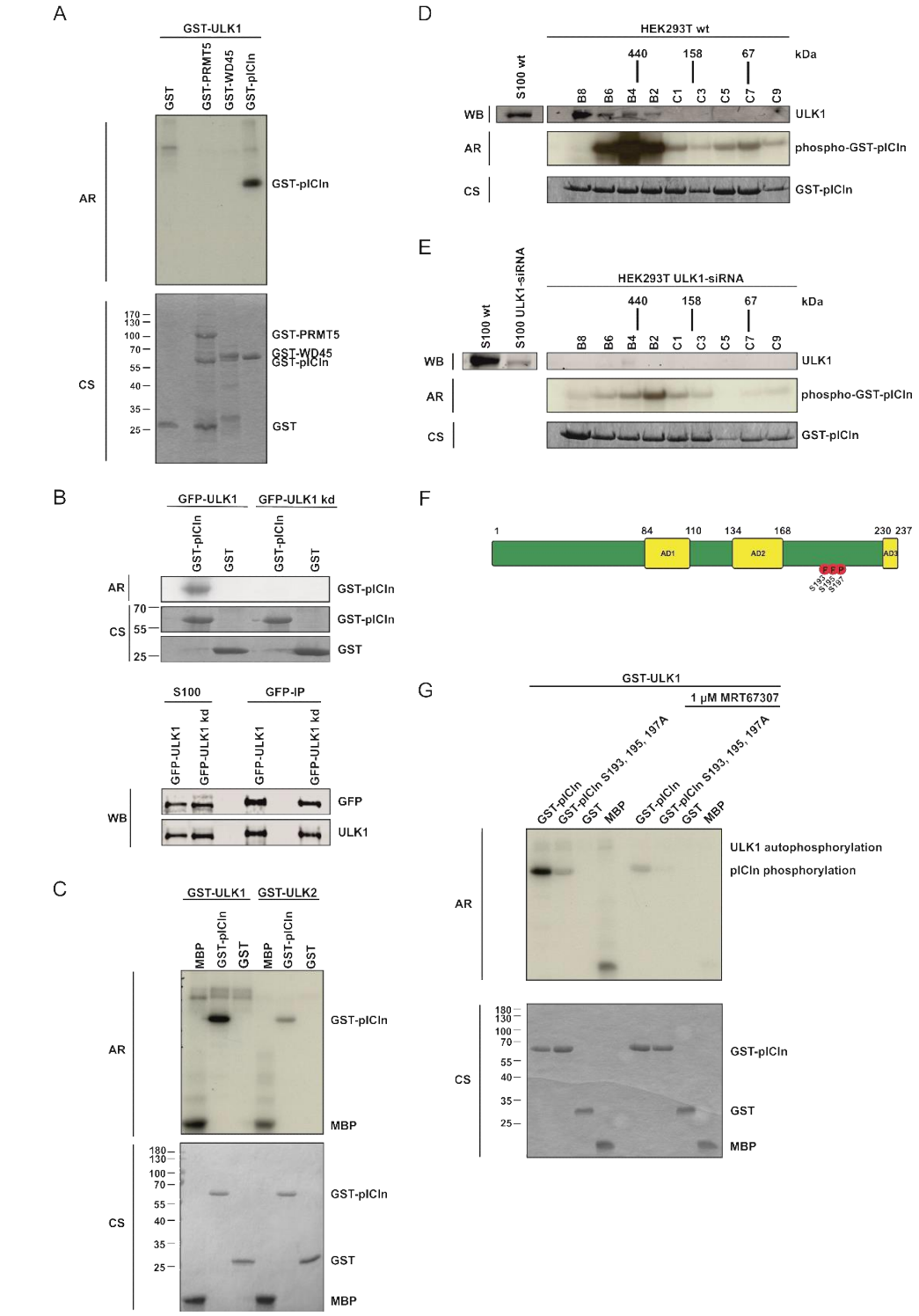

Figure 2. ULK1 phosphorylates pICln in the C-terminal region on residues S193, S195, and S197. (A) *In vitro* kinase assay using recombinant active GST-ULK1 expressed in Sf9 insect cells and GST-PRMT5, -WD45 and -pICln purified from *E. coli* as substrate proteins were incubated with 10 µCi [32P]-ATP for 45 min. at 30 °C. Samples were separated by Tris/Glycine-SDS-PAGE and analyzed by autoradiography. (B) *In vitro* kinase assay with purified GFP-ULK1 or GFP-ULK1 kinase-dead mutant (GFP-ULK1kd) overexpressed in Flp-In T-REx 293 cells and GST-pICln was executed as described in (A). Amounts of the GFP precipitation from GFP-ULK1 and GFP-ULK1 kinase-dead were compared by Tris/Glycine-SDS-PAGE and Western-Blot analysis using antibodies against ULK1 and GFP. (C) *In vitro* kinase assay using recombinant active GST-ULK1 or -ULK2 expressed in Sf9 cells and GST-pICln was executed as described in (A). (D; E) Gel filtration was performed with HEK293T wild type (D) and HEK293T ULK1-siRNA knockdown (E) S100 extracts

fractionated by a Superdex 200 column and evaluated by western blotting. Appropriate fractions were used for in vitro kinase assay using exogenous GST-pICln substrate protein and 10 µCi [32P]-ATP for 45 min. at 30 °C and analyzed by autoradiography (Exposure time of 30 minutes for (D) and (E)). (F) Schematic view of pICln protein with its three acidic domains (AD1-3) and the ULK1-dependent phosphorylation sites. *In vitro* kinase assay was performed with recombinant active GST-ULK1 from Sf9 cells and GST-pICln as described in (A). After Tris/Glycine-SDS-PAGE and coomassie blue staining, the pICln band was excised and phosphorylation status was analyzed by mass spectrometry (LC-MS/MS). Three phosphosites were detected: S193 (p=3.05E-05, 94.5%), S195 (p=2.3E-07, 100%), S197 (p=2.8E-06, 100%). (G) Recombinant active GST-ULK1 from Sf9 insect cells was incubated with 1 µM ULK inhibitor MRT67307 for 30 min. at 30 °C. *In vitro* kinase assay with inhibitor-treated and non-treated GST-ULK1 was performed using substrate proteins GST-pICln wild type and alanine mutant purified from *E. coli* as described in (A). AR: autoradiography, CS: coomassie blue staining, WB: western blotting. See also Supplementary Figure S2.

Since ULK2 is known to compensate for the activity of ULK1 in the regulation of autophagic processes (Lee et al., 2011), we investigated whether ULK2 can also phosphorylate pICln. In contrast to ULK1, ULK2 was not proficient to phosphorylate pICln with comparable efficiency (Fig. 2C). To evaluate whether ULK1 represents the pICln-associated kinase in cellular extracts we incubated the fractions of a size exclusion chromatography experiment of HEK293T cells with recombinant purified GST-pICln and ^{32}P γ-ATP. Autoradiographic analysis of these particular fractions showed strongly phosphorylated GST-pICln in fractions B2, B4, and B6 (Fig. 2D). Interestingly, predominant phosphorylation of pICln was observed in fraction B4 that corresponds to the entire PRMT5 complex of ~440 kDa consisting of all components (PRMT5, WD45, pICln, and ULK1) (SD Fig. 2A).

To further confirm the specificity of ULK1 dependent phosphorylation of pICln *in vivo,* we performed siRNA knockdown experiments of ULK1 in HEK293T followed by size exclusion chromatography and subsequent assessment of pICln phosphorylation status by kinase assays using recombinant purified GST-pICln as substrate and ^{32}P γ-ATP. By these means, we observed an almost complete reduction in phosphorylation of pICln (Fig. 2E), whereas the composition of the PRMT5 complex was not affected (SD Fig. 2B). Remarkably, the whole PRMT5 complex migrates in a lower size range if ULK1 is absent (SD Fig. 2A, B).

To identify the respective ULK1 phosphorylation sites of pICln, we performed *in vitro* kinase assays following SDS-PAGE, in-gel digestion, and NanoLC-MS/MS analysis. Thereby we identified three novel phosphorylation sites in the C-terminal region of pICln on serine residues 193, 195, and 197 (Fig. 2F).

The substitution of all three serines by alanine residues prevented the phosphorylation of pICln by active ULK1 (Fig. 2G). Also, pharmacological inhibition of active ULK1 with the ULK1/ULK2 specific inhibitor MRT67307 (Petherick et al., 2015) significantly reduces

phosphorylation of pICln (Fig. 2G). Taken together, we demonstrated by amino acid exchange within pICln as well as ULK1 specific inhibition, ULK1 siRNA, and ULK1 kinase-dead mutant that ULK1 binds and phosphorylates pICln on newly identified sites within its C-terminal region.

ULK1 dependent phosphorylation of pICln regulated binding of pICln towards SmG

pICln is part of the methylosome complex (Friesen et al., 2001b, Meister et al., 2001b). For this, we investigate to which extent phosphorylation of pICln does affect PRMT5-mediated methylation of Sm proteins. Hence we performed *in vitro* methylation assays using the substrate proteins SmB, D1, and D3 with or without the presence of pICln wildtype and phosphomutants thereof. For the methylation of SmB and D3, the presence of pICln does not seem to be necessary, confirming so far findings by Neuenkirchen and colleagues (Neuenkirchen et al., 2015). This is in clear contrast to SmD1, as SmD1 is only methylated in the presence of pICln. However, comparing the methylation efficiency of Sm proteins, we see no difference using pICln wildtype or the phosphomutants thereof (SD Fig. 3A-B). To this end methylation of SmD1 is pICln-dependent but independent of the phosphostatus of pICln (SD Fig. 3B).

Figure 3

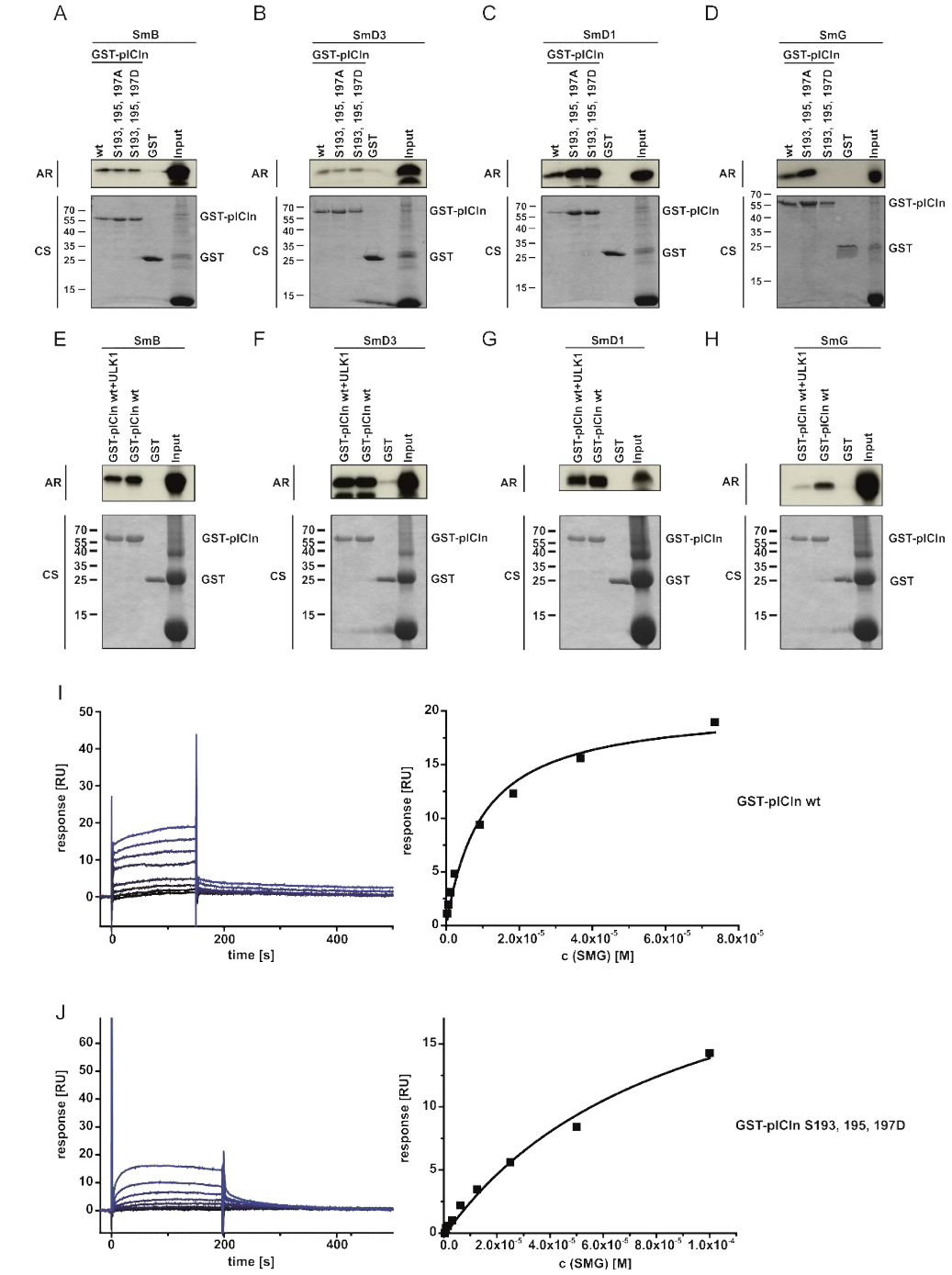

Figure 3. ULK1 dependent phosphorylation of pICln regulated binding of pICln towards SmG. (A-D) *In vitro* translated L-[35S]-Methionine labeled Sm Proteins D1, D3, B, and G were applied to an interaction assay with GST-pICln wt and phospho mutants purified from *E. coli*. After incubation for 1.5 h at 4 °C and two times washing, purified proteins were separated by Tris/Glycine-SDS-PAGE and analyzed by autoradiography. (E-H) *In vitro* translated L-[35S]-Methionine labeled Sm Proteins D1, D3, B, and G were applied to an interaction assay with GST-pICln wt and GST-pICln pre-phosphorylated by ULK1. Pre- phosphorylation of pICln was performed for 1.5 h with 100 ng of active ULK1. After incubation for 1.5 h at 4 °C with translated Sm Proteins and two times washing, purified proteins were separated by Tris/Glycine- SDS-PAGE and analyzed by autoradiography. (I; J) SmG (analyte), and GST-pICln (ligand) wild type and aspartate mutant were purified from *E. coli*. Affinity dissociation constants were analyzed by surface plasmon resonance by steady-state analysis (SmG – GST-pICln wt, Kd 11.5 ± 1.5 µM; SmG – GST-pICln S193,195,197D, Kd 84.7 ± 14.7 µM; n = 3). AR: autoradiography, CS: coomassie blue staining.

Extensive and conclusive analysis by A. Chari and coworkers revealed the function of pICln as an assembly chaperone in the biogenesis of UsnRNPs (Chari et al., 2008). In this function, pICln forms two subcomplexes: One consisting of pICln, the Sm proteins B and D3 (SmB/D3) and the other subcomplex consists of pICln and the Sm proteins D1, D2, E, F, and G (SmD1/D2/E/F/G, see also Fig. 8). In the latter case pICln directly binds to SmD1 and G and builds a highly stable hexameric ring structure, also known as 6S complex (Fisher et al., 1985, Friesen et al., 2001b, Chari et al., 2008). Consequently, we investigated to which extend the phosphorylation status of pICln affects its binding to the Sm proteins B, D3, D1, and G. To this end, we used GST-tagged recombinant pICln and phosphomutants thereof to analyze the interaction with *in vitro* translated ^{35}S-labelled SmB, SmD3, SmD1 and SmG (Fig. 3A-D). Neither the phospho-inactivating serine-to-alanine nor the phospho-mimicking serine-to-aspartate substitutions at positions 193, 195, and 197 affected the binding capacity of pICln to the Sm proteins B, D3, and D1 (Fig. 3A-C). In striking contrast, the phospho-mimicking aspartate mutations of pICln displayed no interaction with SmG, whereas the phospho-inactivating alanine mutations of pICln exhibited increased binding to SmG (Fig. 3D).

In addition to these results binding of GST-pICln wildtype, phosphorylated by ULK1 does not effect association to the Sm proteins B, D3, and D1 (Fig. 3E-G). In contrast, pICln, phosphorylated by ULK1 shows dramatically reduced interaction with SmG compared to unphosphorylated pICln (Fig. 3H).

These results were further corroborated by surface plasmon resonance measurement. The affinity of wild type pICln for SmG yielded a dissociation constant (K_d) of 11.5 ± 1.5 µM (Fig. 3I). The introduction of phospho-mimicking aspartate mutations (S193, 195, 197D) within pICln reduced the affinity for SmG by almost one order of magnitude to a K_d of 84.7 ± 14.7 µM (Fig. 3J).

Summarizing results so far, we see that phosphorylation of pICln in its C-terminal part by ULK1 does not alter binding properties to SmD1 but does block its binding towards SmG.

Phosphorylation of pICln by ULK1 alters the structure of the 6S complex

These findings are in line with Grimm and colleagues, who proposed the pICln-SmG contact surface as a “mobility hotspot” of the 6S structure by *in silico* prediction (Grimm et al., 2013). From their comprehensive work, the authors concluded that the 6S ring structure has

to be transiently opened on the pICln-SmG interface to be able to load Sm proteins onto the SMN complex. To evaluate if phosphorylation of pICln within the 6S complex also alters its composition or structure *in vivo* we used analytical ultracentrifugation (AUC). AUC analysis is an absolute method to determine the size and shape of macromolecules in solution. The sedimentation of macromolecules in a centrifugal force field depends on molecular mass, as well as shape according to the Svedberg equation (SV) (Chaturvedi et al., 2017). SV analysis was applied to detect potential differences in the conformations of wild type pICln complex and pICln complex with S193, S195, S197D mutations. The used GFP tagged phosphomutants of pICln can interact with its well-known binding partners PRMT5, WD45, and SMN to the same extend as wildtype pICln does (SD Fig. 3A). Also, no differences in interaction with Sm proteins or methylation efficiency could be detected (SD Fig. 3A; B), ensuring the functionality of used mutated constructs. A closed ring structure is expected to sediment faster than an elongated open ring structure of the same mass because of less friction. For this experiment, a GFP variant of pICln was used. This specific labeling allowed tracing of pICln in its diverse states during ultracentrifugation, using SV-AUC equipped with a fluorescence detection system, in the presence of cytoplasm extract. Other non- fluorescing proteins or macromolecules also present in the S100 extract are invisible. As shown in Figure 4A, the SV analysis of the wild type complex revealed a major species with a weight averaged s_{app}-value of 4.7 S and a minor species at 16.1 S. For the mutated complex, however, only one species with a weight averaged s_{app}-value of 3.5 S was detected. Concomitantly, the weight average frictional ratio (f/f_0), which is informative on the hydrodynamic shape of a molecule in solution, was higher in the c(s) analysis for the serine- to-aspartate mutant pICln complex. Assuming that the molar mass of the complex stays constant during centrifugation, the SV analysis suggests that the mutant form of the complex has a different, more elongated conformation than the wild type complex. Since density and viscosity of the cytoplasm extract were unknown only the relative differences between wild type and mutant complex can be reported as apparent sedimentation coefficients $s_{app.}$. These results are in agreement with our model of a closed ring conformation for the wild type and an open ring structure for the serine-to-aspartate mutant pICln-complex (for the model also see Fig. 8).

Figure 4

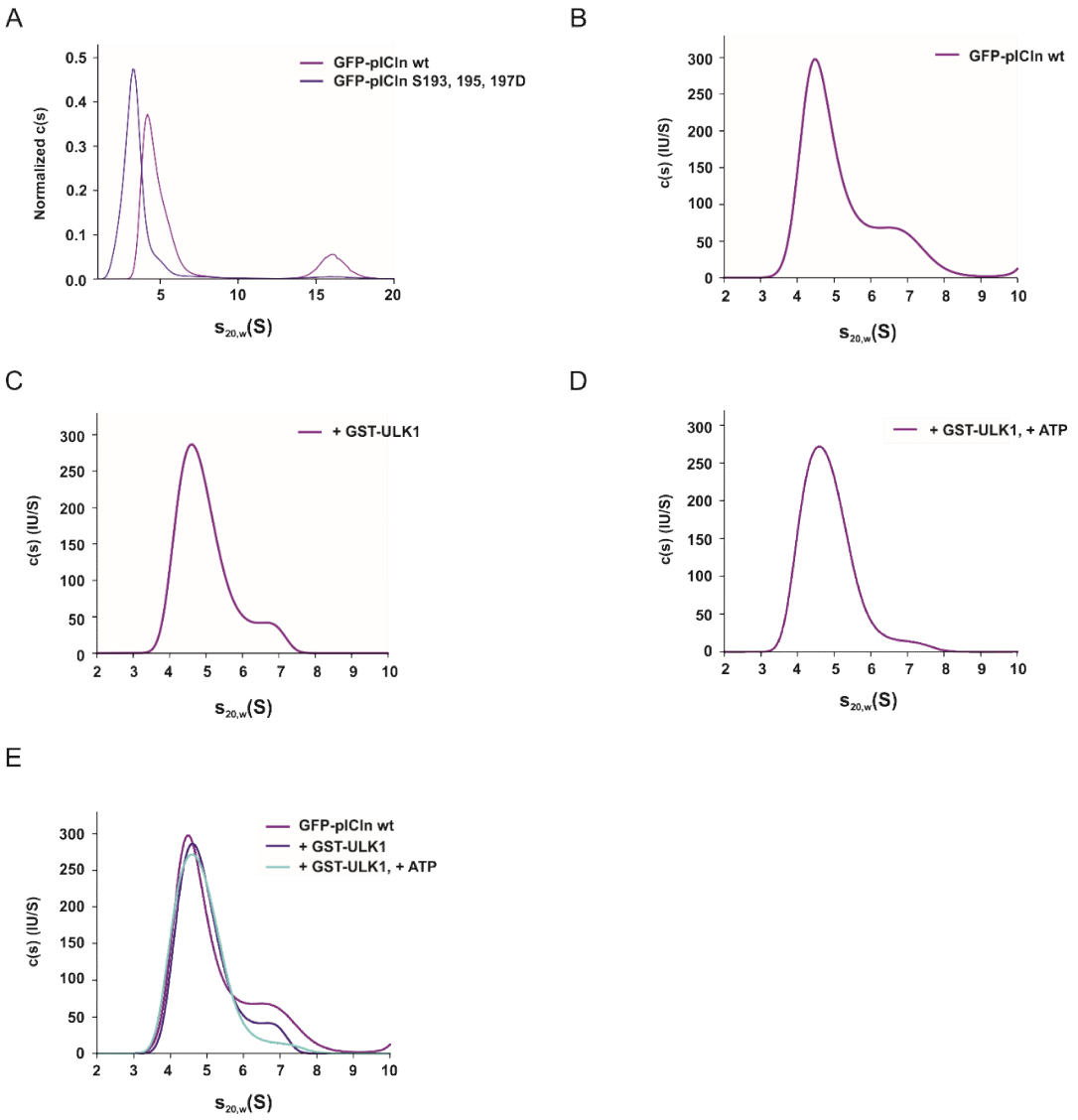

Figure 4. Phosphorylation of pICln by ULK1 alters the structure of the 6S complex. (A) Sedimentation velocity (SV) analysis of GFP-pICln wild type and aspartate mutant in S100 extracts. The c(s) distributions for wild type pICln complex (magenta curve) and pICln complex with S193, S195, S197D mutations (blue curve) obtained from SV analysis at 40,000 rpm at 20 °C for 5 hours are shown. For better comparability normalization according to the area under the curve was done. (B-E), Size exclusion chromatography of Flp-In T-REx 293-GFP-pICln S100 extract using a Superdex 200 increase column was performed following a sedimentation velocity analysis (B) for GFP-pICln wild type of the 6S fractions B13 and B12. (C) Sedimentation coefficient distribution for wild type pICln complex incubated with recombinant active GST-ULK1. (D) Sedimentation coefficient distribution for wild type pICln complex incubated with recombinant active GST-ULK1 and ATP. (E) Overlay of c(s) distributions for all three samples acquired under the same conditions. All measurements were performed at 40,000 rpm at 20 °C for 5 hours. See also Supplementary Figure S3.

To examine whether the phosphorylation of pICln leads to a conformational change of the 6S complex and thus to a reduced sedimentation velocity, we purified the 6S complex containing GFP-pICln by size exclusion chromatography (pooled fractions B12 and B13, SD Fig. 3C) and incubated it with active GST-ULK1 and ATP. As a control, we included

the active kinase ULK1 but no additional ATP to demonstrate that the observed effects are not due to the presence of the kinase only but require phosphorylation of pICln. As can be seen from Figure 4B the wild type pICln complex displayed a heterogeneous distribution pattern in our experiment, with a major peak at 4.5 S and a shoulder peak at about 6.3 S. A very similar distribution was observed in pICln complex incubated with ULK1 (Fig. 4C). However, the addition of ATP to pICln complex with ULK1 significantly reduced the fraction of the species at ~6.3 S, as depicted in Fig. 4D, suggesting that the closed-ring structures have been converted to open-ring structures in the presence of ULK1 and ATP.

The measured *s*-value of the complex in the present study is in agreement with the literature for the 6S ring-shaped complexes (Grimm et al., 2013). The SV analysis demonstrated that the phospho-mimicking pICln complex is indeed more elongated than the wild type complex (Fig. 4A). Additionally, we could show that phosphorylation of pICln within the wild type 6S complex by ULK1 favors the formation of open ring structures (Fig. 4B-E).

Phosphorylated pICln is not able to build the 6S complex and to promote the subsequent Sm protein transfer onto the SMN complex

To prove whether the phospho-dependent interaction between pICln and SmG is crucial for the biogenesis of the 6S complex *in vivo*, we performed pulldown assays with recombinant GST-tagged wild type, phospho-mimicking (S193, 195, 197D) and -inactivating (S193, 195, 197A) pICln proteins in HEK293T derived cytosolic extracts. Pulldowns were followed by protein identification and relative protein quantification by mass spectrometry analysis (for details see materials and methods section). Thus both, the phospho-mimicking and -inactivating pICln mutants pulled down the same amount of the SmB/D3 subcomplex normalized to pICln wild type (Fig. 5A). In contrast, all components of the 6S complex (SmD1/D2/E/F/G) displayed a substantial reduction in binding to phospho-mimicking pICln mutant whereas the binding capacity of the phospho-inactivating pICln mutant was only slightly affected (Fig. 5A). These data underscore that the phosphorylation status of pICln represents a crucial event in the assembly of the 6S complex: phosphorylated pICln is not able to bind SmD1/D2/E/F/G to the same extent as non-phosphorylated pICln.

Figure 5

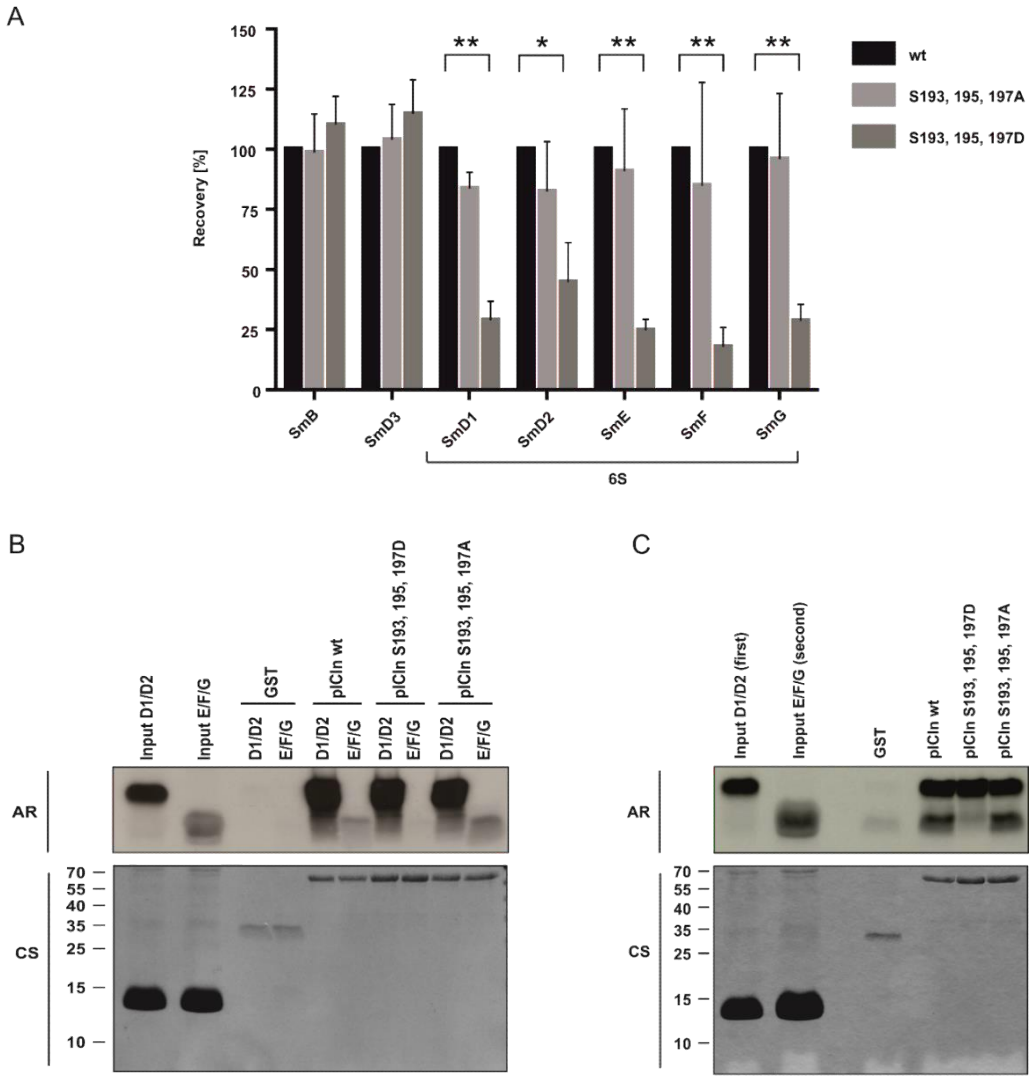

Figure 5. Phosphorylated pICln is not able to build the 6S complex and to promote the subsequent Sm protein transfer onto the SMN complex. (A) Pulldown experiments using GST-pICln wild type and phospho mutants were executed in HEK293T S100 extract overnight at 4 °C and co-purified Sm proteins were quantified by mass spectrometry and normalized to pICln wild type (LC-MS/MS; * $p<0.05$; ** $p<0.01$). (B) Sm proteins D1, D2, E, F, and G were *in vitro* translated and labeled with L-[35S]-Methionine. D1/D2 and E/F/G were pre-incubated for 1 h at 30 °C and applied to an interaction assay with GST-pICln wt and phospho mutants purified from *E. coli*. Following incubation for 1.5 h at 4 °C and 3 times washing purified proteins were separated by Tris/Glycine-SDS-PAGE and analyzed by autoradiography. (C) Sm proteins D1, D2, E, F, and G were *in vitro* translated and labeled with L-[35S]-Methionine. To form the 6S structure D1/D2 and E/F/G were pre-incubated for 1 h at 30 °C. To assess the influence of pICln as "assembly chaperone" Sm protein complex D1/D2 was first incubated (1 h at 4 °C) using GST-pICln wt or phospho mutants purified from *E. coli*. After three times washing of the resulting pICln- SmD1/D2 complex, SmE/F/G complex was added to the mixture for further 1 h at 4 °C. After 3 times washing purified proteins were separated by Tris/Glycine-SDS- PAGE and analyzed by autoradiography. AR: autoradiography, CS: coomassie blue staining.

Neuenkirchen et al. postulate a model in which pICln binds first to SmD1 and D2 and recruits it for methylation by PRMT5/WD45. After methylation of SmD1 pICln further recruits the subcomplex of SmE/F/G to assemble the final 6S complex that stays associated with the

PRMT5 complex (Neuenkirchen et al., 2015). Beyond that, we could now show that ULK1 interacts with the PRMT5/6S complex and phosphorylates the C-terminus of pICln. To test the influence of ULK1 mediated pICln phosphorylation towards the biogenesis of the 6S complex, we executed direct binding studies. For this, we used GST-tagged recombinant pICln and phosphomutants thereof to investigate the interaction with *in vitro* translated ^{35}S-labeled preformed Sm protein subcomplexes D1/D2 and E/F/G (Fig. 5B-C). Neither the serine-to-alanine nor the phospho-mimicking serine-to-aspartate substitutions at positions 193, 195, and 197 affected the binding capacity of pICln to the SmD1/D2 subcore (Fig. 5B). In contrast, the phospho-mimicking aspartate mutant of pICln did not interact with the SmE/F/G subcore in comparison to the serine-to-alanine mutant and the wild type protein (Fig. 5B). Next, we reconstituted the entire 6S complex in a stepwise process, using *in vitro* translated ^{35}S-labelled Sm proteins. In a first step, we incubated GST-tagged recombinant pICln or phosphomutants with *in vitro* translated ^{35}S-labelled subcomplex SmD1/D2. In a subsequent step and after intensive washing, we added *in vitro* translated ^{35}S-labelled subcomplex SmE/F/G. Consistent with our previous data Sm proteins E/F/G only bind to the pICln-SmD1/D2 subcomplex with the wild type protein and the serine-to-alanine mutant of pICln, but not to the pICln-SmD1/D2 subcomplex with the serine-to-aspartate mutant (Fig. 5C). We also observed that the binding of the SmE/F/G subcomplex to pICln wt and alanine mutant was increased after incubation with the SmD1/D2 subcomplex (Fig. 5B-C), supporting the model of a sequential binding of Sm protein subcomplexes during 6S assembly.

Our results demonstrate that binding of single Sm proteins, Sm-subcomplexes as well as the formation of a reconstituted entire 6S complex depend on the phosphorylation status of the C-terminus of pICln and its interaction with SmG.

Inhibition of ULK1 results in a decreased number of Cajal bodies

Complementary to the results before, ULK1 inhibition should result in the reduction of nuclear UsnRNP levels. Therefore we treated HEK293T cells with ULK1 and ULK2 siRNA followed by immunofluorescence using SMN and Coilin specific antibodies to visualize the quantity of Cajal bodies (CBs) as a marker of snRNP assembly capability (Nizami et al., 2010, Strzelecka et al., 2010, Mao et al., 2011) (Fig. 6A, B). The number of CBs per nucleus (mean) was significantly decreased in ULK1 knockdown HEK cells (1.10) compared to

HEK control cells (1.54) without cumulative effect by concurrent knockdown for ULK2 (1.10 compared to 1.06) (Fig. 6A. B).

Figure 6

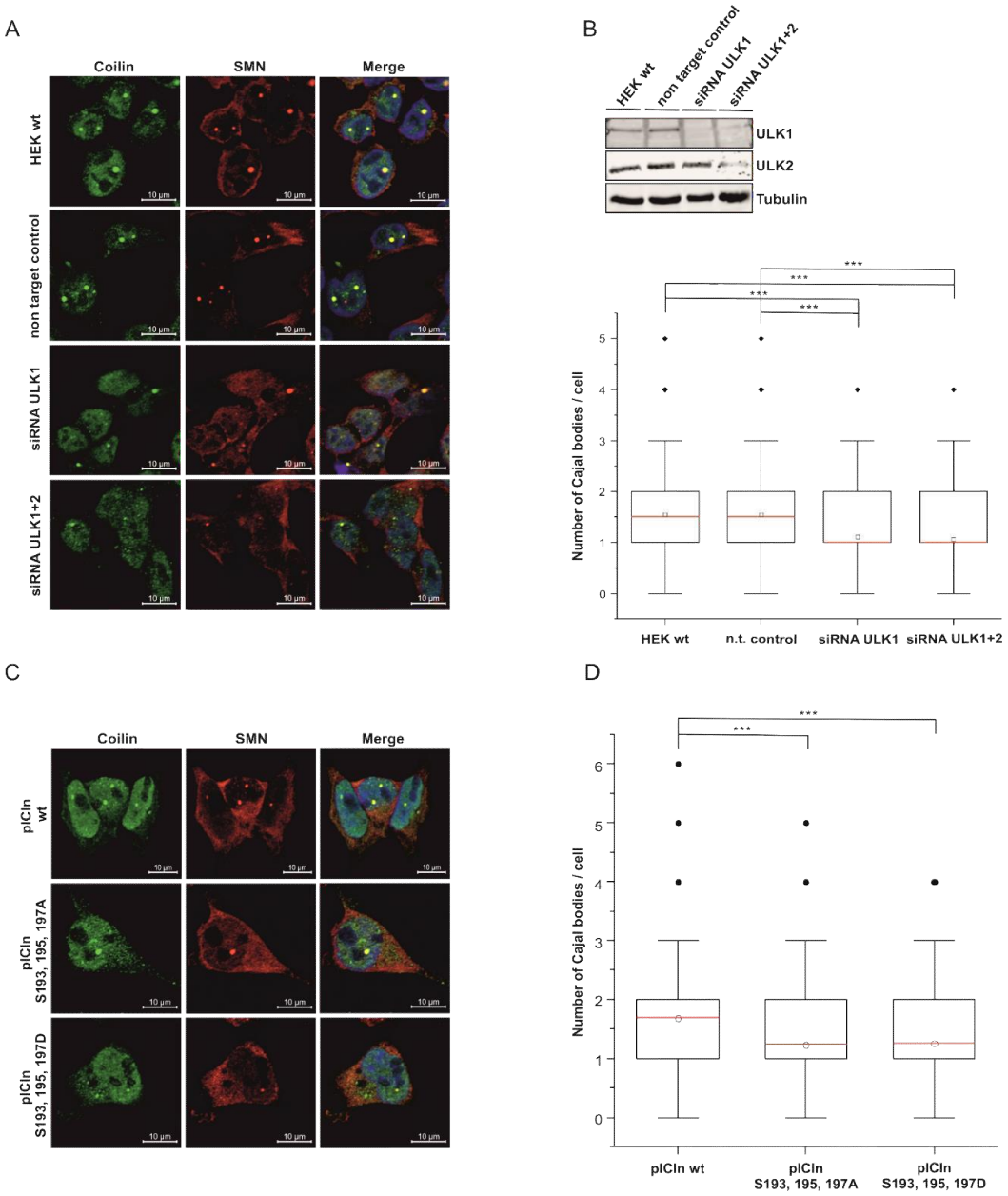

Figure 6. Decrease of endogenous ULK1 results in a decreased number of Cajal bodies. (A; B) HEK293T cells were treated with 50 nM ULK1,2 siRNA or non-targeting control for 48 h. (A; C) The cells were fixed and Cajal bodies were visualized with antibody staining against Coilin (green) and SMN (red). The DNA was stained with DAPI (blue). (B) Cell lysates of siRNA treated cells were analyzed by Tris/Glycine-SDS-PAGE using antibodies against ULK1, ULK2, and Tubulin. Downregulation of ULK1 causes a reduction in the snRNP storage pool. In the boxplot diagram, the "box" represents 25-75% of all values and the mean (red), standard deviation, and out layers are visualized. HEK293T cells show an average of 1.54 (n=500) Cajal bodies. Treatment of cells with siRNA caused a 1. significant decrease in the number of Cajal bodies. (C; D) The phosphorylation status of pICln influences the number of Cajal bodies per cell. (D) Overexpression of pICln in Flp-In T-Rex cells causes an increase in the number of Cajal bodies, mean 1.69 (n = 502). Phospho-mutants of pICln (S193, 195, 197A or D), cause a decrease in the number of Cajal bodies per cell. The p-value was calculated with Origin using the Mann-Whitney U test. ***P < 0.005; scale bars: 10 µm (A and C).

Comparable results were obtained when we investigated the number of CBs in HEK cells overexpressing phospho-mimicking (S193, 195, 197D) and -inactivating (S193, 195, 197A) pICln proteins (Fig. 6C, D). The mean of CBs in HEK Flp-In T-Rex cells overexpressing the pICln phosphomutants was decreased (1.22 for the alanine mutant and 1.26 for the aspartate mutant) compared to 1.64 in HEK Flp-In T-Rex cells overexpressing the wildtype protein (Fig. 6C, D). Immunostaining, as well as analysis of the composition of endogenous Sm proteins, thus clearly shows alter composition and content of UsnRNPs upon ULK1 dependent phosphorylation of pICln in the cell.

ULK1 regulates UsnRNP biogenesis

As the phosphorylation status of pICln influences the nuclear Cajal bodies, we asked whether ULK1 directly regulates the UsnRNP assembly activity. By using native polyacrylamide gel electrophoresis we demonstrate that immobilized GFP-pICln derived from HEK Flp-In T-Rex cells can generate U1snRNP cores super-shifted by the anti-Sm antibody Y12 upon incubation with a human *in vitro* transcribed ^{32}P-labeled U1snRNA (Fig. 7A compare lanes 2 and 3). This assembly reaction is remarkably increasable by adding ATP (Fig. 7A compare lanes 3 and 5) confirming the ATP dependency of the UsnRNP biogenesis by previous studies (Meister et al., 2001a, Pellizzoni et al., 2002b, Grimmler et al., 2005b). It also implies that the corresponding kinase is associated with the immunoprecipitated complex, capable of UsnRNP assembly. The addition of purified ULK1 to the immobilized GFP-pICln/U1 snRNA mixture without extra ATP does not affect the assembly efficiency (Fig. 7A compare lanes 3 and 7). In striking contrast, the simultaneous addition of ULK1 and ATP strongly increases the ability of U1 snRNP core biogenesis (Fig. 7A lane 9). UsnRNP assembly efficiency increases up to 2.6 fold upon the addition of ATP and active ULK1 (see enlarged part of Fig. 7A). In striking contrast, the addition of active ULK2 has no stimulatory effect of the UsnRNP assembly efficiency (Fig. 7B).

Figure 7

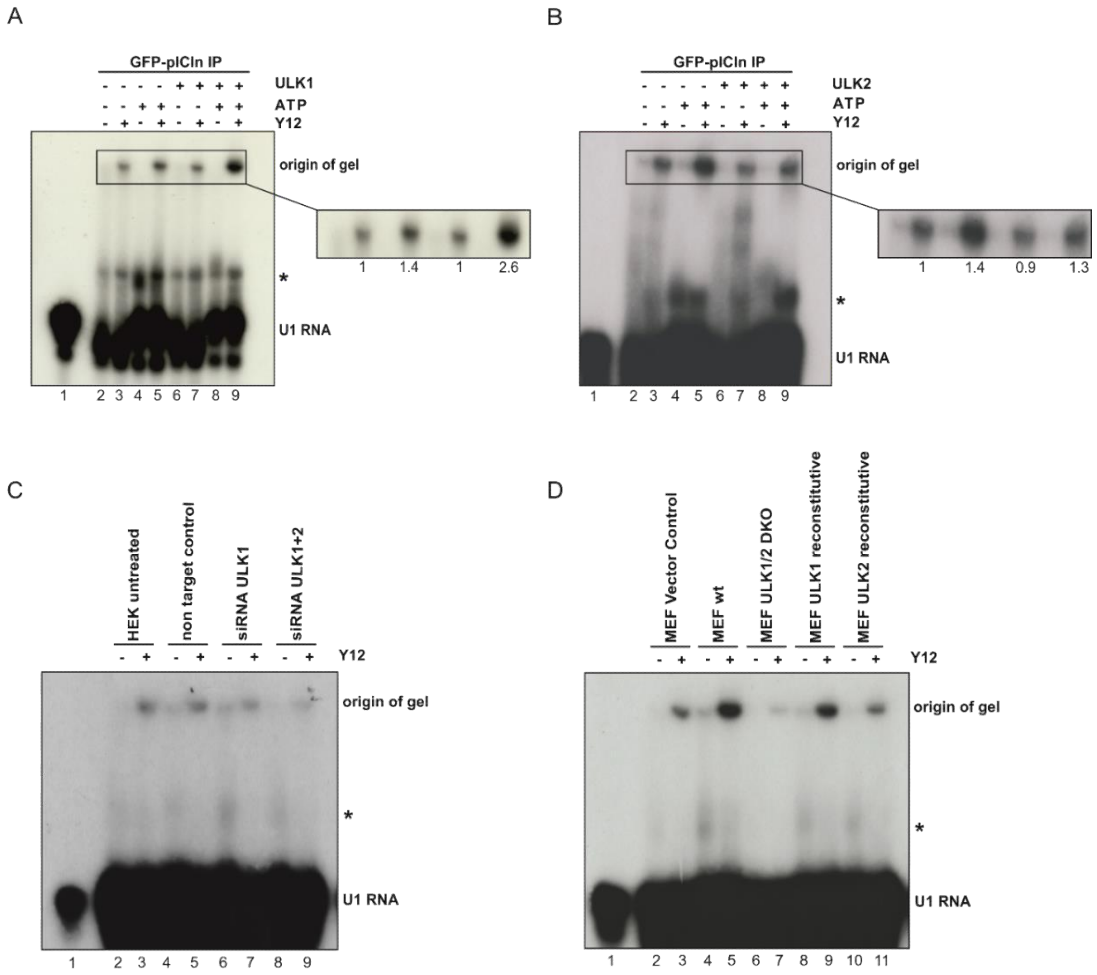

Figure 7. ULK1 phosphorylation of pICln regulates UsnRNP biogenesis. (A; B) GFP-pICln IP contains all proteins necessary for U1 snRNP core assembly. *In vitro* transcribed U1 snRNA labeled with 10 µCi [32P]-UTP was incubated with GFP-pICln IP. After incubation samples were directly analyzed by native gel electrophoresis (2, 4, 6, 8), or the same samples were subjected to supershift analysis with the Y12 antibody to show the specific formation of snRNPs (3, 5, 7, 9). The formation of snRNPs was quantified with Image Studio to compare the efficiency of the snRNP biogenesis. Adding ATP to the GFP-pICln IP increases efficiency (1.4) while adding ATP and ULK1 (2.6) leads to the highest efficiency in snRNP formation compared to the GFP-pICln IP alone. Adding ULK2 and ATP to the GFP-pICln IP caused no effect at all (1.3). (C) *In vitro* transcribed U1 snRNA labeled with 10 µCi [32P]-UTP was incubated with S100 extract from HEK293T cells treated with siRNA against ULK1, ULK 1+2, or a non-targeting control. After a native gel electrophoresis supershift analysis was performed using the Y12 antibody. (D) S100 extract from Mouse Embryonic Fibroblasts (MEF´s) lacking ULK1/2, or reconstituted with vector control, ULK1 or ULK2 were incubated with [32P] labeled U1 snRNA, after a native gel electrophoresis supershift analysis occurred.

Complementary to these results HEK cells treated with siRNA against ULK1 and ULK1/ULK2 shown reduced assembly UsnRNP assembly activity (Fig. 7C). A comparable reduction was observed in constitutive ULK1/ULK2-double knockout MEF cells (Fig. 7D). Only double-knockout cells reconstituted with ULK1 but not ULK2 alone can assemble snRNPs with comparable efficiency as MEF wild-type cells do (Fig. 7D).

This data demonstrates that an isolated, purified assembly complex directly is capable to increase UsnRNP biogenesis upon the addition of ATP. It further clearly shows that only ULK1 stimulates UsnRNP biogenesis by direct phosphorylation of pICln. To test whether the observed snRNP biogenesis effects are ULK1-dependent and not due to an overall autophagy-dependent effect we used ATG3 knockouts MEF cells (SD Fig. 4A). Autophagy is completely blocked in this cell line (Sou et al., 2008) (SD Fig. 4A). However, we could detect any difference concerning snRNP assembly activity between normal or ATG3 knockout cells (SD Fig. 4B).

DISCUSSION

Although the ATP dependency of the Sm core assembly and phosphorylation of some key components within the UsnRNP pathway has been known for many years (Meister et al., 2001a, Grimmler et al., 2005a, Husedzinovic et al., 2014, Husedzinovic et al., 2015), neither the responsible kinases nor the structural or mechanistic consequences of the modified residues were known so far. In our study, we identified the Ser/Thr kinase ULK1 as a functional component of the PRMT5 complex and as an essential key regulator of UsnRNP biogenesis by specific phosphorylation of pICln.

The identified phospho-serines 193, 195, and 197 are located in a region of pICln that, based on crystal structures, is not known for Sm protein binding so far. Certainly, the structure determination of pICln has only been executed with pICln of *D. melanogaster*, C-terminal deletions of pICln of *D. melanogaster* (Chari et al., 2008, Grimm et al., 2013, Pelz et al., 2015), or with the isolated N-terminus of canine pICln (Schedlbauer et al., 2003, Furst et al., 2005). Recent studies also have determined the C-terminus of canine pICln by NMR (Schedlbauer et al., 2011). The authors demonstrated that the C-terminus of pICln is highly conserved in vertebrates and natively unstructured with secondary structure elements. These unstructured regions often function as flexible linkers in the assembly of macromolecular systems regulated by post-translational modifications (Dyson et al., 2005). The lack of essential elements of the intrinsic disorder region in initial experiments based on *D. melanogaster* pICln may explain why this region was not addressed for Sm protein binding in the human system so far (SD Fig. 5) (Corpet, 1988). It also may explain the difficulties to solve the crystal structure of the human 6S intermediate complex, containing flexible unstructured regions (Pelz et al., 2015). In the capacity of an assembly chaperone of Sm

proteins (Chari et al., 2008), the conformational flexibility of pICln generated by the disordered C-terminus is an important property in the consecutive transfer of the Sm proteins onto the SMN complex. The work presented here specifically does focus on the exclusive use of human proteins and human snRNA to assess the status and mechanism of human Sm core assembly and UsnRNP biogenesis.

The newly identified ULK1-dependent phosphorylation sites within the C-terminus of pICln regulate the contact surface of pICln and SmG (Fig. 2F, 3D, H-J); consequently, they also influence binding properties towards the SmE/F/G subcomplex (Fig. 5B, C). Consistent with these are the results from the analytical ultracentrifugation analysis, demonstrating that the phosphorylation of purified cytoplasmic 6S complex by ULK1 favors the formation of an open ring structure (Fig. 4E). These results prove the pICln-SmG contact surface as a mobility hotspot of the 6S complex (Grimm et al., 2013). Our data also provide information on the composition and conformation of native human 6S complex and its functional regulation by phosphorylation of pICln.

Figure 8

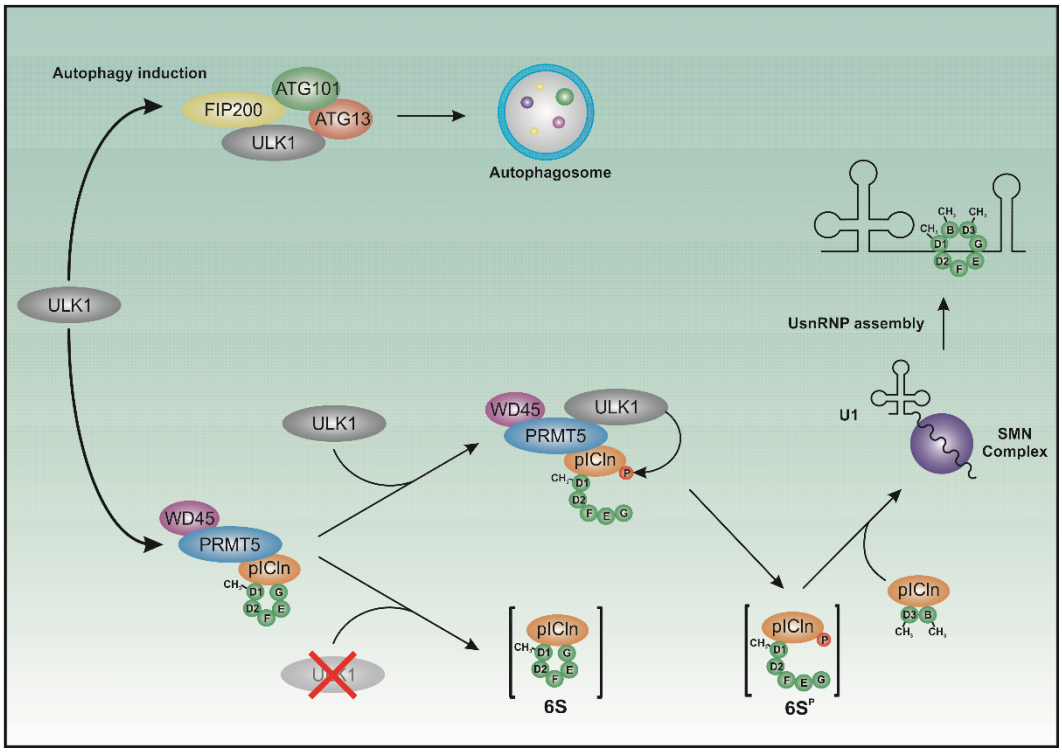

Figure 8. Schematic illustration summarizing the new role of ULK1 in the UsnRNP assembly as well as its well-known function in autophagy induction.

We further show that ULK1 dependent phosphorylation sites within the C-terminus of pICln affect the interaction between pICln and SmG. Recent studies convincingly demonstrated that the SMN subcomplex consisting of SMN and GEMIN2 can directly bind the Sm pentamer via GEMIN2 (Zhang et al., 2011). The authors pointed out that there probably exist at least two sequential occurring mechanisms of Sm pentamer binding: A first step by binding to pICln, as second sequential one by binding to GEMIN2. Future studies of pICln/phospho-pICln and the SMN/SMN subcomplexes are necessary to address the detailed mechanism of how phosphorylated pICln contributes to this step of UsnRNP assembly.

With the autophagy activating kinase ULK1 we identified an unknown player in this complex pathway. Although our data demonstrate a new regulatory function of ULK1 independent of autophagy, the latest studies were also able to link the autophagy pathway with UsnRNP biogenesis by providing evidence of an autophagosome mediated Sm protein degradation pathway during the early phase of UsnRNP biosynthesis (Prusty et al., 2017). The authors showed that only the Sm proteins D1, D2, D3, and B (but not Sm proteins E, F, and G) are degraded by autophagy to avoid toxic Sm protein aggregation in a scenario of pICln deficiency prohibiting disturbances in UsnRNP biogenesis. Our results now show that the autophagy activating Ser/Thr kinase ULK1 attributes an additional key regulatory function in UsnRNP biogenesis by direct phosphorylation of pICln. Phosphorylation of pICln by ULK1 and not by ULK2 results in an enhancement of UsnRNP biogenesis (Fig. 7A, B). Convenient to this, in cell lines deficient for ULK1 and ULK2, the UsnRNP biogenesis is dramatically reduced and could be reestablished by reconstitution of ULK1 only (Fig. 7D). If ULK1 dependent phosphorylation of pICln is blocked the Cajal bodies in the nucleus are altered (Fig. 6A-D). The observations from Prusty and colleagues together with our results demonstrate that not only the amount of free available pICln but also the phosphorylation status of pICln is a critical parameter for the storage pool of Sm proteins and an efficient assembly reaction. It will be right of interesting to investigate in future eg. by using ULK1 deficient cells lacking pICln phosphorylation, how the Sm protein balance is regulated, but even more of interest to answer the question of how the activity of ULK1 is regulated in this pathway. In this context, it is very much relevant to note, that recent studies already demonstrated a connection of the intracellular energy sensor mTOR to the spliceosomal proteins, especially to SmE (Quidville et al., 2013) and to motor neuron development in context to SMA (Piras et al., 2017).

The data presented in this work provide the molecular basis of how the transient opening of the 6S ring, catalyzed by ULK1, lowers the energy barrier during UsnRNP biogenesis. The provided data prove the contact area of pICln and SmG as the predetermined breaking point of the 6S ring to initiate the transfer of the open 6S entity onto the SMN complex *in vivo* and show that ULK1 mediated phosphorylation is a crucial regulatory and essential step of efficient UsnRNP biogenesis.

Our data also show that the PRMT5-ULK1-complex conjoins two distinct post-translational mechanisms of regulation in one complex: Symmetrical dimethylation and phosphorylation of the 6S complex to allow for the efficient and highly ordered assembly of UsnRNPs.

A highly ordered and efficient assembly reaction is a prerequisite to keep the responsive gene to protein balance by mRNA transcription of a cell. Mutations or metabolic disorders within this spliceosomal process lead to a dramatic medical outcome like in amyotrophic lateral sclerosis (ALS), *Retinitis pigmentosa,* or spinal muscular atrophy (SMA) in humans. The evolutionary conserved Unc-51-like kinase (ULK1) was first identified in *C. elegans* as the main factor in early neuronal differentiation and axonal elongation (Ogura et al., 1994). The new mechanism of phosphorylation of pICln by ULK1 may help to explain and address specific neuronal aspects associated with inefficient or reduced UsnRNP assembly in this kind of neuronal human diseases. Intensive work will be necessary to understand in more detail the molecular impact of ULK1 within neuronal disorders and the regulation of ULK1activity in this context.

AVAILABILITY

All data and constructs are available upon request to christoph.peter@uni-duesseldorf.de

SUPPLEMENTARY DATA

Supplementary Data are available at NAR online.

ACKNOWLEDGEMENT

We thank Alexander Lang for technical help and critical discussion on the manuscript. We also thank our colleagues Maria Jose Mendiburo, Niklas Berleth, Philip Böhler, and

Wenxian Wu for comments on the manuscript. Furthermore, we thank Alexander K. Büll and Nicola Vettore for their technical support.

FUNDING

Stefan Klinker and Dieter Willbold received funding from the Deutsche Forschungsgemeinschaft (DFG) via the SFB974 and Dieter Willbold received funding from the DFG via the SFB1208. Financial support of Luitgard Nagel-Steger was provided by "Portfolio Technology and Medicine", the Helmholtz-Validierungsfonds of the Impuls and Vernetzungs-Fonds der Helmholtzgemeinschaft.

CONFLICT OF INTEREST

The authors declare that they have no conflict of interest.

REFERENCES

Brautigam, C. A. 2015. *'Calculations and Publication-Quality Illustrations for Analytical Ultracentrifugation Data', **Methods Enzymol**, 562: 109-33.*

Chan, E. Y., A. Longatti, N. C. McKnight, and S. A. Tooze. 2009. *'Kinase-inactivated ULK proteins inhibit autophagy via their conserved C-terminal domains using an Atg13-independent mechanism', **Mol Cell Biol**, 29: 157-71.*

Chari, A., and U. Fischer. 2010. *'Cellular strategies for the assembly of molecular machines', **Trends Biochem Sci**, 35: 676-83.*

Chari, A., M. M. Golas, M. Klingenhäger, N. Neuenkirchen, B. Sander, C. Englbrecht, A. Sickmann, H. Stark, and U. Fischer. 2008. *'An assembly chaperone collaborates with the SMN complex to generate spliceosomal SnRNPs', **Cell**, 135: 497-509.*

Chaturvedi, S. K., J. Ma, H. Zhao, and P. Schuck. 2017. *'Use of fluorescence-detected sedimentation velocity to study high-affinity protein interactions', **Nat Protoc**, 12: 1777-91.*

Corpet, F. 1988. *'Multiple sequence alignment with hierarchical clustering', **Nucleic Acids Res**, 16: 10881-90.*

Dignam, J. D., R. M. Lebovitz, and R. G. Roeder. 1983. *'Accurate transcription initiation by RNA polymerase II in a soluble extract from isolated mammalian nuclei', **Nucleic Acids Res**, 11: 1475-89.*

Dubiel, D., W. Bintig, T. Kahne, W. Dubiel, and M. Naumann. 2017. *'Cul3 neddylation is crucial for gradual lipid droplet formation during adipogenesis', **Biochim Biophys Acta**, 1864: 1405-12.*

Dyson, H. J., and P. E. Wright. 2005. *'Intrinsically unstructured proteins and their functions', **Nat Rev Mol Cell Biol**, 6: 197-208.*

Fischer, U., Q. Liu, and G. Dreyfuss. 1997. *'The SMN-SIP1 complex has an essential role in spliceosomal snRNP biogenesis',* ***Cell****, 90: 1023-9.*

Fisher, D. E., G. E. Conner, W. H. Reeves, R. Wisniewolski, and G. Blobel. 1985. *'Small nuclear ribonucleoprotein particle assembly in vivo: demonstration of a 6S RNA-free core precursor and posttranslational modification',* ***Cell****, 42: 751-8.*

Friesen, W. J., S. Paushkin, A. Wyce, S. Massenet, G. S. Pesiridis, G. Van Duyne, J. Rappsilber, M. Mann, and G. Dreyfuss. 2001. *'The methylosome, a 20S complex containing JBP1 and pICln, produces dimethylarginine-modified Sm proteins',* ***Mol Cell Biol****, 21: 8289-300.*

Friesen, W. J., A. Wyce, S. Paushkin, L. Abel, J. Rappsilber, M. Mann, and G. Dreyfuss. 2002. *'A novel WD repeat protein component of the methylosome binds Sm proteins',* ***J Biol Chem****, 277: 8243-7.*

Furst, J., A. Schedlbauer, R. Gandini, M. L. Garavaglia, S. Saino, M. Gschwentner, B. Sarg, H. Lindner, M. Jakab, M. Ritter, C. Bazzini, G. Botta, G. Meyer, G. Kontaxis, B. C. Tilly, R. Konrat, and M. Paulmichl. 2005. *'ICln159 folds into a pleckstrin homology domain-like structure. Interaction with kinases and the splicing factor LSm4',* ***J Biol Chem****, 280: 31276-82.*

Grimm, C., A. Chari, J. P. Pelz, J. Kuper, C. Kisker, K. Diederichs, H. Stark, H. Schindelin, and U. Fischer. 2013. *'Structural basis of assembly chaperone- mediated snRNP formation',* ***Mol Cell****, 49: 692-703.*

Grimmler, M., L. Bauer, M. Nousiainen, R. Körner, G. Meister, and U. Fischer. 2005. *'Phosphorylation regulates the activity of the SMN complex during assembly of spliceosomal U snRNPs',* ***EMBO Rep****, 6: 70-6.*

Grimmler, M., S. Otter, C. Peter, F. Muller, A. Chari, and U. Fischer. 2005. *'Unrip, a factor implicated in cap-independent translation, associates with the cytosolic SMN complex and influences its intracellular localization',* ***Hum Mol Genet****, 14: 3099-111.*

Guderian, G., C. Peter, J. Wiesner, A. Sickmann, K. Schulze-Osthoff, U. Fischer, and M. Grimmler. 2011. *'RioK1, a new interactor of protein arginine methyltransferase 5 (PRMT5), competes with pICln for binding and modulates PRMT5 complex composition and substrate specificity',* ***J Biol Chem****, 286: 1976-86.*

Hieke, N., A. S. Loffler, T. Kaizuka, N. Berleth, P. Bohler, S. Driessen, F. Stuhldreier, O. Friesen, K. Assani, K. Schmitz, C. Peter, B. Diedrich, J. Dengjel, P. Holland, A. Simonsen, S. Wesselborg, N. Mizushima, and B. Stork. 2015. *'Expression of a ULK1/2 binding-deficient ATG13 variant can partially restore autophagic activity in ATG13-deficient cells',* ***Autophagy****, 11: 1471-83.*

Hosokawa, N., T. Hara, T. Kaizuka, C. Kishi, A. Takamura, Y. Miura, S. Iemura, T. Natsume, K. Takehana, N. Yamada, J. L. Guan, N. Oshiro, and N. Mizushima. 2009. *'Nutrient-dependent mTORC1 association with the ULK1-Atg13-FIP200 complex required for autophagy',* ***Mol Biol Cell****, 20: 1981-91.*

Husedzinovic, A., B. Neumann, J. Reymann, S. Draeger-Meurer, A. Chari, H. Erfle, U. Fischer, and O. J. Gruss. 2015. *'The catalytically inactive tyrosine phosphatase HD-PTP/PTPN23 is a novel regulator of SMN complex localization',* ***Mol Biol Cell****, 26: 161-71.*

Husedzinovic, A., F. Oppermann, S. Draeger-Meurer, A. Chari, U. Fischer, H. Daub, and O. J. Gruss. 2014. *'Phosphoregulation of the human SMN complex',* ***Eur J Cell Biol****, 93: 106-17.*

Kambach, C., S. Walke, R. Young, J. M. Avis, E. de la Fortelle, V. A. Raker, R. Lührmann, J. Li, and K. Nagai. 1999. *'Crystal structures of two Sm protein complexes and their implications for the assembly of the spliceosomal snRNPs',* ***Cell****, 96: 375-87.*

Laemmli, U. K. 1970. *'Cleavage of structural proteins during the assembly of the head of bacteriophage T4',* ***Nature****, 227: 680-5.*

Lee, E. J., and C. Tournier. 2011. *'The requirement of uncoordinated 51-like kinase 1 (ULK1) and ULK2 in the regulation of autophagy',* ***Autophagy****, 7: 689-95.*

Liu, Q., U. Fischer, F. Wang, and G. Dreyfuss. 1997. *'The spinal muscular atrophy disease gene product, SMN, and its associated protein SIP1 are in a complex with spliceosomal snRNP proteins',* ***Cell****, 90: 1013-21.*

Löffler, A. S., S. Alers, A. M. Dieterle, H. Keppeler, M. Franz-Wachtel, M. Kundu, D. G. Campbell, S. Wesselborg, D. R. Alessi, and B. Stork. 2011. *'Ulk1-mediated phosphorylation of AMPK constitutes a negative regulatory feedback loop',* ***Autophagy****, 7: 696-706.*

MacLean, B., D. M. Tomazela, N. Shulman, M. Chambers, G. L. Finney, B. Frewen, R. Kern, D. L. Tabb, D. C. Liebler, and M. J. MacCoss. 2010. *'Skyline: an open source document editor for creating and analyzing targeted proteomics experiments',* ***Bioinformatics****, 26: 966-8.*

Mao, Y. S., B. Zhang, and D. L. Spector. 2011. *'Biogenesis and function of nuclear bodies',* ***Trends Genet****, 27: 295-306.*

Matera, A. G., and Z. Wang. 2014. *'A day in the life of the spliceosome',* ***Nat Rev Mol Cell Biol****, 15: 108-21.*

Meister, G., D. Bühler, R. Pillai, F. Lottspeich, and U. Fischer. 2001a. *'A multiprotein complex mediates the ATP-dependent assembly of spliceosomal U snRNPs',* ***Nat Cell Biol****, 3: 945-9.*

Meister, G., C. Eggert, D. Bühler, H. Brahms, C. Kambach, and U. Fischer. 2001b. *'Methylation of Sm proteins by a complex containing PRMT5 and the putative U snRNP assembly factor pICln',* ***Curr Biol****, 11: 1990-4.*

Meister, G., and U. Fischer. 2002b. *'Assisted RNP assembly: SMN and PRMT5 complexes cooperate in the formation of spliceosomal UsnRNPs',* ***Embo j****, 21: 5853-63.*

Neuenkirchen, N., C. Englbrecht, J. Ohmer, T. Ziegenhals, A. Chari, and U. Fischer. 2015. *'Reconstitution of the human U snRNP assembly machinery reveals stepwise Sm protein organization',* ***EMBO J****, 34: 1925-41.*

Newman, A. J., and K. Nagai. 2010. *'Structural studies of the spliceosome: blind men and an elephant',* ***Curr Opin Struct Biol****, 20: 82-9.*

Niewalda, T., B. Michels, R. Jungnickel, S. Diegelmann, J. Kleber, T. Kahne, and B. Gerber. 2015. *'Synapsin determines memory strength after punishment- and relief-learning',* ***J Neurosci****, 35: 7487-502.*

Nizami, Z., S. Deryusheva, and J. G. Gall. 2010. *'The Cajal body and histone locus body',* ***Cold Spring Harb Perspect Biol****, 2: a000653.*

Ogura, K., C. Wicky, L. Magnenat, H. Tobler, I. Mori, F. Müller, and Y. Ohshima. 1994. *'Caenorhabditis elegans unc-51 gene required for axonal elongation encodes a novel serine/threonine kinase',* ***Genes Dev****, 8: 2389-400.*

Pellizzoni, L., J. Yong, and G. Dreyfuss. 2002b. *'Essential role for the SMN complex in the specificity of snRNP assembly',* ***Science****, 298: 1775-9.*

Pelz, J. P., H. Schindelin, K. van Pee, J. Kuper, C. Kisker, K. Diederichs, U. Fischer, and C. Grimm. 2015. *'Crystallizing the 6S and 8S spliceosomal assembly intermediates: a complex project', **Acta Crystallogr D Biol Crystallogr**, 71: 2040-53.*

Petherick, K. J., O. J. Conway, C. Mpamhanga, S. A. Osborne, A. Kamal, B. Saxty, and I. G. Ganley. 2015. *'Pharmacological inhibition of ULK1 kinase blocks mammalian target of rapamycin (mTOR)-dependent autophagy', **J Biol Chem**, 290: 11376-83.*

Piras, A., L. Schiaffino, M. Boido, V. Valsecchi, M. Guglielmotto, E. De Amicis, J. Puyal, A. Garcera, E. Tamagno, R. M. Soler, and A. Vercelli. 2017. *'Inhibition of autophagy delays motoneuron degeneration and extends lifespan in a mouse model of spinal muscular atrophy', **Cell Death Dis**, 8: 3223.*

Prusty, A. B., R. Meduri, B. K. Prusty, J. Vanselow, A. Schlosser, and U. Fischer. 2017. *'Impaired spliceosomal UsnRNP assembly leads to Sm mRNA down-regulation and Sm protein degradation', **J Cell Biol**, 216: 2391-407.*

Quidville, V., S. Alsafadi, A. Goubar, F. Commo, V. Scott, C. Pioche-Durieu, I. Girault, S. Baconnais, E. Le Cam, V. Lazar, S. Delaloge, M. Saghatchian, P. Pautier, P. Morice, P. Dessen, S. Vagner, and F. André. 2013. *'Targeting the deregulated spliceosome core machinery in cancer cells triggers mTOR blockade and autophagy', **Cancer Res**, 73: 2247-58.*

Sanchez-Olea, R., F. Emma, M. Coghlan, and K. Strange. 1998. *'Characterization of pICln phosphorylation state and a pICln-associated protein kinase', **Biochim Biophys Acta**, 1381: 49-60.*

Schedlbauer, A., R. Gandini, G. Kontaxis, M. Paulmichl, J. Furst, and R. Konrat. 2011. *'The C-terminus of ICln is natively disordered but displays local structural preformation', **Cell Physiol Biochem**, 28: 1203-10.*

Schedlbauer, A., G. Kontaxis, M. Konig, J. Furst, M. Jakab, M. Ritter, L. Garavaglia, G. Botta, G. Meyer, M. Paulmichl, and R. Konrat. 2003. *'Sequence-specific resonance assignments of ICln, an ion channel cloned from epithelial cells', **J Biomol NMR**, 27: 399-400.*

Schuck, P. 2000. *'Size-distribution analysis of macromolecules by sedimentation velocity ultracentrifugation and lamm equation modeling', **Biophys J**, 78: 1606-19.*

Schuck, P. *'SEDFIT website, http://www.analyticalultracentrifugation.com/'. http://www.analyticalultracentrifugation.com/.*

Shevchenko, A., M. Wilm, O. Vorm, and M. Mann. 1996. *'Mass spectrometric sequencing of proteins silver-stained polyacrylamide gels', **Anal Chem**, 68: 850-8.*

Sou, Y. S., S. Waguri, J. Iwata, T. Ueno, T. Fujimura, T. Hara, N. Sawada, A. Yamada, N. Mizushima, Y. Uchiyama, E. Kominami, K. Tanaka, and M. Komatsu. 2008. *'The Atg8 conjugation system is indispensable for proper development of autophagic isolation membranes in mice', **Mol Biol Cell**, 19: 4762-75.*

Strzelecka, M., S. Trowitzsch, G. Weber, R. Luhrmann, A. C. Oates, and K. M. Neugebauer. 2010. *'Coilin-dependent snRNP assembly is essential for zebrafish embryogenesis', **Nat Struct Mol Biol**, 17: 403-9.*

Taus, T., T. Kocher, P. Pichler, C. Paschke, A. Schmidt, C. Henrich, and K. Mechtler. 2011. *'Universal and confident phosphorylation site localization using phosphoRS', **J Proteome Res**, 10: 5354-62.*

Zhang, R., B. R. So, P. Li, J. Yong, T. Glisovic, L. Wan, and G. Dreyfuss. 2011. *'Structure of a key intermediate of the SMN complex reveals Gemin2's crucial function in snRNP assembly', **Cell**, 146: 384-95.*

SD Figure 1

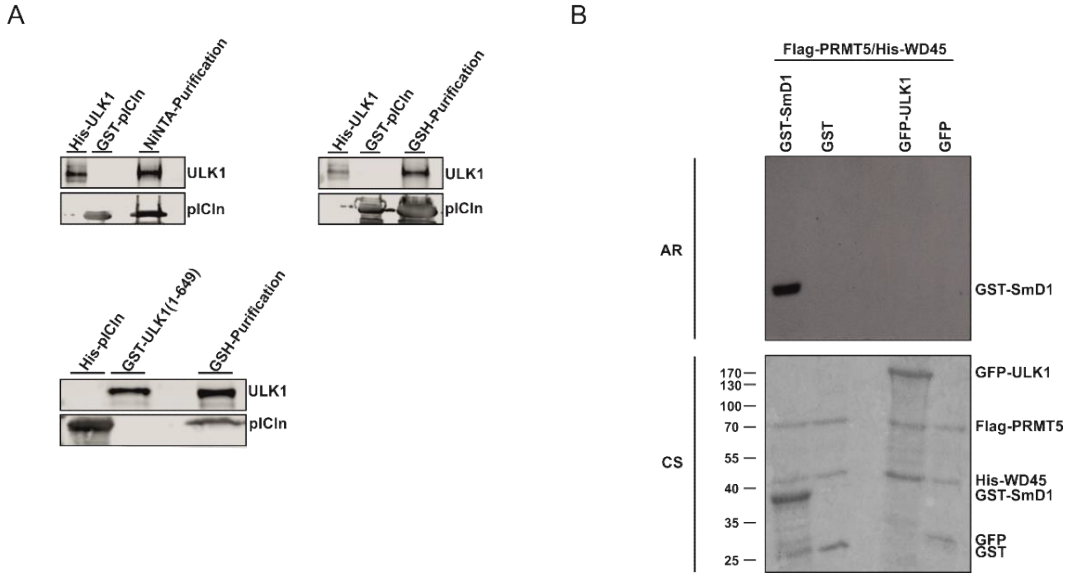

Supplementary Data Figure 1
rULK1 interacts direct with rpICln *in vitro*
A, Recombinant His-ULK1, GST-pICln, GST-ULK1(1-649) or His-pICln were purified with GSH-beads or NiNTA. rULK1 and rpICln were incubated at 4 °C for 1,5 h, afterwards they were purified together for 1 h at 4 °C. Protein binding was analyzed by Tris/Glycine-SDS-PAGE and western blotting using antibodies against ULK1 and pICln. **B,** 1 µg recombinant active Flag-PRMT5/His-WD45 was incubated with GFP-ULK1 or GST-SmD1 (positive control) and 1 µCi [^{3}H]-SAM for 1 h at 37 °C. Samples were separated by Tris/Glycine-SDS-PAGE and analyzed by autoradiography. AR: autoradiography, CS: coomassie blue staining.

SD Figure 2

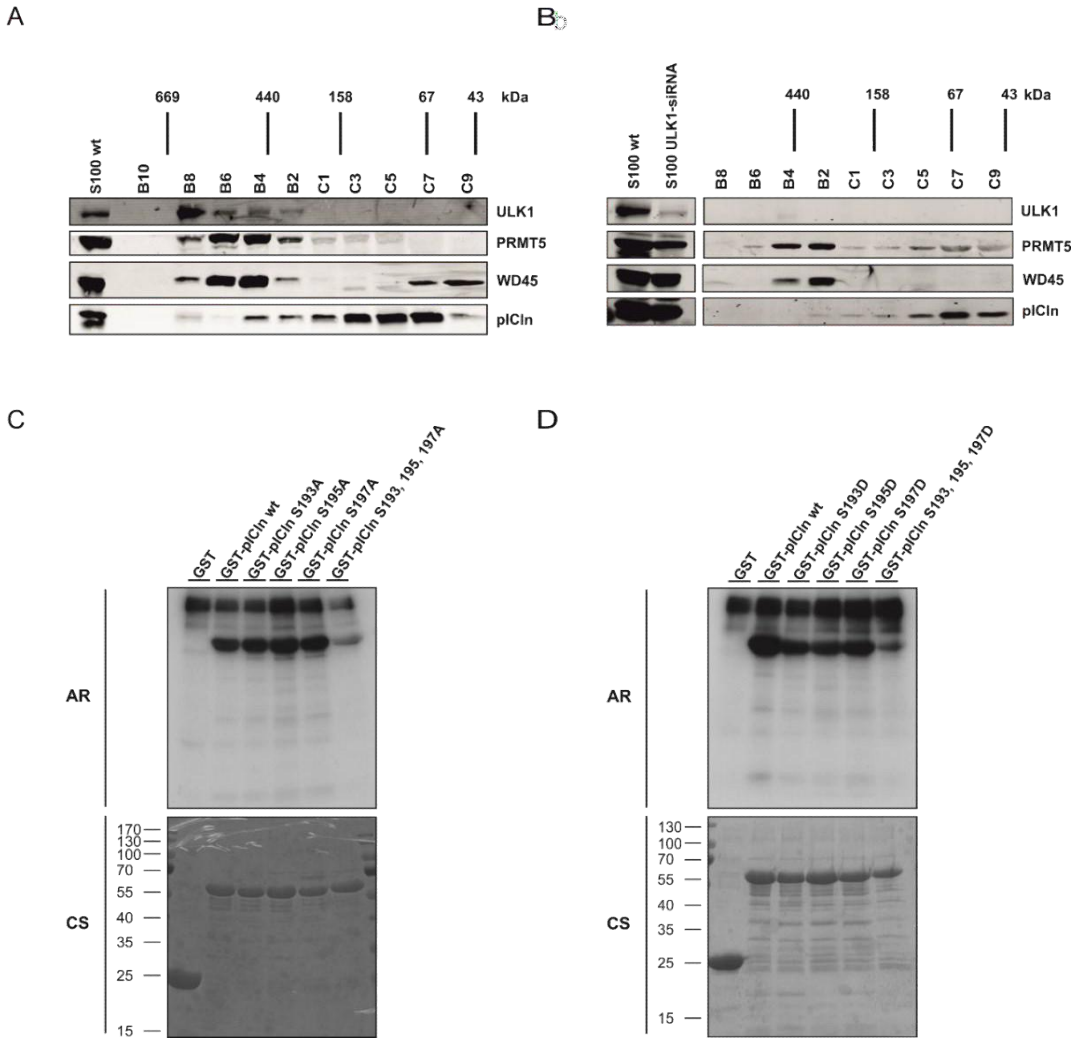

Supplementary Data Figure 2

Western Blot of size exclusion chromatography of wild type HEK293T and HEK293T ULK1-siRNA knockdown S100 extracts

A, **B**, After S100 extraction of wild type HEK293T cells (wt) and HEK293T-ULK1-siRNA knockdown (ULK1-KD) cells a gel filtration was performed using a Superdex 200 column. Complexes were analyzed by Tris/Glycine-SDS-PAGE and western blotting using antibodies against ULK1, PRMT5, WD45 and pICln. **C**, **D**, ULK1 phosphorylates pICln in the C-terminal region on residues S193, S195, and S197. **C,** *In vitro* kinase assay using recombinant active GST-ULK1 expressed in Sf9 insect cells and GST-pICln wt, -pICln S193A, -pICln S195A, -pICln S197A, -pICln S193, 195, 197A and GST purified from *E. coli* as substrate proteins were incubated with 10 µCi [32P]-ATP for 45 min. at 30 °C. Samples were separated by Tris/Glycine-SDS-PAGE and analyzed by autoradiography. **D**, *In vitro* kinase assay was performed as descriped in **C** using recombinant active GST-ULK1 expressed in Sf9 insect cells and GST-pICln wt, -pICln S193D, -pICln S195D, -pICln S197D, -pICln S193, 195, 197D and GST purified from *E. coli* as substrate.

SD Figure 3

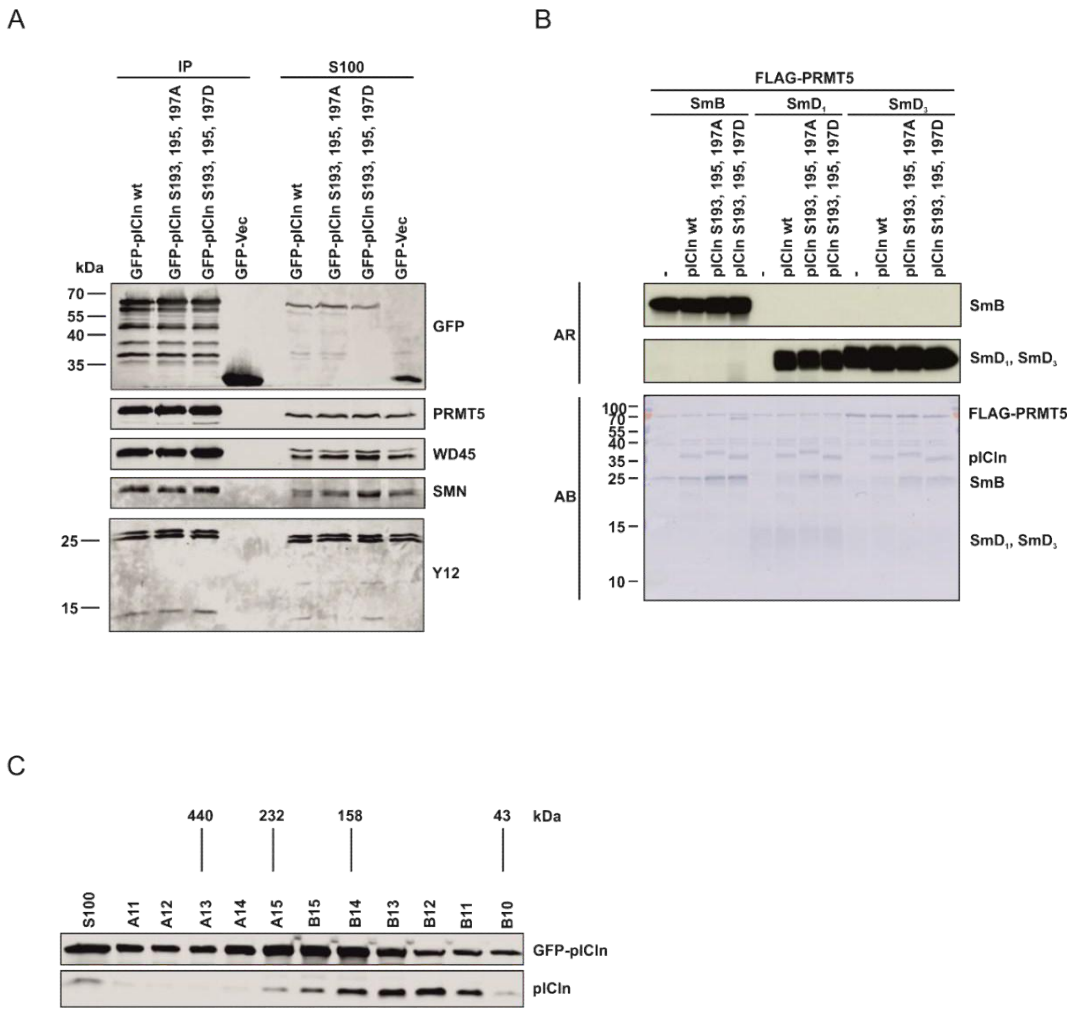

Supplementary Data Figure 3
Influence of the PRMT5 complex composition and activity in dependency of the pICln phosphomutants. **A**, GFP-IP was performed and analyzed by Tris/Glycine-SDS-PAGE and western blotting using antibodies against GFP, PRMT5, WD45, SMN and Y12. **B**, Radioactive methylation assay of SmB, SmD1 and SmD3 by PRMT5. 500 ng of Sm proteins were pre-incubated with or without (-) pICln and the corresponding mutants for 30 min. Methylation assay was performed for 1.5 h at 37 °C with 150 ng of active PRMT5. C, For velocity analysis a gel filtration was performed with S100 extract of Flp-In T-REx 293-GFP-pICln cells using a Superdex 200 increase column. Separation of GFP-pICln and endogenous pICln were analyzed by Tris/Glycine-SDS-PAGE and western blotting using antibodies against GFP and pICln.

SD Figure 4

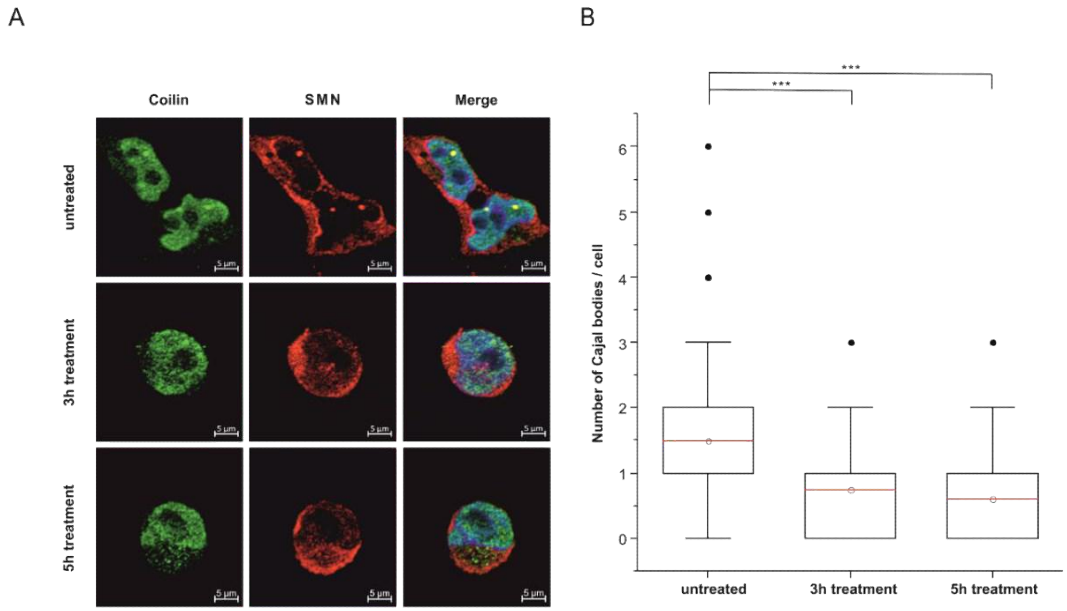

Supplementary Data Figure 4
Inhibition of ULK1 results in a decreased number of Cajal bodies
A,B, HEK293T cells were treated with 30 µM ULK inhibitor MRT67307 for 3 and 5 h. **A**, The cells were fixed and Cajal bodies were visualized with antibody staining against Coilin (green) and SMN (red). The DNA was stained with DAPI (blue). **B**, Inhibition of ULK causes a reduction in the snRNP storage pool. In the boxplot diagram the "box" represents 25-75% of all values and the mean (red), standard deviation and out layers are visualized. HEK293T cells show an average of 1.49 (n = 518) Cajal bodies. Treatment of cells with ULK inhibitor caused a significant decrease in number of Cajal bodies. The p-value was calculated with Origin using the Mann-Whitney U test. ***$P < 0.005$; scale bars: 5 µm (**A**).

SD Figure 5

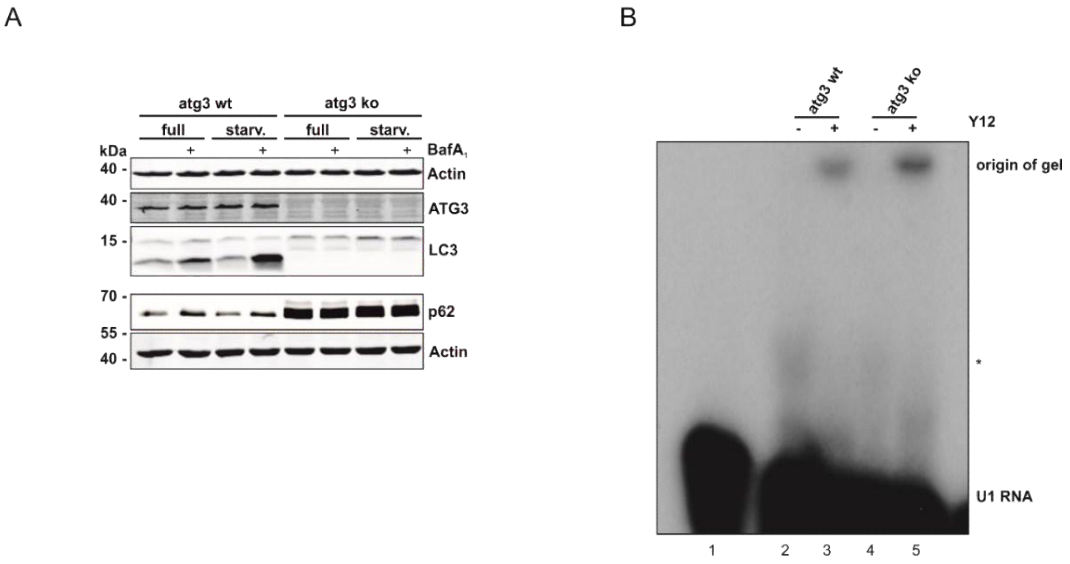

Supplementary Data Figure 5
ATG3 deficient cells are capable for UsnRNP biogenesis.
A, MEF cells, which express wild type atg3 or are deficient for ATG3, were treated with full or starvation medium (EBSS) in absence or presence of bafilomycin A1 (BafA1; 10 nM) for 2 h. Afterwards, cells were harvested, lysed and cleared cellular lysates were subjected to SDS-PAGE and immunoblotting for ATG3, p62, LC3, and Actin. **B**, *In vitro* transcribed U1 snRNA labelled with 10 µCi [32P]-UTP was incubated with S100 extracts from MEF cells either lacking ATG3 or cells reconstituted with ATG3 wt. After incubation samples were directly analyzed by native gel electrophoresis or same samples were subjected to supershift analysis with the Y12 antibody to show the specific formation of snRNPs.

SD Figure 6

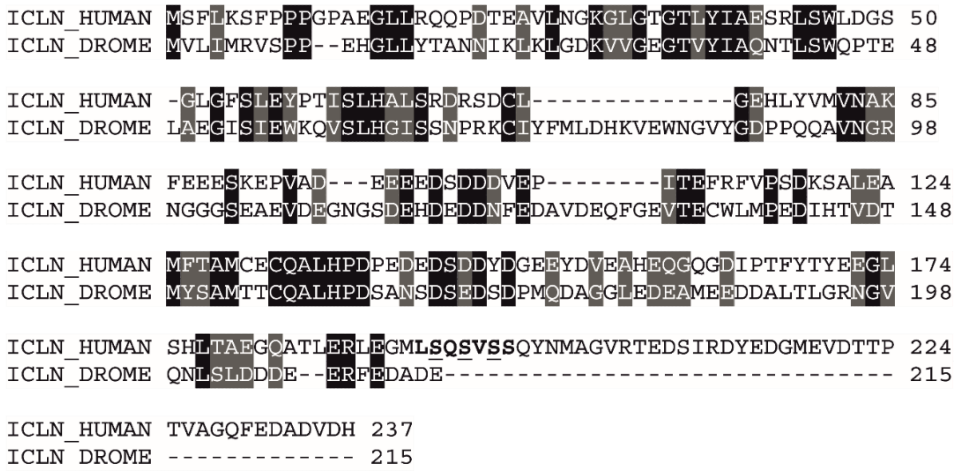

Supplementary Data Figure 6
Sequence alignemnt of human pICln
Sequence alignment (multalin) of human pICln (P54105-1) and drosophila pICln (A1ZAW5-1). Black shade indicates identical amino acids whereas grey shade indicates similar amino acids. Sequence identity: 22.05%. Underlined serines indicate phosphorylation sites of ULK1 in human pICln at positions 193, 195 and 197. These phosphorylation sites are missing in drosophila pICln.

7.3 Chapter 3 - Phosphorylation of pICln by the autophagy activating kinase ULK1 regulates snRNP biogenesis and splice activity of the cell

Title:	**Phosphorylation of pICln by the autophagy activating kinase ULK1 regulates snRNP biogenesis and splice activity of the cell**
Authors:	Lea Marie Esser, Katharina Schmitz, Frank Hillebrand, Steffen Erkelenz, Heiner Schaal, Björn Stork, Matthias Grimmler, Sebastian Wesselborg and Christoph Peter
Published in:	*Computational and Structural Biotechnology Journal* Volume 16, Issue 21, **March 2023**, Pages 2100–2109 DOI: 10.1016/j.csbj.2023.03.015
Impact factor:	6,0
Proportional work on this manuscript:	50% Protein purifications *In vitro* kinase assay *In vivo* labeling experiments Size exclusion experiments Immunofluorescence analysis and quantification *In vitro* assembly assays Preparation of figure Contributing in writing the manuscript

Phosphorylation of pICln by the autophagy activating kinase ULK1 regulates snRNP biogenesis and splice activity of the cell

Lea Marie Esser[1], Katharina Schmitz[1], Frank Hillebrand[2], Steffen Erkelenz[2], Heiner Schaal[2], Björn Stork[1], Matthias Grimmler[3†], Sebastian Wesselborg[1], Christoph Peter[1*]

[1]Institute of Molecular Medicine I, Medical Faculty, Heinrich Heine University Düsseldorf, Düsseldorf, Germany; [2]Institute of Virology, University Hospital Düsseldorf, Düsseldorf, Germany; [3]HOCHSCHULEN FRESENIUS gem. Trägergesellschaft mbH, University of Applied Sciences, Limburger Straße 2, 65510 Idstein, Germany; †Present address: DiaSys Diagnostic Systems GmbH, Holzheim, Germany

*Correspondence: christoph.peter@uni-duesseldorf.de

Abstract

The spliceosome, responsible for all mature protein-coding transcripts of eukaryotic intron-containing genes, consists of small uridine-rich nuclear ribonucleoproteins (UsnRNPs). The assembly of UsnRNPs depends, on one hand, on the arginine methylation of Sm proteins catalyzed by the PRMT5 complex. On the other hand, it depends on the phosphorylation of the PRMT5 subunit pICln by the Uncoordinated Like Kinase 1 (ULK1). In consequence, phosphorylation of pICln affects the stability of the UsnRNP assembly intermediate, the so-called 6S complex. The detailed mechanisms of phosphorylation-dependent integrity and subsequent UsnRNP assembly of the 6S complex *in vivo* have not yet been analyzed.

By using a phospho-specific antibody against ULK1-dependent phosphorylation sites of pICln, we visualize the intracellular distribution of phosphorylated pICln. Furthermore, we detect the colocalization of ULK1 with phospho-pICln by size-exclusion chromatography and immunofluorescence techniques. We also show that phosphorylated pICln is predominantly present in the 6S complex. The addition of ULK1 to *in vitro* produced 6S complex, as well as the reconstitution of ULK1 in ULK1-deficient cells, increases the efficiency of snRNP biogenesis. Accordingly, inhibition of ULK1 and the associated decreased pICln phosphorylation lead to accumulation of the 6S complex and reduction in the spliceosomal activity of the cell.

Keywords: Autophagy/PRMT5/pICln/ULK1/UsnRNP/spliceosomal activity

1. Introduction

Pre-mRNA splicing in eukaryotes is catalyzed by the spliceosome, a multimegadalton complex comprised of five small uridine-rich nuclear ribonucleoproteins (UsnRNPs) (Maniatis et al., 1987, Matera et al., 2014). Each UsnRNPs consists of a specific UsnRNA (U1, U2, U4, U5, or U6) and, except for the U6 snRNP, a common set of seven Sm proteins (B, D1, D2, D3, E, F, and G), which form a ring-shaped structure around the UsnRNA and thus form the functional snRNP (Kambach et al., 1999, Matera et al., 2014). The assembly of Sm proteins and their respective snRNAs is mainly arranged by the cooperated action of two multiprotein complexes: the PRMT5 (Protein arginine N-methyltransferase 5), also called methylosome, and the SMN (Survival of motor neuron) complex (Fischer et al., 1997, Liu et al., 1997, Bühler et al., 1999, Friesen et al., 2001b, Meister et al., 2001b, Meister et al., 2002b). The PRMT5 complex, consisting of the Protein Arginine Methyltransferase 5 (PRMT5), the WD-repeat protein WD45, and pICln, catalyzes the arginine methylation of the Sm proteins B, D1, and D3 and subsequently transfers them onto the SMN complex (Brahms et al., 2001, Friesen et al., 2001b, Meister et al., 2001b, Meister et al., 2002b). The SMN multiprotein complex consists of the survival of motor neuron (SMN) protein, its binding partners known as Gemins 2-8, and the UNR interacting protein (UNRIP) (Fischer et al., 1997, Meister et al., 2001a, Selenko et al., 2001, Grimmler et al., 2005b, Otter et al., 2007, Kroiss et al., 2008). The SMN protein and Gemin2 form the functional core of the SMN complex that is responsible for binding the Sm proteins (Kroiss et al., 2008, Zhang et al., 2011, Veepaschit et al., 2021). The interaction of the PRMT5 and the SMN multiprotein complexes in the assembly of snRNPs is a tightly regulated process in which pICln attributes a key role: on the one hand it recruits the Sm proteins as substrates for PRMT5 and on the other hand it also functions as an assembly chaperone by forming a stable ring-shaped RNA-free intermediate with the Sm proteins D1, D2, E, F, and G. This structure is called the 6S complex (Fisher et al., 1985, Chari et al., 2008). To form functional snRNP, pICln must be released from this intermediate 6S ring structure and needs to be replaced by the two missing Sm proteins B and D3. It has been speculated that this key substitutional step may be regulated by phosphorylation processes (Chari et al., 2008). In our recent work, we have shown that the autophagy activating Ser/Thr Unc-51-like kinase (ULK1) catalyzes the phosphorylation of specific serine residues of pICln in its C-terminus and mediates the release of Sm Proteins onto the SMN complex upon phosphorylation (Schmitz et al., 2021).

In our work presented here, we focus on the characterization of the phospho-status and cellular distribution of endogenous pICln and its influence on the efficiency of new synthesis of UsnRNPs, by using a phospho-pICln-specific antibody. We also address the subsequent ULK1-mediated /phospho-pICln-specific spliceosomal activity *in vivo*.

2. Experimental procedures

2.1 Antibodies

The following primary antibodies were used for immunoblotting and immunofluorescence: α-pICln C5 (sc-130668, Santa Cruz, mouse), Antibody recognizing phosphorylated pICln generated by Eurogentec (rabbit), Antibody recognizing pICln has been described previously (Guderian et al., 2011), α-SMN (05-1532, Merck, mouse), α-SmE (NBP243792, Novus Biologicals, rabbit), α-SmF (SAB2102258, Sigma Aldrich, rabbit), α-SmG (PA5- 49365, Invitrogen, rabbit), α-SmD1 (AV40693, Sigma Aldrich, rabbit), α-SmD2 (SAB2102257, Sigma Aldrich, rabbit), α-2,2,7-Trimethylguanosin (MABE302, Merck, mouse), α-ULK1 (8054; CST, rabbit), α-ULK1 (HPA063990; Prestige Antibodies Sigma Aldrich, rabbit), α-ULK1 F4 (sc-390904; Santa Cruz, mouse). The detection of proteins was carried out with the following fluorescent secondary antibodies: IRDye 680LT goat α-rabbit, IRDye 680LT goat α-mouse, IRDye 800CW donkey α-rabbit, IRDye 800CW donkey α- mouse. For the detection of proteins *in vivo* via IF the following secondary antibodies were used: Goat anti-Mouse IgG (H+L) Cross-Adsorbed Secondary Antibody, Alexa Fluor 488 (A11001, Invitrogen), Donkey anti-Rabbit IgG (H+L) Highly Cross-Adsorbed Secondary Antibody, Alexa Fluor 647 (A31573, Invitrogen).

2.2 Plasmids and proteins

ULK1/2 inhibitor MRT67307 was obtained through the MRC PPU Reagents and Services facility (MRC PPU, College of Life Sciences, University of Dundee, Scotland, mrcppureagents.dundee.ac.uk).

For all *in vitro* assays, the used plasmids were described previously (Schmitz et al., 2021).

To analyze the influence of the ULK inhibition on the cellular splicing process, transient transfection with the following plasmids were used: SV SRSF2 (2X) SD1 Δvpuenv-eGFP, SV SRSF2 (2X) -1G3U Δvpuenv-eGFP (for cloning strategy see (Kammler et al., 2001, Erkelenz et al., 2013)); pUCBΔU1, pUCU1 6A (for cloning strategy see (Kammler et al.,

2001)). pXGH5 expressing the human growth hormone 1 (hGH1) under control of the mouse metallothionein-1 promoter was co-transfected for normalization and to monitor transfection efficiencies.

2.3 Cell lines and Cell culture

All cells were cultivated at 37°C, 5% CO_2 in a humidified area in Dulbecco´s Modified Eagle Medium (4,5 g/L D-glucose, 41965-039, Gibco) supplemented with 10% (v/v) Fetal Bovine Serum (FCS) (F0804, Sigma Aldrich), 100 U/ml Penicillin and 100 µg/ml Streptomycin (15140-122, Sigma Aldrich). HEK293T cells for immunofluorescence were seeded one day before the treatment with $1x10^5$ per well. For knockdown of ULK1 for immunofluorescence analysis, HEK293T cells were transfected in 24-well plates using DharmaFECT1 (T-2001-02, GE Dharmacon) with 50 nM ULK1 siRNA (L-005049-00-0010, SMARTpool, ON-TARGETplus, GE Dharmacon) or 50 nM of the On-TARGET plus Non-targeting Control Pool (D-001810-10-20, GE Dharmacon) for 72 h. For inhibition of ULK1 in immunofluorescence analysis, cells were pre-incubated for 5 hours with 30 µM ULK1 inhibitor MRT67307. For splicing assays, HEK293T cells were seeded in six-well plates with 2.5 $x10^5$ cells per well. Before transfection, cells were pre-incubated for three hours with 30 µM of the ULK inhibitor MRT67307. Transient transfection was carried out by using the TransIT-LT1 reagent (Mirus Bio LLC) following the manufacturer's instructions and described previously (Erkelenz et al., 2015). Cells were harvested for total RNA isolation 20 h after ULK inhibitor addition. MEF ULK1/DKO cells were reconstituted as described before (Schmitz et al., 2021).

2.4 Protein expression and purification

Recombinant proteins were overexpressed in BL21 competent *E. coli* at RT for 4 h after induction with 1 mM IPTG. For cell lysis, the lysis buffer containing 300 mM NaCl, 50 mM Tris/HCl pH 7.5, 5 mM EDTA, 5 mM EGTA, 0.01% (v/v) Igepal, protease inhibitor cocktail (4693132001, Roche), 50 mg/ml Lysozyme (12650-88-3, Serva) was used as well as sonication. After centrifugation at 15,000 rpm for 1 h, the lysate was incubated with Glutathione-Sepharose 4B (17-0756-01, Cytivia) for 1.5 h at 4°C and subsequently washed 3 times with lysis buffer before use in *in vitro* assays.

2.5 Cytoplasm extraction (S100) and size exclusion chromatography

HEK293T cells were incubated with Roeder A buffer (Dignam et al., 1983) in three times cell volume for 10 min at room temperature, dounced 10 times with a tight douncer, and

adjusted to a NaCl concentration of 150 mM. After centrifugation at 13,000 rpm for 30 min, the supernatants (S100 extracts) were filtrated with Millex-HA, 0.45 µm filter unit (Merck Millipore) and either used for immunopurification or applied to a Superdex 200 HiLoad 16/600 or Superdex 200 increase 10/300 GL column (GE Healthcare). For size exclusion chromatography 1 ml of the sample was fractionated in running buffer (150 mM NaCl, 50 mM Tris/HCl pH 7.5) and 0.5 ml fractions were collected and analyzed by immunoblotting. The columns were calibrated with thyroglobulin (669 kDa), ferritin (440 kDa), aldolase (158 kDa), and RNase (14 kDa) (GE Healthcare).

2.6 Immunoblotting and immunopurification

The protein concentration of S100 cytoplasm extract was measured by the Bradford method. The samples were separated by Tris/Tricine or Tris/Glycine SDS gel electrophoresis (Laemmli, 1970) and transferred to PVDF membranes (Immobilon-FL, Merck Millipore). For immunoblot analysis, indicated antibodies and signals were detected with an Odyssey LI-COR Imaging System. For endogenous immunopurification, Protein-G-Sepharose (GE17-0618-01, GE Healthcare) was coated with 1 µg of the specific antibody for 1 h rotating. Afterward, pre-cleared lysates were bound to the Sepharose for 3 h at 4°C. Purified proteins were washed 3 times with washing buffer (50 mM Hepes-NaOH, pH 7.5, 150 mM NaCl, 1% Igepal, 2.5 mM $MgCl_2$, 0.8 U/µl RNase Inhibitor (N2611, Promega) and protease inhibitor cocktail (4693132001, Roche). The elution was obtained in sample buffer (375 mM Tris pH 7.5; 25.8% (w/v) glycerol; 12.3% (w/v) SDS; 0.06% (w/v) Bromophenol blue; 6% (v/v) β-mercaptoethanol; pH 6.8) and analyzed by immunoblotting.

2.7 Immunofluorescence microscopy

For Immunofluorescence $1x10^5$ HEK293T cells per well were seeded on coverslips in 24-well plates in a humidified area at 37°C, 5% CO_2 in Dulbecco´s Modified Eagle Medium (4.5 g/L D-glucose, 41965-039, Gibco) supplemented with 10% (v/v) FCS (F0804, Sigma Aldrich), 100 U/ml Penicillin and 100 µg/ml Streptomycin (15140-122, Sigma Aldrich) one day before staining. On the next day, cells were fixed with 4% paraformaldehyde for 10 min and permeabilized with 0,2% Triton X-100, after these steps cells were washed three times with Dulbecco´s phosphate-buffered saline (DPBS, 14190-094, Gibco). Blocking of the cells was carried out with 5% BSA for 1 h at RT. For detection of pICln total, (both antibodies 1:500), phospho-specific pICln (1:500), and ULK1 total (both antibodies 1:500) cells were incubated for 2 h. For colocalization experiments with pICln-phospho, which is an antibody

with rabbit host, and ULK1 F4 (sc-390904) antibody, which is a mouse host, were co-stained. For comparison as a control pICln total antibody from also rabbit host was used. To control whether ULK1 siRNA worked and if the inhibition or knockdown of ULK1 total has an effect on pICln total localization the following antibodies were used: ULK1 Prestige Antibody Sigma (HPA063990) rabbit host and pICln C5 antibody Santa Cruz mouse host (sc-130668). For immunofluorescence quantification pICln phospho/total the pICln C5 antibody was co-stained with the phospho-specific one. The secondary Alexa Fluor 488 and Alexa Fluor 647 antibodies were incubated for 1 h and the DNA was stained with DAPI. Microscopy was carried out with an Axio Observer microscope from Zeiss with an ApoTome.2 and a 40 x oil immersion objective.

2.8 Immunofluorescence Quantification with Fiji

For the quantification of the intensity ratio between phospho-specific pICln and pICln total, a macro was written in Fiji software which measured the intensity of pICln total and pICln phospho in the area of each cell. Therefore, the macro recognized pICln total staining which is distributed all over the cell as the area of the cell, and the DAPI staining as the area of the nucleus. The total area of the cell was divided by the total DAPI count per picture which in consequence is the relative area of the cell per picture. Subsequently, the measured intensity for pICln total and phospho-specific pICln each was divided by the relative area of the cell which results in the relative fluorescence intensity of those two stainings per cell. For calculation, the value of the pICln phospho signal per cell was normalized on the value of the pICln total. Afterward, the values for MRT67307 treatment were normalized on HEK wt value, and the values for ULK1 siRNA were normalized on Non-targeting control. For every condition at least 300 cells were analyzed. The diagram and the calculation of the standard deviation as well as the statistics were made in Origin Software. To test the significance of the values the data were analyzed using a Mann-Whitney U test where the p value was below 0.005, meaning that the samples were significantly different from each other.

2.9 *In vitro* translation and interaction assay

The proteins were [^{35}S] methionine-labelled (Hartmann Analytic) by using the TNT Quick Coupled Transcription/Translation System (Promega). For interaction assay *in vitro* translated proteins were incubated with GST fusion proteins purified with Glutathione-Sepharose 4B (17-0756-01, Cytivia) rotating for 1.5 h at 4°C in interaction buffer (300 mM NaCl, 50 mM Tris/HCl pH 7.5, 1 mM EGTA, 1 mM EDTA, 1 mM DTT, and 0.01% (v/v)

Igepal). The GST fusion proteins were washed 2 times with interaction buffer and eluted by adding sample buffer, following SDS-PAGE, coomassie staining, and autoradiography.

2.10 *In vivo* labelling

For *in vivo* labelling cells were seeded in six-well plates in DMEM (4.5 g/L D-glucose, 41965-039, Gibco) supplemented with 10% FCS (F0804, Sigma Aldrich) with a density of $1x10^6$ cells per well. The cells were starved in media without methionine and cysteine (D0422, Sigma Aldrich) for 30 minutes. For the labelling cells were incubated with 100 µl media containing 10 % dialyzed FCS, 20 mM Hepes pH 7,4, and 25 µCi/ml [^{35}S] methionine-label for 3.5 h at 37°C. Afterward, cells were washed with DPBS (14190-094, Gibco) 3 times and the pellet was harvested for cell lysis. For cell lysis a buffer containing 50 mM Hepes-NaOH, pH 7.5, 150 mM NaCl, 1% NP-40, 2.5 mM $MgCl_2$, 0.8 U/µl RNase Inhibitor (N2611, Promega), and protease inhibitor cocktail (4693132001, Roche) was used. Endogenous immunopurification was done as described above and after the separation by SDS-PAGE followed by a coomassie staining the gels were dried and analyzed by autoradiography.

2.11 RNA-isolation and quantitative RT-PCR (qPCR)

Total RNA was collected and the mRNAs were reverse transcribed as described in (Erkelenz et al., 2015) and (Chomczynski et al., 1987). Quantitative RT-PCR analysis was performed by using Precision 2× real-time PCR MasterMix with SYBR green (Primerdesign, UK) using LightCycler 1.5 (Roche). For quantification of the spliced and unspliced mRNA species the following primer pairs were used: spliced: #3210 (5'- TGAGGAGGCTTTTTTGGAGG) and #3211 (5'-TTCACTAATCGAATGGATCTGTC),
unspliced: #3210 and #640 (5'-CAATACTACTTCTTGTGGGTTGG). For normalization, primers #1224 (5'-TCTTCCAGCCTCCCATCAGCGTTTGG) and #1225 (5'-CAACAGAAATCCAACCTAGAGCTGCT) were used to monitor the expression of the hGH1-mRNA of the co-transfected pXGH5 plasmid.

3 Results

3.1 Characterization of the phosphorylation state of pICln

To investigate the phospho-status of pICln we generated a phospho-specific pICln antibody against phosphorylated peptides of the C-terminal region. The specificity of the phospho-pICln antibody was tested by Western blotting, using recombinant non-phosphorylated pICln wildtype (wt) and the phospho-deficient mutants 193, 196, 197 A and D as negative control and S100 cytoplasm extract as a positive control. As shown in Figure 1A, the phospho-specific antibody only recognized pICln from the S100 extract and not the recombinant non-phosphorylated proteins. This is in clear contrast to a pan-pICln antibody. To verify the specificity of the phospho-specific antibody concerning phosphorylation sites within the C-terminus of pICln at the serines 193, 195, and 197, recombinant wt pICln and the two phospho-deficient mutants 193, 195, 197A and 193, 195, 197D were subjected to a phosphorylation experiment with active ULK1 and non-radioactive ATP. As shown in Figure 1B, the phospho-specific antibody recognizes only recombinant wt protein that is phosphorylated. The two pICln mutants, which cannot be phosphorylated by ULK1 in the C-terminus, gave no signal with the phospho-specific antibody (Fig.1B).

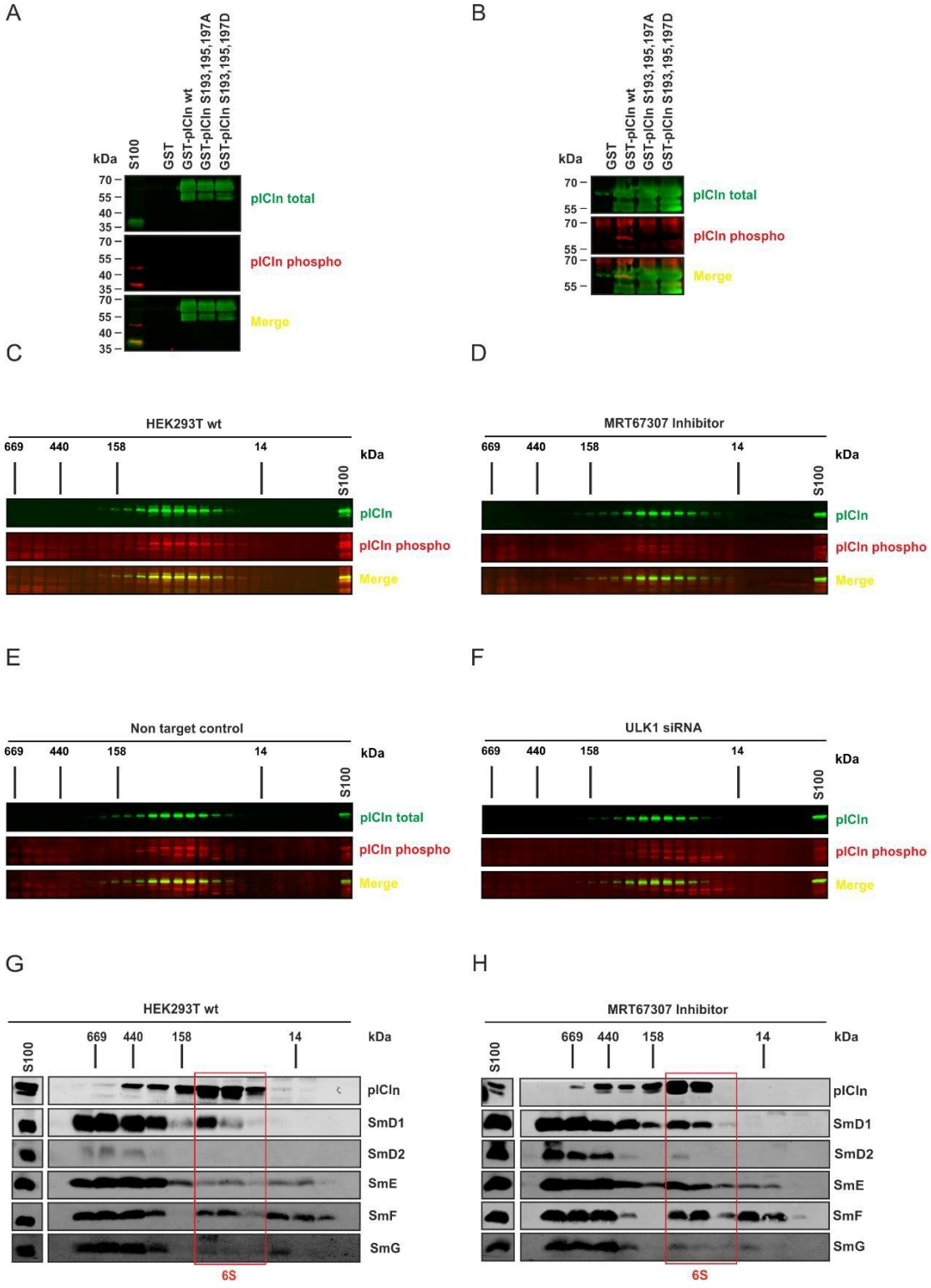

Figure 1
Validation of pICln phosphorylation *in vitro* and *in vivo*.
A, S100 extract of HEK293T cells and recombinant GST, GST-pICln wt, GST-pICln S193,195,197A, and GST-pICln S193,195,197D were analyzed by Tris/Glycine-SDS-PAGE and western blotting using antibodies against phosphorylated pICln and total pICln. **B**, Recombinant GST, GST-pICln wt, GST-pICln S193,195,197A, and GST-pICln S193,195,197D were incubated with 500 ng active GST-ULK1 and ATP for 1 h at 30°C. The phosphorylation status of the proteins was analyzed by Tris/Glycine-SDS-PAGE and western blotting as described in **A**. **C, D** S100 extracts of untreated HEK293T cells or pre-treated cells (10 µM ULK inhibitor MRT67307) were generated with a douncer and applied to a Superdex 200 increase column. Fractions

were analyzed by Tris/Glycine-SDS-PAGE and immunoblotting using antibodies against phosphospecific pICln and total pICln. **E, F,** HEK293T cells were transfected with 50 nM Non-targeting control pool (**E**) or ULK1 siRNA (**F**) for 72 h. The protein complexes of the S100 extract generated with a douncer were separated in a gel filtration with a Superdex 200 increase column. Protein complexes were analyzed by Tris/Glycine-SDS-PAGE and western blotting as described in **C**, **D**. **G, H,** HEK293T cells were treated with 10 µM ULK inhibitor MRT67307 for 1 h followed by S100 extraction and subsequent gel filtration using a Superdex 200 HiLoad 16/600 column. Obtained complexes were analyzed in comparison to untreated HEK293T cells by Tris/Tricine-SDS-PAGE and western blotting using antibodies against the Sm proteins. The 6S complex is highlighted by the red box.

To analyze endogenous pICln and the phospho-content of pICln, HEK293T wild-type cell lysate was separated by size exclusion chromatography, following immunoblot analysis using pan-specific and phospho-specific antibodies against pICln. Total pICln (represented in green color) is distributed in a wide range, whereas pICln, phosphorylated in its C-terminus (represented in red) is only detectable in the distinct molecular weight range from 400 kDa to 100 kDa, including the 6S complex, the size of 158 kDa (Fig. 1C). In contrast, treatment of HEK293T wild-type cells with the inhibitor MRT67307 and the knockdown of ULK1 with siRNA (SD 1G) resulted in a marked decrease in the intensity of the phosphoantibody signal in Western blot analyzes after size-exclusion chromatography (Fig. 1D-F). This observation indicates that phosphorylated endogenous pICln is part of the 6S complex. Since we already have shown in previous work (Schmitz et al., 2021), that ULK1 is responsible for the specific phosphorylation of pICln within its C-terminus, we investigated the influence of ULK1 activity on the integrity of the 6S complex.

To test this scenario, we performed size exclusion chromatography with lysates of HEK293T cells, cultivated in the absence or presence of the inhibitor MRT67307 and detected the respective Sm proteins by immunoblotting. We observed an accumulation of SmD1/D2/E/F/G within the 6S complex upon ULK1 inhibition (Fig. 1G, H; red box). On the one hand, these data show the composition and distribution of the entire endogenous 6S for the first time. On the other hand, the data confirm that phosphorylation of pICln by ULK1 reduces the amount of the intracellular 6S intermediate (Fig. 1G).

Using immunofluorescence analyses with the newly generated phospho-specific antibody against pICln and the ULK1-specific antibody, we next assessed the intracellular distribution and the interactions of pICln, phospho-pICln, and ULK1. Both total pICln and phospho-pICln co-localize with ULK1 predominantly in the cytoplasm. Total pICln signal intensity is significantly higher, compared to that of phospho-pICln (Fig. 2A).

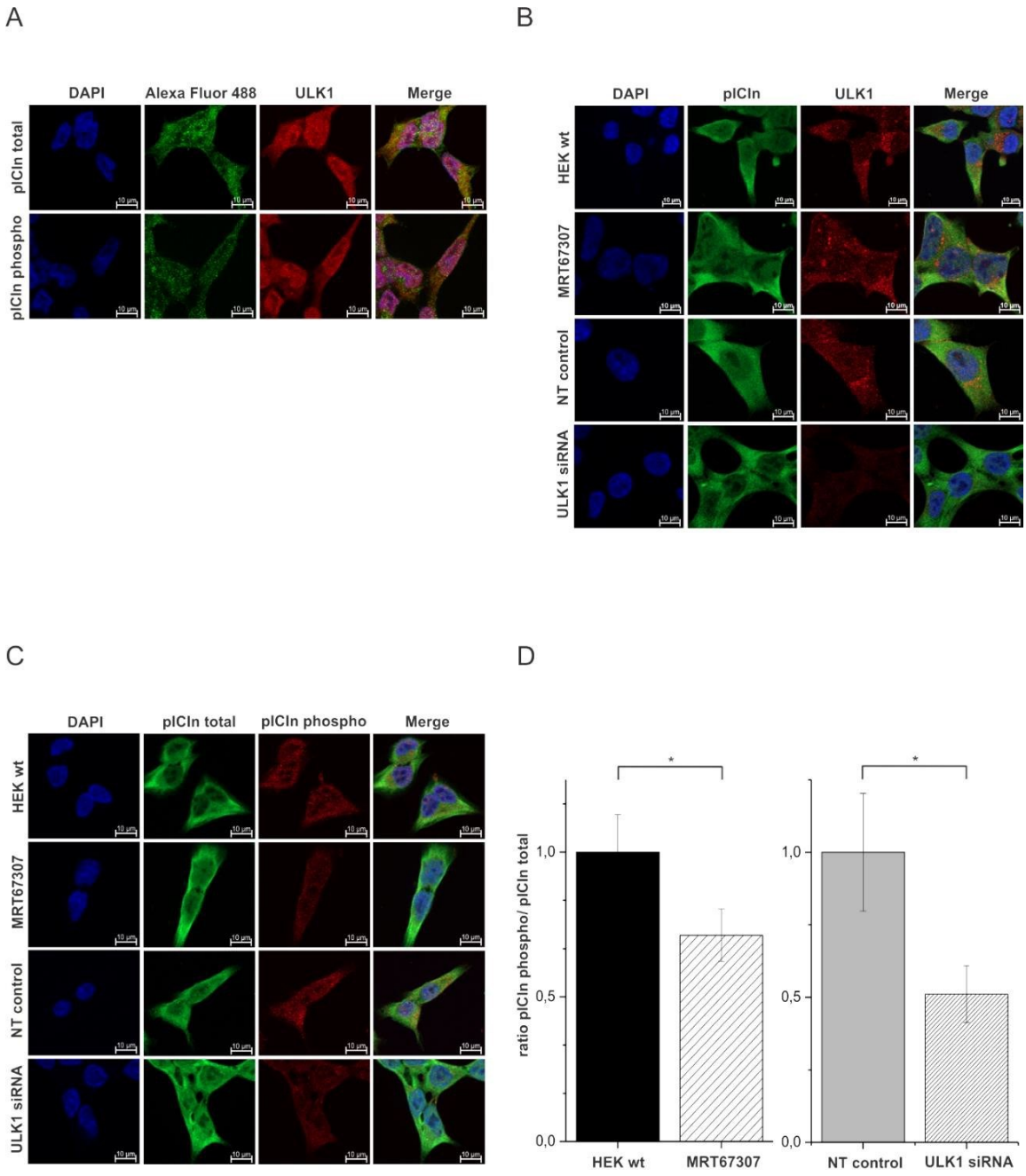

Figure 2
Inhibition of ULK1 results in a decrease of pICln phosphorylation *in vivo*
A, Colocalization of ULK1 and pICln phospho and total. Cells were fixed with 4% PFA and afterwards permeabilized with Triton X-100 to visualize ULK1 (red) and pICln total or phosphospecific pICln (green). The DNA was stained with DAPI (blue), scale bars 10 µm. **B,** HEK293T cells were treated with 30 µM ULK inhibitor MRT67307 for 5 h or transfected with 50 nM Non-targeting control pool (NT) control or ULK1 siRNA for 72 h. Cells were fixed as described in **A** to visualize ULK1 (red) and pICln total (green). The DNA was stained with DAPI (blue), scale bars 10 µm. **C,** HEK293T cells were treated as described in **B** to visualize phosphospecific pICln (red) and pICln total (green). The DNA was stained with DAPI (blue), scale bars 10 µm. **D,** Inhibition or knockdown of ULK1 decreases pICln phosphorylation *in vivo*. Quantification of the intensity ratio between phosphospecific pICln and pICln total was made in Fiji and the diagram in Origin, the values for MRT67307 treatment are normalized on HEK wt value, and the values for ULK1 siRNA are normalized on NT control. The significance of the values was analyzed using a Mann-Whitney U test, the p-value of HEK wt vs. MRT67307 and NT control vs. ULK1 siRNA was below 0.005, indicating significant differences between the values.

Knockdown of ULK1 by siRNA has no effect on the signal intensity of total pICln, nor has the inhibition of kinase activity by ULK-specific kinase inhibitor MRT67307 (Fig. 2B). However, the signal intensity of phosphorylated pICln significantly decreases upon both, inhibitor treatment and ULK1-knockdown (Fig. 2C). Relative to total pICln, there is a 40% reduction in phospho-pICln upon ULK1-knockdown and a 50% reduction after inhibitor treatment (Fig. 2D). This demonstrated, that in the cell, the phospho-status of pICln is directly regulated by ULK1.

Since we have previously shown (Schmitz et al., 2021), that the C-terminal phosphorylation of pICln by ULK1 regulates the binding properties of pICln to Sm proteins and thus snRNP biogenesis, we asked, whether phosphorylation of pICln affects the transfer efficiency of Sm proteins to the SMN complex.

To answer this question, we assessed the pICln-mediated transfer of ^{35}S-labelled reconstituted human 6S complex onto immunopurified human SMN complex. Indeed, the 6S complex sufficed for the transfer of the Sm proteins to the SMN complex. However, after treatment of the 6S complex with recombinant active GST-ULK1 and ATP, the transfer rate of the Sm proteins is strongly enhanced (Fig. 3A and Supplemental Data (SD) 2A). This finding indicated that ULK1-dependent phosphorylation of pICln enables a more efficient transfer of Sm proteins onto the SMN complex and is less involved in the turnover or degradation of pICln.

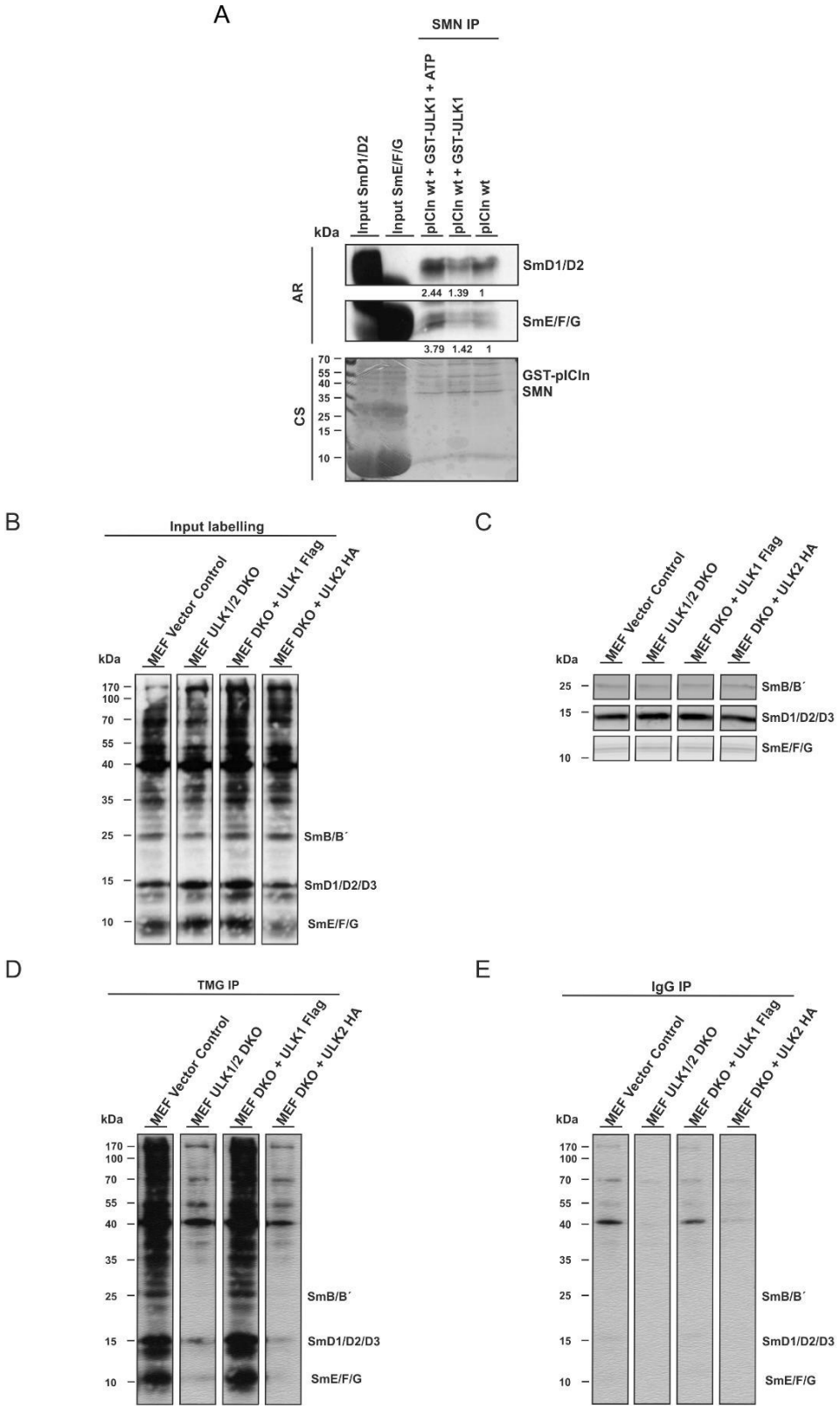

Figure 3

ULK1 phosphorylation of pICln increases Sm protein transfer and late UsnRNP biogenesis

A, pICln-mediated transfer of [^{35}S]-labelled reconstituted human 6S complex onto immunopurified human SMN complex. To test the influence of ULK1 on the Sm protein transfer, immunopurified SMN complex was incubated with active GST-ULK1 with or without addition of ATP which increased the binding capacity of the SMN complex. **B**, As control of the metabolic labelling experiment, 10 % of the [^{35}S] methionine lysate of ULK1/ULK2-double knockout MEF cells as well as individually reconstituted ones with Vector control. ULK1

Flag or ULK2 HA were analyzed by a Tris-Glycine SDS-PAGE and respective western blot. **C**, Whole cell lysate of MEF cells was analyzed by Tris/Glycine-SDS-PAGE and western blotting using antibodies against the Sm proteins for size comparison. **D,** Analysis of late assembly machinery *in vivo*. Therefore metabolic labelling with [^{35}S] methionine in constitutive ULK1/ULK2-double knockout MEF cells, individually reconstituting Vector control, ULK1 Flag, or ULK2 HA only was performed. After metabolic labelling immunopurification using an antibody recognizing the m_3G/m^7G-cap was performed. Only MEF cells reconstituted with ULK1 are capable to transfer Sm proteins onto UsnRNA to the same extent as MEF Vector control cells.

Because the SMN complex has a crucial role in the late assembly state of UsnRNPs we tested the consequence of ULK1-mediated phosphorylation of pICln to the late assembly machinery *in vivo.* To this end we performed metabolic labelling studies with [^{35}S] methionine in constitutive ULK1/ULK2-double knockout (DKO) MEF cells, individually reconstituting ULK1 or ULK2 only (Fig. 3B-E; SD 2B; C). Immunopurifications using an antibody specifically recognizing the m_3G/m^7G-cap of the snRNA, revealed that the Sm protein transfer onto the UsnRNA is dramatically reduced in ULK1 knockout cells in comparison to the corresponding vector control (Fig. 3D). Only MEF cells, reconstituted with ULK1 are capable to transfer Sm proteins onto UsnRNA to the same extent as the used control cells (Fig. 3D). This data confirms the crucial role of ULK1, but not the closely related kinase ULK2, in the UsnRNP assembly *in vivo*.

3.2 ULK1 regulates splice activity via enhanced snRNP biogenesis

To further investigate the influence of pICln phosphorylation on UsnRNP biogenesis *in vivo*, we analyzed the influence of ULK1 on subsequent U1 spliceosomal activity. Therefore, we pre-incubated HEK293T cells with the inhibitor MRT67307 and transfected them with the previously described splicing-reporter constructs (Kammler et al., 2001, Erkelenz et al., 2013). These reporter constructs contain either a splice donor (D1) which is recognized by the endogenous U1 snRNA or the mutant splice donor site 3U that requires co-expression of the complementary U1 6A snRNA. Thus, co-transfection of the 3U reporter and the U1 6A snRNA expression vector allows for exclusive detection of the splicing activity which is dependent only on newly synthesized UsnRNPs (Fig. 4A).

A

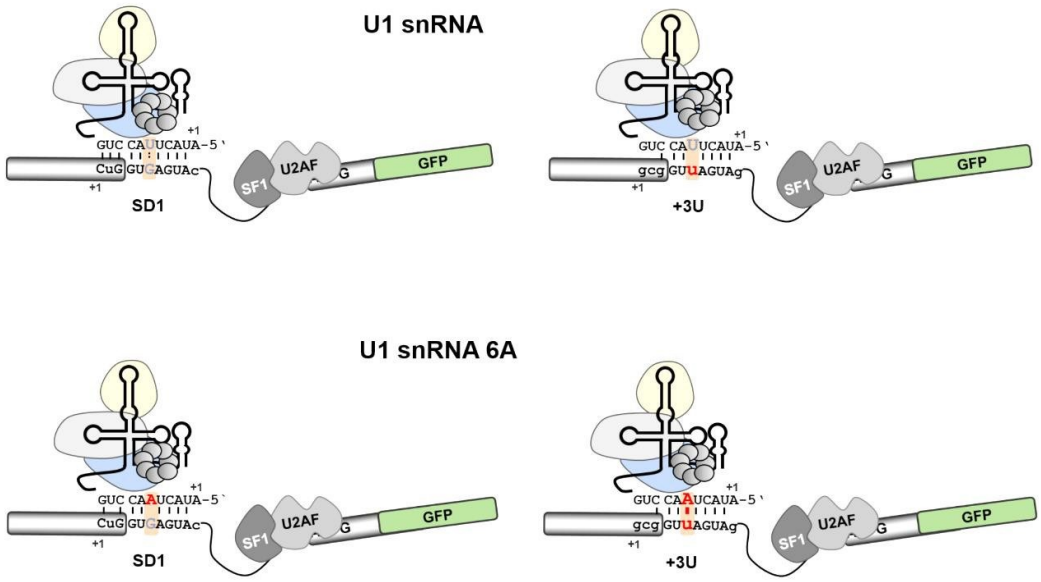

B

Averages	mean spliced [%]			mean unspliced [%]		
	untreated	MRT67307	difference	untreated	MRT67307	difference
D1 splice site	90,89	81,23	-9,66	9,11	18,77	+9,66
3U splice site	8,51	2,59	-5,92	91,49	97,41	+5,92
3U splice site + U1 6A	86,91	55,20	-31,72	13,09	44,80	+31,72

C

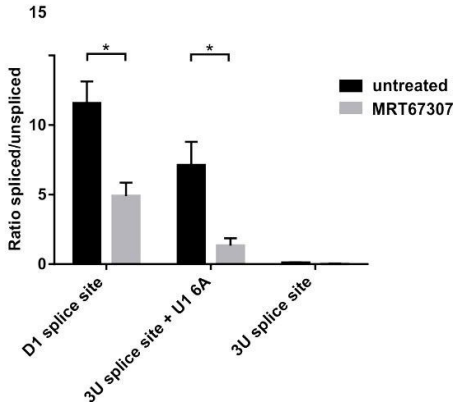

Figure 4
ULK1 phosphorylation of pICln increases UsnRNP biogenesis and spliceosomal activity
A, The HIV-1-based splicing reporter contains a test 5'splice site (5'ss) with a mutated version of viral 5'ss D4 termed „-1G3U". This splice site carries two nucleotide substitutions: A-to-G at position -1 (-1G) and A- to-U at position +3 (+3U) and is poorly recognized by the endogenous U1 snRNA due to a mismatch at position +3. However, splice site recognition is efficiently restored following the co-expression of a U1 snRNA with a compensatory U-to-A nucleotide exchange at position +6, indicating that the modified U1 is assembled into functional snRNP particles within the cell. Uppercase letters within the splice site sequences represent complementary residues, while lowercase letters represent mismatches to the U1. Mutations are highlighted in red. Base-pairing at position +3 is highlighted by a light red box and increased font size. **B; C,** HEK293T cells were treated with 30 µM inhibitor MRT67307 and transiently transfected with different splicing reporter constructs (see methods section for more details). After 20 h of inhibitor treatment cells were harvested to perform RNA isolation. Quantitative RT-PCR was executed and mRNA was analyzed by assessing the respective ratio of spliced/unspliced form, the p value was below 0.005 (**B**). The equal averages including differences between inhibitor-treated and untreated spliced and unspliced forms are listed in **C** (n = 3).

To monitor the influence of ULK inhibition on the splicing of this specific reporter-construct derived RNAs, we performed qPCR analysis to determine the relative amount of spliced and unspliced mRNA of the respective constructs and calculated the spliced/unspliced mRNA ratio.

As expected, in the absence of the ULK inhibitor we observed predominantly spliced mRNA for both reporter constructs (90.9% for the D1 reporter and 86.9% for the 3U reporter, when the U1 6A snRNA was co-expressed) and a relatively small amount of unspliced mRNA (9.1% for the D1 and 13.1% for the 3U reporter, when the U1 6A snRNA was co-expressed) (Fig. 4B). In the absence of U1 6A snRNA, we mainly detected unspliced mRNA when using the 3U reporter (8.5% of spliced and 91.5% of unspliced mRNA) (Fig. 4B), demonstrating the requirement for of the U1 6A snRNA expression. However, when cells were incubated with the ULK inhibitor MRT67307, we observed a substantially reduced spliced/unspliced ratio (Fig. 4C) with a decrease in spliced mRNA by 31.7% for the U1 6A snRNA-dependent and 9.7% for the endogenous D1 splice site (Fig. 4B) with a concomitant increase in unspliced mRNA (Fig. 4B). These results clearly demonstrate that ULK inhibition reduces UsnRNP biogenesis and subsequent spliceosome activity *in vivo*.

4 Discussion

The Ser/Thr kinase ULK1 acts as a functional component of the PRMT5 complex by specific phosphorylation of pICln (Schmitz et al., 2021). Here we characterize the phosphorylation status of endogenous pICln in depth, by using a phospho-specific antibody against the C-terminal, ULK1-specific phosphorylation sites of pICln. This allowed us to study the distribution of phospho-pICln at the endogenous level. Using immunofluorescence microscopy, it becomes evident, that phosphorylated pICln predominantly is detectable in the cytoplasm together with ULK1, and both methods, pharmacological inhibition or knockdown of ULK1 by siRNA led to a clear decrease in the signal intensity of phosphorylated pICln (Fig. 2D). However, originally developed as a ULK1/2 inhibitor (Petherick et al., 2015), it turned out that the MRT67307 compound also inhibits TBK1 and IKKepsilon just as efficiently concerning kinase activities (Saric et al., 2016). Both kinases have their main function predominantly in the immunological context or in immune cells (Clark et al., 2011). Recently, however, it has been shown that TBK1/IKKepsilon also plays a role in energy metabolism and autophagy (Chiang et al., 2009, Reilly et al., 2013). So far,

we cannot exclude that TBK1 or IKKepsilon may have some indirect influence on snRNP-biogenesis. It will be interesting in future work to investigate the role of both kinases in snRNP-biogenesis.

Our results are in line with the work of Sanchez-Olena et al. (Sanchez-Olea et al., 1998) and Grimmler and colleagues (Grimmler et al., 2005a). Both groups could independently show, that endogenous pICln is phosphorylated and a putative kinase activity can be detected on pICln immuno-purified from the cytoplasm. This suggests that pICln interacts with a kinase in the cytoplasm and is consequently phosphorylated.

Interestingly, the major amount of phosphorylated pICln is found in the size range around 158 kDa, which overlaps with the 6S complex of Sm proteins (Figure 1C; E). The intermediate 6S complex plays a key role in UsnRNP biogenesis. The work by Chari and colleagues suggested, that the 6S complex may be a kinetic trap, that is released by the phosphorylation of pICln to keep snRNP biogenesis ongoing (Chari et al., 2008). Complementary to our previous work, in which we showed by *in vitro* binding studies, that ULK1 regulates the formation of the 6S complex by phosphorylating pICln, our results show that pICln is largely phosphorylated in the 6S complex.

Concordant with this data, one should expect that, when the kinase activity of ULK1 is inhibited, there should be an enrichment of the 6S complex in the cell. This is indeed the case, as shown in Figures 1G and H. Conversely, the transfer of Sm proteins to the SMN complex from the 6S complex should be increased in the presence of ULK1. This is likewise the case (Fig. 3A, B), demonstrating that ULK1 activity is responsible for the equilibrium of endogenous 6S complex-bound Sm proteins in the cytoplasm. Since snRNPs are the building blocks of the spliceosome (Newman et al., 2010, Matera et al., 2014), the influence of ULK1 should also be reflected in the overall splice activity. We were also able to determine this by utilizing a splicing reporter assay (Fig. 4). In summary, it can be concluded that the interaction between ULK1 and pICln regulates snRNP biogenesis and consequently also influences subsequent splicing activity *in vivo*.

The crucial role of pICln in neurodegenerative diseases (Winkler et al., 2005) and the unexpected link to ULK1, a key regulator of neurodifferentiation and axonal elongation in *C. elegans*, mice, and humans (Ogura et al., 1994, Tomoda et al., 1999, Loh et al., 2008), make both, pICln as well as ULK1 to a new relevant target for further studies and potential therapies of SMA and other (motor) neuronal diseases. The successful introduction of

antisense oligonucleotides (AONs) such as nusinersen (Hoy, 2017) or gene replacement therapy (Mendell et al., 2017), has dramatically increased the prospects for successful treatment of SMA patients. These novel treatments focus exclusively on increasing the protein levels of SMN. The long-term consequences caused by SMN overexpression are as yet unclear (Aslesh et al., 2022). A simultaneous increase in snRNP biogenesis via activation of ULK1 could represent a new additional target for successful therapy. Much work will be necessary to gather more experimental data on this – but the association of pICln with ULK1 gives a new starting option on this so far blind alley to answer the question of why general spliceosomal defects predominantly do lead to neuronal manifestations.

Funding

This work was supported by grants from Deutsche Forschungsgemeinschaft [RTG 2158 (to B.S. and S.W.), RTG 2578 (to B.S. and S.W.), and STO 864/4-3 (to B.S.)] and the Düsseldorf School of Oncology (funded by the Comprehensive Cancer Center Düsseldorf/Deutsche Krebshilfe and the Medical Faculty of the Heinrich Heine University Düsseldorf; to B.S. and S.W.).

Declaration of Competing Interest

The authors declare that they have no known competing financial interests or personal relationships that could have appeared to influence the work reported in this paper.

Acknowledgments

We gratefully acknowledge Maximilian Jüdt, Qiaoping Li, David Schlütermann, Seda Akgün and Maria Jose Mendiburo for valuable discussions and technical support.

Author contributions

L.E. performed *in vivo* labelling experiments as well as the Western blots of S100 extract of MEF cells, Western Blot analysis of recombinant pICln and pre-phosphorylated recombinant pICln, size exclusion with or without inhibitor-/ siRNA-treatment using the phospho-specific pICln antibody, immunofluorescence analysis and *in vitro* assembly assays; Ka.Sc.

performed the gel filtrations with and without inhibitor treatment, and *in vitro* assembly assays; S.E., H.F., and H.S. performed and interpreted splicing analysis; B.S. and S.W. discussed the results; M.G. and C.P. designed the experiments and supervised the project; all authors contributed to the writing of the manuscript.

Data availability

All data and material are available upon request to christoph.peter@uni-duesseldorf.de

References

Aslesh, T., and T. Yokota. 2022. '*Restoring SMN Expression: An Overview of the Therapeutic Developments for the Treatment of Spinal Muscular Atrophy*', ***Cells***, 11.

Brahms, H., L. Meheus, V. de Brabandere, U. Fischer, and R. Lührmann. 2001. '*Symmetrical dimethylation of arginine residues in spliceosomal Sm protein B/B' and the Sm-like protein LSm4, and their interaction with the SMN protein*', ***Rna***, 7: 1531-42.

Bühler, D., V. Raker, R. Lührmann, and U. Fischer. 1999. '*Essential role for the tudor domain of SMN in spliceosomal U snRNP assembly: implications for spinal muscular atrophy*', ***Hum Mol Genet***, 8: 2351-7.

Chari, A., M. M. Golas, M. Klingenhäger, N. Neuenkirchen, B. Sander, C. Englbrecht, A. Sickmann, H. Stark, and U. Fischer. 2008. '*An assembly chaperone collaborates with the SMN complex to generate spliceosomal SnRNPs*', ***Cell***, 135: 497-509.

Chiang, S. H., M. Bazuine, C. N. Lumeng, L. M. Geletka, J. Mowers, N. M. White, J. T. Ma, J. Zhou, N. Qi, D. Westcott, J. B. Delproposto, T. S. Blackwell, F. E. Yull, and A. R. Saltiel. 2009. '*The protein kinase IKKepsilon regulates energy balance in obese mice*', ***Cell***, 138: 961-75.

Chomczynski, P., and N. Sacchi. 1987. '*Single-step method of RNA isolation by acid guanidinium thiocyanate-phenol-chloroform extraction*', ***Anal Biochem***, 162: 156-9.

Clark, K., M. Peggie, L. Plater, R. J. Sorcek, E. R. Young, J. B. Madwed, J. Hough, E. G. McIver, and P. Cohen. 2011. '*Novel cross-talk within the IKK family controls innate immunity*', ***Biochem J***, 434: 93-104.

Dignam, J. D., R. M. Lebovitz, and R. G. Roeder. 1983. '*Accurate transcription initiation by RNA polymerase II in a soluble extract from isolated mammalian nuclei*', ***Nucleic Acids Res***, 11: 1475-89.

Erkelenz, S., F. Hillebrand, M. Widera, S. Theiss, A. Fayyaz, D. Degrandi, K. Pfeffer, and H. Schaal. 2015. '*Balanced splicing at the Tat-specific HIV-1 3'ss A3 is critical for HIV-1 replication*', ***Retrovirology***, 12: 29.

Erkelenz, S., W. F. Mueller, M. S. Evans, A. Busch, K. Schoneweis, K. J. Hertel, and H. Schaal. 2013. '*Position-dependent splicing activation and repression by SR and hnRNP proteins rely on common mechanisms*', ***RNA***, 19: 96-102.

Fischer, U., Q. Liu, and G. Dreyfuss. 1997. '*The SMN-SIP1 complex has an essential role in spliceosomal snRNP biogenesis*', ***Cell***, 90: 1023-9.

Fisher, D. E., G. E. Conner, W. H. Reeves, R. Wisniewolski, and G. Blobel. 1985. '*Small nuclear ribonucleoprotein particle assembly in vivo: demonstration of a 6S RNA-free core precursor and posttranslational modification*', ***Cell***, 42: 751-8.

Friesen, W. J., S. Paushkin, A. Wyce, S. Massenet, G. S. Pesiridis, G. Van Duyne, J. Rappsilber, M. Mann, and G. Dreyfuss. 2001b. '*The methylosome, a 20S complex containing JBP1 and pICln, produces dimethylarginine-modified Sm proteins*', ***Mol Cell Biol***, 21: 8289-300.

Grimmler, M., L. Bauer, M. Nousiainen, R. Körner, G. Meister, and U. Fischer. 2005a. '*Phosphorylation regulates the activity of the SMN complex during assembly of spliceosomal U snRNPs*', ***EMBO Rep***, 6: 70-6.

Grimmler, M., S. Otter, C. Peter, F. Muller, A. Chari, and U. Fischer. 2005b. '*Unrip, a factor implicated in cap-independent translation, associates with the cytosolic SMN complex and influences its intracellular localization*', ***Hum Mol Genet***, 14: 3099-111.

Guderian, G., C. Peter, J. Wiesner, A. Sickmann, K. Schulze-Osthoff, U. Fischer, and M. Grimmler. 2011. '*RioK1, a new interactor of protein arginine methyltransferase 5 (PRMT5), competes with pICln for binding and modulates PRMT5 complex composition and substrate specificity*', ***J Biol Chem***, 286: 1976-86.

Hoy, S. M. 2017. '*Nusinersen: First Global Approval*', ***Drugs***, 77: 473-79.

Kambach, C., S. Walke, R. Young, J. M. Avis, E. de la Fortelle, V. A. Raker, R. Lührmann, J. Li, and K. Nagai. 1999. '*Crystal structures of two Sm protein complexes and their implications for the assembly of the spliceosomal snRNPs*', ***Cell***, 96: 375-87.

Kammler, S., C. Leurs, M. Freund, J. Krummheuer, K. Seidel, T. O. Tange, M. K. Lund, J. Kjems, A. Scheid, and H. Schaal. 2001. '*The sequence complementarity between HIV-1 5' splice site SD4 and U1 snRNA determines the steady-state level of an unstable env pre-mRNA*', ***RNA***, 7: 421-34.

Kroiss, M., J. Schultz, J. Wiesner, A. Chari, A. Sickmann, and U. Fischer. 2008. '*Evolution of an RNP assembly system: a minimal SMN complex facilitates formation of UsnRNPs in Drosophila melanogaster*', ***Proc Natl Acad Sci U S A***, 105: 10045-50.

Laemmli, U. K. 1970. '*Cleavage of structural proteins during the assembly of the head of bacteriophage T4*', ***Nature***, 227: 680-5.

Liu, Q., U. Fischer, F. Wang, and G. Dreyfuss. 1997. '*The spinal muscular atrophy disease gene product, SMN, and its associated protein SIP1 are in a complex with spliceosomal snRNP proteins*', ***Cell***, 90: 1013-21.

Loh, S. H., L. Francescut, P. Lingor, M. Bahr, and P. Nicotera. 2008. '*Identification of new kinase clusters required for neurite outgrowth and retraction by a loss-of-function RNA interference screen*', ***Cell Death Differ***, 15: 283-98.

Maniatis, T., and R. Reed. 1987. '*The role of small nuclear ribonucleoprotein particles in pre-mRNA splicing*', ***Nature***, 325: 673-8.

Matera, A. G., and Z. Wang. 2014. '*A day in the life of the spliceosome*', ***Nat Rev Mol Cell Biol***, 15: 108-21.

Meister, G., D. Bühler, R. Pillai, F. Lottspeich, and U. Fischer. 2001a. '*A multiprotein complex mediates the ATP-dependent assembly of spliceosomal U snRNPs*', ***Nat Cell Biol***, 3: 945-9.

Meister, G., C. Eggert, D. Bühler, H. Brahms, C. Kambach, and U. Fischer. 2001b. '*Methylation of Sm proteins by a complex containing PRMT5 and the putative U snRNP assembly factor pICln*', ***Curr Biol***, 11: 1990-4.

Meister, G., and U. Fischer. 2002b. '*Assisted RNP assembly: SMN and PRMT5 complexes cooperate in the formation of spliceosomal UsnRNPs*', ***Embo j***, 21: 5853-63.

Mendell, J. R., S. Al-Zaidy, R. Shell, W. D. Arnold, L. R. Rodino-Klapac, T. W. Prior, L. Lowes, L. Alfano, K. Berry, K. Church, J. T. Kissel, S. Nagendran, J. L'Italien, D. M. Sproule, C. Wells, J. A. Cardenas, M. D. Heitzer, A. Kaspar, S. Corcoran, L. Braun, S. Likhite, C. Miranda, K. Meyer, K. D. Foust, A. H. M. Burghes, and B. K. Kaspar. 2017. '*Single-Dose Gene-Replacement Therapy for Spinal Muscular Atrophy*', ***N Engl J Med***, 377: 1713-22.

Newman, A. J., and K. Nagai. 2010. '*Structural studies of the spliceosome: blind men and an elephant*', ***Curr Opin Struct Biol***, 20: 82-9.

Ogura, K., C. Wicky, L. Magnenat, H. Tobler, I. Mori, F. Müller, and Y. Ohshima. 1994. '*Caenorhabditis elegans unc-51 gene required for axonal elongation encodes a novel serine/threonine kinase*', ***Genes Dev***, 8: 2389-400.

Otter, S., M. Grimmler, N. Neuenkirchen, A. Chari, A. Sickmann, and U. Fischer. 2007. '*A comprehensive interaction map of the human survival of motor neuron (SMN) complex*', ***J Biol Chem***, 282: 5825-33.

Petherick, K. J., O. J. Conway, C. Mpamhanga, S. A. Osborne, A. Kamal, B. Saxty, and I. G. Ganley. 2015. '*Pharmacological inhibition of ULK1 kinase blocks mammalian target of rapamycin (mTOR)-dependent autophagy*', ***J Biol Chem***, 290: 11376-83.

Reilly, S. M., S. H. Chiang, S. J. Decker, L. Chang, M. Uhm, M. J. Larsen, J. R. Rubin, J. Mowers, N. M. White, I. Hochberg, M. Downes, R. T. Yu, C. Liddle, R. M. Evans, D. Oh, P. Li, J. M. Olefsky, and A. R. Saltiel. 2013. '*An inhibitor of the protein kinases TBK1 and IKK-varepsilon improves obesity-related metabolic dysfunctions in mice*', ***Nat Med***, 19: 313-21.

Sanchez-Olea, R., F. Emma, M. Coghlan, and K. Strange. 1998. '*Characterization of pICln phosphorylation state and a pICln-associated protein kinase*', ***Biochim Biophys Acta***, 1381: 49-60.

Saric, A., V. E. Hipolito, J. G. Kay, J. Canton, C. N. Antonescu, and R. J. Botelho. 2016. '*mTOR controls lysosome tubulation and antigen presentation in macrophages and dendritic cells*', ***Mol Biol Cell***, 27: 321-33.

Schmitz, K., J. Cox, L. M. Esser, M. Voss, K. Sander, A. Löffler, F. Hillebrand, S. Erkelenz, H. Schaal, T. Kähne, S. Klinker, T. Zhang, L. Nagel-Steger, D. Willbold, S. Seggewiß, D. Schlütermann, B. Stork, M. Grimmler, S. Wesselborg, and C. Peter. 2021. '*An essential role of the autophagy activating kinase ULK1 in snRNP biogenesis*', ***Nucleic Acids Res***, 49: 6437-55.

Selenko, P., R. Sprangers, G. Stier, D. Buhler, U. Fischer, and M. Sattler. 2001. '*SMN tudor domain structure and its interaction with the Sm proteins*', ***Nat Struct Biol***, 8: 27-31.

Tomoda, T., R. S. Bhatt, H. Kuroyanagi, T. Shirasawa, and M. E. Hatten. 1999. '*A mouse serine/threonine kinase homologous to C. elegans UNC51 functions in parallel fiber formation of cerebellar granule neurons*', ***Neuron***, 24: 833-46.

Veepaschit, J., A. Viswanathan, R. Bordonne, C. Grimm, and U. Fischer. 2021. '*Identification and structural analysis of the Schizosaccharomyces pombe SMN complex*', ***Nucleic Acids Res***, 49: 7207-23.

Winkler, C., C. Eggert, D. Gradl, G. Meister, M. Giegerich, D. Wedlich, B. Laggerbauer, and U. Fischer. 2005. '*Reduced U snRNP assembly causes motor axon degeneration in an animal model for spinal muscular atrophy*', ***Genes Dev***, 19: 2320-30.

Zhang, R., B. R. So, P. Li, J. Yong, T. Glisovic, L. Wan, and G. Dreyfuss. 2011. '*Structure of a key intermediate of the SMN complex reveals Gemin2's crucial function in snRNP assembly*', ***Cell***, 146: 384-95.

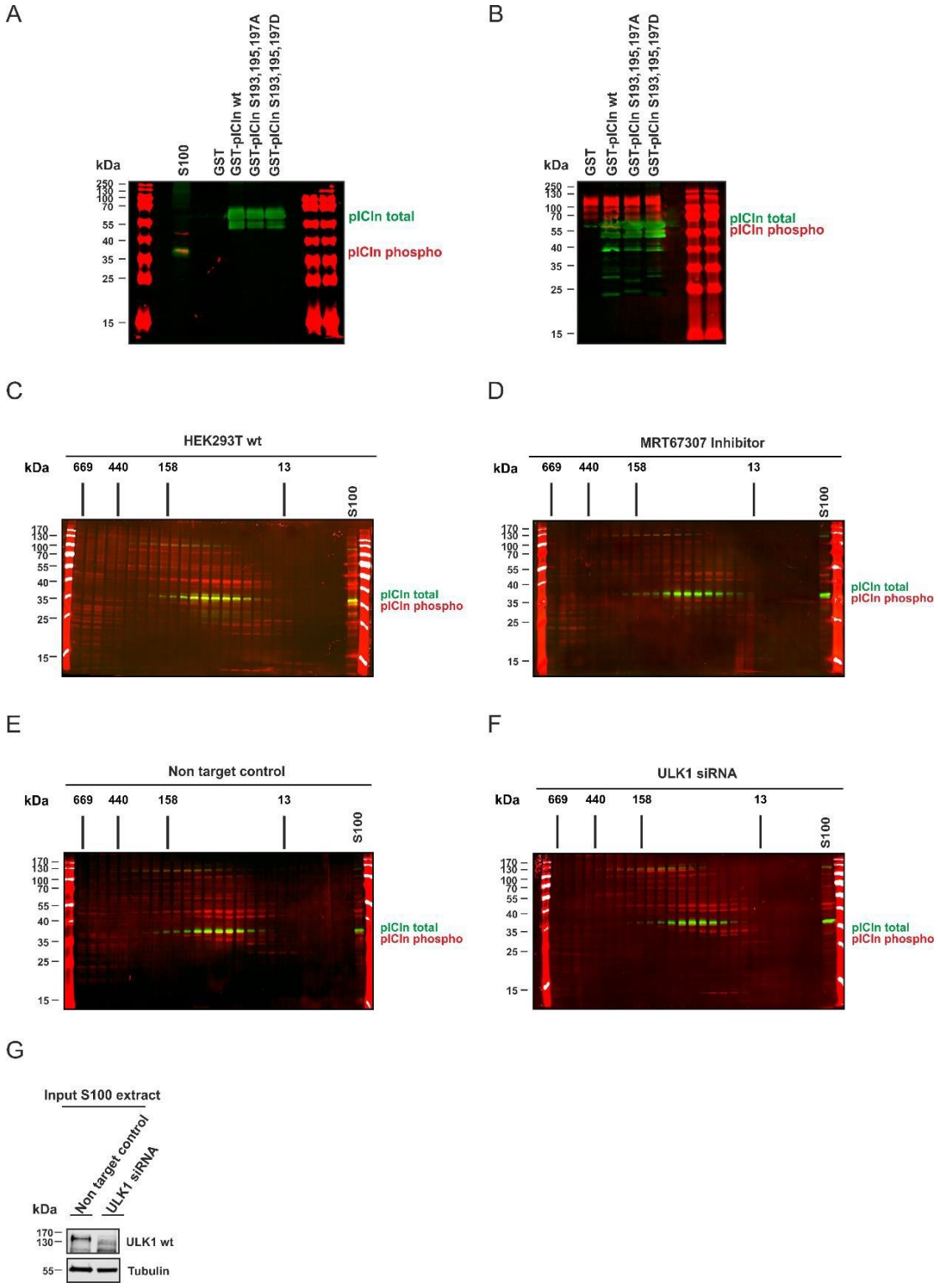

SD Figure 1
Validation of pICln phosphorylation *in vitro* and *in vivo*.
A, B, Whole membranes **Figure 1 A, B,** samples were separated by Tris/Glycine-SDS-Page. Western blot of pICln total is shown in green, phosphorylated pICln is shown in red. **C-F,** Whole membranes **Figure 1 C-F,** samples collected after size exclusion chromatography were separated by Tris/Gycine-SDS-Page. Western blotting of phospho pICln is shown in red and pICln total in green. **G**, HEK293T cell lysate was analyzed by Tris/Glycine-SDS-PAGE as well as western blotting after transfection of ULK1 siRNA or Non-targeting control using antibodies against ULK1 wt and β-Tubulin (control for **Figure 1 E**,**F**).

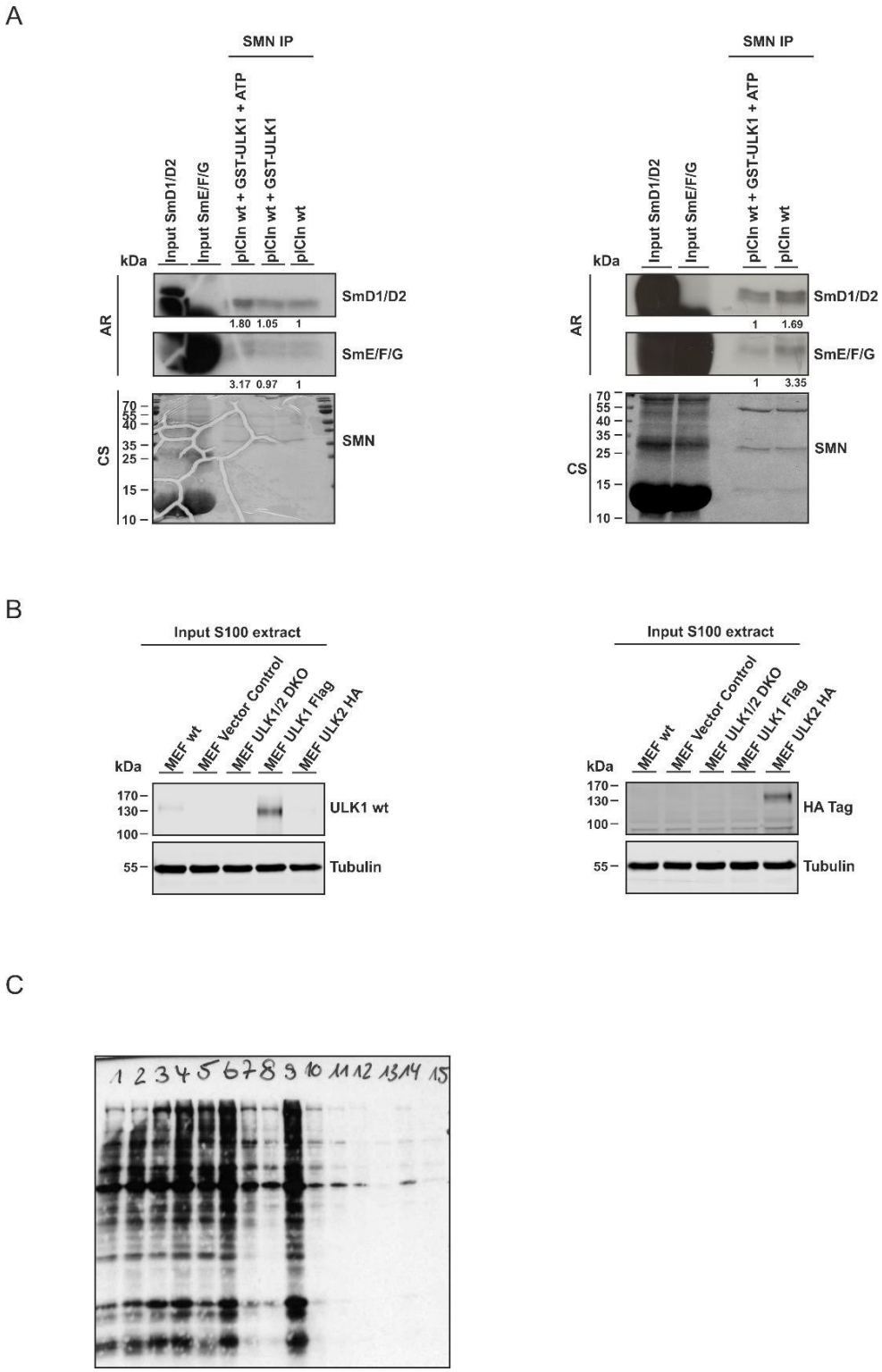

SD Figure 2

ULK1 phosphorylation of pICln increases UsnRNP biogenesis and spliceosomal activity

A, pICln mediated transfer of [^{35}S]-labelled reconstituted human 6S complex onto immunopurified human SMN complex. Replicates of Figure **3 A**. **B,** MEF whole cell lysate was analyzed by Tris/Glycine-SDS-PAGE and western blotting using antibodies against ULK1 wt and HA-Tag for ULK2. The expression of ULK1 Flag and ULK2 HA after the reconstitution of ULK1/2 deficient MEF cells is comparable. **C**, Whole membrane **Figure 3 B-D**. Lanes for **Figure 3 B**: 2: MEF VC; 3: MEF DKO, 4: MEF DKO + ULK1 Flag, 5: MEF DKO + ULK2 HA. Lanes for **Figure 3 C**: 11: MEF VC, 13: MEF DKO, 14: MEF DKO + ULK1 Flag, 15: MEF DKO + ULK2 HA. Lanes for **Figure 3 D**: 6: MEF VC, 8: MEF DKO, 9: MEF DKO + ULK1 Flag, 10: MEF DKO + ULK2 HA.

7.4 Chapter 4 - The Impact of p70S6 Kinase-Dependent Phosphorylation of Gemin2 in UsnRNP Biogenesis

Title:	**The Impact of p70S6 Kinase-Dependent Phosphorylation of Gemin2 in UsnRNP Biogenesis**
Authors:	Lea Marie Esser, Qiaoping Li, Maximilian Jüdt, Thilo Kähne, Björn Stork, Matthias Grimmler, SebastianWesselborg and Christoph Peter
Published in:	*International Journal of Molecular Sciences* Volume 24, Issue 21, October 2023, Pages 15552 DOI: 10.3390/ijms242115552
Impact factor:	5,6
Proportional work on this manuscript:	65% Protein purifications *In vitro* kinase assays Generation of inducible GFP cell lines Immunofluorescence analysis and quantification Immunopurification experiments Size exclusion chromatography Preparation of figures Contributing in writing the manuscript

The Impact of p70S6 Kinase-Dependent Phosphorylation of Gemin2 in UsnRNP Biogenesis

Lea Marie Esser [1], Qiaoping Li [1], Maximilian Jüdt [1], Thilo Kähne [2], Björn Stork [1], Matthias Grimmler [3,4], Sebastian Wesselborg [1] and Christoph Peter [1,*]

Institute of Molecular Medicine I, Medical Faculty, Heinrich Heine University Düsseldorf, 40225 Düsseldorf, Germany;
Institute of Experimental Internal Medicine, Otto von Guericke University, 39120 Magdeburg, Germany;
Institute for Biomolecular Research, Hochschule Fresenius gGmbH, University of Applied Sciences, 65510 Idstein, Germany;
DiaServe Laboratories GmbH, 82393 Iffeldorf, Germany
Correspondence: christoph.peter@uni-duesseldorf.de; Tel: +49-(0)-211-81-12196

Abstract

The survival motor neuron (SMN) complex is a multi-megadalton complex involved in post-transcriptional gene expression in eukaryotes via promotion of the biogenesis of uridine-rich small nuclear ribonucleoproteins (UsnRNPs). The functional center of the complex is formed from the SMN/Gemin2 subunit. By binding the pentameric ring made up of the Sm proteins SmD1/D2/E/F/G and allowing for their transfer to a uridine-rich short nuclear RNA (UsnRNA), the Gemin2 protein in particular is crucial for the selectivity of the Sm core assembly. It is well established that post-translational modifications control UsnRNP biogenesis. In our work presented here, we emphasize the crucial role of Gemin2, showing that the phospho-status of Gemin2 influences the capacity of the SMN complex to condense in Cajal bodies (CBs) *in vivo*. Additionally, we define Gemin2 as a novel and particular binding partner and phosphorylation substrate of the mTOR pathway kinase ribosomal protein S6 kinase beta-1 (p70S6K). Experiments using size exclusion chromatography further demonstrated that the Gemin2 protein functions as a connecting element between the 6S complex and the SMN complex. As a result, p70S6K knockdown lowered the number of CBs, which in turn inhibited in vivo UsnRNP synthesis. In summary, these findings reveal a unique regulatory mechanism of UsnRNP biogenesis.

Keywords: UsnRNP biogenesis; Gemin2; p70S6K; mTOR pathway; post-translational modification

1. Introduction

The biogenesis of uridine-rich small nuclear ribonucleoproteins (UsnRNPs) plays a key role in post-transcriptional gene expression in eukaryotes, including pre-messenger RNA (pre-mRNA) splicing and the inhibition of premature termination (Staley et al., 1998, Wahl et al., 2009, Kaida et al., 2010). Each UsnRNP is composed of a specific, uridine-rich small nuclear RNA (UsnRNA), as well as the seven Sm proteins B, D1, D2, D3, E, F, and G. The Sm proteins form a stable heptameric ring structure, binding the so-called Sm site (Sm core) on the common snRNAs U1, U2, U4 or U5 (Mattaj et al., 1985, Kambach et al., 1999, Will et al., 2001, Newman et al., 2010, Weber et al., 2010). The assembly of the Sm core occurs stepwise in cells and is highly regulated by two cooperating protein complexes: the protein arginine methyltransferase 5 (PRMT5) and the survival of motor neuron (SMN) complex (Liu et al., 1997, Friesen et al., 2001b, Meister et al., 2001a).

The SMN complex consists of the survival motor neuron (SMN) protein, Gemins 2–8, and the UNR interacting protein (UNRIP) (Liu et al., 1997, Charroux et al., 1999, Baccon et al., 2002, Carissimi et al., 2005, Grimmler et al., 2005b, Carissimi et al., 2006). Within the SMN complex, the SMN protein and Gemin2 act as a functional core, responsible for Sm protein binding, which forces the transfer of the Sm proteins onto the Sm site of the snRNA and thus the formation of a core snRNP (Pellizzoni et al., 2002b, Kroiss et al., 2008, Zhang et al., 2011). After hypermethylation of the snRNA cap, the entire complex is reimported into the nucleus (Fischer et al., 1990, Pellizzoni et al., 2002b). Before being active in mRNA splicing, the snRNPs mature in aggregates within the nucleus, the so-called Cajal bodies (CBs), containing SMN complex components and coilin (Carmo-Fonseca et al., 1992, Liu et al., 1996, Bellini et al., 1999).

Further research already revealed a crucial role for post-translational modifications as a key regulation regulator in the biogenesis of snRNPs (Meister et al., 2001b, Grimmler et al., 2005a, Chari et al., 2008, Husedzinovic et al., 2014, Schmitz et al., 2021). Although several studies have showed that the SMN complex is highly phosphorylated, and the ATP-dependency of the snRNP core formation has been known for many years (Meister et al., 2001a, Grimmler et al., 2005a, Husedzinovic et al., 2014), the structural or mechanistic consequences of these post-translational modifications have not been identified so far. The work from Schilling et al. (Schilling et al., 2021) recently identified kinases from the mTOR pathway as interacting with core components of the SMN complex. Our work presents here the important role of the Gemin2 protein within this complex. Further research (Zhang et al.,

2011) has identified Gemin2 as binding the pentamer of Sm proteins independent from pICln. These results are in contradiction with previous work (Bühler et al., 1999, Pu et al., 1999, Meister et al., 2001b, Chari et al., 2008), indicating that the assembly chaperone protein pICln is necessary for the binding of the Sm proteins. In our recent work, we were able not only to demonstrate the necessity of pICln concerning the binding of the Sm proteins but also to show the importance of pICln phosphorylation, catalyzed by the autophagy-activating Unc-51-like kinase (ULK1), another kinase from the mTOR pathway, which mediates the release of Sm proteins onto the SMN complex (Schmitz et al., 2021). In this work, we identified Gemin2 as a new p70S6 kinase-specific binding partner and phosphorylation substrate. We focus on the characterization of the phospho-status of Gemin2 and its influence on nuclear SMN condensation, visualized via the number of nuclear CBs via immunofluorescence, as a readout for the efficiency of UsnRNP biogenesis. Furthermore, we demonstrate that the upstream phosphorylation of the mTOR-related kinase p70S6 regulates Gemin2 activity and, as a consequence, UsnRNP formation *in vivo* (Figure 1).

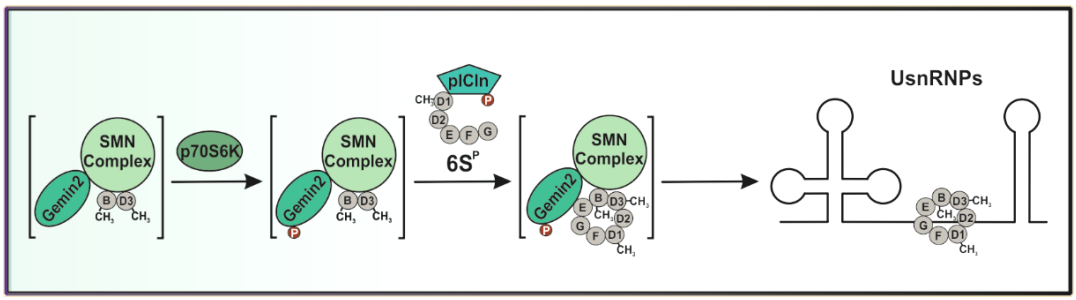

Figure 1. p70S6 kinase influences UsnRNP biogenesis via binding and phosphorylation of Gemin2, a core component of the human SMN complex.

2. Results

2.1. The p70S6 Kinase Is a New Interaction Partner of the SMN Complex

The SMN complex is a multi-megadalton protein complex consisting of the SMN protein itself, Gemins 2–8, and UNRIP (Liu et al., 1997, Charroux et al., 1999, Baccon et al., 2002, Gubitz et al., 2002, Pellizzoni et al., 2002a, Carissimi et al., 2005, Grimmler et al., 2005b, Carissimi et al., 2006). Gemin2 is, along with the SMN protein, one of the essential elements of the SMN complex (Ogawa et al., 2007). It is well established that phosphorylation events play a major role in controlling the SMN complex, and Gemin2 may have putative phosphorylation sites (Husedzinovic et al., 2014). Earlier studies have shown

that mTOR/-p70S6K-dependent phosphorylation events play an important role in this context, although the molecular mechanisms are yet unknown (Schilling et al., 2021). Our present study aims to clarify the role of p70S6K as a regulator of UsnRNP formation (Figure 1). Immunofluorescence studies were conducted to ascertain the role of p70S6K. In line with previous work (Liu et al., 1997, Carvalho et al., 1999), Gemin2 localizes predominantly in the cytoplasm, as well as in so-called Cajal bodies (CBs) within the nucleus of the cell (Figure 2A). p70S6K also localizes in the cytoplasm (Figure 2B), where it co-localizes with Gemin2 (Figure 2C).

To test whether Gemin2 directly interacts with p70S6K, immunopurification studies were performed. To this end, we established an inducible expression system for the GFP-immunopurification of a GFP-Vector control (GFP), GFP-Gemin2 wt, and GFP-SMN wt in Flp-In T-REx 293 cells. In this context, it is interesting to note that each Gemin (Gemin2–5) and the SMN protein bind in amounts comparable to both GFP-SMN and GFP-Gemin2 wild type, indicating that the overexpressed proteins are functional in the formation of the entire SMN complex. However, only Gemin2 showed an interaction with p70S6K. Thus, we identified p70S6K as a new, Gemin2-specific binding partner of the SMN complex (Figure 2D). To further validate this survey, we performed endogenous immunopurification and immunoblot analysis from the two potential interaction partners Gemin2 and p70S6K, showing that the two proteins also interact in vivo (Figure 2E).

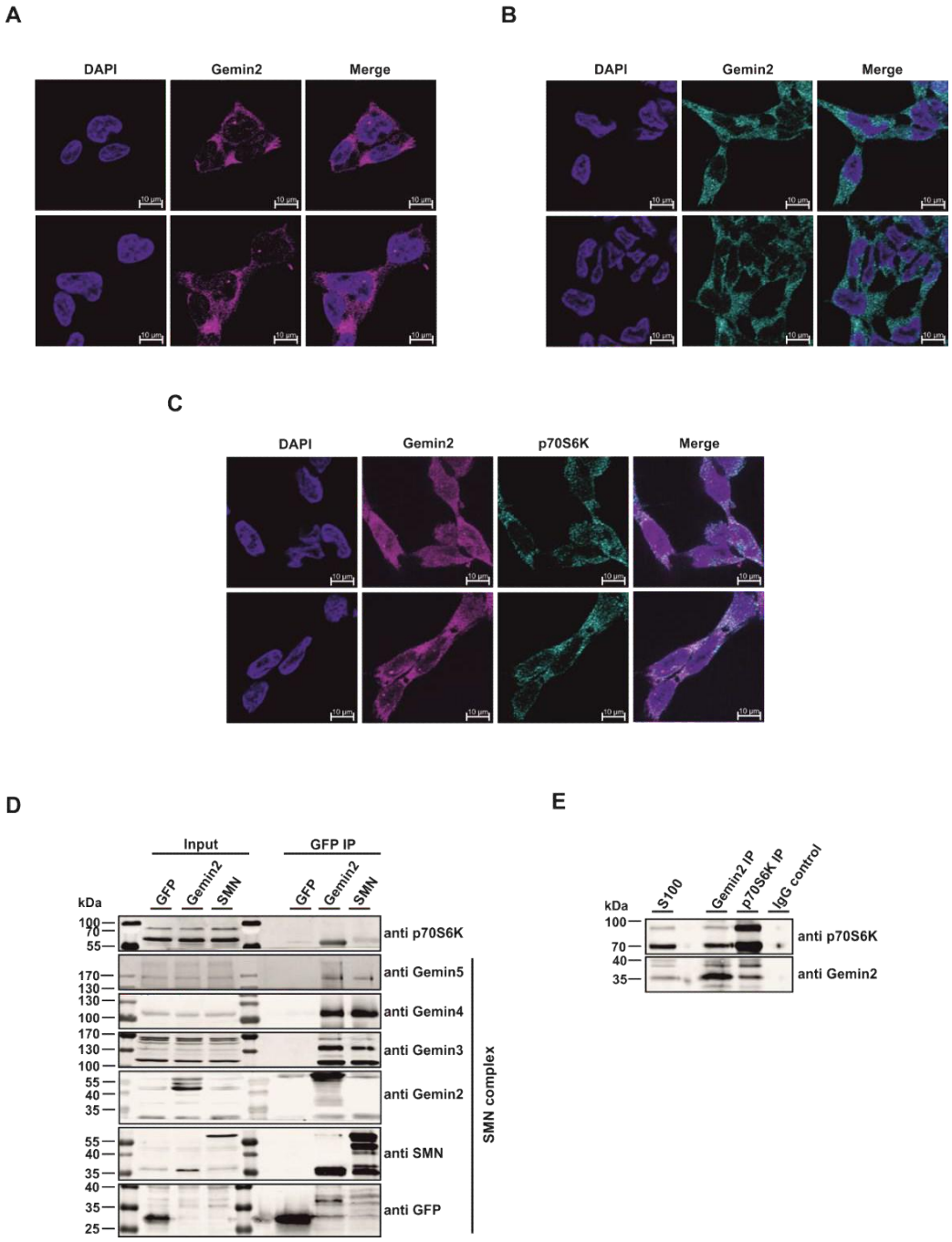

Figure 2. The kinase p70S6 interacts with the core components of the SMN complex in cells. (**A**) Gemin2 localizes in the cytoplasm and Cajal bodies in HEK293T wt cells. All cells were fixed with 4% paraformaldehyde and permeabilized with Triton X-100 to visualize Gemin2 (magenta). DAPI (blue) was used as a DNA marker, with scale bars of 10 µm. (**B**) The staining procedure for HEK293T cells was executed as described in (**A**), to visualize p70S6K (cyan) via specific antibody. The DNA was stained with DAPI (blue), with scale bars of 10 µm. (**C**) Gemin2 (magenta) co-localizes with p70S6K (cyan) predominantly in the cytoplasm. HEK293T cells were treated as described in (**A**). DAPI (blue) was used as a DNA marker, with scale bars of 10 µm. (**D**) Immunopurification (IP) of GFP Vector control (GFP), GFP-Gemin2 wt, and GFP-SMN wt overexpressing cells. Expression of GFP proteins was induced with 0.1 µg/mL doxycycline for 24 h. After cell lysis via douncing, GFP-IP was performed and analyzed with Tris/Glycine-SDS-PAGE and Western blotting, using antibodies against p70S6K, GFP, and core components of the SMN complex. As an input, 25 µg of total protein was loaded. The p70S6K did bind more efficiently to GFP-Gemin2 wt than to GFP-SMN wt. (**E**) Endogenous immunopurification studies revealed that Gemin2 and p70S6K interact in vivo. S100 extract of HEK293 cells was used for performing an endogenous IP experiment with each 1 µg antibody and 1 mg of total protein lysate. Afterward, the IP samples and an input sample were subjected to Tris/Glycine- SDS-PAGE followed by Western blot analysis.

2.2. The SMN Complex Core Subunit Gemin2 Is a New Substrate of the p70S6 Kinase

To determine whether Gemin2 is a new and so-far unknown substrate of p70S6K, we performed in vitro kinase assays using recombinant purified GST-fusion proteins of Gemin2 and SMN as substrates and active 6xHis-p70S6K purified from Sf21 insect cells. All used substrates showed ^{32}P incorporation upon incubation with active His-p70S6K. Although Gemin2 does not have many putative phosphorylation sites (two threonines and four serines) (Husedzinovic et al., 2014, Schilling et al., 2021), it showed a strong ^{32}P incorporation (Figure 3A). Based on earlier mass spectrometry results from Schilling et al. (Schilling et al., 2021), the potential phosphorylation sites serine 81 and serine 166 within Gemin2 were mutated. Each potential phosphorylation site was mutated to an alanine, as a phospho-deficient, and to an aspartate, as a putative phospho-mimicking mutant. To verify these potential p70S6K phosphorylation sites within Gemin2, we performed in vitro kinase assays with GST-Gemin2 wt, GST-Gemin2 S81A, GST-Gemin2 S166A, GST-Gemin2 S81D, GST-Gemin2 S166D, and GST only. Gemin2 wt and Gemin2 S166's mutation to alanine and to aspartate showed a strong ^{32}P incorporation. Interestingly, the Gemin2 S81 mutation to alanine and to aspartate showed a strong decrease in phosphorylation signal, meaning that this was a p70S6K-specific residue (Figure 3B). However, the phosphorylation was not blocked completely, indicating that this was not the only p70S6K-specific phosphorylation site within Gemin2 in this setting. A pulldown assay was performed with these recombinant Gemin2 phosphorylation mutants to see whether the binding capacity of these proteins was also affected. GST-Gemin2 wild type (wt), GST-Gemin2 S81A, GST-Gemin2 S166A, GST-Gemin2 S81D, and GST-Gemin2 S166D bind SMN and SmB/B' (Y12 antibody) to the same extent. This indicates that the mutations at the respective serines within Gemin2 do not affect the overall protein structure or formation of the SMN complex. Only the Gemin2 S81 alanine mutant showed a decrease in p70S6K binding. As this is also the mutant that showed a decrease in phosphorylation, these results indicate on one hand that S81 is the major site of phosphorylation but also may represent the area of direct binding of Gemin2 and p70S6K (Figure 3C).

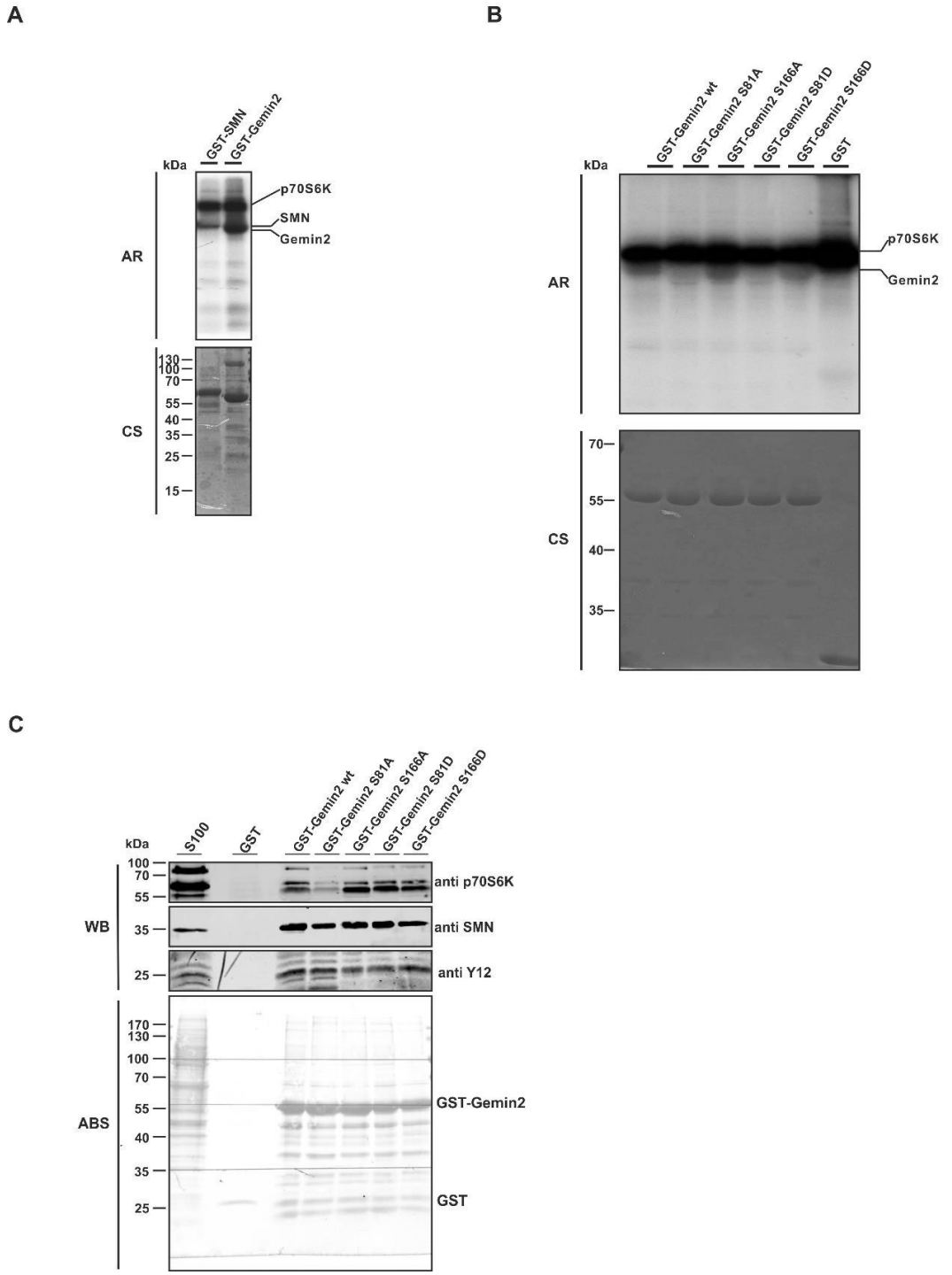

Figure 3. The p70S6 kinase phosphorylates Gemin2 at specific residues. (**A**) The p70S6K phosphorylates components of the SMN complex. In vitro kinase assay using recombinant active His-tagged p70S6K expressed in Sf21 insect cells and GST-SMN and GST-Gemin2 purified from *E. coli* as substrate proteins were incubated with 10 µCi [32P]-ATP for 45 min at 30 °C. Samples were separated via Tris/Glycine-SDS-PAGE and after coomassie staining (CS) analyzed by autoradiography (AR). (**B**) The p70S6K phosphorylates Gemin2 at S81. Kinase assay using His-tagged p70S6K with the substrates GST-Gemin2 wt, GST-Gemin2 SA81, GST- Gemin2 SA166, GST-Gemin2 SD81, and GST-Gemin2 SD166 as recombinant proteins purified from *E. coli* was performed as described in (**A**). (**C**) Pulldown assays using recombinant GST-Gemin2 wild type (wt), GST-Gemin2 SA81, GST-Gemin2 SA166, GST-Gemin2 SD81 and GST-Gemin2 SD166 and GST purified from *E. coli* were executed in HEK293T cytoplasmic extracts for 2 h at 4 °C. Afterward, samples were analyzed via Tris/Glycine-SDS-PAGE and Western blotting (WB), using antibodies against p70S6 kinase, SMN and SmB/B´ (Y12) and amido black staining (ABS) of the whole membrane was used as a loading control for the recombinant proteins.

2.3. The p70S6 Kinase-Dependent Phosphorylation Influences Binding towards Gemin2

We identified Gemin2 as a new, p70S6K-specific interaction partner and substrate; however, the question of the cellular effect of Gemin2 phosphorylation remained unclear. To further investigate the effect of the Gemin2 phospho-status, Flp-In T-REx 293 cells overexpressing GFP-Vector control, GFP-SMN wt, GFP-Gemin2 wt, GFP-Gemin2 A81, GFP-Gemin2 A166, GFP-Gemin2 D81, and GFP-Gemin2 D166 were used. To test the expression efficiency of the cell lines, immunoblot analyses were performed with cytoplasmic extract (S100) as well as a GFP-immunopurification of these extracts. All generated cell lines expressed the GFP-tagged fusion proteins in comparable amounts (Figure 4A). The localization of the GFP-tagged proteins was visualized using immunofluorescence analysis. While GFP-Vector control, GFP-Gemin2 wt, GFP-Gemin2 A81, GFP-Gemin2 A166, GFP-Gemin2 D81, and GFP-Gemin2 D166 localized in the cytoplasm and the nucleus, GFP-SMN wt mainly aggregated in dots in the cytoplasm of the cell (Figure 4B). To see whether the overexpression of GFP-Vector control, GFP-Gemin2 wt, and the GFP-Gemin2 phospho-mutants influenced endogenous Gemin2 complex building, S100 extracts of these cell lines were separated with size exclusion chromatography with a Superose 6 column. Via immunoblot analysis, when a pan-specific antibody against Gemin2 was used, it was evident that Gemin2 is distributed in a complex in the higher molecular size range around 2000 kDa and in addition in the distinct lower molecular weight range from 158 kDa to 100 kDa, comigrating with the so-called 6S complex, an RNA-free intermediate consisting of the chaperone protein pICln and the Sm proteins D1, D2, E, F, and G (Esser et al., 2023).

The overexpression of neither GFP-Gemin2 wt nor the GFP-Gemin2 phosphorylation-mutant variants of Gemin2 affected the Gemin2 distribution pattern (Figure 4C). To test the scenario of whether Gemin2 phosphorylation status influences the binding of interaction partners, a GFP-immunopurification with cytoplasmic extracts of those cell lines was performed. All core components of the SMN complex, Gemin2–5, and SMN bind in equal amounts to the Gemin2 phospho-mutants. This indicated that the complex composition of the SMN core-complex is not affected by overexpression (Figure 4D).

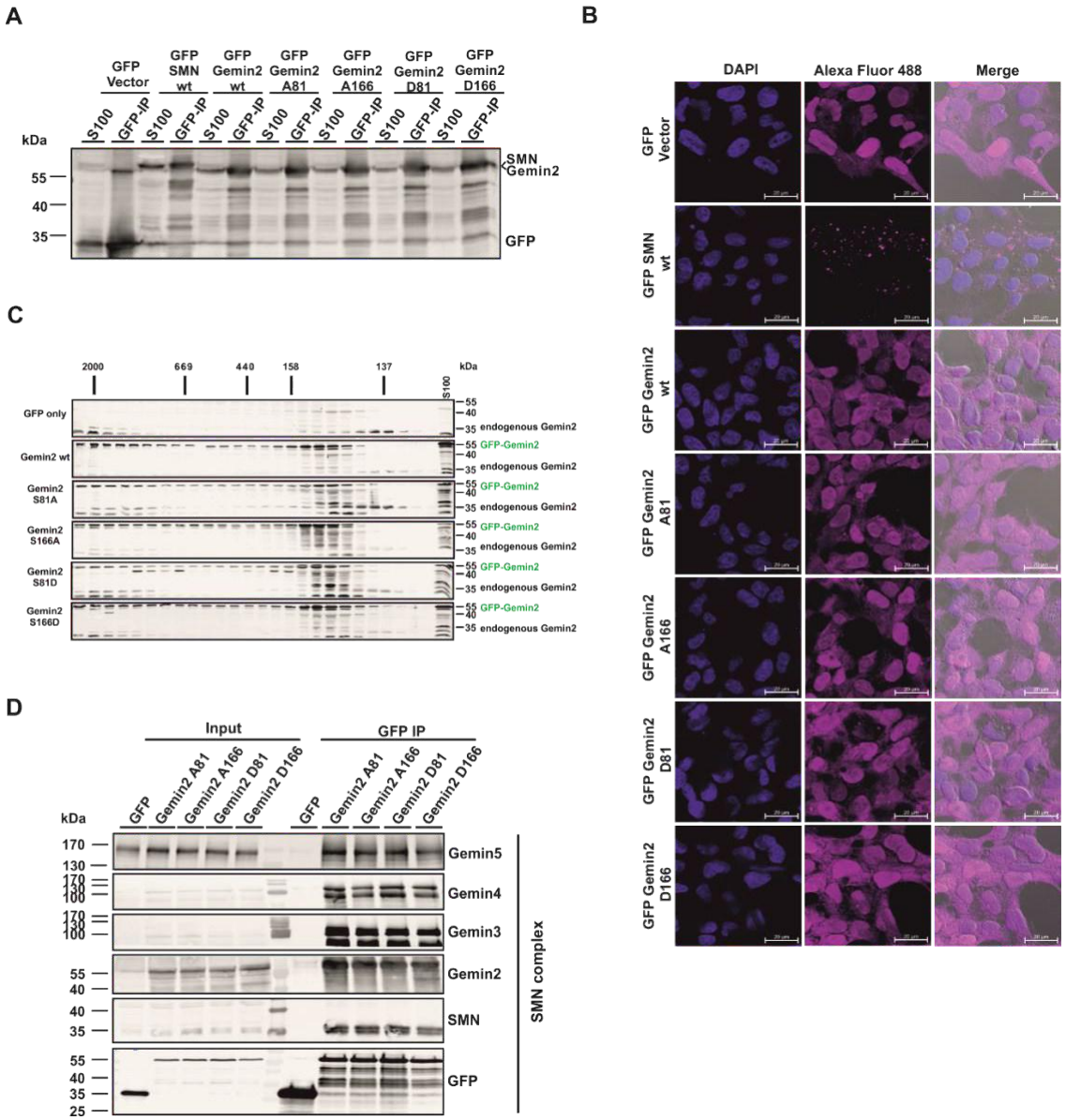

Figure 4. The phosphorylation status of Gemin2 does not influence the binding of the SMN complex components. *(***A**) Expression of newly generated cell lines was tested using Western blot analysis of HEK293T S100 extracts and GFP-immunopurification. IP was performed with S100 extract from GFP-Vector control, GFP-SMN wt, GFP-Gemin2 wt, GFP-Gemin2 A81, GFP-Gemin2 A166, GFP-Gemin2 D81, and GFP-Gemin2 D166 overexpressing cells. Protein expression was induced with 0.1 µg/mL doxycycline for 24 h. After cell lysis, GFP-IP was performed and together with 25 µg of total protein was analyzed via Tris/Glycine-SDS-PAGE and Western blotting, using an antibody against GFP. (**B**) Immunofluorescence studies of GFP-Vector, GFP-SMN wt, GFP-Gemin2 wt, GFP-Gemin2 A81, GFP-Gemin2 A166, GFP-Gemin2 D81, and GFP-Gemin2 D166 in overexpressing cells. Protein expression was induced as described in (**A**). Cells were fixed with 4% PFA and permeabilized with Triton X-100 to visualize the GFP overexpressed proteins (magenta). The DNA was stained with DAPI (blue), with scale bars of 20 µm. (**C**) S100 extracts of inducible Flp-In T-REx 293 cells overexpressing GFP-Vector control (GFP), GFP-Gemin2 wt, GFP-Gemin2 A81, GFP-Gemin2 A166, GFP-Gemin2 D81, and GFP-Gemin2 D166, generated by douncing, were applied to a Superose 6 column. Afterward, fractions were analyzed via Tris/Glycine-SDS-PAGE and immunoblotting using antibodies against Gemin2. Each of the overexpressed GFP and the GFP-Gemin2 variants (green) as well as the endogenous Gemin2 (black) were visualized via this analysis. (**D**) IP of GFP, GFP-Gemin2 A81, GFP-Gemin2 A166, GFP-Gemin2 D81, and GFP-Gemin2 D166 overexpressing cells. Expression of GFP proteins was induced as described in (**A**). After cell lysis, GFP-IP was performed with S100 extract and analyzed via Tris/Glycine-SDS-PAGE and Western blotting, using antibodies against GFP and core components of the SMN complex.

2.4. The Phosphorylation Status of Gemin2 Influences UsnRNP Biogenesis and Inhibition of p70S6K Results in a Decreased Number of Cajal Bodies

So far, this study identified p70S6K as a specific interaction partner of the SMN complex and revealed Gemin2 as a phosphorylation substrate of this kinase. This data raised the question of whether the Gemin2 phospho-status has a direct impact on the regulation of UsnRNP biogenesis. In the late stage of UsnRNP biogenesis, the UsnRNP matures in an aggregate in the nucleus, within the CBs, which can be visualized as SMN and coilin positive dots via immunofluorescence (Liu et al., 1996, Schmitz et al., 2021). To test the SMN condensation, the GFP-Vector control, GFP-SMN wt, GFP-Gemin2 wt, GFP-Gemin2 A81, GFP-Gemin2 A166, GFP-Gemin2 D81, and GFP-Gemin2 D166 overexpressing cells were seeded on coverslips and stained with antibodies against SMN and coilin (Figure 5A). All numbers of CBs mentioned in this work are the mean of 1000 cells per condition. The overexpression of GFP-SMN wt (2.44) caused a strong increase in the number of CBs compared to the GFP-Vector control (1.19). Expression of GFP-Gemin2 wild-type protein and the corresponding phospho-mutants had only a slight effect on the number of Cajal bodies (Figure 5B); this can be explained by the presence of endogenous Gemin2. Therefore, we treated HEK293T cells with p70S6K-siRNA, followed by immunofluorescence against SMN and coilin, to visualize the quantity of CBs (Figure 5C,D). The number of CBs per nucleus (mean) was significantly decreased in p70S6K knockdown HEK293T cells (0.75) compared to untreated control HEK293T cells (1.43) and cells transfected with non-target control siRNA (1.31) (Figure 5D).

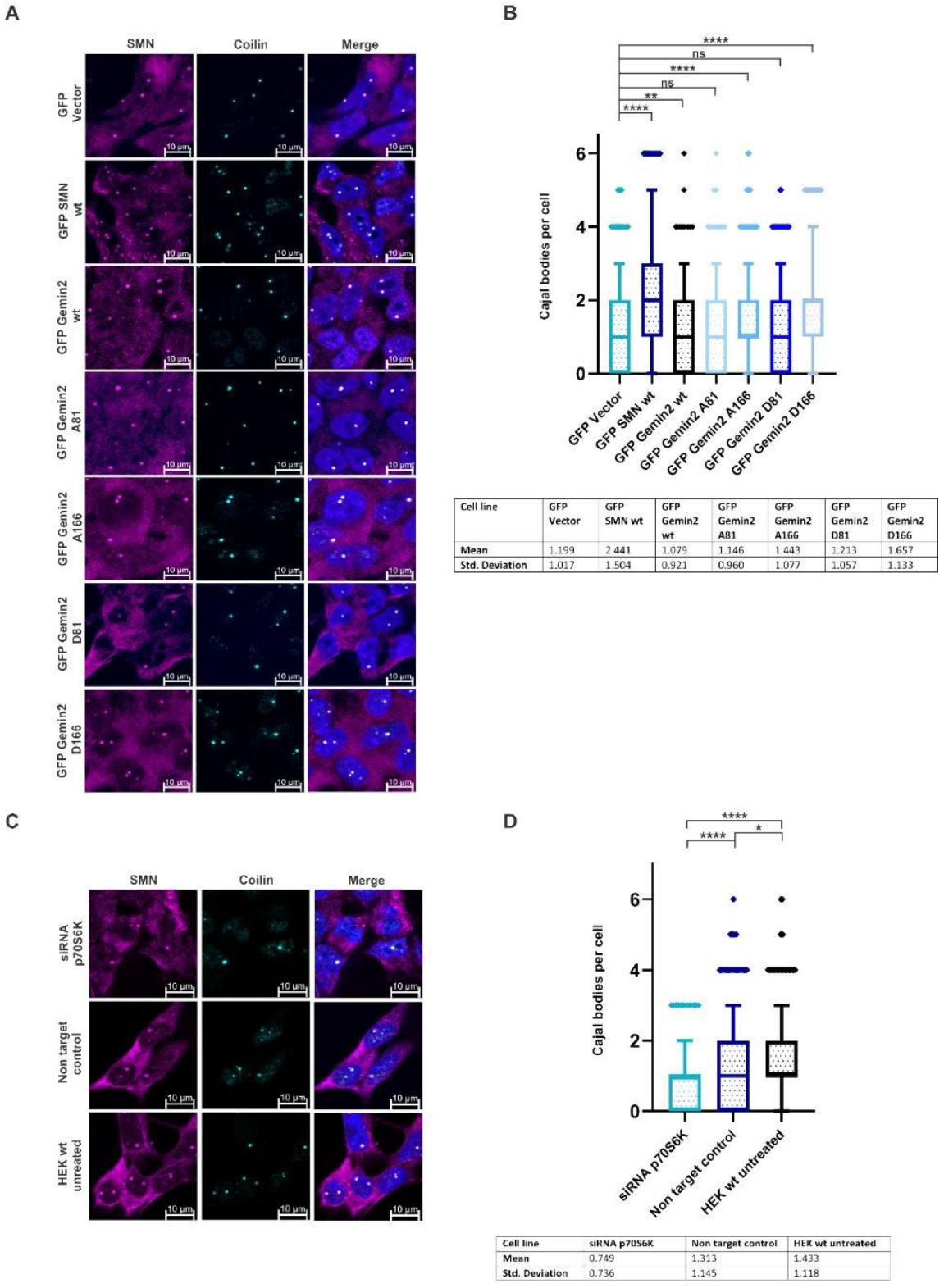

Cell line	GFP Vector	GFP SMN wt	GFP Gemin2 wt	GFP Gemin2 A81	GFP Gemin2 A166	GFP Gemin2 D81	GFP Gemin2 D166
Mean	1.199	2.441	1.079	1.146	1.443	1.213	1.657
Std. Deviation	1.017	1.504	0.921	0.960	1.077	1.057	1.133

Cell line	siRNA p70S6K	Non target control	HEK wt untreated
Mean	0.749	1.313	1.433
Std. Deviation	0.736	1.145	1.118

Figure 5. **Gemin2 phospho-status and p70S6 kinase influence UsnRNP biogenesis in vivo.** (**A**) Quantification of Cajal bodies in GFP-Vector control, GFP-SMN wt, GFP-Gemin2 wt, GFP-Gemin2 A81, GFP-Gemin2 A166, GFP-Gemin2 D81, and GFP-Gemin2 D166 overexpressing cells. Protein expression was induced with 0.1 µg/mL doxycycline for 24 h. Cells were fixed with 4% PFA and permeabilized with Triton X-100 to visualize SMN (magenta) and coilin (cyan). DAPI (blue) was used as a DNA marker, with scale bars of 10 µm. (**B**) Overexpression of GFP-SMN as well as GFP-Gemin2 A166 and GFP-Gemin2 D166 in Flp-In T-Rex cells caused an increase in the number of Cajal bodies compared to the GFP-Vector control and GFP-Gemin2 wt cells. The box in the boxplot diagram represents 5–95% of the data; outliers are shown as stacked rectangles. The *p*-value, calculated with Prism using an unpaired *t*-test, was **** $p < 0.0001$. (**C**) HEK293T

cells were treated with 50 nM p70S6K siRNA or non-targeting control for 72 h. Untreated HEK293T cells, as well as the transfected ones, were fixed with 4% PFA, and Cajal bodies were visualized with antibody staining against coilin (cyan) and SMN (magenta). The DNA was stained with DAPI (blue), with scale bars of 10 µm. (**D**) Decrease of endogenous p70S6K resulted in a dramatic reduction in the number of Cajal bodies compared to untreated cells and non-target control. Statistics and presentation of the data were performed as described in (**B**).

Taken together, Gemin2 is a newly identified p70S6 kinase substrate. The mutation of Gemin2 phospho-sites has an impact on the binding of the kinase, but not on SMN complex integrity. Knockdown of p70S6K in cells has also a strong impact on UsnRNP biogenesis, indicating that this kinase influences the regulation of this process via phosphorylation of Gemin2.

3. Discussion

The SMN complex fulfills a key role in the biogenesis of uridine-rich small nuclear ribonucleoproteins (UsnRNPs), which is a well-organized stepwise mechanism highly regulated via post-translational modifications (Meister et al., 2001b, Grimmler et al., 2005a, Chari et al., 2008, Husedzinovic et al., 2014). Recent research has demonstrated a significant role of kinases from the mTOR pathway in this context (Schilling et al., 2021, Schmitz et al., 2021, Esser et al., 2023). In our study presented here, we show that p70S6 kinase interacts with the SMN complex via Gemin2 and influences UsnRNP biogenesis via phosphorylation of Gemin2 (Figure 1).

Immunofluorescence analyses showed colocalization of Gemin2 and p70S6K in the cytoplasm (Figure 2A–C). Subsequent endogenous immunopurification studies have revealed that p70S6K is co-precipitated with Gemin2 but also interacts with it via direct binding (Figure 2D,E). The significantly weaker detection of p70S6K in the GFP-SMN IP compared with the GFP-Gemin2 IP likely indicates indirect binding via endogenous coprecipitated Gemin2 (Figure 2D).

This is consistent with previous work showing that phosphorylation of the SMN complex and the resulting regulation occurs predominantly in the cytoplasm (Grimmler et al., 2005a, Schmitz et al., 2021). Although in vitro phosphorylation studies have demonstrated that both SMN and Gemin2 proteins can be phosphorylated via p70S6K (Figure 3A,B), results from immunopurification studies suggest that Gemin2 is the major substrate and binding partner of p70S6K within the SMN complex (Figure 2D,E).

The phosphorylation sites of Gemin2, serine 81 and serine 166, as postulated in the work of Schilling and colleagues, were mutated to an alanine, as a phospho-deficient, and to an aspartate, as a phospho-mimicking mutant (Schilling et al., 2021). Interestingly, in in vitro kinase assay, Gemin2 S81 mutations to alanine and to aspartate showed a strong decrease in phosphorylation signal, identifying serine 81 as a p70S6K-specific target (Figure 3B). Nevertheless, the phosphorylation was not blocked completely, meaning there may be more phosphorylation sites within Gemin2, consistent with the earlier mass spectrometry analysis by Schilling and colleagues (Schilling et al., 2021). The in vitro binding studies using these recombinant Gemin2 phosphorylation mutants revealed that the binding towards SMN and SmB/B′ is not affected, indicating that the phospho-mutations do not affect SMN core complex building (Figures 3C and 4D). Indeed, the Gemin2 S81-to-alanine mutant showed a decrease in p70S6K-dependent phosphorylation and a slight decrease in p70S6K binding, suggesting that the reduced binding affinity of the Gemin2 S81 mutant affects the phosphorylation efficiency, too (Figure 3B,C).

To address the question of the intracellular effect of Gemin2 phosphorylation, cells which inducibly overexpress GFP, GFP-SMN wt, GFP-Gemin2 wt, GFP-Gemin2 A81, GFP-Gemin2 A166, GFP-Gemin2 D81, and GFP-Gemin2 D166 were generated (Figure 4A,B). Size exclusion chromatography pointed out that Gemin2 is distributed in a higher molecular complex as well as in the distinct molecular weight range from 158 kDa to 100 kDa, the same size range as the 6S complex (Esser et al., 2023). This suggests that the 6S complex, consisting of pICln and the Sm proteins D1, D2, E, F, and G, might be a kinetic trap involved in the transfer of Sm proteins onto the SMN complex to keep snRNP biogenesis ongoing (Chari et al., 2008). Our findings now identify Gemin2 as co-migrating in the size of the 6S complex by using size exclusion chromatography in vivo (Figure 4C). Further in vitro studies revealed Gemin2 to organize the stepwise formation of the Sm core by binding the Sm protein pentamer and at the same time prevent it from binding RNAs. Gemin2 was shown to have an open confirmation, where the C- and N-terminus of the protein wrap around the pentamer of the Sm proteins SmD1/D2 and SmE/F and G, connected by an unstructured loop region (Zhang et al., 2011). This data strengthens the assumption that Gemin2 is a bridging factor between the 6S complex and the SMN complex involved in the transfer of the Sm proteins from the 6S complex onto the snRNA (Meister et al., 2002b, Zhang et al., 2011).

During UsnRNP biogenesis, the snRNPs mature in the nucleus, within the CBs (Liu et al., 1996, Schmitz et al., 2021). According to earlier studies (Husedzinovic et al., 2014, Schilling et al., 2021), the subcellular location of the SMN complex and, consequently, its nuclear condensation in CBs, is controlled via the phosphorylation of serine/threonine residues as a regulatory mechanism. Due to this, we investigated how Gemin2's phosphorylation status affected the SMN complex's ability to condense in the nucleus. When compared to the GFP-Vector control (1.19), the overexpression of the GFP-Gemin2 wild-type protein and the corresponding phospho-mutants (1.08) had no discernible impact (Figure 5A,B). This can be explained on the one hand by the fact that the phosphorylation state of Gemin2 is not the sole factor for the number of Cajal bodies and on the other hand by the fact that in the overexpressing Gemin2 model systems, the endogenous Gemin2 is still present and performs this function. However, HEK293T cells treated with p70S6K siRNA (0.75) revealed a significant decrease in the number of CBs per cell compared to HEK293T untreated control cells (1.43) or cells transfected with non-target control siRNA (1.31) (Figure 5C,D). It is interesting to note that the SMN complex fails to condense in CBs in spinal muscle atrophy (SMA) patients (Coovert et al., 1997, Lefebvre et al., 1997). As the siRNA-mediated knockdown of p70S6K in cells has a strong impact on the condensation of the nuclear SMN complex in vivo, this identifies p70S6K as a new putative target for the treatment of SMA patients. As mentioned above, earlier studies have linked Gemin2's crucial role in snRNP biogenesis through regulating the binding of the Sm protein pentamer independent from pICln and thus increasing RNA binding specificity. In line with these results, a mutation in the SMN protein aborting the binding towards Gemin2, which is known to be SMA-causing, links the so-far missing mechanism of the Gemin2-mediated Sm pentamer recruitment to SMA (Zhang et al., 2011). Still, it is crucial that the role of pICln be discussed, as it is clear that it builds an RNA-free intermediate, the 6S complex, containing the Sm proteins SmD1, D2, E, F, and G. To form a functional UsnRNP, the two Sm proteins B and D3 must replace pICln. This replacement is catalyzed via phosphorylation of an mTOR pathway kinase, ULK1, which enables the transfer of the Sm proteins onto the SMN complex (Meister et al., 2002b, Schmitz et al., 2021, Esser et al., 2023). The new mechanism of Gemin2 phosphorylation caused by p70S6K identified here may help to explain the regulation of Sm protein transfer within UsnRNP assembly. As the phospho-status of Gemin2, influenced by the p70S6 kinase from the mTOR pathway, influences the nuclear SMN condensation in vivo, our results strengthen the assumption that Gemin2 is acting as a bridging factor between the SMN complex and the 6S complex. Thus, regulation

of Gemin2 activity could have a direct influence on the formation of core UsnRNPs by mediating the transfer of Sm proteins onto the UsnRNA (Zhang et al., 2011). We hypothesize a strongly phospho-dependent mechanism of Sm protein transfer onto the SMN complex: on the one hand regulated by ULK1 via pICln (Schmitz et al., 2021, Esser et al., 2023) and on the other hand regulated transfer by p70S6K via Gemin2, receiving the Sm proteins from pICln. As Gemin2 conformation was shown to be open while the protein wraps around the Sm proteins (Zhang et al., 2011), this conformation may be forced by phosphorylation mechanisms. Intensive work will be necessary to understand in more detail the molecular impact of p70S6K within UsnRNP biogenesis and the regulation of Gemin2 activity in this context.

4. Materials and Methods

4.1. Antibodies

The following primary antibodies were used for immunoblotting and immunofluorescence: α-coilin (Invitrogen, Carlsbad, CA, USA, #PA5-29531, rabbit), α-Gemin2 (Santa Cruz, CA, USA, #sc-166162, mouse), α-Gemin3 (Santa Cruz, CA, USA, #sc-374373, mouse), α-Gemin4 (Santa Cruz, CA, USA, #sc-365424, mouse), α-Gemin5 (Santa Cruz, CA, USA, #sc-136200, mouse), α-GFP (Invitrogen, Carlsbad, CA, USA, #14-6674-82, mouse), α-p70S6K (CST, Danvers, Massachusetts, USA, #9202, rabbit) α-SMN (Merck Millipore, Billerica, Massachusetts, USA, #05-1532, mouse), and α-SmB (Y12, Novus biologicals, Colorado USA, #NB600-456, mouse). The detection of proteins after transfer onto PVDF membranes occurred with the following fluorescent secondary antibodies: IRDye 680LT goat α-rabbit and IRDye 800CW donkey α-mouse. For the detection of proteins in vivo via immunofluorescence, the following secondary antibodies were used: Goat anti-Mouse IgG (H + L) Cross-Adsorbed Secondary Antibody, Alexa Fluor 488 (Invitrogen, Carlsbad, CA, USA, #A11001), Donkey anti-Rabbit IgG (H + L) Highly Cross-Adsorbed Secondary Antibody, Alexa Fluor 647 (Invitrogen, Carlsbad, CA, USA, #A31573), and Alexa Fluor 568 donkey anti-mouse (Invitrogen, Carlsbad, CA, USA, #A10037).

4.2. Plasmids and Proteins

Plasmids containing SMN wt, and Gemin2 wt in pGEX-6P-1 Vector for protein expression were synthesized with GeneArt (Thermo Fisher Scientific, Waltham,

Massachusetts, USA). For all cloning procedures, the Q5 High-Fidelity 2x Master Mix (New ENGLAND BioLabs, Germany, #M0494S) and KLD Enzyme Mix (New ENGLAND BioLabs, Germany, #M0554S) were used.

For cloning of the constructs in the GST-tagged pGEX-6P-1 protein expression vector, the following primers were used:

pGEX-6P-1-SMN wt, 5′-CTCGAGATGGCGATGAGCAGCGG-3′

5′-GCCCTTTTAATTTAAGGAATGTGAGCACC-3′

pGEX-6P-1-Gemin2 wt, 5′-GAATTCATGCGCCGAGCGGAAC-3′

5′-CTCGAGTCAAGATGGCTCATCAGCTAAA-3′

For cloning the Gemin2 phosphorylation mutants the following primers were used:

Gemin2 A81, 5′-GCAGTGAATATTTCTCTTTCAGGATGCCAAC-3′

5′-TTGCTTCCTTTTCAACTTCTTTGGGTC-3′

Gemin2 D81, 5′-GACGTGAATATTTCTCTTTCAGGATGCCAAC-3′

5′-TTGCTTCCTTTTCAACTTCTTTGGGTC-3′

Gemin2 A166, 5′-GCACCTGGAATAGATTATGTACAAATTGGTTTTCC-3′

5′- TTCATTTGTGGCTGGTCCAACAG-3′

Gemin2 D166, 5′-GACCCTGGAATAGATTATGTACAAATTGGTTTTCC-3′

5′-TTCATTTGTGGCTGGTCCAACAG-3′

pcDNA-FRT-TO-GFP is the vector used for the generation of inducible Flp-In T-REx 293 cells. For cloning of GFP-SMN wt, GFP-Gemin2 wt, GFP-Gemin2 A81, GFP-Gemin2 A166, GFP-Gemin2 D81, and GFP-Gemin2 D166 cell lines restriction enzymes were used with a following ligation with T4 ligase (Thermo Fisher, Waltham, Massachusetts, USA #EL0011).

4.3. Cell Lines and Cell Culture

Generation of inducible Flp-In T-REx 293 cell system expressing GFP, GFP-SMN wt, GFP-Gemin2 wt, GFP-Gemin2 S81A, GFP-Gemin2 S166A, GFP-Gemin2 S81D, and GFP-Gemin2 S166D were carried out according to the manufacturer's instructions (Invitrogen, Thermo Fisher Scientific, #R78007). The generation of pcDNA5-FRT-TO-eGFP plasmid has been described previously (Löffler et al., 2011). Cells were selected with 200 µg/mL Hygromycin B Gold (Invivogen, #ant-hg-1) and 5 µg/mL Blasticidin (Invivogen, #ant-bl-05). Protein expression of Flp-In T-REx 293 cell lines was induced with 0.1 µg/mL Doxycycline (Clontech, Mountain View, CA, USA, #564-25-0) for 24 h. For p70S6K

knockdown, HEK293T cells were transfected with 50 nM p70S6K siRNA (Dharmacon, #L-003616-00-0020) or SMARTpool non-targeting control (ON-TARGETplus, Dharmacon, Lafayette, CO, USA, #D-001810-10-20) for 72 h using DharmaFECT1 (Dharmacon, Lafayette, CO, USA, #T-2001-02). All cell lines were cultured at 37 °C in DMEM high glucose media (Gibco, Thermo Fisher Scientific, Waltham, Massachusetts, USA, #41965062) supplemented with 10% (v/v) FCS (Sigma Aldrich, St. Louis, USA, #F9665), 100 U/mL Penicillin and 100 µg/mL Streptomycin (Gibco, Thermo Fisher Scientific, Waltham, Massachusetts, USA, # 15140122) in a 5% CO_2 humidified atmosphere. For transfection of siRNA, opti-MEM (Gibco, USA, #31985062) was used as a serum-reduced transfection medium.

4.4. Protein Expression and Purification

All proteins were expressed in BL21 DE3 Arctic express competent *E. coli* (Agilent Santa Clara, Kalifornien, USA, #230192). Bacterial lysis was carried out in a buffer containing 50 mM Tris/HCl pH 7.5, 5 mM EDTA, 5 mM EGTA, 0.01% (v/v) Igepal, EDTA-free protease inhibitor cocktail (cOmplete, Roche, Switzerland, #04693132001), 50 mg/mL Lysozyme (Serva, Germany, #12650-88-3) and via sonication. After centrifugation at 15.000 rpm for 1 h, the lysate of GST-tagged proteins was incubated with pre-washed glutathione Sepharose 4B (Cytivia, Malborough, Massachusetts, USA, #17-0756-01) for 2 h at 4 °C and afterward washed 3 times with lysis buffer. For pulldown assays, recombinant proteins were incubated 2 h at 4 °C with HEK293T S100 extract and subsequently washed 3 times with lysis buffer. As a positive control, 25 µg of total protein was loaded; as a negative control, a pulldown assay with the GST protein was performed. For further analysis of the proteins, a Tris/Glycine SDS-PAGE and Western blotting with specific antibodies were carried out. As a loading control after immunoblotting, the whole membrane was stained with amido black staining (40% Methanol (v/v), 10% Acetic acid (v/v), 0.1% Amido black 10B (w/v)).

4.5. Cytoplasm Extraction (S100) and Size Exclusion Chromatography

After harvesting, HEK293T cells were incubated in Roeder A buffer in 3 times the volume of the weight of the cells for 10 min at room temperature. Then cells were dounced 10 times, and the lysate was adjusted to 150 mM NaCl. After centrifugation at 12,000 rpm for 30 min the supernatants (S100 extracts) were filtrated with Millex-HA, 0.45 µm filter unit (Merck Millipore, Billerica, Massachusetts, USA #HAWP04700) and applied to a Superose6 increase 10/300 GL column (GE Healthcare, Malborough, Massachusetts, USA,

#GE29-0915-96). A 1 mL quantity as a fraction volume was loaded, and each 0.5 mL fraction was collected in running buffer (150 mM NaCl, 50 mM Tris/HCl pH 7.5) and analyzed via immunoblotting. The columns were calibrated with thyroglobulin (669 kDa), ferritin (440 kDa), catalase (232 kDa), aldolase (158 kDa), albumin (67 kDa), ovalbumin (43 kDa), and RNase (14 kDa) (GE Healthcare, Malborough, Massachusetts, USA).

4.6. Immunoblotting and Immunopurification

Protein amounts of cleared S100 cytoplasm extracts were measured via the Bradford method. Samples were separated via Tris/Glycine SDS gel electrophoresis and transferred onto PVDF membranes (Immobilon-FL, Merck Millipore, Billerica, Massachusetts, USA #IPFL00010). For the immunoblot analysis, the membranes were incubated in protein-specific primary antibodies and signals were detected with fluorescent secondary antibodies and the Odyssey LI-COR Imaging System. For GFP immunopurification, S100 extracts were incubated with pre-washed GFP-Trap beads (ChromoTek, Germany, #gta-20) for at least 2 h at 4 °C while rotating. Immunopurified proteins were washed 3 times with Dulbecco's phosphate-buffered saline-DPBS (Gibco, USA, #14190144). The elution of proteins occurred in sample buffer [375mM Tris pH 7.5; 25.8% (w/v) glycerol; 12.3% (w/v) SDS; 0.06% (w/v) Bromophenol blue; 6% (v/v) β-mercaptoethanol; pH 6.8] and analysis of samples was carried out via immunoblotting. For endogenous immunopurification, 20 µL of a 1:1 ratio mix of protein G (Cytivia, Malborough, Massachusetts, USA). #17061801): protein A (Cytivia, Malborough, Massachusetts, USA). #17127901) beads per sample was pre-incubated with 1 µg of the indicated antibody for 2 h at 4 °C. Afterward, the antibody-coated beads were incubated with HEK293T S100 extract for 2 h at 4 °C while rotating for immunopurification. After washing the samples 3 times with washing buffer (50 mM Tris pH 7.5, 150 mM NaCl, 1 mM EDTA, 1 mM EGTA, 0.01% Igepal and protease inhibitor cocktail (cOmplete, Roche, Switzerland, #04693132001)), immunoblot analysis was performed.

4.7. Immunofluorescence Microscopy

Each of the 1×10^5 cells of HEK293T and Flp-In T-REx 293 cell lines were seeded in DMEM high glucose media (Gibco, Thermo Fisher Scientific, #41965062) with 10% FCS (Sigma Aldrich, #F9665), Penicillin and Streptomycin (Gibco, Thermo Fisher Scientific, # 15140122) on coverslips one-day prior staining. After adhering to the cells for one night, the cells were washed once with DPBS and thus fixed with 4% paraformaldehyde for 10 min at

RT. For permeabilization, cells were incubated with 0.2% Triton X-100/PBS for 10 min and blocked with 5% BSA for 30 min. Proteins were detected by incubating the following primary antibodies for 2 h: anti-Gemin2 (1:500), anti-p70S6K (1:500), anti-GFP (1:500), anti-SMN clone 2B1 (1:500), and anti-coilin antibody (1:500). As a secondary antibody, Alexa Fluor 488 (1:200; shown in magenta), Alexa Fluor 568 (1:200; shown in magenta), and Alexa Fluor 647 (1:200; shown in cyan) were used. Microscopic analysis of the antibody staining was performed with an Axio Observer microscope from ZEISS (Germany) with an ApoTome.2 and a 40x oil immersion objective.

4.8. Immunofluorescence Quantification with Fiji

For the quantification of the number of Cajal bodies per cell, a macro was written in the software program Fiji, which measured the number of SMN and coilin double-positive dots within the nucleus. The macro recognized the DAPI staining, which is distributed all over the nucleus, as a region of interest (ROI). The number of either SMN or coilin dots was measured separately within the ROI. Only the ones that were SMN- and coilin-positive were counted as Cajal bodies. For every condition, 1000 cells were analyzed. The diagram and the calculation of the standard deviation as well as the statistics were made in Prism. To test the significance of the values, the data sets were analyzed using an unpaired *t*-test; the samples which were significantly different from each other had a **** $p < 0.001$. The box in the boxplot diagram represents 5–95% of the data, and outliers are shown.

4.9. *In vitro* Phosphorylation

GST-SMN, and GST-Gemin2 wt, GST-Gemin2 S81A, GST-Gemin2 S166A, GST-Gemin2 S81D, GST-Gemin2 S166D, and GST were purified from BL21 DE3 *E. coli* (Agilent, Santa Clara, Kalifornien, USA, #230192). Recombinant active human His-p70S6K purified from Sf21 cells (Sigma Aldrich, St. Louis, USA, #14-486-M) and the substrates in appropriate amounts were incubated in 2 µM ATP, 10 µCi [32P]-ATP (Hartmann Analytic, Germany, #SRP-301), 2.5 mM Tris/HCl pH 7.5, 5 µM EGTA, 50 µM DTT, and 3.75 mM $Mg(CH_3COO)_2$ for 45 min at 30 °C. After terminating the reaction by adding sample buffer, samples were subjected to SDS-PAGE, and a coomassie staining following auto-radiographic analysis with Amersham Hyperfilm MP (Cytivia, #28906844) was performed.

Author Contributions: L.M.E. performed immunofluorescence analysis and quantification, immunopurification experiments, generation of inducible overexpressing GFP cell lines, size exclusion chromatography, and in vitro phosphorylation experiments.

Q.L. also performed GFP immunopurification experiments and the corresponding Western blot analysis. M.J., T.K., B.S. and S.W. discussed the results; M.G. and C.P. designed the experiments and supervised the project. All authors have read and agreed to the published version of the manuscript.

Funding: Qiaoping Li was funded by China Scholarship Council (CSC grant number 202108440212). This work was supported by grants from the Deutsche Forschungsgemeinschaft [DFG, German Research Foundation; GRK 2158 (S.W.), 417677437/GRK 2578 (S.W.) and the Düsseldorf School of Oncology (funded by the Comprehensive Cancer Center Düsseldorf/Deutsche Krebshilfe and the Medical Faculty of the Heinrich Heine University Düsseldorf; to S.W.).

Institutional Review Board Statement: Not applicable.

Informed Consent Statement: Not applicable.

Data Availability Statement: All data and material are available upon request to christoph.peter@uni-duesseldorf.de.

Acknowledgments: We gratefully acknowledge Karina Krings for technical support.

Conflicts of Interest: The authors declare no conflict of interest

References

Baccon, J., L. Pellizzoni, J. Rappsilber, M. Mann, and G. Dreyfuss. 2002. '*Identification and characterization of Gemin7, a novel component of the survival of motor neuron complex*', ***J Biol Chem***, 277: 31957-62.

Bellini, M., and J. G. Gall. 1999. '*Coilin shuttles between the nucleus and cytoplasm in Xenopus oocytes*', ***Mol Biol Cell***, 10: 3425-34.

Bühler, D., V. Raker, R. Lührmann, and U. Fischer. 1999. '*Essential role for the tudor domain of SMN in spliceosomal U snRNP assembly: implications for spinal muscular atrophy*', ***Hum Mol Genet***, 8: 2351-7.

Carissimi, C., J. Baccon, M. Straccia, P. Chiarella, A. Maiolica, A. Sawyer, J. Rappsilber, and L. Pellizzoni. 2005. '*Unrip is a component of SMN complexes active in snRNP assembly*', ***FEBS Lett***, 579: 2348-54.

Carissimi, C., L. Saieva, J. Baccon, P. Chiarella, A. Maiolica, A. Sawyer, J. Rappsilber, and L. Pellizzoni. 2006. '*Gemin8 is a novel component of the survival motor neuron complex and functions in small nuclear ribonucleoprotein assembly*', ***J Biol Chem***, 281: 8126-34.

Carmo-Fonseca, M., R. Pepperkok, M. T. Carvalho, and A. I. Lamond. 1992. '*Transcription-dependent colocalization of the U1, U2, U4/U6, and U5 snRNPs in coiled bodies*', ***J Cell Biol***, 117: 1-14.

Carvalho, T., F. Almeida, A. Calapez, M. Lafarga, M. T. Berciano, and M. Carmo-Fonseca. 1999. '*The spinal muscular atrophy disease gene product, SMN: A link between snRNP biogenesis and the Cajal (coiled) body*', ***J Cell Biol***, 147: 715-28.

Chari, A., M. M. Golas, M. Klingenhäger, N. Neuenkirchen, B. Sander, C. Englbrecht, A. Sickmann, H. Stark, and U. Fischer. 2008. '*An assembly chaperone collaborates with the SMN complex to generate spliceosomal SnRNPs*', ***Cell***, 135: 497-509.

Charroux, B., L. Pellizzoni, R. A. Perkinson, A. Shevchenko, M. Mann, and G. Dreyfuss. 1999. '*Gemin3: A novel DEAD box protein that interacts with SMN, the spinal muscular atrophy gene product, and is a component of gems*', ***J Cell Biol***, 147: 1181-94.

Coovert, D. D., T. T. Le, P. E. McAndrew, J. Strasswimmer, T. O. Crawford, J. R. Mendell, S. E. Coulson, E. J. Androphy, T. W. Prior, and A. H. Burghes. 1997. '*The survival motor neuron protein in spinal muscular atrophy*', ***Hum Mol Genet***, 6: 1205-14.

Esser, L. M., K. Schmitz, F. Hillebrand, S. Erkelenz, H. Schaal, B. Stork, M. Grimmler, S. Wesselborg, and C. Peter. 2023. '*Phosphorylation of pICln by the autophagy activating kinase ULK1 regulates snRNP biogenesis and splice activity of the cell*', ***Comput Struct Biotechnol J***, 21: 2100-09.

Fischer, U., and R. Lührmann. 1990. '*An essential signaling role for the m3G cap in the transport of U1 snRNP to the nucleus*', ***Science***, 249: 786-90.

Friesen, W. J., S. Paushkin, A. Wyce, S. Massenet, G. S. Pesiridis, G. Van Duyne, J. Rappsilber, M. Mann, and G. Dreyfuss. 2001. '*The methylosome, a 20S complex containing JBP1 and pICln, produces dimethylarginine-modified Sm proteins*', ***Mol Cell Biol***, 21: 8289-300.

Grimmler, M., L. Bauer, M. Nousiainen, R. Körner, G. Meister, and U. Fischer. 2005a. '*Phosphorylation regulates the activity of the SMN complex during assembly of spliceosomal U snRNPs*', ***EMBO Rep***, 6: 70-6.

Grimmler, M., S. Otter, C. Peter, F. Müller, A. Chari, and U. Fischer. 2005b. '*Unrip, a factor implicated in cap-independent translation, associates with the cytosolic SMN complex and influences its intracellular localization*', ***Hum Mol Genet***, 14: 3099-111.

Gubitz, A. K., Z. Mourelatos, L. Abel, J. Rappsilber, M. Mann, and G. Dreyfuss. 2002. '*Gemin5, a novel WD repeat protein component of the SMN complex that binds Sm proteins*', ***J Biol Chem***, 277: 5631-6.

Husedzinovic, A., F. Oppermann, S. Draeger-Meurer, A. Chari, U. Fischer, H. Daub, and O. J. Gruss. 2014. '*Phosphoregulation of the human SMN complex*', ***Eur J Cell Biol***, 93: 106-17.

Kaida, D., M. G. Berg, I. Younis, M. Kasim, L. N. Singh, L. Wan, and G. Dreyfuss. 2010. '*U1 snRNP protects pre-mRNAs from premature cleavage and polyadenylation*', ***Nature***, 468: 664-8.

Kambach, C., S. Walke, R. Young, J. M. Avis, E. de la Fortelle, V. A. Raker, R. Lührmann, J. Li, and K. Nagai. 1999. '*Crystal structures of two Sm protein complexes and their implications for the assembly of the spliceosomal snRNPs*', ***Cell***, 96: 375-87.

Kroiss, M., J. Schultz, J. Wiesner, A. Chari, A. Sickmann, and U. Fischer. 2008. '*Evolution of an RNP assembly system: a minimal SMN complex facilitates formation of UsnRNPs in Drosophila melanogaster*', ***Proc Natl Acad Sci U S A***, 105: 10045-50.

Lefebvre, S., P. Burlet, Q. Liu, S. Bertrandy, O. Clermont, A. Munnich, G. Dreyfuss, and J. Melki. 1997. '*Correlation between severity and SMN protein level in spinal muscular atrophy*', ***Nat Genet***, 16: 265-9.

Liu, Q., and G. Dreyfuss. 1996. '*A novel nuclear structure containing the survival of motor neurons protein*', ***Embo j***, 15: 3555-65.

Liu, Q., U. Fischer, F. Wang, and G. Dreyfuss. 1997. '*The spinal muscular atrophy disease gene product, SMN, and its associated protein SIP1 are in a complex with spliceosomal snRNP proteins*', ***Cell***, 90: 1013-21.

Löffler, A. S., S. Alers, A. M. Dieterle, H. Keppeler, M. Franz-Wachtel, M. Kundu, D. G. Campbell, S. Wesselborg, D. R. Alessi, and B. Stork. 2011. '*Ulk1-mediated phosphorylation of AMPK constitutes a negative regulatory feedback loop*', ***Autophagy***, 7: 696-706.

Mattaj, I. W., and E. M. De Robertis. 1985. '*Nuclear segregation of U2 snRNA requires binding of specific snRNP proteins*', ***Cell***, 40: 111-8.

Meister, G., D. Bühler, R. Pillai, F. Lottspeich, and U. Fischer. 2001a. '*A multiprotein complex mediates the ATP-dependent assembly of spliceosomal U snRNPs*', ***Nat Cell Biol***, 3: 945-9.

Meister, G., C. Eggert, D. Bühler, H. Brahms, C. Kambach, and U. Fischer. 2001b. '*Methylation of Sm proteins by a complex containing PRMT5 and the putative U snRNP assembly factor pICln*', ***Curr Biol***, 11: 1990-4.

Meister, G., and U. Fischer. 2002b. '*Assisted RNP assembly: SMN and PRMT5 complexes cooperate in the formation of spliceosomal UsnRNPs*', ***Embo j***, 21: 5853-63.

Newman, A. J., and K. Nagai. 2010. '*Structural studies of the spliceosome: blind men and an elephant*', ***Curr Opin Struct Biol***, 20: 82-9.

Ogawa, C., K. Usui, M. Aoki, F. Ito, M. Itoh, C. Kai, M. Kanamori-Katayama, Y. Hayashizaki, and H. Suzuki. 2007. '*Gemin2 plays an important role in stabilizing the survival of motor neuron complex*', ***J Biol Chem***, 282: 11122-34.

Pellizzoni, L., J. Baccon, J. Rappsilber, M. Mann, and G. Dreyfuss. 2002a. '*Purification of native survival of motor neurons complexes and identification of Gemin6 as a novel component*', ***J Biol Chem***, 277: 7540-5.

Pellizzoni, L., J. Yong, and G. Dreyfuss. 2002b. '*Essential role for the SMN complex in the specificity of snRNP assembly*', ***Science***, 298: 1775-9.

Pu, W. T., G. B. Krapivinsky, L. Krapivinsky, and D. E. Clapham. 1999. '*pICln inhibits snRNP biogenesis by binding core spliceosomal proteins*', ***Mol Cell Biol***, 19: 4113-20.

Schilling, M., A. B. Prusty, B. Boysen, F. S. Oppermann, Y. L. Riedel, A. Husedzinovic, H. Rasouli, A. König, P. Ramanathan, J. Reymann, H. Erfle, H. Daub, U. Fischer, and O. J. Gruss. 2021. '*TOR signaling regulates liquid phase separation of the SMN complex governing snRNP biogenesis*', ***Cell Rep***, 35: 109277.

Schmitz, K., J. Cox, L. M. Esser, M. Voss, K. Sander, A. Löffler, F. Hillebrand, S. Erkelenz, H. Schaal, T. Kähne, S. Klinker, T. Zhang, L. Nagel-Steger, D. Willbold, S.

Seggewiß, D. Schlütermann, B. Stork, M. Grimmler, S. Wesselborg, and C. Peter. 2021. '*An essential role of the autophagy activating kinase ULK1 in snRNP biogenesis*', ***Nucleic Acids Res***, 49: 6437-55.

Staley, J. P., and C. Guthrie. 1998. '*Mechanical devices of the spliceosome: motors, clocks, springs, and things*', ***Cell***, 92: 315-26.

Wahl, M. C., C. L. Will, and R. Lührmann. 2009. '*The spliceosome: design principles of a dynamic RNP machine*', ***Cell***, 136: 701-18.

Weber, G., S. Trowitzsch, B. Kastner, R. Lührmann, and M. C. Wahl. 2010. '*Functional organization of the Sm core in the crystal structure of human U1 snRNP*', ***Embo j***, 29: 4172-84.

Will, C. L., and R. Lührmann. 2001. '*Spliceosomal UsnRNP biogenesis, structure and function*', ***Curr Opin Cell Biol***, 13: 290-301.

Zhang, R., B. R. So, P. Li, J. Yong, T. Glisovic, L. Wan, and G. Dreyfuss. 2011. '*Structure of a key intermediate of the SMN complex reveals Gemin2's crucial function in snRNP assembly*', ***Cell***, 146: 384-95.

8 Discussion

The biogenesis of UsnRNPs plays a key role during post-transcriptional gene expression (Matera et al., 2014). UsnRNP biogenesis is executed by the mode of action of two protein complexes: The PRMT5 complex and the SMN complex (Fischer et al., 1997, Liu et al., 1997, Friesen et al., 2001b, Meister et al., 2001b, Friesen et al., 2002, Zhang et al., 2011). With NF90, we could validate a new substrate of the PRMT5-WD45-RioK1 protein complex, thereby increasing the PRMT5 substrate diversity (Chapter 7.1). Furthermore, the role of pICln, an adapter protein of the PRMT5 complex, was identified to be regulated by the ULK1 kinase (Chapter 7.2, 7.3). The phosphorylation of pICln leads to a termination of the 6S structure *in vivo* (Chapter 7.2), leading to an increased transfer efficiency of Sm proteins in UsnRNP biogenesis and a higher spliceosomal activity (Chapter 7.2, Chapter 7.3). Moreover, we demonstrated a regulatory role of the p70S6K in this pathway, via the interaction with and phosphorylation of Gemin2 (Chapter 7.4).

8.1 NF90 as a new PRMT5 methylation target

PRMT5 belongs to a conserved enzymatic protein family, the protein arginine methyltransferases (PRMTs), that catalyzes different forms of arginine methylation (Bachand, 2007). PRMT5 builds two subcomplexes *in vivo* (PRMT5-WD45-RioK1 and PRMT5-WD45-pICln), to this date, only nucleolin was identified to be recruited via the adapter protein RioK1 (Guderian et al., 2011). Within this thesis, we identified the Nuclear Factor 90 (NF90), as a new interaction partner of the PRMT5-WD45-RioK1 complex (Fig. 1A, B; Chapter 7.1). Some methylation targets occurred to be fully methylated *in vivo* (Herrmann et al., 2004), disabling additional *in vitro* methylation assays. After a treatment with the universal methyltransferase inhibitor adenosine dialdehyde (Adox) (Chen et al., 2004), we could show that endogenous NF90 represents a fully methylated PRMT5 target *in vivo* (Fig. 3C, D; Chapter 7.1). So far in the literature, next to already described PRMT5 substrates like nucleolin, or the Sm proteins SmD1, D3, and B (Brahms et al., 2000, Brahms et al., 2001, Friesen et al., 2001b, Teng et al., 2007), NF90 represents the only fully methylated target of PRMT5 (Chapter 7.1). NF90 is an RNA-binding protein (Shi et al., 2005), as arginine residues play an important role in RNA-protein interactions (Bedford et al., 2005), the newly identified PTM is probably involved in the regulation of the biological function of NF90. The fact, that the methylation of RGG-motifs can increase the basicity of

the guanidino group of the arginine, and therefore modulate the interaction between this motif and RNAs as well as proteins (Thandapani et al., 2013), strengthens this hypothesis.

8.2 The regulatory role of post-translational modifications in UsnRNP biogenesis

8.2.1 Targeting UsnRNP biogenesis on the level of pICln

Within the cell, large amounts of Sm proteins are stored in the cytoplasm, which are awaiting the transcription of the snRNA, when the time copious amounts of spliceosomal snRNPs are assembled (Zeller et al., 1983). As the Sm proteins have a hydrophobic nature that likely aggregates and needs to be shielded before their assembly into the core (Prusty et al., 2017), and the fact that cellular protein aggregation has been linked to several diseases (Ross et al., 2004), the cell needs to solve this problem. This process is regulated via pICln that was shown to directly accept Sm protein binding after their transcription at the ribosome (Paknia et al., 2016). The pICln protein builds a stable, ring-shaped, 6S structure, with a subset of Sm proteins, thereby preventing their assembly with the UsnRNA as a kinetic trap (Chari et al., 2008). However, the structure of the 6S complex needs to be solved to overcome this kinetic trap. In the preliminary work of our group, we could identify the Ser/Thr kinase Unc-51-like kinase 1 (ULK1), usually regulating the autophagy pathway, as a new potential interaction partner of the methylosome in a mass spectrometry screen (Löffler et al., 2011). In our study presented in this thesis, we could verify the first specific kinase-substrate interaction in the regulation of UsnRNP biogenesis, by identifying pICln as an interaction partner and phosphorylation substrate of ULK1 (Chapter 7.2). We could map the ULK1-dependend phosphorylation to individual phospho-serines within the C-terminus of pICln (Fig. 2 F, G; Chapter 7.2), which consequently solves the 6S complex by lowering the pICln-SmG contact side, which acts as a kind of intended breaking point (Chari et al., 2008). The C-terminus of pICln is a highly conserved, unstructured region (Dyson et al., 2005, Schedlbauer et al., 2011). Unstructured regions are known to be regulated by PTMs (Dyson et al., 2005), thus functioning as flexible linkers in the assembly of higher-ordered molecular systems. This flexible structure of the protein probably contributes to its role of transferring Sm proteins onto the SMN complex. Besides this research, the generation of a phospho-antibody against the ULK1-specific phosphorylation sites allowed us to compare exclusively different subspecies of pICln *in vivo* (Chapter 7.3). Size exclusion chromatography revealed that the main amount of phosphorylated pICln is distributed in a size range overlapping with

the 6S complex (Fig. 1C, E; Chapter 7.3). This shows for the first time that mostly phosphorylated pICln binds the Sm proteins *in vivo*. Interestingly, the complex integrity as well as the amount of phosphorylated pICln is directly coupled to ULK1 activity in cells. After depletion of ULK1 we demonstrated a markedly reduction of pICln phosphorylation *in vivo* (Fig. 1C-H, 2C, D; Chapter 7.3). This raises the hypothesis that the transfer of Sm proteins from the PRMT5 complex onto the SMN complex could be directly influenced by ULK1 activity, and indeed, we could prove this hypothesis (Fig. 3A, Chapter 7.3) by showing the importance of a direct, ULK1-dependent, pICln regulation *in vivo* within the ongoing assembly of the Sm core.

8.2.2 The role of Gemin2 as a regulatory unit within UsnRNP biogenesis

The SMN-Gemin2 complex is the regulatory unit in the SMN complex that maintains the transfer of Sm proteins onto the Sm site of the UsnRNA (Pellizzoni et al., 2002b, Kroiss et al., 2008, Zhang et al., 2011). However, the regulation of the SMN complex activity within UsnRNP biogenesis remains unclear. In our latest research, we were able to identify Gemin2 as a novel interaction partner and phosphorylation substrate of the ribosomal protein S6 kinase beta-1 (p70S6K) (Fig. 2D, E; 3A, B; Chapter 7.4), revealing a potential regulation mechanism. Gemin2 has a crucial role within UsnRNP biogenesis, it acts like an arm of the SMN complex, which binds the pentamer of Sm proteins (consisting of SmD1, D2, E, F, and G) in an RNA-free complex, thereby wrapping around the pentamer of Sm proteins from the outer and inner pocket (Zhang et al., 2011). In line with these results, we identified Gemin2 to join a higher molecular complex and additionally a lower molecular complex in size exclusion chromatography, with the distinct weight range from 158 to 100 kDa (Fig. 4C; Chapter 7.4), which corresponds to the 6S complex (Chapter 7.3). Based on our research in addition to the work from Zhang et al., (Zhang et al., 2011), we hypothesize a model in which Gemin2 acts as a bridging molecule for the Sm proteins between the SMN and the PRMT5 complex (Chapter 7.4). Here, Gemin2, regulated by the p70S6K, fulfills a role additional to the one from pICln serving as a kinetic trap (Chari et al., 2008), mediated by ULK1 (Chapter 7.2, 7.3), via receiving the Sm proteins from pICln and preventing their binding from snRNAs, thus increasing RNA binding specificity (Chapter 7.4), (Zhang et al., 2011). These findings maintain the stepwise organization of the Sm core assembly so that the Sm proteins B and D3 can be transferred onto the snRNA with the involvement of the SMN complex (Meister et al., 2002b).

As the siRNA-mediated knockdown of the p70S6K resulted in a dramatically reduced condensation of the nuclear SMN complex in CBs (Fig. 5C, D; Chapter 7.4), it became clear that the kinase has a regulatory role within UsnRNP biogenesis. However, despite these new insights, still a lot of research will be necessary to understand the exact role of the p70S6K within this pathway and the involvement of Gemin2 activity regulation in this context.

8.2.3 Who regulates the regulators?

As discussed above, we identified two kinases as novel modulators in the regulation of the UsnRNP biogenesis pathway, ULK1 and p70S6K (Chapter 7.2, 7.3, 7.4). Whereas ULK1 is mainly known for its role in autophagy, an evolutionarily conserved pathway, in which proteins and organelles are degraded through their engulfment within lysosomes (Klionsky, 2007, Mizushima, 2010), the p70S6K is a key regulator in protein synthesis via phosphorylation of the S6 ribosomal protein (Stewart et al., 1994, Ruvinsky et al., 2006). Although our research revealed new insides in the mode of action of these kinases, these findings imply the question of how these kinases are regulated within their different functions. As we identified the role of ULK1 in UsnRNP biogenesis to be independent from autophagy (Chapter 7.2), it was controverting, that the over-expression of U1snRNA leads to the induction of autophagy (Cheng et al., 2018). In addition, in the absence of pICln autophagy is initiated for an autophagosome-induced Sm protein degradation, to avoid toxicity induced by Sm protein aggregation (Prusty et al., 2017). Interestingly, the avoiding of the aggregation of proteins as well as the accumulation of misfolded proteins is a common feature of neurodegenerative diseases like Alzheimer´s disease, Parkinson´s disease, and Huntington´s disease (Harris et al., 2011, Ciechanover et al., 2015). Consequently, the induction of autophagy reveals a treatment strategy, which targets those proteins by the degradation through the autophagy pathway. As ULK1 acts within different complexes to fulfill its role in autophagy and the UsnRNP biogenesis ((Mizushima, 2010); Chapter 7.2, 7.3)), the role of ULK1 needs to be tightly regulated, as it cannot simultaneously perform both functions.

The Ser/Thr kinase mTOR is a main regulator within autophagy, it is able to inhibit autophagy (Noda et al., 1998, Klionsky, 2007, Mizushima, 2007). Besides this role, mTOR regulates the cell cycle progression via the integration of nutrients and growth factors (Shamji et al., 2003). Early research hypothesized that mTOR influences SMN activity, as it

was known before that cell cycle-dependent signaling regulates the nuclear accumulation of UsnRNPs and SMN (Carmo-Fonseca et al., 1993). Another working group identified a putative function for mTOR within UsnRNP biogenesis via a mass spectrometry screen revealing a potential phosphorylation of SMN complex components (Schilling et al., 2021). This data just assumes an involvement of the mTOR signaling in UsnRNP biogenesis, via the identification of p70S6K-dependent phosphorylation of Gemin2 we could prove this now (Chapter 7.4). The mTOR kinase is part of two distinct protein complexes, mTORC1 and mTORC2, which differ in complex composition and thereby are involved in different signaling pathways (Hara et al., 2002, Kim et al., 2002, Jacinto et al., 2004, Sarbassov et al., 2004). It would be smart for the cell to involve mTOR in the regulation of UsnRNP biogenesis, as this would link this pathway to cellular energy levels and the UsnRNP biogenesis which is a process that is dependent on high availability of cellular energy in the form of ATP (Meister et al., 2001a, Grimmler et al., 2005a, Husedzinovic et al., 2014), (Chapter 7.2, 7.3, 7.4). Furthermore, the biogenesis of UsnRNPs is, as a part of the splicing machinery, crucial for genome stability (Matera et al., 2014), therefore the cell needs to keep this process ongoing, at least partially, in phases of nutrient starvation. With this knowledge, it is interesting to note, that the mTORC1 complex is on the one hand regulating ULK1 activity through phosphorylation and on the other hand the p70S6K, thus showing that mTOR can regulate the activity of both kinases (Banerjee et al., 1990, Kuo et al., 1992, Burnett et al., 1998, Hara et al., 2002, Jung et al., 2009). Here, the mTOR kinase could act in the role of a molecular switch to maintain the balance between growth and autophagy-related cell death, as a response to physiologic conditions and environmental stress (Jung et al., 2010), regulating the involvement of ULK1 and the p70S6K within the UsnRNP biogenesis, dependent on the physiological conditions. Indeed, a link between mTOR and snRNP assembly could be verified, as a knockdown of SmE leads to a strong decrease in mTOR mRNA and protein abundance and in addition, to a global deregulation of the mTOR signaling and a consequent autophagy initiation (Quidville et al., 2013). The depletion of SmE was further characterized to impair splicing activity (Chen et al., 2019). These studies demonstrated a direct relation between mTOR activity and the induction of autophagy, however, the knockdown of another spliceosomal protein, SmD1, did not affect effect mTOR but still led to autophagy induction (Quidville et al., 2013). As a lot of research highlights the importance of the relation between the splicing machinery and mTOR, especially in the background of diseases, this reveals the process of mRNA maturation and splicing as a major

target for future drug targeting research (Quidville et al., 2013). In line with this assumption, latest research identified the spliceosome machinery as the main regulator of the mTORC1 signaling pathway in model organism Drosophila melanogaster (Lindquist et al., 2011). In future research, the splicing machinery-mTOR signaling axis should be targeted as a potential regulation mechanism in the view of a treatment against SMA, especially as there is evidence that autophagy is dysregulated in SMA and the fact that autophagy inhibitors prolonged the life span of the SMA mice (Piras et al., 2017). However, this knowledge does not exclude the possibility that the activity of ULK1 in UsnRNP biogenesis, bound in the PRMT5 complex (Chapter 7.2), is not regulated by mTOR, maybe this just represents a potential influence from autophagy on UsnRNP biogenesis for energy conservation in the cell. Although some insights into the regulation of the UsnRNP biogenesis were gained, the question of how enzymes inducing PTMs in this pathway are regulated remains unclear. As the mTOR kinase has somehow a relation to the kinases ULK1 and the p70S6K, involved in UsnRNP biogenesis regulation, it is a potential target to answer this question in future research.

8.3 Conclusions and further perspectives

Within this thesis, we could identify a new, fully methylated, substrate of the PRMT5-WD45-RioK1 protein complex (Chapter 7.1). Furthermore, the regulation of the assembly chaperone pICln was investigated, and the newly identified phosphorylation via the Ser/Thr ULK1 kinase induced a termination of the hexameric 6S structure *in vivo* (Chapter 7.2), leading to an increase of the transfer efficiency of Sm proteins onto the SMN complex and as a consequence to a rise of spliceosome activity (Chapter 7.2, Chapter 7.3). Moreover, as the siRNA-mediated knockdown of the p70S6K caused a severe decrease in UsnRNP assembly activity, we identified another kinase as a novel regulator in this pathway, which directly interacts with and phosphorylates Gemin2 (Chapter 7.4). In summary, the main achievements presented in this thesis were the identification of two kinases of the mTOR pathway as key regulators in UsnRNP biogenesis, as well as the molecular mechanisms caused by these regulations.

The findings presented in the discussion generated a link between the autophagy pathway and the spliceosomal activity and represent an interesting future research target. As we could show that the function of ULK1 in UsnRNP biogenesis is independent from autophagy, the

key question is how ULK1 activity is regulated on the protein level, so that the kinase either functions in the PRMT5-pICln-ULK1 complex or the autophagy initiation complex. As it is known that ULK1 activity in the autophagy pathway (Hara et al., 2002, Jung et al., 2009), as well as p70S6K activity in ribosome biogenesis (Banerjee et al., 1990, Kuo et al., 1992, Burnett et al., 1998), is regulated via phosphorylation from mTOR, future research should target the phosphorylated protein subspecies of those two kinases in the background of activity regulation in their different cellular functions.

Since Gemin2 activity is regulated by phosphorylation, this raises the question of whether other Gemini in the SMN complex are also potential phosphorylation targets.

The neuromuscular disease SMA, which causes the degeneration of α-motor neurons (Crawford et al., 1996), is so far treated with ASOs rescuing the amount of the disease-causing *SMN1* gene and therefore increasing the amount of active SMN protein (Schorling et al., 2020). Although these treatments block the progression of the SMA phenotype, they do not cure the disease, making further research indispensable. The protein level of Gemini was found to be reduced in the spinal cord SMA mice (Gabanella et al., 2007, Zhang et al., 2008), moreover, a dysfunction of Gemin2 and pICln led to an impairment of the neuromuscular activity (Borg et al., 2015, Borg et al., 2016), which identifies them as a potential therapeutic targets. But still, as the change in the level of SMN complex components, at least in cells, disrupts its function (Borg et al., 2015), it is unclear if this effect is specific to Gemin2 or due to complex instability as a consequence of reduced cellular SMN levels. As ULK1 is evolutionarily conserved and the fact that the kinase was first identified as a main factor in the early differentiation of neurons and axonal elongation, the role of ULK1 in the background of SMA should be targeted further (Ogura et al., 1994). In addition, the reduction of SMN leads to reduced ATP levels in the background of SMA (Acsadi et al., 2009, Miller et al., 2016). Concluding from this the cellular energy sensor mTOR is an interesting potential therapeutic target. Taken together the discussed data as well as the data provided in this thesis, it became clear that not only the protein abundance, but also the protein activity is a severe factor for a proper function of the protein within a signaling pathway. As SMA is dependent on snRNP assembly activity in the spinal cord (Workman et al., 2009), maybe the activity regulation of SMN in form of PTMs in combination with the already used therapeutic approaches could cure SMA. Therefore, future research should especially target the mTOR-ULK1-p70S6K axis as a major regulatory unit of ATP-dependent protein activity regulation in UsnRNP biogenesis.

9 Bibliography

Acsadi, G., I. Lee, X. Li, M. Khaidakov, A. Pecinova, G. C. Parker, and M. Hüttemann. 2009. *'Mitochondrial dysfunction in a neural cell model of spinal muscular atrophy',* ***J Neurosci Res****, 87: 2748-56.*

Antonysamy, S., Z. Bonday, R. M. Campbell, B. Doyle, Z. Druzina, T. Gheyi, B. Han, L. N. Jungheim, Y. Qian, C. Rauch, M. Russell, J. M. Sauder, S. R. Wasserman, K. Weichert, F. S. Willard, A. Zhang, and S. Emtage. 2012. *'Crystal structure of the human PRMT5:MEP50 complex',* ***Proc Natl Acad Sci U S A****, 109: 17960-5.*

Araujo, R. P., L. A. Liotta, and E. F. Petricoin. 2007. *'Proteins, drug targets and the mechanisms they control: the simple truth about complex networks',* ***Nat Rev Drug Discov****, 6: 871-80.*

Aslesh, T., and T. Yokota. 2022. *'Restoring SMN Expression: An Overview of the Therapeutic Developments for the Treatment of Spinal Muscular Atrophy',* ***Cells****, 11.*

Baccon, J., L. Pellizzoni, J. Rappsilber, M. Mann, and G. Dreyfuss. 2002. *'Identification and characterization of Gemin7, a novel component of the survival of motor neuron complex',* ***J Biol Chem****, 277: 31957-62.*

Bachand, F. 2007. *'Protein arginine methyltransferases: from unicellular eukaryotes to humans',* ***Eukaryot Cell****, 6: 889-98.*

Baillat, D., M. A. Hakimi, A. M. Näär, A. Shilatifard, N. Cooch, and R. Shiekhattar. 2005. *'Integrator, a multiprotein mediator of small nuclear RNA processing, associates with the C-terminal repeat of RNA polymerase II',* ***Cell****, 123: 265-76.*

Banerjee, P., M. F. Ahmad, J. R. Grove, C. Kozlosky, D. J. Price, and J. Avruch. 1990. *'Molecular structure of a major insulin/mitogen-activated 70-kDa S6 protein kinase',* ***Proc Natl Acad Sci U S A****, 87: 8550-4.*

Bäumer, D., S. Lee, G. Nicholson, J. L. Davies, N. J. Parkinson, L. M. Murray, T. H. Gillingwater, O. Ansorge, K. E. Davies, and K. Talbot. 2009. *'Alternative splicing events are a late feature of pathology in a mouse model of spinal muscular atrophy',* ***PLoS Genet****, 5: e1000773.*

Bedford, M. T., and S. Richard. 2005. *'Arginine methylation an emerging regulator of protein function',* ***Mol Cell****, 18: 263-72.*

Bedford, M. T., and S. G. Clarke. 2009. *'Protein arginine methylation in mammals: who, what, and why',* ***Mol Cell****, 33: 1-13.*

Bellini, M., and J. G. Gall. 1999. *'Coilin shuttles between the nucleus and cytoplasm in Xenopus oocytes',* ***Mol Biol Cell****, 10: 3425-34.*

Berget, S. M., C. Moore, and P. A. Sharp. 1977. *'Spliced segments at the 5' terminus of adenovirus 2 late mRNA',* ***Proc Natl Acad Sci U S A****, 74: 3171-5.*

Blanc, R. S., and S. Richard. 2017. *'Arginine Methylation: The Coming of Age',* ***Mol Cell****, 65: 8-24.*

Bludau, I., and R. Aebersold. 2020. *'Proteomic and interactomic insights into the molecular basis of cell functional diversity',* ***Nat Rev Mol Cell Biol****, 21: 327-40.*

Borg, R. M., R. Bordonne, N. Vassallo, and R. J. Cauchi. 2015. *'Genetic Interactions between the Members of the SMN-Gemins Complex in Drosophila',* ***PLoS One****, 10: e0130974.*

Borg, R. M., B. Fenech Salerno, N. Vassallo, R. Bordonne, and R. J. Cauchi. 2016. *'Disruption of snRNP biogenesis factors Tgs1 and pICln induces phenotypes that*

*mirror aspects of SMN-Gemins complex perturbation in Drosophila, providing new insights into spinal muscular atrophy', **Neurobiol Dis**, 94: 245-58.*

Bottger, A., M. S. Islam, R. Chowdhury, C. J. Schofield, and A. Wolf. 2015. *'The oxygenase Jmjd6--a case study in conflicting assignments', **Biochem J**, 468: 191-202.*

Brahms, H., J. Raymackers, A. Union, F. de Keyser, L. Meheus, and R. Lührmann. 2000. *'The C-terminal RG dipeptide repeats of the spliceosomal Sm proteins D1 and D3 contain symmetrical dimethylarginines, which form a major B-cell epitope for anti-Sm autoantibodies', **J Biol Chem**, 275: 17122-9.*

Brahms, H., L. Meheus, V. de Brabandere, U. Fischer, and R. Lührmann. 2001. *'Symmetrical dimethylation of arginine residues in spliceosomal Sm protein B/B' and the Sm-like protein LSm4, and their interaction with the SMN protein', **Rna**, 7: 1531-42.*

Branlant, C., A. Krol, J. P. Ebel, E. Lazar, B. Haendler, and M. Jacob. 1982. *'U2 RNA shares a structural domain with U1, U4, and U5 RNAs', **Embo j**, 1: 1259-65.*

Brautigam, C. A. 2015. *'Calculations and Publication-Quality Illustrations for Analytical Ultracentrifugation Data', **Methods Enzymol**, 562: 109-33.*

Brzustowicz, L. M., T. Lehner, L. H. Castilla, G. K. Penchaszadeh, K. C. Wilhelmsen, R. Daniels, K. E. Davies, M. Leppert, F. Ziter, D. Wood, and et al. 1990. *'Genetic mapping of chronic childhood-onset spinal muscular atrophy to chromosome 5q11.2-13.3', **Nature**, 344: 540-1.*

Bühler, D., V. Raker, R. Lührmann, and U. Fischer. 1999. *'Essential role for the tudor domain of SMN in spliceosomal U snRNP assembly: implications for spinal muscular atrophy', **Hum Mol Genet**, 8: 2351-7.*

Burnett, P. E., R. K. Barrow, N. A. Cohen, S. H. Snyder, and D. M. Sabatini. 1998. *'RAFT1 phosphorylation of the translational regulators p70 S6 kinase and 4E-BP1', **Proc Natl Acad Sci U S A**, 95: 1432-7.*

Burset, M., I. A. Seledtsov, and V. V. Solovyev. 2000. *'Analysis of canonical and non-canonical splice sites in mammalian genomes', **Nucleic Acids Res**, 28: 4364-75.*

Carissimi, C., J. Baccon, M. Straccia, P. Chiarella, A. Maiolica, A. Sawyer, J. Rappsilber, and L. Pellizzoni. 2005. *'Unrip is a component of SMN complexes active in snRNP assembly', **FEBS Lett**, 579: 2348-54.*

Carissimi, C., L. Saieva, J. Baccon, P. Chiarella, A. Maiolica, A. Sawyer, J. Rappsilber, and L. Pellizzoni. 2006. *'Gemin8 is a novel component of the survival motor neuron complex and functions in small nuclear ribonucleoprotein assembly', **J Biol Chem**, 281: 8126-34.*

Carmo-Fonseca, M., R. Pepperkok, M. T. Carvalho, and A. I. Lamond. 1992. *'Transcription-dependent colocalization of the U1, U2, U4/U6, and U5 snRNPs in coiled bodies', **J Cell Biol**, 117: 1-14.*

Carmo-Fonseca, M., J. Ferreira, and A. I. Lamond. 1993. *'Assembly of snRNP-containing coiled bodies is regulated in interphase and mitosis--evidence that the coiled body is a kinetic nuclear structure', **J Cell Biol**, 120: 841-52.*

Carvalho, T., F. Almeida, A. Calapez, M. Lafarga, M. T. Berciano, and M. Carmo-Fonseca. 1999. *'The spinal muscular atrophy disease gene product, SMN: A link between snRNP biogenesis and the Cajal (coiled) body', **J Cell Biol**, 147: 715-28.*

Chan-Penebre, E., K. G. Kuplast, C. R. Majer, P. A. Boriack-Sjodin, T. J. Wigle, L. D. Johnston, N. Rioux, M. J. Munchhof, L. Jin, S. L. Jacques, K. A. West, T. Lingaraj, K. Stickland, S. A. Ribich, A. Raimondi, M. P. Scott, N. J. Waters, R. M. Pollock, J. J. Smith, O. Barbash, M. Pappalardi, T. F. Ho, K. Nurse, K. P. Oza, K. T. Gallagher,

R. Kruger, M. P. Moyer, R. A. Copeland, R. Chesworth, and K. W. Duncan. 2015. *'A selective inhibitor of PRMT5 with in vivo and in vitro potency in MCL models',* ***Nat Chem Biol****, 11: 432-7.*

Chan, E. Y., A. Longatti, N. C. McKnight, and S. A. Tooze. 2009. *'Kinase-inactivated ULK proteins inhibit autophagy via their conserved C-terminal domains using an Atg13-independent mechanism',* ***Mol Cell Biol****, 29: 157-71.*

Chang, B., Y. Chen, Y. Zhao, and R. K. Bruick. 2007. *'JMJD6 is a histone arginine demethylase',* ***Science****, 318: 444-7.*

Chari, A., M. M. Golas, M. Klingenhäger, N. Neuenkirchen, B. Sander, C. Englbrecht, A. Sickmann, H. Stark, and U. Fischer. 2008. *'An assembly chaperone collaborates with the SMN complex to generate spliceosomal SnRNPs',* ***Cell****, 135: 497-509.*

Chari, A., and U. Fischer. 2010. *'Cellular strategies for the assembly of molecular machines',* ***Trends Biochem Sci****, 35: 676-83.*

Charroux, B., L. Pellizzoni, R. A. Perkinson, A. Shevchenko, M. Mann, and G. Dreyfuss. 1999. *'Gemin3: A novel DEAD box protein that interacts with SMN, the spinal muscular atrophy gene product, and is a component of gems',* ***J Cell Biol****, 147: 1181-94.*

Charroux*, B. P., L.;* Perkinson*, R.; Young, J.;* Shevchenko*, A.; & MANN, M. A. D., G. 2000. Gemin4: A Novel Component of the SMN Complex That Is Found in both Gems and Nucleoli.* ***J Cell Biol****, 148: 1177-86.*

Chaturvedi, S. K., J. Ma, H. Zhao, and P. Schuck. 2017. *'Use of fluorescence-detected sedimentation velocity to study high-affinity protein interactions',* ***Nat Protoc****, 12: 1777-91.*

Chen, D. H., K. T. Wu, C. J. Hung, M. Hsieh, and C. Li. 2004. *'Effects of adenosine dialdehyde treatment on in vitro and in vivo stable protein methylation in HeLa cells',* ***J Biochem****, 136: 371-6.*

Chen, T., B. Zhang, T. Ziegenhals, A. B. Prusty, S. Fröhler, C. Grimm, Y. Hu, B. Schaefke, L. Fang, M. Zhang, N. Kraemer, A. M. Kaindl, U. Fischer, and W. Chen. 2019. *'A missense mutation in SNRPE linked to non-syndromal microcephaly interferes with U snRNP assembly and pre-mRNA splicing',* ***PLoS Genet****, 15: e1008460.*

Cheng, Z., Z. Du, B. Zhai, Z. Yang, and T. Zhang. 2018. *'U1 small nuclear RNA overexpression implicates autophagic-lysosomal system associated with AD',* ***Neurosci Res****, 136: 48-55.*

Chiang, S. H., M. Bazuine, C. N. Lumeng, L. M. Geletka, J. Mowers, N. M. White, J. T. Ma, J. Zhou, N. Qi, D. Westcott, J. B. Delproposto, T. S. Blackwell, F. E. Yull, and A. R. Saltiel. 2009. *'The protein kinase IKKepsilon regulates energy balance in obese mice',* ***Cell****, 138: 961-75.*

Chomczynski, P., and N. Sacchi. 1987. *'Single-step method of RNA isolation by acid guanidinium thiocyanate-phenol-chloroform extraction',* ***Anal Biochem****, 162: 156-9.*

Chow, L. T., R. E. Gelinas, T. R. Broker, and R. J. Roberts. 1977. *'An amazing sequence arrangement at the 5' ends of adenovirus 2 messenger RNA',* ***Cell****, 12: 1-8.*

Ciechanover, A., and Y. T. Kwon. 2015. *'Degradation of misfolded proteins in neurodegenerative diseases: therapeutic targets and strategies',* ***Exp Mol Med****, 47: e147.*

Clark, K., M. Peggie, L. Plater, R. J. Sorcek, E. R. Young, J. B. Madwed, J. Hough, E. G. McIver, and P. Cohen. 2011. *'Novel cross-talk within the IKK family controls innate immunity',* ***Biochem J****, 434: 93-104.*

Coovert, D. D., T. T. Le, P. E. McAndrew, J. Strasswimmer, T. O. Crawford, J. R. Mendell, S. E. Coulson, E. J. Androphy, T. W. Prior, and A. H. Burghes. 1997. *'The survival motor neuron protein in spinal muscular atrophy',* ***Hum Mol Genet****, 6: 1205-14.*

Corpet, F. 1988. *'Multiple sequence alignment with hierarchical clustering',* ***Nucleic Acids Res****, 16: 10881-90.*

Crawford, T. O., and C. A. Pardo. 1996. *'The neurobiology of childhood spinal muscular atrophy',* ***Neurobiol Dis****, 3: 97-110.*

Cullen, B. R. 2003. *'Nuclear RNA export',* ***J Cell Sci****, 116: 587-97.*

De Klerk, E., and P. A. t Hoen. 2015. *'Alternative mRNA transcription, processing, and translation: insights from RNA sequencing',* ***Trends Genet****, 31: 128-39.*

Dignam, J. D., R. M. Lebovitz, and R. G. Roeder. 1983. *'Accurate transcription initiation by RNA polymerase II in a soluble extract from isolated mammalian nuclei',* ***Nucleic Acids Res****, 11: 1475-89.*

Dubiel, D., W. Bintig, T. Kahne, W. Dubiel, and M. Naumann. 2017. *'Cul3 neddylation is crucial for gradual lipid droplet formation during adipogenesis',* ***Biochim Biophys Acta****, 1864: 1405-12.*

Dyson, H. J., and P. E. Wright. 2005. *'Intrinsically unstructured proteins and their functions',* ***Nat Rev Mol Cell Biol****, 6: 197-208.*

Eggert, C., A. Chari, B. Laggerbauer, and U. Fischer. 2006. *'Spinal muscular atrophy: the RNP connection',* ***Trends Mol Med****, 12: 113-21.*

Erkelenz, S., W. F. Mueller, M. S. Evans, A. Busch, K. Schoneweis, K. J. Hertel, and H. Schaal. 2013. *'Position-dependent splicing activation and repression by SR and hnRNP proteins rely on common mechanisms',* ***RNA****, 19: 96-102.*

Erkelenz, S., F. Hillebrand, M. Widera, S. Theiss, A. Fayyaz, D. Degrandi, K. Pfeffer, and H. Schaal. 2015. *'Balanced splicing at the Tat-specific HIV-1 3'ss A3 is critical for HIV-1 replication',* ***Retrovirology****, 12: 29.*

Esser, L. M., K. Schmitz, F. Hillebrand, S. Erkelenz, H. Schaal, B. Stork, M. Grimmler, S. Wesselborg, and C. Peter. 2023. *'Phosphorylation of pICln by the autophagy activating kinase ULK1 regulates snRNP biogenesis and splice activity of the cell',* ***Comput Struct Biotechnol J****, 21: 2100-09.*

Finkel, R. S., C. A. Chiriboga, J. Vajsar, J. W. Day, J. Montes, D. C. De Vivo, M. Yamashita, F. Rigo, G. Hung, E. Schneider, D. A. Norris, S. Xia, C. F. Bennett, and K. M. Bishop. 2016. *'Treatment of infantile-onset spinal muscular atrophy with nusinersen: a phase 2, open-label, dose-escalation study',* ***Lancet****, 388: 3017-26.*

Fisher, D. E., G. E. Conner, W. H. Reeves, R. Wisniewolski, and G. Blobel. 1985. *'Small nuclear ribonucleoprotein particle assembly in vivo: demonstration of a 6S RNA-free core precursor and posttranslational modification',* ***Cell****, 42: 751-8.*

Fischer, U., and R. Lührmann. 1990. *'An essential signaling role for the m3G cap in the transport of U1 snRNP to the nucleus',* ***Science****, 249: 786-90.*

Fischer, U., Q. Liu, and G. Dreyfuss. 1997. *'The SMN-SIP1 complex has an essential role in spliceosomal snRNP biogenesis',* ***Cell****, 90: 1023-9.*

Friesen, W. J., Massenet, S., Paushkin, S., Wyce, A. & Dreyfuss, G. 2001a. *SMN, the product of the spinal muscular atrophy gene, binds preferentially to dimethylarginine-containing protein targets.* ***Mol Cell****, 7****,*** *1111-7.*

Friesen, W. J., S. Paushkin, A. Wyce, S. Massenet, G. S. Pesiridis, G. Van Duyne, J. Rappsilber, M. Mann, and G. Dreyfuss. 2001b. *'The methylosome, a 20S complex containing JBP1 and pICln, produces dimethylarginine-modified Sm proteins',* ***Mol Cell Biol****, 21: 8289-300.*

Friesen, W. J., A. Wyce, S. Paushkin, L. Abel, J. Rappsilber, M. Mann, and G. Dreyfuss. 2002. *'A novel WD repeat protein component of the methylosome binds Sm proteins',* ***J Biol Chem****, 277: 8243-7.*

Furst, J., A. Schedlbauer, R. Gandini, M. L. Garavaglia, S. Saino, M. Gschwentner, B. Sarg, H. Lindner, M. Jakab, M. Ritter, C. Bazzini, G. Botta, G. Meyer, G. Kontaxis, B. C. Tilly, R. Konrat, and M. Paulmichl. 2005. *'ICln159 folds into a pleckstrin homology domain-like structure. Interaction with kinases and the splicing factor LSm4',* ***J Biol Chem****, 280: 31276-82.*

Gabanella, F., M. E. Butchbach, L. Saieva, C. Carissimi, A. H. Burghes, and L. Pellizzoni. 2007. *'Ribonucleoprotein assembly defects correlate with spinal muscular atrophy severity and preferentially affect a subset of spliceosomal snRNPs',* ***PLoS One****, 2: e921.*

Grimm, C., A. Chari, J. P. Pelz, J. Kuper, C. Kisker, K. Diederichs, H. Stark, H. Schindelin, and U. Fischer. 2013. *'Structural basis of assembly chaperone- mediated snRNP formation',* ***Mol Cell****, 49: 692-703.*

Grimmler, M., L. Bauer, M. Nousiainen, R. Körner, G. Meister, and U. Fischer. 2005a. *'Phosphorylation regulates the activity of the SMN complex during assembly of spliceosomal U snRNPs',* ***EMBO Rep****, 6: 70-6.*

Grimmler, M., S. Otter, C. Peter, F. Muller, A. Chari, and U. Fischer. 2005b. *'Unrip, a factor implicated in cap-independent translation, associates with the cytosolic SMN complex and influences its intracellular localization',* ***Hum Mol Genet****, 14: 3099-111.*

Gubitz, A. K., Z. Mourelatos, L. Abel, J. Rappsilber, M. Mann, and G. Dreyfuss. 2002. *'Gemin5, a novel WD repeat protein component of the SMN complex that binds Sm proteins',* ***J Biol Chem****, 277: 5631-6.*

Guderian, G., C. Peter, J. Wiesner, A. Sickmann, K. Schulze-Osthoff, U. Fischer, and M. Grimmler. 2011. *'RioK1, a new interactor of protein arginine methyltransferase 5 (PRMT5), competes with pICln for binding and modulates PRMT5 complex composition and substrate specificity',* ***J Biol Chem****, 286: 1976-86.*

Hadjikyriacou, A., Y. Yang, A. Espejo, M. T. Bedford, and S. G. Clarke. 2015. *'Unique Features of Human Protein Arginine Methyltransferase 9 (PRMT9) and Its Substrate RNA Splicing Factor SF3B2',* ***J Biol Chem****, 290: 16723-43.*

Han, G., J. Li, Y. Wang, X. Li, H. Mao, Y. Liu, and C. D. Chen. 2012. *'The hydroxylation activity of Jmjd6 is required for its homo-oligomerization',* ***J Cell Biochem****, 113: 1663-70.*

Hara, K., Y. Maruki, X. Long, K. Yoshino, N. Oshiro, S. Hidayat, C. Tokunaga, J. Avruch, and K. Yonezawa. 2002. *'Raptor, a binding partner of target of rapamycin (TOR), mediates TOR action',* ***Cell****, 110: 177-89.*

Harada, Y., R. Sutomo, A. H. Sadewa, T. Akutsu, Y. Takeshima, H. Wada, M. Matsuo, and H. Nishio. 2002. *'Correlation between SMN2 copy number and clinical phenotype of spinal muscular atrophy: three SMN2 copies fail to rescue some patients from the disease severity',* ***J Neurol****, 249: 1211-9.*

Harris, H., and D. C. Rubinsztein. 2011. *'Control of autophagy as a therapy for neurodegenerative disease', **Nat Rev Neurol**, 8: 108-17.*

Henry, R. W., V. Mittal, B. Ma, R. Kobayashi, and N. Hernandez. 1998. *'SNAP19 mediates the assembly of a functional core promoter complex (SNAPc) shared by RNA polymerases II and III', **Genes Dev**, 12: 2664-72.*

Hernandez, N., and A. M. Weiner. 1986. *'Formation of the 3' end of U1 snRNA requires compatible snRNA promoter elements', **Cell**, 47: 249-58.*

Herrmann, F., M. Bossert, A. Schwander, E. Akgün, and F. O. Fackelmayer. 2004. *'Arginine methylation of scaffold attachment factor A by heterogeneous nuclear ribonucleoprotein particle-associated PRMT1', **J Biol Chem**, 279: 48774-9.*

Hieke, N., A. S. Loffler, T. Kaizuka, N. Berleth, P. Bohler, S. Driessen, F. Stuhldreier, O. Friesen, K. Assani, K. Schmitz, C. Peter, B. Diedrich, J. Dengjel, P. Holland, A. Simonsen, S. Wesselborg, N. Mizushima, and B. Stork. 2015. *'Expression of a ULK1/2 binding-deficient ATG13 variant can partially restore autophagic activity in ATG13-deficient cells', **Autophagy**, 11: 1471-83.*

Hosokawa, N., T. Hara, T. Kaizuka, C. Kishi, A. Takamura, Y. Miura, S. Iemura, T. Natsume, K. Takehana, N. Yamada, J. L. Guan, N. Oshiro, and N. Mizushima. 2009. *'Nutrient-dependent mTORC1 association with the ULK1-Atg13-FIP200 complex required for autophagy', **Mol Biol Cell**, 20: 1981-91.*

Hoy, S. M. 2017. *'Nusinersen: First Global Approval', **Drugs**, 77: 473-79.*

Hsieh-Li, H. M., J. G. Chang, Y. J. Jong, M. H. Wu, N. M. Wang, C. H. Tsai, and H. Li. 2000. *'A mouse model for spinal muscular atrophy', **Nat Genet**, 24: 66-70.*

Hua, Y., K. Sahashi, G. Hung, F. Rigo, M. A. Passini, C. F. Bennett, and A. R. Krainer. 2010. *'Antisense correction of SMN2 splicing in the CNS rescues necrosis in a type III SMA mouse model', **Genes Dev**, 24: 1634-44.*

Hung, K. H., and W. E. Stumph. 2011. *'Regulation of snRNA gene expression by the Drosophila melanogaster small nuclear RNA activating protein complex (DmSNAPc)', **Crit Rev Biochem Mol Biol**, 46: 11-26.*

Husedzinovic, A., F. Oppermann, S. Draeger-Meurer, A. Chari, U. Fischer, H. Daub, and O. J. Gruss. 2014. *'Phosphoregulation of the human SMN complex', **Eur J Cell Biol**, 93: 106-17.*

Husedzinovic, A., B. Neumann, J. Reymann, S. Draeger-Meurer, A. Chari, H. Erfle, U. Fischer, and O. J. Gruss. 2015. *'The catalytically inactive tyrosine phosphatase HD-PTP/PTPN23 is a novel regulator of SMN complex localization', **Mol Biol Cell**, 26: 161-71.*

Jacinto, E., R. Loewith, A. Schmidt, S. Lin, M. A. Rüegg, A. Hall, and M. N. Hall. 2004. *'Mammalian TOR complex 2 controls the actin cytoskeleton and is rapamycin insensitive', **Nat Cell Biol**, 6: 1122-8.*

Jung, C. H., C. B. Jun, S. H. Ro, Y. M. Kim, N. M. Otto, J. Cao, M. Kundu, and D. H. Kim. 2009. *'ULK-Atg13-FIP200 complexes mediate mTOR signaling to the autophagy machinery', **Mol Biol Cell**, 20: 1992-2003.*

Jung, C. H., S. H. Ro, J. Cao, N. M. Otto, and D. H. Kim. 2010. *'mTOR regulation of autophagy', **FEBS Lett**, 584: 1287-95.*

Kaida, D., M. G. Berg, I. Younis, M. Kasim, L. N. Singh, L. Wan, and G. Dreyfuss. 2010. *'U1 snRNP protects pre-mRNAs from premature cleavage and polyadenylation', **Nature**, 468: 664-8.*

Kambach, C., S. Walke, R. Young, J. M. Avis, E. de la Fortelle, V. A. Raker, R. Lührmann, J. Li, and K. Nagai. 1999. *'Crystal structures of two Sm protein complexes and their implications for the assembly of the spliceosomal snRNPs', **Cell**, 96: 375-87.*

Kammler, S., C. Leurs, M. Freund, J. Krummheuer, K. Seidel, T. O. Tange, M. K. Lund, J. Kjems, A. Scheid, and H. Schaal. 2001. *'The sequence complementarity between HIV-1 5' splice site SD4 and U1 snRNA determines the steady-state level of an unstable env pre-mRNA', **RNA**, 7: 421-34.*

Kim, D. H., D. D. Sarbassov, S. M. Ali, J. E. King, R. R. Latek, H. Erdjument-Bromage, P. Tempst, and D. M. Sabatini. 2002. *'mTOR interacts with raptor to form a nutrient-sensitive complex that signals to the cell growth machinery', **Cell**, 110: 163-75.*

Klionsky, D. J. 2007. *'Autophagy: from phenomenology to molecular understanding in less than a decade', **Nat Rev Mol Cell Biol**, 8: 931-7.*

Kroiss, M., J. Schultz, J. Wiesner, A. Chari, A. Sickmann, and U. Fischer. 2008. *'Evolution of an RNP assembly system: a minimal SMN complex facilitates formation of UsnRNPs in Drosophila melanogaster', **Proc Natl Acad Sci U S A**, 105: 10045-50.*

Krzyzanowski, A., R. Gasper, H. Adihou, P. t Hart, and H. Waldmann. 2021. *'Biochemical Investigation of the Interaction of pICln, RioK1 and COPR5 with the PRMT5-MEP50 Complex', **Chembiochem**.*

Kuo, C. J., J. Chung, D. F. Fiorentino, W. M. Flanagan, J. Blenis, and G. R. Crabtree. 1992. *'Rapamycin selectively inhibits interleukin-2 activation of p70 S6 kinase', **Nature**, 358: 70-3.*

Laemmli, U. K. 1970. *'Cleavage of structural proteins during the assembly of the head of bacteriophage T4', **Nature**, 227: 680-5.*

Lapeyre, B., F. Amalric, S. H. Ghaffari, S. V. Rao, T. S. Dumbar, and M. O. Olson. 1986. *'Protein and cDNA sequence of a glycine-rich, dimethylarginine-containing region located near the carboxyl-terminal end of nucleolin (C23 and 100 kDa)', **J Biol Chem**, 261: 9167-73.*

Lee, E. J., and C. Tournier. 2011. *'The requirement of uncoordinated 51-like kinase 1 (ULK1) and ULK2 in the regulation of autophagy', **Autophagy**, 7: 689-95.*

Lefebvre, S., L. Bürglen, S. Reboullet, O. Clermont, P. Burlet, L. Viollet, B. Benichou, C. Cruaud, P. Millasseau, M. Zeviani, and et al. 1995. *'Identification and characterization of a spinal muscular atrophy-determining gene', **Cell**, 80: 155-65.*

Lefebvre, S., P. Burlet, Q. Liu, S. Bertrandy, O. Clermont, A. Munnich, G. Dreyfuss, and J. Melki. 1997. *'Correlation between severity and SMN protein level in spinal muscular atrophy', **Nat Genet**, 16: 265-9.*

Lefebvre, S., L. Bürglen, J. Frézal, A. Munnich, and J. Melki. 1998. *'The role of the SMN gene in proximal spinal muscular atrophy', **Hum Mol Genet**, 7: 1531-6.*

Lerner, M. R., J. A. Boyle, S. M. Mount, S. L. Wolin, and J. A. Steitz. 1980. *'Are snRNPs involved in splicing?', **Nature**, 283: 220-4.*

Lindquist, R. A., K. A. Ottina, D. B. Wheeler, P. P. Hsu, C. C. Thoreen, D. A. Guertin, S. M. Ali, S. Sengupta, Y. D. Shaul, M. R. Lamprecht, K. L. Madden, A. R. Papallo, T. R. Jones, D. M. Sabatini, and A. E. Carpenter. 2011. *'Genome-scale RNAi on living-cell microarrays identifies novel regulators of Drosophila melanogaster TORC1-S6K pathway signaling', **Genome Res**, 21: 433-46.*

Lischwe, M. A., K. D. Roberts, L. C. Yeoman, and H. Busch. 1982. *'Nucleolar specific acidic phosphoprotein C23 is highly methylated', **J Biol Chem**, 257: 14600-2.*

Lischwe, M. A., R. L. Ochs, R. Reddy, R. G. Cook, L. C. Yeoman, E. M. Tan, M. Reichlin, and H. Busch. 1985. *'Purification and partial characterization of a nucleolar scleroderma antigen (Mr = 34,000; pI, 8.5) rich in NG,NG-dimethylarginine',* ***J Biol Chem****, 260: 14304-10.*

Liu, Q., and G. Dreyfuss. 1996. *'A novel nuclear structure containing the survival of motor neurons protein',* ***Embo j****, 15: 3555-65.*

Liu, Q., U. Fischer, F. Wang, and G. Dreyfuss. 1997. *'The spinal muscular atrophy disease gene product, SMN, and its associated protein SIP1 are in a complex with spliceosomal snRNP proteins',* ***Cell****, 90: 1013-21.*

Liu, W., Q. Ma, K. Wong, W. Li, K. Ohgi, J. Zhang, A. Aggarwal, and M. G. Rosenfeld. 2013. *'Brd4 and JMJD6-associated anti-pause enhancers in regulation of transcriptional pause release',* ***Cell****, 155: 1581-95.*

Löffler, A. S., S. Alers, A. M. Dieterle, H. Keppeler, M. Franz-Wachtel, M. Kundu, D. G. Campbell, S. Wesselborg, D. R. Alessi, and B. Stork. 2011. *'Ulk1-mediated phosphorylation of AMPK constitutes a negative regulatory feedback loop',* ***Autophagy****, 7: 696-706.*

Loh, S. H., L. Francescut, P. Lingor, M. Bahr, and P. Nicotera. 2008. *'Identification of new kinase clusters required for neurite outgrowth and retraction by a loss-of-function RNA interference screen',* ***Cell Death Differ****, 15: 283-98.*

Lorson, C. L., E. Hahnen, E. J. Androphy, and B. Wirth. 1999. *'A single nucleotide in the SMN gene regulates splicing and is responsible for spinal muscular atrophy',* ***Proc Natl Acad Sci U S A****, 96: 6307-11.*

Lorson, C. L., and E. J. Androphy. 2000. *'An exonic enhancer is required for inclusion of an essential exon in the SMA-determining gene SMN',* ***Hum Mol Genet****, 9: 259-65.*

Lunn, M. R., and C. H. Wang. 2008. *'Spinal muscular atrophy',* ***Lancet****, 371: 2120-33.*

MacLean, B., D. M. Tomazela, N. Shulman, M. Chambers, G. L. Finney, B. Frewen, R. Kern, D. L. Tabb, D. C. Liebler, and M. J. MacCoss. 2010. *'Skyline: an open source document editor for creating and analyzing targeted proteomics experiments',* ***Bioinformatics****, 26: 966-8.*

Maniatis, T., and R. Reed. 1987. *'The role of small nuclear ribonucleoprotein particles in pre-mRNA splicing',* ***Nature****, 325: 673-8.*

Mao, Y. S., B. Zhang, and D. L. Spector. 2011. *'Biogenesis and function of nuclear bodies',* ***Trends Genet****, 27: 295-306.*

Massenet, S., L. Pellizzoni, S. Paushkin, I. W. Mattaj, and G. Dreyfuss. 2002. *'The SMN complex is associated with snRNPs throughout their cytoplasmic assembly pathway',* ***Mol Cell Biol****, 22: 6533-41.*

Matera, A. G., and Z. Wang. 2014. *'A day in the life of the spliceosome',* ***Nat Rev Mol Cell Biol****, 15: 108-21.*

Mattaj, I. W., and E. M. De Robertis. 1985. *'Nuclear segregation of U2 snRNA requires binding of specific snRNP proteins',* ***Cell****, 40: 111-8.*

Mattaj, I. W. 1986. *'Cap trimethylation of U snRNA is cytoplasmic and dependent on U snRNP protein binding',* ***Cell****, 46: 905-11.*

McKinney, D. C., B. J. McMillan, M. J. Ranaghan, J. A. Moroco, M. Brousseau, Z. Mullin-Bernstein, M. O'Keefe, P. McCarren, M. F. Mesleh, K. M. Mulvaney, F. Robinson, R. Singh, B. Bajrami, F. F. Wagner, R. Hilgraf, M. J. Drysdale, A. J. Campbell, A. Skepner, D. E. Timm, D. Porter, V. K. Kaushik, W. R. Sellers, and A. Ianari. 2021.

'Discovery of a First-in-Class Inhibitor of the PRMT5-Substrate Adaptor Interaction', ***J Med Chem****, 64: 11148-68.*

Meister, G.;, D. Bühler, R. Pillai, F. Lottspeich, and U. Fischer. 2001a. *'A multiprotein complex mediates the ATP-dependent assembly of spliceosomal U snRNPs',* ***Nat Cell Biol****, 3: 945-9.*

Meister, G.;, C.; Eggert, D.; Bühler, H.; Brahms, C.; Kambach, and U. Fischer. 2001b. *'Methylation of Sm proteins by a complex containing PRMT5 and the putative U snRNP assembly factor pICln',* ***Curr Biol****, 11: 1990-4.*

Meister, Gunter, Christian Eggert, and Utz Fischer. 2002a. *'SMN-mediated assembly of RNPs: a complex story',* ***Trends in Cell Biology****, 12: 472-78.*

Meister, G., and U. Fischer. 2002b. *'Assisted RNP assembly: SMN and PRMT5 complexes cooperate in the formation of spliceosomal UsnRNPs',* ***Embo j****, 21: 5853-63.*

Melki, J., S. Abdelhak, P. Sheth, M. F. Bachelot, P. Burlet, A. Marcadet, J. Aicardi, A. Barois, J. P. Carriere, M. Fardeau, and et al. 1990. *'Gene for chronic proximal spinal muscular atrophies maps to chromosome 5q',* ***Nature****, 344: 767-8.*

Mendell, J. R., S. Al-Zaidy, R. Shell, W. D. Arnold, L. R. Rodino-Klapac, T. W. Prior, L. Lowes, L. Alfano, K. Berry, K. Church, J. T. Kissel, S. Nagendran, J. L'Italien, D. M. Sproule, C. Wells, J. A. Cardenas, M. D. Heitzer, A. Kaspar, S. Corcoran, L. Braun, S. Likhite, C. Miranda, K. Meyer, K. D. Foust, A. H. M. Burghes, and B. K. Kaspar. 2017. *'Single-Dose Gene-Replacement Therapy for Spinal Muscular Atrophy',* ***N Engl J Med****, 377: 1713-22.*

Miller, N., H. Shi, A. S. Zelikovich, and Y. C. Ma. 2016. *'Motor neuron mitochondrial dysfunction in spinal muscular atrophy',* ***Hum Mol Genet****, 25: 3395-406.*

Mizushima, N. 2007. *'Autophagy: process and function',* ***Genes Dev****, 21: 2861-73. 2010. 'The role of the Atg1/ULK1 complex in autophagy regulation',* ***Curr Opin Cell Biol****, 22: 132-9.*

Mizushima, N. 2010. *The role of the Atg1/ULK1 complex in autophagy regulation.* ***Curr Opin Cell Biol****, 22, 132-9.*

Monani, U. R., C. L. Lorson, D. W. Parsons, T. W. Prior, E. J. Androphy, A. H. Burghes, and J. D. McPherson. 1999. *'A single nucleotide difference that alters splicing patterns distinguishes the SMA gene SMN1 from the copy gene SMN2',* ***Hum Mol Genet****, 8: 1177-83.*

Mulvaney, K. M., C. Blomquist, N. Acharya, R. Li, M. J. Ranaghan, M. O'Keefe, D. J. Rodriguez, M. J. Young, D. Kesar, D. Pal, M. Stokes, A. J. Nelson, S. S. Jain, A. Yang, Z. Mullin-Bernstein, J. Columbus, F. K. Bozal, A. Skepner, D. Raymond, S. LaRussa, D. C. McKinney, Y. Freyzon, Y. Baidi, D. Porter, A. J. Aguirre, A. Ianari, B. McMillan, and W. R. Sellers. 2021. *'Molecular basis for substrate recruitment to the PRMT5 methylosome',* ***Mol Cell****, 81: 3481-95 e7.*

Murn, J., and Y. Shi. 2017. *'The winding path of protein methylation research: milestones and new frontiers',* ***Nat Rev Mol Cell Biol****, 18: 517-27.*

Musiani, D., J. Bok, E. Massignani, L. Wu, T. Tabaglio, M. R. Ippolito, A. Cuomo, U. Ozbek, H. Zorgati, U. Ghoshdastider, R. C. Robinson, E. Guccione, and T. Bonaldi. 2019. *'Proteomics profiling of arginine methylation defines PRMT5 substrate specificity',* ***Sci Signal****, 12.*

Neuenkirchen, N., C. Englbrecht, J. Ohmer, T. Ziegenhals, A. Chari, and U. Fischer. 2015. *'Reconstitution of the human U snRNP assembly machinery reveals stepwise Sm protein organization',* ***EMBO J****, 34: 1925-41.*

Newman, A. J., and K. Nagai. 2010. *'Structural studies of the spliceosome: blind men and an elephant',* ***Curr Opin Struct Biol****, 20: 82-9.*

Niewalda, T., B. Michels, R. Jungnickel, S. Diegelmann, J. Kleber, T. Kahne, and B. Gerber. 2015. *'Synapsin determines memory strength after punishment- and relief-learning',* ***J Neurosci****, 35: 7487-502.*

Nilsen, T. W., and B. R. Graveley. 2010. *'Expansion of the eukaryotic proteome by alternative splicing',* ***Nature****, 463: 457-63.*

Nizami, Z., S. Deryusheva, and J. G. Gall. 2010. *'The Cajal body and histone locus body',* ***Cold Spring Harb Perspect Biol****, 2: a000653.*

Noda, T., and Y. Ohsumi. 1998. *'Tor, a phosphatidylinositol kinase homologue, controls autophagy in yeast',* ***J Biol Chem****, 273: 3963-6.*

Ogawa, C., K. Usui, M. Aoki, F. Ito, M. Itoh, C. Kai, M. Kanamori-Katayama, Y. Hayashizaki, and H. Suzuki. 2007. *'Gemin2 plays an important role in stabilizing the survival of motor neuron complex',* ***J Biol Chem****, 282: 11122-34.*

Ogura, K., C. Wicky, L. Magnenat, H. Tobler, I. Mori, F. Müller, and Y. Ohshima. 1994. *'Caenorhabditis elegans unc-51 gene required for axonal elongation encodes a novel serine/threonine kinase',* ***Genes Dev****, 8: 2389-400.*

Ohno, M., A. Segref, S. Kuersten, and I. W. Mattaj. 2002. *'Identity elements used in export of mRNAs',* ***Mol Cell****, 9: 659-71.*

Otter, S., M. Grimmler, N. Neuenkirchen, A. Chari, A. Sickmann, and U. Fischer. 2007. *'A comprehensive interaction map of the human survival of motor neuron (SMN) complex',* ***J Biol Chem****, 282: 5825-33.*

Paknia, E., A. Chari, H. Stark, and U. Fischer. 2016. *'The Ribosome Cooperates with the Assembly Chaperone pICln to Initiate Formation of snRNPs',* ***Cell Rep****, 16: 3103-12.*

Pal, S., S. N. Vishwanath, H. Erdjument-Bromage, P. Tempst, and S. Sif. 2004. *'Human SWI/SNF-associated PRMT5 methylates histone H3 arginine 8 and negatively regulates expression of ST7 and NM23 tumor suppressor genes',* ***Mol Cell Biol****, 24: 9630-45.*

Patel, A. A., and J. A. Steitz. 2003. *'Splicing double: insights from the second spliceosome',* ***Nat Rev Mol Cell Biol****, 4: 960-70.*

Pearn, J. 1980. *'Classification of spinal muscular atrophies',* ***Lancet****, 1: 919-22.*

Pellizzoni, L., N. Kataoka, B. Charroux, and G. Dreyfuss. 1998. *'A novel function for SMN, the spinal muscular atrophy disease gene product, in pre-mRNA splicing',* ***Cell****, 95: 615-24.*

Pellizzoni, L., J. Baccon, J. Rappsilber, M. Mann, and G. Dreyfuss. 2002a. *'Purification of native survival of motor neurons complexes and identification of Gemin6 as a novel component',* ***J Biol Chem****, 277: 7540-5.*

Pellizzoni, L., J. Yong, and G. Dreyfuss. 2002b. *'Essential role for the SMN complex in the specificity of snRNP assembly',* ***Science****, 298: 1775-9.*

Pelz, J. P., H. Schindelin, K. van Pee, J. Kuper, C. Kisker, K. Diederichs, U. Fischer, and C. Grimm. 2015. *'Crystallizing the 6S and 8S spliceosomal assembly intermediates: a complex project',* ***Acta Crystallogr D Biol Crystallogr****, 71: 2040-53.*

Perrett, D. 2007. *'From 'protein' to the beginnings of clinical proteomics',* ***Proteomics Clin Appl****, 1: 720-38.*

Petherick, K. J., O. J. Conway, C. Mpamhanga, S. A. Osborne, A. Kamal, B. Saxty, and I. G. Ganley. 2015. *'Pharmacological inhibition of ULK1 kinase blocks mammalian target of rapamycin (mTOR)-dependent autophagy', **J Biol Chem**, 290: 11376-83.*

Piras, A., L. Schiaffino, M. Boido, V. Valsecchi, M. Guglielmotto, E. De Amicis, J. Puyal, A. Garcera, E. Tamagno, R. M. Soler, and A. Vercelli. 2017. *'Inhibition of autophagy delays motoneuron degeneration and extends lifespan in a mouse model of spinal muscular atrophy', **Cell Death Dis**, 8: 3223.*

Pollack, B. P., S. V. Kotenko, W. He, L. S. Izotova, B. L. Barnoski, and S. Pestka. 1999. *'The human homologue of the yeast proteins Skb1 and Hsl7p interacts with Jak kinases and contains protein methyltransferase activity', **J Biol Chem**, 274: 31531-42.*

Porensky, P. N., C. Mitrpant, V. L. McGovern, A. K. Bevan, K. D. Foust, B. K. Kaspar, S. D. Wilton, and A. H. Burghes. 2012. *'A single administration of morpholino antisense oligomer rescues spinal muscular atrophy in mouse', **Hum Mol Genet**, 21: 1625-38.*

Poulard, C., J. Rambaud, N. Hussein, L. Corbo, and M. Le Romancer. 2014. *'JMJD6 regulates ERalpha methylation on arginine', **PLoS One**, 9: e87982.*

Prior, T. W., M. E. Leach, and E. Finanger. 1993. *'Spinal Muscular Atrophy.' in M. P. Adam, J. Feldman, G. M. Mirzaa, R. A. Pagon, S. E. Wallace, L. J. H. Bean, K. W. Gripp and A. Amemiya (eds.), **GeneReviews**(®) (University of Washington, Seattle Copyright © 1993-2023, University of Washington, Seattle. GeneReviews is a registered trademark of the University of Washington, Seattle. All rights reserved.: Seattle (WA)).*

Prusty, A. B., R. Meduri, B. K. Prusty, J. Vanselow, A. Schlosser, and U. Fischer. 2017. *'Impaired spliceosomal UsnRNP assembly leads to Sm mRNA down-regulation and Sm protein degradation', **J Cell Biol**, 216: 2391-407.*

Pu, W. T., G. B. Krapivinsky, L. Krapivinsky, and D. E. Clapham. 1999. *'pICln inhibits snRNP biogenesis by binding core spliceosomal proteins', **Mol Cell Biol**, 19: 4113-20.*

Quidville, V., S. Alsafadi, A. Goubar, F. Commo, V. Scott, C. Pioche-Durieu, I. Girault, S. Baconnais, E. Le Cam, V. Lazar, S. Delaloge, M. Saghatchian, P. Pautier, P. Morice, P. Dessen, S. Vagner, and F. André. 2013. *'Targeting the deregulated spliceosome core machinery in cancer cells triggers mTOR blockade and autophagy', **Cancer Res**, 73: 2247-58.*

Raker, V. A., G. Plessel, and R. Lührmann. 1996. *'The snRNP core assembly pathway: identification of stable core protein heteromeric complexes and an snRNP subcore particle in vitro', **Embo j**, 15: 2256-69.*

Reilly, S. M., S. H. Chiang, S. J. Decker, L. Chang, M. Uhm, M. J. Larsen, J. R. Rubin, J. Mowers, N. M. White, I. Hochberg, M. Downes, R. T. Yu, C. Liddle, R. M. Evans, D. Oh, P. Li, J. M. Olefsky, and A. R. Saltiel. 2013. *'An inhibitor of the protein kinases TBK1 and IKK-varepsilon improves obesity-related metabolic dysfunctions in mice', **Nat Med**, 19: 313-21.*

Richard, S., M. Morel, and P. Cleroux. 2005. *'Arginine methylation regulates IL-2 gene expression: a role for protein arginine methyltransferase 5 (PRMT5)', **Biochem J**, 388: 379-86.*

Ross, C. A., and M. A. Poirier. 2004. *'Protein aggregation and neurodegenerative disease', **Nat Med**, 10 Suppl: S10-7.*

Ruvinsky, I., and O. Meyuhas. 2006. *'Ribosomal protein S6 phosphorylation: from protein synthesis to cell size',* ***Trends Biochem Sci****, 31: 342-8.*

Sanchez-Olea, R., F. Emma, M. Coghlan, and K. Strange. 1998. *'Characterization of pICln phosphorylation state and a pICln-associated protein kinase',* ***Biochim Biophys Acta****, 1381: 49-60.*

Sarbassov, D. D., S. M. Ali, D. H. Kim, D. A. Guertin, R. R. Latek, H. Erdjument-Bromage, P. Tempst, and D. M. Sabatini. 2004. *'Rictor, a novel binding partner of mTOR, defines a rapamycin-insensitive and raptor-independent pathway that regulates the cytoskeleton',* ***Curr Biol****, 14: 1296-302.*

Saric, A., V. E. Hipolito, J. G. Kay, J. Canton, C. N. Antonescu, and R. J. Botelho. 2016. *'mTOR controls lysosome tubulation and antigen presentation in macrophages and dendritic cells',* ***Mol Biol Cell****, 27: 321-33.*

Schedlbauer, A., G. Kontaxis, M. Konig, J. Furst, M. Jakab, M. Ritter, L. Garavaglia, G. Botta, G. Meyer, M. Paulmichl, and R. Konrat. 2003. *'Sequence-specific resonance assignments of ICln, an ion channel cloned from epithelial cells',* ***J Biomol NMR****, 27: 399-400.*

Schedlbauer, A., R. Gandini, G. Kontaxis, M. Paulmichl, J. Furst, and R. Konrat. 2011. *'The C-terminus of ICln is natively disordered but displays local structural preformation',* ***Cell Physiol Biochem****, 28: 1203-10.*

Schilling, M., A. B. Prusty, B. Boysen, F. S. Oppermann, Y. L. Riedel, A. Husedzinovic, H. Rasouli, A. König, P. Ramanathan, J. Reymann, H. Erfle, H. Daub, U. Fischer, and O. J. Gruss. 2021. *'TOR signaling regulates liquid phase separation of the SMN complex governing snRNP biogenesis',* ***Cell Rep****, 35: 109277.*

Schmitz, K., J. Cox, L. M. Esser, M. Voss, K. Sander, A. Löffler, F. Hillebrand, S. Erkelenz, H. Schaal, T. Kähne, S. Klinker, T. Zhang, L. Nagel-Steger, D. Willbold, S. Seggewiß, D. Schlütermann, B. Stork, M. Grimmler, S. Wesselborg, and C. Peter. 2021. *'An essential role of the autophagy activating kinase ULK1 in snRNP biogenesis',* ***Nucleic Acids Res****, 49: 6437-55.*

Schorling, D. C., A. Pechmann, and J. Kirschner. 2020. *'Advances in Treatment of Spinal Muscular Atrophy - New Phenotypes, New Challenges, New Implications for Care',* ***J Neuromuscul Dis****, 7: 1-13.*

Schuck, P. 2000. *'Size-distribution analysis of macromolecules by sedimentation velocity ultracentrifugation and lamm equation modeling',* ***Biophys J****, 78: 1606-19.*

Schuck, P. *'SEDFIT website, http://www.analyticalultracentrifugation.com/'.*

Selenko, P., R. Sprangers, G. Stier, D. Buhler, U. Fischer, and M. Sattler. 2001. *'SMN tudor domain structure and its interaction with the Sm proteins',* ***Nat Struct Biol****, 8: 27-31.*

Shamji, A. F., P. Nghiem, and S. L. Schreiber. 2003. *'Integration of growth factor and nutrient signaling: implications for cancer biology',* ***Mol Cell****, 12: 271-80.*

Shevchenko, A., M. Wilm, O. Vorm, and M. Mann. 1996. *'Mass spectrometric sequencing of proteins silver-stained polyacrylamide gels',* ***Anal Chem****, 68: 850-8.*

Shi, L., G. Zhao, D. Qiu, W. R. Godfrey, H. Vogel, T. A. Rando, H. Hu, and P. N. Kao. 2005. *'NF90 regulates cell cycle exit and terminal myogenic differentiation by direct binding to the 3'-untranslated region of MyoD and p21WAF1/CIP1 mRNAs',* ***J Biol Chem****, 280: 18981-9.*

Simms, S. A., A. M. Stock, and J. B. Stock. 1987. *'Purification and characterization of the S-adenosylmethionine:glutamyl methyltransferase that modifies membrane chemoreceptor proteins in bacteria',* ***J Biol Chem****, 262: 8537-43.*

Sou, Y. S., S. Waguri, J. Iwata, T. Ueno, T. Fujimura, T. Hara, N. Sawada, A. Yamada, N. Mizushima, Y. Uchiyama, E. Kominami, K. Tanaka, and M. Komatsu. 2008. *'The Atg8 conjugation system is indispensable for proper development of autophagic isolation membranes in mice',* ***Mol Biol Cell****, 19: 4762-75.*

Staley, J. P., and C. Guthrie. 1998. *'Mechanical devices of the spliceosome: motors, clocks, springs, and things',* ***Cell****, 92: 315-26.*

Stewart, M. J., and G. Thomas. 1994. *'Mitogenesis and protein synthesis: a role for ribosomal protein S6 phosphorylation?',* ***Bioessays****, 16: 809-15.*

Strzelecka, M., S. Trowitzsch, G. Weber, R. Luhrmann, A. C. Oates, and K. M. Neugebauer. 2010. *'Coilin-dependent snRNP assembly is essential for zebrafish embryogenesis',* ***Nat Struct Mol Biol****, 17: 403-9.*

Taus, T., T. Kocher, P. Pichler, C. Paschke, A. Schmidt, C. Henrich, and K. Mechtler. 2011. *'Universal and confident phosphorylation site localization using phosphoRS',* ***J Proteome Res****, 10: 5354-62.*

Teng, Y., A. C. Girvan, L. K. Casson, W. M. Pierce, Jr., M. Qian, S. D. Thomas, and P. J. Bates. 2007. *'AS1411 alters the localization of a complex containing protein arginine methyltransferase 5 and nucleolin',* ***Cancer Res****, 67: 10491-500.*

Thandapani, P., T. R. O'Connor, T. L. Bailey, and S. Richard. 2013. *'Defining the RGG/RG motif',* ***Mol Cell****, 50: 613-23.*

Tisdale, S., and L. Pellizzoni. 2015. *'Disease mechanisms and therapeutic approaches in spinal muscular atrophy',* ***J Neurosci****, 35: 8691-700.*

Tomoda, T., R. S. Bhatt, H. Kuroyanagi, T. Shirasawa, and M. E. Hatten. 1999. *'A mouse serine/threonine kinase homologous to C. elegans UNC51 functions in parallel fiber formation of cerebellar granule neurons',* ***Neuron****, 24: 833-46.*

Tsai, W. C., L. C. Reineke, A. Jain, S. Y. Jung, and R. E. Lloyd. 2017. *'Histone arginine demethylase JMJD6 is linked to stress granule assembly through demethylation of the stress granule-nucleating protein G3BP1',* ***J Biol Chem****, 292: 18886-96.*

Turunen, J. J., E. H. Niemelä, B. Verma, and M. J. Frilander. 2013. *'The significant other: splicing by the minor spliceosome',* ***Wiley Interdiscip Rev RNA****, 4: 61-76.*

Veepaschit, J., A. Viswanathan, R. Bordonne, C. Grimm, and U. Fischer. 2021. *'Identification and structural analysis of the Schizosaccharomyces pombe SMN complex',* ***Nucleic Acids Res****, 49: 7207-23.*

Wahl, M. C., C. L. Will, and R. Lührmann. 2009. *'The spliceosome: design principles of a dynamic RNP machine',* ***Cell****, 136: 701-18.*

Wandrey, Franziska, Christian Montellese, Krisztian Koos, Lukas Badertscher, Lukas Bammert, Atlanta G. Cook, Ivo Zemp, Peter Horvath, and Ulrike Kutay. 2015. *'The NF45/NF90 Heterodimer Contributes to the Biogenesis of 60S Ribosomal Subunits and Influences Nucleolar Morphology',* ***Molecular and Cellular Biology****, 35: 3491-503.*

Webby, C. J., A. Wolf, N. Gromak, M. Dreger, H. Kramer, B. Kessler, M. L. Nielsen, C. Schmitz, D. S. Butler, J. R. Yates, 3rd, C. M. Delahunty, P. Hahn, A. Lengeling, M. Mann, N. J. Proudfoot, C. J. Schofield, and A. Bottger. 2009. *'Jmjd6 catalyses lysyl-hydroxylation of U2AF65, a protein associated with RNA splicing',* ***Science****, 325: 90-3.*

Weber, G., S. Trowitzsch, B. Kastner, R. Lührmann, and M. C. Wahl. 2010. *'Functional organization of the Sm core in the crystal structure of human U1 snRNP',* ***Embo j****, 29: 4172-84.*

Widmann, B., F. Wandrey, L. Badertscher, E. Wyler, J. Pfannstiel, I. Zemp, and U. Kutay. 2012. *'The kinase activity of human Rio1 is required for final steps of cytoplasmic maturation of 40S subunits',* ***Mol Biol Cell****, 23: 22-35.*

Will, C. L., and R. Lührmann. 2001. *'Spliceosomal UsnRNP biogenesis, structure and function',* ***Curr Opin Cell Biol****, 13: 290-301.*

Will, C. L. & Lührmann, R. 2011. *Spliceosome structure and function.* ***Cold Spring Harb Perspect Biol****, 3.*

Winkler, C., C. Eggert, D. Gradl, G. Meister, M. Giegerich, D. Wedlich, B. Laggerbauer, and U. Fischer. 2005. *'Reduced U snRNP assembly causes motor axon degeneration in an animal model for spinal muscular atrophy',* ***Genes Dev****, 19: 2320-30.*

Workman, E., L. Saieva, T. L. Carrel, T. O. Crawford, D. Liu, C. Lutz, C. E. Beattie, L. Pellizzoni, and A. H. Burghes. 2009. *'A SMN missense mutation complements SMN2 restoring snRNPs and rescuing SMA mice',* ***Hum Mol Genet****, 18: 2215-29.*

Yildirim, M. A., K. I. Goh, M. E. Cusick, A. L. Barabási, and M. Vidal. 2007. *'Drug-target network',* ***Nat Biotechnol****, 25: 1119-26.*

Zeller, R., T. Nyffenegger, and E. M. De Robertis. 1983. *'Nucleocytoplasmic distribution of snRNPs and stockpiled snRNA-binding proteins during oogenesis and early development in Xenopus laevis',* ***Cell****, 32: 425-34.*

Zhang, Z., F. Lotti, K. Dittmar, I. Younis, L. Wan, M. Kasim, and G. Dreyfuss. 2008. *'SMN deficiency causes tissue-specific perturbations in the repertoire of snRNAs and widespread defects in splicing',* ***Cell****, 133: 585-600.*

Zhang, R., B. R. So, P. Li, J. Yong, T. Glisovic, L. Wan, and G. Dreyfuss. 2011. *'Structure of a key intermediate of the SMN complex reveals Gemin2's crucial function in snRNP assembly',* ***Cell****, 146: 384-95.*

Zhou, J., X. Zheng, and H. Shen. 2012. *'Targeting RNA-splicing for SMA treatment',* ***Mol Cells****, 33: 223-8.*

10 Acknowledgments

An dieser Stelle möchte ich allen Beteiligten, die mich bei der Erstellung meiner Dissertation unterstützt haben, meine große Dankbarkeit aussprechen.

Ganz besonders bedanken möchte ich mich bei meinem Doktorvater Christoph Peter für die hervorragende Betreuung sowie die zahlreichen konstruktiven Diskussionen. Vielen Dank für die uneingeschränkte Unterstützung und die überdurchschnittliche Erreichbarkeit während der gesamten Zeit meiner Promotion und die Vergabe eines für mich besonders spannenden Themas.

Mein herzlicher Dank gilt auch Prof. Sebastian Wesselborg, der mir die Möglichkeit gab, meine Dissertation in seinem Institut für Molekulare Medizin I realisieren zu dürfen sowie stets ein offenes Ohr und interessante Anregungen für mich hatte. Des Weiteren bedanke ich mich für die uneingeschränkte Unterstützung auch bei bürokratischen Angelegenheiten.

Weiterhin möchte ich mich bei Prof. Henrike Heise für die Übernahme des Zweit Gutachtens bedanken.

Darüber hinaus möchte ich mich bei allen Co-Autoren und Kooperationspartnern bedanken. Vor allen gilt mein Dank hier Prof. Dr. Matthias Grimmler für die gute Zusammenarbeit und das offene Feedback.

Außerdem möchte ich mich bei allen aktuellen und ehemaligen Mitgliedern der Molekularen Medizin I für die Unterstützung und die sehr schöne Zeit nicht nur im Labor bedanken. Ihr habt mir die Arbeit auch an langen Laborabenden erleichtert und mir stets ein Lächeln ins Gesicht gezaubert.

Auch meinen Eltern, vor allem meiner Mutter, möchte ich danken. Ihr habt Zeit meines Lebens schon immer ein offenes Ohr für mich und habt mich immer bei der Verwirklichung aller meiner Träume und Ziele im Leben unterstützt. Meine Eltern haben mir nie Druck gemacht und meinen gesamten Bildungsweg konnte ich immer frei gestalten, ich weiß dies sehr zu schätzen.

Zu guter Letzt möchte ich meinem Freund danken, Patrick Linsen, der maßgeblich zu dem Gelingen dieser Arbeit beigetragen hat. Du hast mich immer zu einhundert Prozent unterstützt und mir den Rücken freigehalten, was meinen Erfolg erst möglich gemacht hat. Dir und meinen Eltern ist diese Arbeit gewidmet.

11 Declaration

Ich versichere an Eides Statt, dass die Dissertation von mir selbständig und ohne unzulässige fremde Hilfe unter Beachtung der „Grundsätze zur Sicherung guter wissenschaftlicher Praxis an der Heinrich-Heine-Universität Düsseldorf' erstellt worden ist. Die Dissertation wurde in der vorgelegten oder in ähnlicher Form noch bei keiner anderen Fakultät eingereicht. Ich habe bisher keine erfolglosen und erfolgreichen Promotionsversuche unternommen.

Düsseldorf, 03.01.2024

Ort, Datum	Lea Marie Esser